Optimization of mesostructured CeO_2 synthesis using SBA-15 as a template

Álvaro Moreno-de la Calle[1], Pedro J. Megía[1], José A. Calles[1,2], Arturo J. Vizcaíno[1,*], and Alicia Carrero[1,2]
[1]Chemical and Environmental Engineering Group, Universidad Rey Juan Carlos, Móstoles, Spain
[2] Institute of Sustainable Technologies, Universidad Rey Juan Carlos, Móstoles, Spain
[*] Corresponding author (arturo.vizcaíno@urjc.es)

INTRODUCTION

Mesostructured materials with well-ordered molecular sieves have garnered significant attention from the scientific community, owing to their remarkable characteristics in different catalytic applications. In this regard, mesostructured metal oxides characterized by their extensive surface area have attracted considerable attention given their capability to interact with molecules, ions, and atoms[1]. CeO_2, has multiple applications in heterogeneous catalysis due to its redox properties, and high oxygen mobility. However, its application in catalysis can be constrained due to its non-porous structure. Despite different authors have reported the synthesis of mesostructured ceria, so far there is no suitable synthesis for these structures in terms of the ordering degree and thermal stability[2].

EXPERIMENTAL/THEORETICAL STUDY

There are different methods to synthesize ordered porous metal oxides: soft-templating, hard-templating, or colloid crystal templating. In this work, mesostructured CeO_2 was prepared via nanocasting by incorporating ceria precursors, $Ce(NO_3)_3{\cdot}6H_2O$ or $CeCl_3{\cdot}7H_2O$, onto SBA-15 used as template. The procedure was repeated six times to evaluate differences in the textural properties of the prepared nanocomposites before removing the SBA-15 with a 2 M solution of NaOH. All the prepared materials were characterized by XRD, N_2-physisorption, and TEM.

RESULTS AND DISCUSSION

After the successive impregnations on the SBA-15, there is a gradual increase in CeO_2 crystallites reaching values near the maximum pore size of the template. Differences in the crystallite distribution within the SBA-15 channels can be distinguished, with a better distribution with $CeCl_3$ After the SBA-15 removal, mesoporous ceria particles were calcined at 600 °C and subsequently characterized. In this sense, Fig.1 shows the TEM micrographs after 5 successive impregnations, where smaller mesoporous CeO_2 particles with a low degree of order can be appreciated for the sample synthesized with $Ce(NO_3)_3$ leading to slightly higher BET surface areas. On the contrary, more ordered structures using $CeCl_3$ were obtained in line with the expected inverse structure of SBA-15, even for three impregnations.

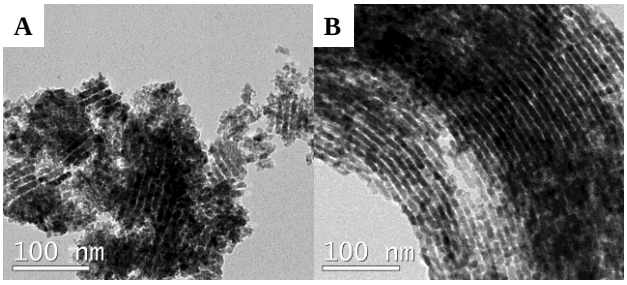

Fig. 1. TEM images after 5 impregnations of SBA-15 with $Ce(NO_3)_3$ (A) and $CeCl_3$ (B)

CONCLUSION

Mesostructured ceria was synthesized via nanocasting using $Ce(NO_3)_3$ and $CeCl_3$ as ceria precursors and SBA-15 as the template. The results showed more ordered structures when using $CeCl_3$ as precursor making easier its diffusion through both mesopores and micropores of SBA-15 material.

REFERENCES

1. Y. Wang et at., J. Mater. Chem. A Mater. 5, 8825–8846 (2017).
2. M. Dubey et al., Appl. Surf. Sci. 12, 100340 (2022).

ACKNOWLEDGMENTS

The authors acknowledge the financial support from the Spanish Ministry of Science and Innovation (Projects PID2020-117273RB-I00 and TED2021-131499B-I00) and the Community of Madrid in the framework of the Multiannual Agreement with the Rey Juan Carlos University in line of action 1, “Encouragement of Young Ph.D. students investigation” (Project Ref. M2743 with the acronym HYDROGREFOX).

Engineering New Nanostructured Multi-Material Inks for 3D Printing for Bone-Regeneration

Adriana Lungu[1*], Izabela-Cristina Stancu[1], Horia Iovu[1], Sorina Dinescu[2], Roxana Balahura (Stămat)[2], Anca Hermenean[3]

[1]Advanced Polymer Materials Group, National University of Science and Technology Politehnica Bucharest, Romania, corresponding author (adriana.lungu@upb.ro);

[2]Department of Biochemistry and Molecular Biology, University of Bucharest, Romania;

[3]"Aurel Ardelean" Institute of Life Sciences, "Vasile Goldis" Western University of Arad, Romania

INTRODUCTION

Taking advantage of both naturally derived polymers and nanostructured materials[1], in the current study, we propose new multicomponent hydrogels double reinforced with two complementary nano-fillers developed for bioprinting-based tissue engineering applications.

EXPERIMENTAL STUDY

Cellulose nanofibrils (CNFs) and polyhedral silsesquioxanes (PSS) nanoparticles were immobilized in a photopolymerizable gelatin-pectin matrix. The methacryloyl derivatives of the biopolymers were crosslinked using UV-light to provide optimal conditions for cell encapsulation purposes. The nanocomposite bioinks were supplemented with bone morphogenetic protein 2 (BMP2) to maximize the function of preosteoblasts already engaged to the osteogenic lineage. The 3D-scaffolds' morphology was investigated focusing on PSS dispersion, porosity, and geometrical features of constructs. Bone formation in non-osteogenic and in osteogenic area was performed using CD1 mice[2].

RESULTS AND DISCUSSION

Swelling investigation revealed that all the scaffolds maintained their hydrophilic character with a slight decreasing tendency of the swelling capacity when PSS nanoparticles were incorporated. The *in vitro* cytocompatibility tests indicated a beneficial influence of CNFs and PSS nanoadditives for cell growth. *In vivo* studies revealed that hydrogels supplemented with nanostructured fillers and BMP2 promote improved osteogenesis both in osteogenic and nonosteogenic área. Such behaviour indicated that the scaffolds reinforced with osteogenic growth factors have a big potential to respond to the challenges of the biomaterials and could be a promising option for the regeneration of hard tissues.

CONCLUSION

New bioinspired multi-material nanostructured scaffolds based on natural origin hydrogels and two types of nanomaterials were fabricated through 3D printing. *In vitro* and *in vivo* testing indicated the potential of BMP2 bioactivated scaffolds to induce enhanced bone regeneration.

REFERENCES

1. F. Curti et. al, Mar. Drugs 20, 670. (2022);
2. A. Lungu et al., CEJ, CEJ-D-24-03740, (submitted 2024)

ACKNOWLEDGMENTS

This work was supported from the project Next3DBone, Integrating mechanically-tunable 3D printing with new bioactive multi(nano)materials for next functional personalized bone regenerative scaffolds, PN-III-P4-PCE-2021–1240, no. PCE 88/2022.

Graphene-based Electrodes for PEM Fuel Cells as Integrated Catalytic Layers

Adriana Marinoiu *, Elena Carcadea and Mihai Varlam

National Research and Development Institute for Cryogenic and Isotopic Technologies, Rm Valcea, Romania, adriana.marinoiu@icsi.ro

INTRODUCTION

Fuel cells (FCs), the most promising power sources for stationary and portable electronic devices, represent an alternative for decentralized energy production and long-distance transport, with applications already successfully employed in automotive, aerospace, and maritime transportation. FCs are electrochemical cells that catalytically convert the chemical energy of a fuel (hydrogen being the most common) and an oxidizing agent into electrical energy through coupled redox reactions. Among them, proton exchange membrane fuel cells (PEM FCs) demonstrated indisputable relevant advantages such as renewable source with very low emissions, low operating temperature, high energy efficiency and modularity. Substantial progress has been achieved in MEA development, however more efforts are needed to improve catalyst performance and durability and to reduce production costs, so that FCs can compete with combustion engines. Both performance and durability issues are directly associated with the materials and efficiency of the MEA, which consists of the proton exchange membrane and a catalyst-supporting (anodic or cathodic) gas diffusion layer (GDL). The GDL development secures a good electrical contact between mentioned layers (i.e. the catalyst layer and PEM), allowing the obtaining of high current densities without excessive cathode overpotentials or cell voltage losses.

EXPERIMENTAL/THEORETICAL STUDY

The scope of this paper is to develop, demonstrate, and validate integrated graphene-based electrodes for PEM FCs, that incorporate both gas-diffusion and catalytic layers in a single-layer assembly, and are realized by advanced physico-chemical methods: microwave and chemical processing.

RESULTS AND DISCUSSION

Through this paper, we specifically aim the MEAs of PEM FCs, targeting to produce graphene-based electrodes, including both microporous and macroporous layers as well as catalyst supports providing integrated catalytic layers, for both anode and cathode. The electrodes will use as catalyst, the noble and/or non-noble nanoparticles supported on reduced graphene oxide (rGO) prepared mainly by the microwave-assisted technique. The method brings notable advantages such as low cost, simplicity, short reaction time and overall high productivity in comparison to SoA chemical methods.

This paper assumea comprehensive testing according to the protocols established by the US Department of Energy (the PEM FC industry standard) in our dedicated facilities. Following *ex situ* electrochemical measurements, *in situ* measurements will be carried out in a dedicated PEM FC system with active area of 25 cm^2. The strong dependence to the operation conditions makes sense to include the anticipated degradation as mandatory durability test. Several configurations including developed cathodes will be taken into consideration. Experimental tests will evaluate: the behavior in repeated on/off cycles, the transitory response at various charge levels, functionality at temperatures between 40 and 80 ℃, and the response function for flow and pressure modifications for hydrogen and air supply.

CONCLUSION

The graphenic materials yielded by both microwave and chemical methods are tested and optimized for use as FC components. These can potentially replace the time-consuming and costly methods that currently dominate the industrial manufacturing of nanocarbonic materials for FC components, offering a competitive advantage to the national initiative in hydrogen economy.

REFERENCES

1. A. Marinoiu et. al, Appl Surf Sci. 504, 144511 (2020)

ACKNOWLEDGMENTS

This work was carried out through the Nucleus Program, financed by the Ministry of Education and Research, Romania, project no. PN 23 15 01 03 and project number PN-III-P2-2.1-PED2021-0840 PED 695/202

Green Synthesis of Nd-doped ZnO @ N-doped g-C_3N_4 Nanohybrid for Photocatalytic Degradation of Pharmaceutical Pollutant

Seyed Ali Zargar[1], Mitra Gharivi[1], Omid Bagheri[1], and Adrine Malek Khachatourian[1*]

[1]Department of Materials Science and Engineering, Sharif University of Technology, Tehran, Iran
***Presenting & Corresponding author Email:** khachatourian@sharif.edu

INTRODUCTION

Zinc oxide (ZnO) is a versatile semiconductor known for its excellent optical properties and high photo-redox capability [1]. Furthermore, combining π-conjugative materials such as g-C_3N_4 with ZnO can effectively reduce its band gap and enhance the overall performance [2]. The novel Nitrogen-doped g-C_3N_4 (NCN) / Neodymium-doped ZnO (ZnO:Nd) Z-scheme heterojunction was eco-friendly fabricated, and its photocatalytic ability was evaluated toward tetracycline antibiotic.

EXPERIMENTAL/THEORETICAL STUDY

ZnO:Nd nanoparticles were synthesized using a precipitation method using pomegranate peel extract (PPE). For NCN fabrication, urea and pomegranate peel fine powder were heated in a muffle furnace at 550°C. For NCN/ ZnO:Nd nanohybrid (NZ) fabrication, the synthesized powders were mixed physically by bath-sonication. After that, the suspension was washed with Ethanol and freeze-dried.

RESULTS AND DISCUSSION

Various characterization techniques confirmed the successful fabrication of NZ catalysts. The Field emission scanning electron microscopy (FESEM) and transmission electron microscopy (TEM) micrographs reveal that ZnO:Nd nanoparticles are tightly anchored onto the porous NCN matrix, forming a robust Z-scheme heterojunction. The photocurrent results imply that the NZ sample generates a greater number of photogenerated carriers due to its enhanced charge transfer efficiency and light utilization. Therefore, the NZ photocatalyst exhibits superior degradation of tetracycline as a common pharmaceutical pollutant.

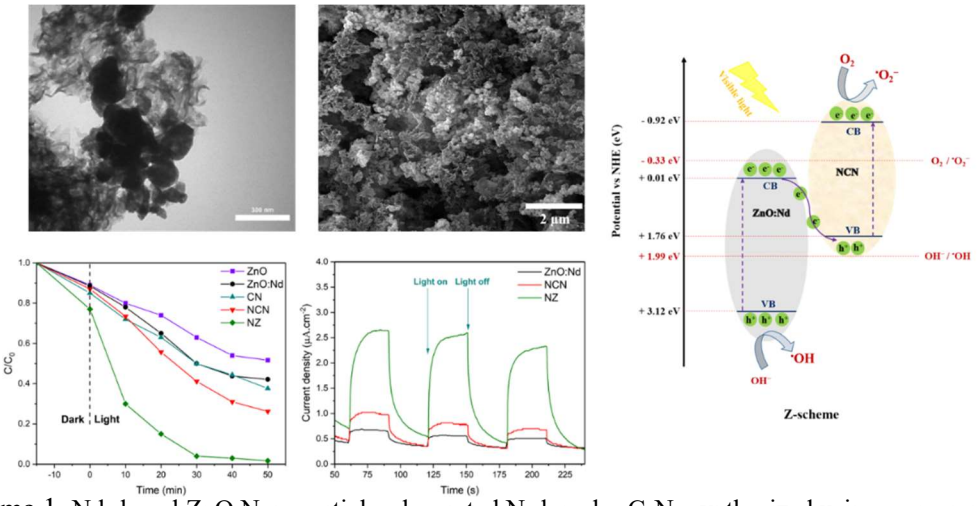

Scheme 1. Nd-doped ZnO Nanoparticles decorated N-doped g-C_3N_4 synthesized using a green route.

CONCLUSION

This work affords a rational method to construct a Z-scheme heterostructure, fulfilling the criteria of environmentally friendly and sustainable chemistry to perform well for wastewater pollutants degradation.

REFERENCES

[1] Manikandan, A., et al., *Rare earth element (REE) lanthanum doped zinc oxide (La: ZnO) nanomaterials: synthesis structural optical and antibacterial studies.* J. Alloys Compd., 2017. **723**: p. 1155-1161.

[2] Luu Thi, L.A., et al., *In situ g-C3N4@ Zno nanocomposite: one-pot hydrothermal synthesis and photocatalytic performance under visible light irradiation.* Adv. Mater. Sci. Eng., 2021. **2021**: p. 1-10.

Potential of Graphene Oxide Laminates as Ion Exchange Membranes for electrochemical cells

A. Fernández-Sotillo [1], D. Botana[1,2], A. Fuerte[1], S. Cavaliere[3] and P. Ferreira-Aparicio* [1]
[1] Department of Energy/CIEMAT, Spain. *Corresponding author (paloma.ferreira@ciemat.es)
[2] Escuela Técnica de Ingeniería Industrial/Universidad Politécnica de Madrid (UPM), Spain.
[3] ICGM, Univ. Montpellier, CNRS, ENSCM, 34095 Montpellier cedex 5, France.

INTRODUCTION

Graphene materials are recently finding very interesting applications in innumerable technological fields as result of their particular physico-chemical properties. Membrane technology is one of these fields of interest[1], in particular for graphene oxide (GO) and reduced graphene oxide (rGO). GO membranes have been reported to allow selective transport of ions, whereas they can be leak-tight to gases.[2] In this study, the proton transport properties of GO laminates have been evaluated and are presented together with their morphological and physicochemical characterization, including their mechanical resistance. Their potential to be used as membranes in electrochemical cells for hydrogen conversion is discussed.

EXPERIMENTAL STUDY

GO films of different thicknesses have been prepared in the range between 5 and 30 microns to evaluate their characteristics and properties as ion exchange membranes for electrochemical cells. Different techniques have been applied for their characterization. Measurements of mechanical resistance and hydrogen permeation tests at different temperatures and values of relative humidity have been performed. SEM examination of GO laminates gives evidence of their internal structure. They have been tested as ion exchange membranes in electrochemical cells.

RESULTS AND DISCUSSION

The prepared laminates consist of stacked GO layers with a "mille-feuille"- like structure, as shown in Fig. 1. These sheets exhibit outstanding mechanical resistance even under high relative humidity at high temperature. Results of performance tests in cells are discussed at the light of the obtained characterization results.

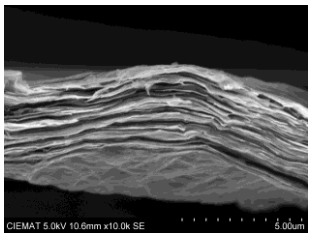

Fig. 1 SEM image of the cross-section of the GO laminates prepared.

CONCLUSION

The study provides evidences of the great potential of graphene oxide laminated to be applied as ion exchange membranes in electrochemical cells.

REFERENCES

1. R. Castro-Muñoz et al. Reviewing the recent developments of using graphene-based nanosized materials in membrane separations. Critical Reviews in Environmental Science and Technology 52(19) 3415-3452 (2022).
2. M. Zhang et al. Controllable ion transport by surface-charged graphene oxide membrane. Nat. Commun. 10, 1253 (2019).

ACKNOWLEDGMENTS

This study has been financed by MCIN/AEI/10.13039/501100011033 and NextGenerationEU"/PRTR funds under project TED2021-131972B-I00. Authors also acknowledge the Regional Government of Madrid and the MCIN of Spain for financing the GREENH2CM project through the Recuperation and Resilience Mechanism with NextGenerationEU funds (PRTR-C17.I1). AFS acknowledges the France Embassy in Spain for funding to support the research collaboration between CIEMAT and the UMR 5253 CNRS-UM-ENSCM in Montpellier (France).

Preliminary Economic Feasibility Study for Graphene Synthesis from King Grass at Laboratory Scale

Santiago Betancur [1]; Erasmo Arriola-Villaseñor [2]; Alba N. Ardila A.[3*,] Lucas Blandón-Naranjo[4]
[1, 2, 3, 4] Grupo de Investigación en Catálisis Ambiental y Energías Renovables, Facultad de Ciencias y Educación, Politécnico Colombiano Jaime Isaza Cadavid, Colombia. Corresponding author: anardila@elpoli.edu.co

INTRODUCTION

Research related to graphene has primarily focused on the study of synthesis methods and their application in the energy field. Based on our literature review, despite the extensive amount of research related to graphene, more than 200,000 studies since 2010 in the ScienceDirect database, we have not identified technical and economic studies that fully support these claims[1]. We propose an alternative microwave process for synthesizing graphene from cellulose King Grass biomass source as an economical raw material, which reduces process costs.

EXPERIMENTAL/THEORETICAL STUDY

Graphene was carried out on a laboratory scale based on one of the experimental procedures indicated in Patent ES2804948T3[2]. To do this, cellulose was first obtained by delignification of the biomass of King Grass grass and monthly production was planned considering 26 batches (including additional time for loading, unloading and cleaning equipment). In each batch, only 153 grams of King Grass were processed. The commercial values of the substances will be estimated based on different sources (Sigma-Aldrich and Merck, various websites, among others).

RESULTS AND DISCUSSION

Spectra of the materials show a pronounced UV absorption band at 270 nm assigned to the sp2 hybridization of the C=C bonds of graphene. In addition, Raman spectra include the G peak around 1580 cm-1 and the 2D peak around 2700 cm^{-1}. These peaks are attributed to the in-plane vibrations of sp2 carbon atoms and second-order zone boundary phonons, respectively. The presence of the D peak at 1336 cm^{-1} is indicative of first-order zone boundary phonons, suggesting the existence of defects or edge effects in the graphene. Technical-economic analysis highlights in its three profitability parameters (Net Present Value: NPV, Internal Rate of Return: IRR, Benefit-Cost Ratio) that the benefits are greater than the costs, where the income is sufficient to cover the expenses of the project, thus generating economic profits.

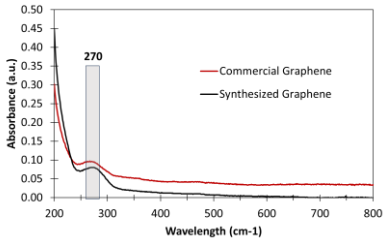

Figure 1. UV-vis absorption spectra of commercial and synthesized graphene.

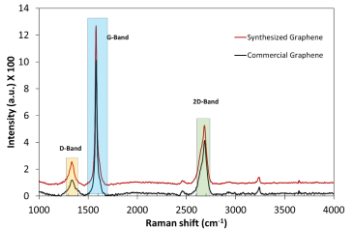

Figure 2. Raman spectra of commercial and synthesized graphene.

Table 2. Results of the economic prefeasibility study (Thousands of dollars).

Item	Value
Initial investment	154.4 USD
Depreciation	4.8 USD
Salvage Value	46.7 USD
NPV	2836.4
IRR	421.5 %
Benefit/Cost ratio	37.74

Table 1. Income and Investments during the useful life of the project (Thousands of dollars).

Period	2023	2024	2025	2026	2027	2028	2029	2030	2031	2032
Sales	583.96	604.4	625.3	647.3	670.1	693.3	717.6	742.9	768.7	795.5
investment	126	131.6	138	144.6	151.5	158.7	166.4	174.3	182.7	180.2

CONCLUSION

The results demonstrate that obtaining graphene from King Grass waste on a laboratory scale is technically and economically viable under current conditions, as revenues exceed expenses. Therefore, it is necessary to thoroughly analyze the possibility of implementing this production system on a pilot or industrial scale, as there is a business opportunity that would make future investment in graphene production attractive.

REFERENCES

1. M. Athanasiou et al. Chem. Eng. J. 446 (2022) 137191.
2. L. Wang et al. ES patent ES2804948T3, 2021.

ACKNOWLEDGMENTS

The authors would like to thank the Politécnico Colombiano Jaime Isaza Cadavid for funding the research projects titled "Desarrollo de sensores electroquímicos basados en nanopartículas metálicas soportadas sobre materiales carbonáceos para la detección de mercurio en matrices líquidas". (AGM) Advanced Graphene Materials.

SPEND BATTERIES VALORIZATION FOR OBTAINING GRAPHENE BY EXFOLIATION IN THE LIQUID PHASE

Erasmo Arriola-Villaseñor [1]; Santiago Bedoya Betancur [2]; Alba N. Ardila A[3]; Luz M. Ocampo-Carmona [4]; José Manuel Romo Herrera [5]; Trino A. Zepeda Partida [6], Sergio A. Gómez[7], Gustavo A. Zurita [8]*

[1,2,3] Research Group on Environmental Catalysis and Renewable Energies, Politécnico Colombiano Jaime Isaza Cadavid, Medellín-Colombia. Corresponding author *anardila@elpoli.edu.co

[4] Facultad de Minas, Universidad Nacional de Colombia Sede Medellín, Medellín Colombia

[5,6] Centro de Nanociencias y Nanotecnología CNyN-UNAM, Ensenada Baja California-México.

[7,8] Universidad Autónoma Metropolitana Iztapalapa, México

INTRODUCTION

In recent years, innovative methods have emerged focused on the use of solvents and ultrasound, with the aim of reducing production costs and using more environmentally friendly raw materials. In general, this scientific research shows that, although graphene is obtained by this method, both the yields for obtaining graphene and its concentration continue to be very low, which shows that to date there is a significant deficiency in the different studies carried out, which lies in the lack of information on the yields obtained in the graphene synthesis process. This information gap extends from the pretreatment of the raw material to the final phase of material synthesis.

EXPERIMENTAL/THEORETICAL STUDY

Graphene was obtained through the exfoliation technique (from graphite carbon previously extracted from BIL) in the liquid phase, assisted by focused ultrasound using deionized water as a solvent.

RESULTS AND DISCUSSION

UV-Vis spectra of all materials showed a band at 265 nm assigned to the sp2 hybridization of the C=C bonds of graphene. Furthermore, the Raman spectra and the I_{2D}/I_G and I_D/I_G ratios confirm the obtaining of multilayer graphene. However, the yields obtained for both the decanted material and that dispersed, demonstrate that graphene of different qualities is produced in both portions of the material, which suggests a separation of both materials for their respective applications. Furthermore, dispersed materials always reveal greater surface area.

Table 1. Physicochemical properties of raw materials, commercial materials and graphene obtained.

No.	Code	BET Surface Area (m^2/g)	Average Pore Volume BJH (cm^3/g)	Average Pore Diameter (nm)	Yield (%)	Graphene Concentration (mg/mL)	I_{2D}/I_G	I_D/I_G
1	Gf-C	2.11	0.008	15.45	-	-	0.66	0.60
2	GPi-Samsung	5.74	0.024	18.89	-	-	0.70	0.67
3	GPi-Nokia	5.13	0.036	22.35	-	-	0.68	0.65
4	Gn-C	49.05	0.096	11.97	-	-	0.66	0.46
5	Gn-S5-2h-De	5.01	0.021	22.53	94.74	0.751	0.53	0.18
6	Gn-S5-2h-Di	14.39	0.060	22.85	5.26	0.435	0.46	0.46
7	Gn-S8-2h-De	4.81	0.020	23.09	93.01	1.503	0.48	0.19
8	Gn-S8-2h-Di	14.75	0.060	17.63	6.99	1.232	0.51	0.32
9	Gn-P7-S5-2h-De	6.44	0.032	21.41	95.04	0.203	0.15	0.21
10	Gn-P7-S5-2h-Di	-	-	-	4.96	0.102	0.42	0.29
11	Gn-P7-S8-2h-De	8.21	0.036	18.88	94.58	0.203	0.22	0.16
12	Gn-P7-S8-2h-Di	-	-	-	5.42	0.102	0.42	0.24
13	Gc-S5-2h-De	3.18	0.010	24.75	95.54	0.430	0.44	0.08
14	Gc-S5-2h-Di	6.97	0.030	38.00	4.46	0.231	0.52	0.15
15	Gc-S8-2h-De	2.06	0.005	39.73	94.24	0.986	0.51	0.13
16	Gc-S8-2h-Di	3.39	0.020	37.56	5.76	0.743	0.63	0.18

CONCLUSION

This work demonstrates that it is possible to valorize the anodic graphitic material waste from spend Li-Ion batteries (BIL) as inputs to obtain multilayer graphene carbonaceous materials to be used in different applications by exfoliation in the liquid phase; a simple, economical and environmentally friendly method.

REFERENCES

1. A. Torkaman-Asadi et al. Comput. Mater. Sci. 210 (2022) 111457.

2. M. Athanasiou et al. Chem. Eng. J. 446 (2022) 137191.

ACKNOWLEDGMENTS

This research was possible thanks to the financing of Minciencias, the National University of Colombia, the Jaime Isaza Cadavid Colombian Polytechnic and the Center for Nanoscience and Nanotechnology. (AGM) Advanced Graphene Materials.

Computational Simulations of the Hydrogen and Methane Storage Capacities on novel JLU MOFs at Room Temperature

Alejandra Granja-DelRío and Iván Cabria

Departamento de Física Teórica, Atómica y Óptica, Universidad de Valladolid, Valladolid, Spain

email: ivan.cabria@uva.es

INTRODUCTION

In recent times, the escalation of global warming threats stemming from fossil fuel consumption has become more pronounced. A crucial technological advancement lies in effectively storing hydrogen and methane to enhance their utilization in electric vehicles fueled by these gases. Hydrogen Fuel Cell Electric Vehicles (HFCEV) offer a carbon dioxide-free alternative, while Natural Gas Vehicles (NGV) aid in diminishing greenhouse gas emissions. The primary challenge is the quest for lightweight solid materials capable of storing hydrogen and methane gases, thereby achieving comparable autonomy to traditional fossil-fuel vehicles. MOFs (Metal-Organic Frameworks) are a large group of light solid porous materials with many technological applications, including gas storage.

THEORETICAL STUDY

Researchers from the Jilin University synthesized recently novel JLU MOFs [1]. GCMC (Grand Canonical Monte Carlo) simulations have been carried out at room temperature and pressures from 0.5 to 35 MPa to assess the hydrogen and methane storage capacities, along with isosteric heats, porosities, densities and pore radii, of two of those novel JLU MOFs, namely JLU-MOF120 (Bi based) and JLU-MOF121 (In based). GCMC simulations were also performed under identical conditions for different groups of MOFs: classical, rest-JLU (the rest of JLU MOFs) and MOFs with similar carbon/metal ratio.

RESULTS AND DISCUSSION

The simulations uncovered that these two newly developed MOFs showcase similar storage capabilities for hydrogen and methane at ambient temperature across pressures from 0.5 to 35 MPa. Particularly noteworthy is their performance at pressures between 25 and 35 MPa, which stands on par with top classical MOFs and other JLU MOFs, even surpassing capacities seen in MOFs incorporating Bi, In, P, Sb, and Al. However, it's essential to highlight that the best classical and rest-JLU MOFs still exhibit superior gravimetric and volumetric capacities for both hydrogen and methane compared to the two JLU-MOFs under scrutiny. Specifically, at 298.15 K and 25 MPa, the JLU MOFs demonstrate usable gravimetric and volumetric hydrogen storage capacities of roughly 2.3 wt.% and 0.015 kg/L, respectively. For usable methane storage at room temperature and 25 MPa, the JLU-MOFs showcase gravimetric and volumetric capacities ranging from 20 to 22 wt.% and from 0.16 to 0.18 kg/L, respectively. The results consistently show that these capabilities are not influenced by the particular type of metal atom involved. Additionally, they illustrate a reverse relationship with density, yet a direct association with porosity and pore size. The storage capabilities of the two studied JLU MOFs are credited to their significant porosity, low density, and relatively wide pores.

ACKNOWLEDGMENTS

This work was supported under MINECO research projects from Spain (Grants PGC2018-093745-B-I00).

REFERENCES

[1] Y. Zhu, J. Cai, L. Xu, G. Li and Y. Liu, Inorg. Chem. 61, 10957-64 (2022)

Partial reduction of $La_{0.6}Sr_{0.4}Co_{0.2}Fe_{0.8}O_{3\pm\delta}$ perovskite shaped as RPC structure for maximizing green H_2 production by thermochemical H_2O splitting

I. Brigidiano[1], A. Pérez[1], E. Díaz[1], M. Orfila[1], M. Linares[1], R. Sanz[1,2], J. Marugán[1,2], R. Molina[1], J.A. Botas[1,2]

[1]Chemical an Environmental Engineering Group, Rey Juan Carlos University,

[2]Instituto de Investigación de Tecnologías para la Sostenibilidad, c/ Tulipán s/n, 28933 Móstoles, Spain

alejandro.perezd@urjc.es

INTRODUCTION

Renewable hydrogen (H_2) is postulated as a key solution for the decarbonization of the economy and the reduction of dependence on fossil fuels. H_2 can be obtained by solar-driven thermochemical water splitting, which is less developed than electrolysis but also ensures obtaining green H_2 from H_2O, using renewable energy and with zero CO_2 emissions [1]. In a two-step thermochemical cycle, a metal oxide is thermally reduced at high temperature (usually higher than 1200-1300 °C), releasing O_2, and then it is reoxidized with H_2O vapor (< 1000 °C), producing H_2 and recovering the starting material. A considerable number of metal oxides have been explored in the literature looking for decreasing the temperature required for the reduction step. Among them, perovskites ($ABO_{3\pm\delta}$) have been proposed as a potential alternative reaching considerable results at reduction temperatures < 1100 °C [2]. Additionally, a proper integration with concentrated solar devices is necessary for furthermore realistic scale application, developing manufacture methods for macroscopic structures for their use in solarised reactors under real operating conditions [2]. Consequently, in this work, the H_2 and O_2 production curves of $La_{0.6}Sr_{0.4}Co_{0.2}Fe_{0.8}O_{3\pm\delta}$ perovskite shaped into RPC (Reticulated Porous Ceramic) macroscopic structures were evaluated for optimize the H_2 production by thermochemical H_2O splitting at moderate temperature.

EXPERIMENTAL/THEORETICAL STUDY

The perovskite $La_{0.6}Sr_{0.4}Co_{0.2}Fe_{0.8}O_{3\pm\delta}$ was synthesized by reactive grinding using a planetary ball milling (PM-100, Retsch) and then characterized by XRD, ICP-AES, TGA and SEM to confirm the perovskite structure. The RPC was prepared following the replica method described elsewhere for other metallic oxides [3], but optimizing the preparation steps (slurry composition, impregnation, and calcination) for this perovskite. The activity of the RPC structure was evaluated in an experimental system with a high temperature tubular furnace operating isothermally at 1000 °C for both reduction and oxidation steps and coupled to a gas analyzer to measure the amount of O_2 and H_2 produced during the thermochemical cycle.

RESULTS AND DISCUSSION

Complete reduction and reoxidation of the RPC at 1000 °C allow obtaining a H_2 production of 16.00 ± 0.03 cm^3 STP/$g_{material}$ in a complete cycle of 143 min (average production rate of 0.112 ± 0.03 cm^3 STP/$g_{material}$·min along the cycle). However, the final part of reduction and oxidation is slower than each initial step. Consequently, a thorough evaluation of the H_2 and O_2 production rate reveals that a partial thermal reduction of 75 % (instead of 100 %) followed by oxidation, theoretically maintains a remarkable production of 12.97 ± 0.06 cm^3 H_2 STP/$g_{material}$, but decreasing the total time required for the cycle from 143 to 67 min (0.194 ± 0.02 cm^3 STP/$g_{material}$·min). This result was experimentally corroborated, obtaining a hydrogen production of 12.35 ± 0.05 cm^3 STP/$g_{material}$ and a production rate of 0.182 ± 0.02 cm^3 STP/$g_{material}$·min, that were maintained during several consecutive cycles.

CONCLUSION

A proper control of the reduction step degree allows it to be carried out up to a partial extension of 75 % which allows to obtain in the subsequent reoxidation step a H_2 production rate 62.5 % higher than imposing a complete reduction step during the thermochemical water splitting. These results are the first step for conceptual design, analysis, and optimization of operation conditions of solar plants for H_2 production by thermochemical water splitting.

REFERENCES

[1] I. Dincer, Int. J. Hydrogen Energy, 40, 11094-1111 (2014).

[2] C. Muhich et al., J. Mater. Chem. A, 5, 15578-15590 (2017).

[3] M. Orfila et al., Int. J. Hydrogen Energy, 46, 17458-17471 (2021).

ACKNOWLEDGMENTS

The authors thank MCIN/AEI/10.13039/501100011033 and European Union "NextGenerationEU"/PRTR for financial support through RHYDROGENALTES (TED2021-132540B-I00) project, and "Comunidad de Madrid" and Rey Juan Carlos University for their financial support to ONEHYDRO Young Researchers R&D Project (M-2733).

The nanostructured GaN template sputtered with thin metal film: new SERS DNA biosensor for detecting mutations in real clinical samples

Aleksandra Michałowska [1*], Agata Kowalczyk [1], Jan L. Weyher [2], Anna M. Nowicka [1] and Andrzej Kudelski [1]

[1*] Faculty of Chemistry, University of Warsaw, Poland, a.michalowska10@uw.edu.pl

[2] Institute of High Pressure Physics of the Polish Academy of Science, Poland

INTRODUCTION

An early and accurate diagnosis of a specific DNA mutations has a decisive role for effective treatment. Especially, when an immediate decision on treatment most needs to be made, the rapid and precise confirmation of clinical findings is vital. One of the methods allowing for quick identification of biomolecules is SERS spectroscopy. In SERS spectroscopy, the efficiency of the generation of Raman signal increases by many orders of magnitude for molecules located close to the plasmonic systems (known as SERS substrates). In some cases, the efficiency of the Raman signal generation is so large that it is possible to obtain a good quality Raman spectrum of a single molecule. An important aspect when conducting research with this technique is the amplification of the signal with appropriately selected material. Currently, the dominant method of producing nanomaterials for medical analytical SERS measurements is to create a repetitively nanostructured surface from a non-metallic material (e.g. GaN or Si) and then spray a layer of the plasmonic metal onto the resulting substrate. In this work, we highlighted the innovative use of Surface Enhanced Raman Scattering (SERS) as a technique for DNA identification, focusing specifically on our novel SERS-based DNA biosensor for the detection of mutations in real clinical samples.[1]

EXPERIMENTAL/THEORETICAL STUDY

The main techniques used to carry out these studies were scanning electron microscopy (SEM), utilized for the structural characterization of the substrate. The performance of the constructed DNA sensor was monitored using surface-enhanced Raman spectroscopy.

RESULTS AND DISCUSSION

The proposed bioactive platforms were based on nanostructured GaN substrates, obtained using photoetching process, and sputtered with different plasmonic metal films. The discussion focuses on the versatility of constructed SERS DNA biosensor in detecting genetic mutations, emphasizing its potential in identifying diverse mutation types with high sensitivity. The identification mechanism in the developed SERS DNA sensor relies on the conformational change (from gauche to trans) of 6-mercaptohexan-1-ol chemisorbed onto nanostructured surfaces. These alterations occur after the hybridization in the presence of the target DNA within the analyzed sample. To evaluate the effectiveness of the novel sensor, we examined different mutation variants in the BRCA1 genes, which causes the increased risk of developing breast cancer. In our study, we used DNA sequences representing fragments of the BRCA1 gene, specifically focusing on pathogenic variants that are prevalent in the population of Poland. During the experiments, we assessed the selectivity of the assay for mutations beyond the specific one targeted by the probe DNA. Additionally, we examined the assay's selectivity in a mixture containing both mutated and non-mutated strands. Furthermore, we also discuss the challenges and future prospects associated with implementing SERS DNA biosensor in clinical diagnostics.

CONCLUSION

In conclusion, our investigation centered on bioactive platforms built upon nanostructured GaN substrates with various plasmonic metal films and underscore the significant influence of the nanostructured surface for efficacity of SERS DNA sensor.

REFERENCES

1. A. Michałowska et. al, RSC Adv., 12, 35192-35198 (2022)

ACKNOWLEDGMENTS

This work was financed by the National Science Centre, Poland, project no. 2019/35/B/ST4/02752.

Production and properties of MoS_2 and WS_2 mesoporous layers

Artem B. Loginov, Valentina A. Eremina, Petr A. Obraztsov, Alexander N. Obraztsov
University of Eastern Finland, Joensuu, Finland

Two-dimensional transition metal dichalcogenides (TMD) attract attention, in particular, due to their properties prospective for numerous applications. A chemical vapor deposition (CVD) is used in this work for production of coatings consisting of tiny flake-like crystallites oriented perpendicular to substrate surface and forming mesoporous layer. The gaseous H_2S and metal (Mo and W) vapor are used as precursors for the CVD synthesis on substrates of different types, including Si and SiO_2/Si, quartz, mica, Al_2O_3 ceramic and other. Atomic structure and morphology of the layers are investigated with scanning and transmission electron microscopy. The typical SEM image of the CVD layer is presented in Fig. 1. HRTEM imaging indicates presence of 1 to 10 single layers in the flakes.

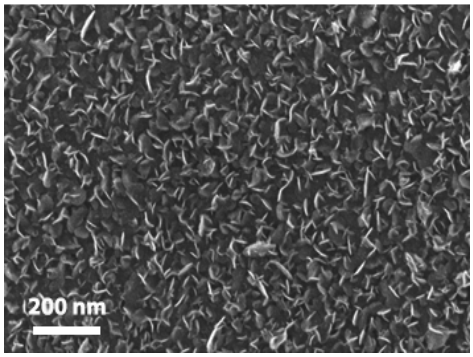

Fig. 1 Typical SEM image of the mesoporous MoS2 layer produced with CVD and consisting of flaky crystallites oriented perpendicular substrate surface.

The samples of the CVD grown layers are characterized with Raman, optical absorption and photoluminescent spectroscopy. Electrical resistivity of the film materials is measured during deposition process. Fig. 2 shows dependence of photoluminescent spectra of MoS_2 and WS_2 deposits measured at for the samples obtained with different deposition process durations (for MoS_2) and different distances from source of evaporated metal to substrate (for WS_2). Material formation mechanism is proposed on basis of obtained results analysis.

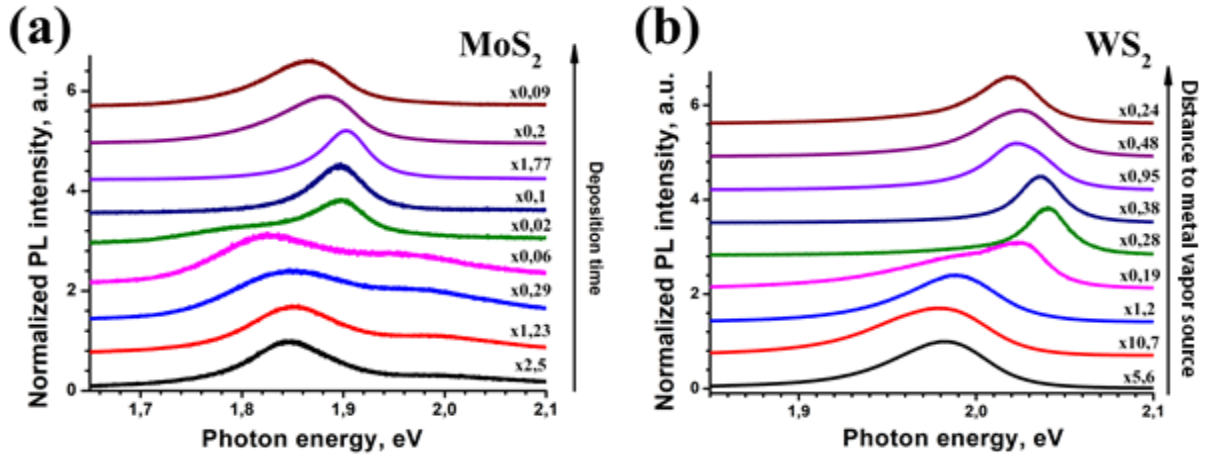

Fig. 2 A set of photoluminescent spectra of MoS_2 (a) and films at different deposition times (a); a set of photoluminescent spectra of WS_2 films at different distances between source of evaporated metal and substrate (b). The scaling factors given at each spectrum indicate ratio of the photoluminescent signal to Raman intensity.

Energy Storage, Photoeffect, and Coulomb Barrier Creation in Graphene and Alumina Nanocapacitors

Alexey Bezryadin, Eduard Ilin, and Irina Burkova
Department of Physics, University of Illinois at Urbana-Champaign, USA
(email: bezryadi@illinois.edu)

INTRODUCTION

Electronic properties of ultrathin dielectric films consistently attract much attention since they play important roles in various electronic devices, such as field effect transistors and memory elements. The dielectric strength of the insulating film limits how much energy can be stored in nanocapacitors. Mechanisms of the energy loss in the nanoscale-dielectric-layer capacitors are not yet well understood. If the leakage current can be reduced and the dielectric strength increased, then nanocapacitors could be used for energy storage. Our research shows that efficient energy storage is possible in nanocapacitor cooled to cryogenic temperatures.

EXPERIMENTAL/THEORETICAL STUDY

First, I will discuss optically transparent Al–Al2O3–graphene nanocapacitors suitable for studying electronic transport in calibrated nanoscale dielectric films under high electric fields and with light exposure. With this device we observe photon-assisted field emission effect, in which the effective barrier height is reduced by a quantity equal to the photon energy. Another finding is a reversed photoeffect.

RESULTS AND DISCUSSION

The main mechanism of energy loss in capacitors with nanoscale dielectric films is leakage currents. Using the example of Al–Al2O3–Al nanocapacitors, we show that there are two main contributions, namely the cold field emission effect and the hopping conductivity through the dielectric. We demonstrate that a significant amount of energy can be stored in the dielectric layer at low temperature, at which hopping conductivity is negligible. Our main finding is that high electric field, ~0.6–0.7 GV/m, causes electrons to penetrate the dielectric and can be used to store energy in the dielectric and, also, to create Coulomb barrier for charge leakage.

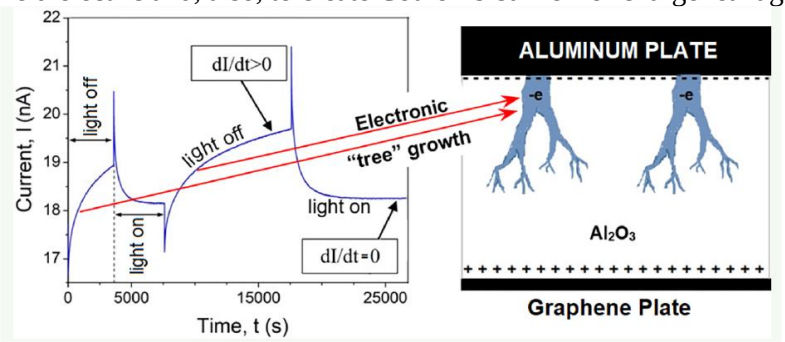

Fig.1 (left) Effect of light exposure on the leakage current. (right) Penetration of charges into alumina.

CONCLUSION

The dielectric strength (breakdown electric field) can increase dramatically if the dielectric layer thickness is reduced to a few nanometers. Hopping conductivity is drastically reduced at cryogenic temperatures. Thus, the leakage current becomes undetectable (practically zero). Charge and energy can be reliably stored in the dielectric nanometer-thick alumina films at liquid nitrogen temperature. The stored charge can be released and measured by increasing temperature.

REFERENCES

1. Reversed photoeffect in transparent graphene nanocapacitors, A. Belkin, E. Ilin, I Burkova, A. Bezryadin, ACS Applied Electronic Materials 1, 2671-2677 (2019).
2. Giant energy storage effect in nanolayer capacitors charged by the field emission tunneling, E. Ilin, I Burkova, E.V. Colla, M. Pak, A. Bezryadin, Nanotechnology 32 (15), 155401 (2021).
3. Coulomb barrier creation by means of electronic field emission in nanolayer capacitors, E. Ilin, I. Burkova, T. Draher, E.V. Colla, A. Hübler, A. Bezryadin, Nanoscale 12, 18761-18770 (2020).

Conjugated polymer nanoparticles for theranostic applications

Miao Zhao[1], Anton Uzunoff[1], Yi Wang[1], Philip Manning[2], Mark Green[1] and Aliaksandra Rakovich* [3*]
[1]Physics Department, King's College London, United Kingdom
[2]Translational and Clinical Research Institute, Newcastle University, United Kingdom
[3*] Physics Department, King's College London, United Kingdom, presenting and corresponding author.

INTRODUCTION

Conjugated polymer nanoparticles (CPN) represent a promising platform for biomedical applications of nanomaterials, particularly in the realm of theranostics, where they offer properties that allow simultaneous diagnostic imaging and optically-activated therapeutic interventions. However, their properties as theranostic probes depend strongly on their composition, fabrication and functionalization, with some aspects of these inter-relations not yet fully investigated[1,2]. This work aims to address some of these omissions.

EXPERIMENTAL/THEORETICAL STUDY

Several types of CPNs, consisting of three different conjugated polymer (CP) cores (PTB7, CN-PPV and MEH-PPV) and different shell materials (bare, PSMA, F127) were fabricated and characterized in terms of their physical, optical and photosensitizing properties. Samples were also tested in various cell lines (A549, HaCaR, HeLa and 3T3) to evaluate their potential as bioimaging and photodynamic therapy probes.

RESULTS AND DISCUSSION

CPNs of various compositions were produced using the nanoprecipitation method. The absorption and emissions properties were found to depend mostly on the CP in the core of the nanoparticle. However, the stabilizing shell of the CPN was found to modify these properties to a degree, corresponding to changes in the packing of the CP chains within the nanoparticles. The selection of shell material was found to have a profound impact on the photosensitizing properties of the CPNs, with PSMA shells often having a detrimental influence on the generation of reactive oxygen species, and the pluronic F127 shell having little or positive impact when compared to bare CPN particles. Furthermore, the stabilizing shell of the nanoparticles was found to strongly affect the attachment of the CPNs to cells, with PSMA shell yielding strong non-specific attachment. Contrary, stabilization of CPNs with pluronic F127 resulted in little non-specific attachment to cells, offering an opportunity for further functionalization of such particles for targeting applications.

CONCLUSION

In conclusion, this study highlights the critical role of composition and surface functionalization in modulating the properties of CPNs for theranostic applications. The choice of core CP and stabilizing shell material significantly influences the optical and photosensitizing properties as well as cellular interactions of CPNs. Specifically, while PSMA shells may compromise photosensitizing capabilities and induce non-specific cell attachment, pluronic F127 offers a promising avenue for minimizing non-specific interactions and facilitating targeted applications. These findings underscore the importance of tailored design strategies in optimizing CPN performance for enhanced theranostic.

REFERENCES

1. M. Zhao *et al.*, ACS Nano 15, 8790-8802 (2021)
2. M. Zhao, A. Uzunoff, M. Green, A. Rakovich, Nanomaterials (Basel), 13, 1543 (2023)

ACKNOWLEDGMENTS

The Authors acknowledge The Royal Society (RF\R\211023, RF\ERE210092, RF\ERE,231032) for funding this work.

Ultrafast charge carriers dynamics in gold nanocrystal superparticles

Cristian Gonzalez,[1] Shengsong Yang,[1] Emanuele Marino,[2] Fabrizio Messina,[2-3] Christopher B. Murray[1] and Alice Sciortino[2-3*]

[1] Department of Chemistry, University of Pennsylvania, Philadelphia, PA, USA

[2*]Dipartimento di Fisica e Chimica – Emilio Segrè, University of Palermo, Palermo, Italy

alice.sciortino02@unipa.it

[3] ATeN Center, University of Palermo, Palermo, Italy

INTRODUCTION

Plasmonic nanoparticles are attracting much interest in the recent literature [1]. Their optical properties have been intensively studied [2] by different experimental and theoretical techniques. Recently, superparticles obtained by the hierarchical assemblies of colloidal nanoparticles have shown great promise in transitioning materials from the nanoscale to the mesoscale, building artificial materials with new properties stemming from the crosstalk between constituent nanoparticles. [3] While significant advances have been made in the self-assembly of semiconductor nanoparticles [3] the fundamental photophysics which governs their optical response remains largely unclear. In particular, little information is available on the dynamics of photoexcited superparticles made from the ordered assembly of plasmonic nanoparticles.

EXPERIMENTAL STUDY

The study was mainly performed by transient absorption spectroscopy.

RESULTS AND DISCUSSION

We synthesized superparticles (SPs) with a size of about 200-300 nm (Fig1a) starting by the self-assembly of 5 nm gold nanoparticles (AuNps) by an oil-in-water emulsion template technique. During the synthesis, the environment conditions, and the length of the ligands between the nanoparticles have been changed.

The optical properties of the SPs were studied by steady state absorption spectroscopy and by transient absorption spectroscopy (TA) in order to reveal the difference between the isolated AuNps and the self-assembled SPs.

The absorption profile of SPs results broader than the isolated AuNps. Moreover, the TA signal depends on the assembly. The shape of the TA signal of the SPs is broader with respect to AuNPs. In addition to this, we also see differences in the charge carrier relaxation dynamics in the first 5-10 ps, where the relaxation of SPs is observed to be faster than isolated AuNps, as a consequence of the mutual interactions between individual nanoparticles.

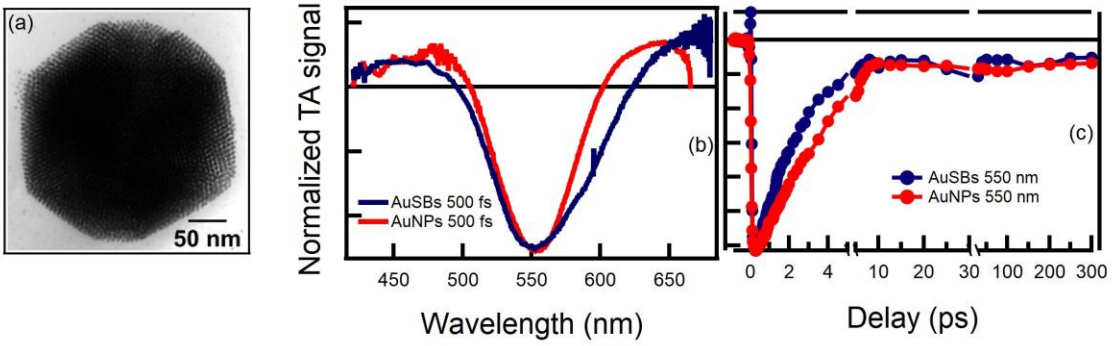

Fig. 1: (a) Normalized FTA spectra recorded after 500 fs from the photoexcitation of gold nanocrystals (red curve) and gold superparticles (blue curve). (b) Normalized FTA kinetics recorded at 550 nm of gold nanocrystals (red curve) and gold superparticles (blue curve).

CONCLUSION

We synthesized new gold nanocrystals superparticles with a size of 200-300 nm. By femtosecond analysis we discovered that the optical properties are regulated by the interactions between the single constituents rather than a simple sum of isolated AuNps contributions and, in particular, the assembly produces a faster recombination of the charge carriers.

REFERENCES

[1] Chem. Rev. 2020, 120, 2, 464–525.

[2] Adv. Funct. Mater. 2020, 30, 2005400.

[3] ACS Nano 2020, 14, 10, 13806–13815.

Mxene/Zirconium Silicate Membranes for PEM Fuel Cells Applications

Reeves Edwin [1], Amani Al-Othman [1]*, and Muhammad Tawalbeh[2]
[1]Department of Chemical and Biological Engineering, American University of Sharjah, UAE
[2] Sustainable and Renewable Energy Engineering Department, University of Sharjah, UAE

INTRODUCTION

Polymer electrolyte membranes, also known as proton exchange membrane fuel cells (PEMFCs), stand out as highly promising platforms for the generation of clean energy. PEMFCs are the most widely preferred fuel cell types due to their high-power density, zero noise pollution, quick startup, and all-solid structure. Currently, PEMFCs operate at temperatures less than 90°C. However, operating them at high temperatures is preferred as it offers a range of advantages, such as enhanced electrode kinetics, better water management, recovery of useful heat, use of less expensive fuels (such as hydrocarbons), and reduction in catalyst poisoning.

EXPERIMENTAL/THEORETICAL STUDY

In this study, an alternative proton-conducting material in lieu of Nafion has been examined. based on zirconium silicates (ZrSi) doped with Mxenes ($Ti_3C_2T_x$)[1,2] and ionic liquids, were utilized and investigated as composite membranes for PEMFCs. Electrochemical spectroscopy (EIS) was utilized to characterize the membranes, revealing encouraging enhancements in proton conductivity upon the incorporation of ILs and Mxenes.

RESULTS AND DISCUSSION

The unmodified ZrSi demonstrated a proton conductivity of $1.73x10^{-4}$S/cm. With the addition of Mxene, the conductivity increased to $4.75x10^{-3}$S/cm. Fig. 1 shows an-SEM analysis for the best conducting membranes presented in this work.

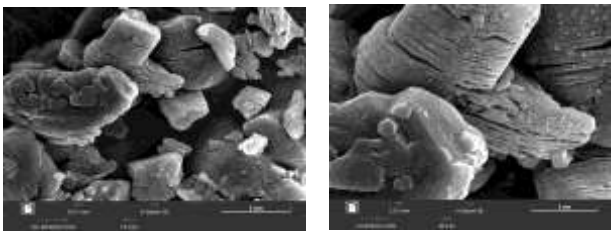

Fig. 1 Scanning electron microscope images for ZrSi/24wt%Mx/28wt%[BMIM][SCN] at magnifications of (e) 15920X, (f)40600X. The figure shows the unique structure of Mxenes. The particle size has changed with the addition of ionic liquids.

CONCLUSION

Composite membranes have been successfully prepared using MXenes and zirconium silicate for the first time. The preceding materials were modified using ionic liquids. A great enhancement in conductivity was observed. Conductivity enhancement can be attributed to the change in surface area.

REFERENCES

References must be numbered. Keep the same style.
1. V. Borysiuk and V. N. Mochalin, “Thermal stability of two-dimensional titanium carbides Tin+1Cn (MXenes) from classical molecular dynamics simulations,” *MRS Commun*, vol. 9, no. 1, pp. 203–208, Mar. 2019, doi: 10.1557/mrc.2019.2.
2. Y. Gogotsi and B. Anasori, “The Rise of MXenes,” *ACS Nano*, vol. 13, no. 8, pp. 8491–8494, Aug. 2019, doi: 10.1021/acsnano.9b06394

ACKNOWLEDGMENTS

The authors would like to acknowledge the financial support provided through AUS graduate program and Petrofac endowed chair funds .

ANM2022 (www.advanced-nanomaterials-conference.com) will host seven simultaneous conference sessions namely,
(ANM) Advanced Nano Materials
(AEM) Advanced Energy Materials
(AGM) Advanced Graphene Materials
(AMM) Advanced Magnetic Materials
(APM) Advanced Polymer Materials
(OLED) Organic Light Emitting Diodes
(HE) Hydrogen Energy
(SEM) Solar Energy Materials

Tungsten trioxide (WO_3)/Graphene-hybrid Membranes for PEM Fuel Cells Applications

Wessam Nimir [1], Amani Al-Othman [1]*, and Muhammad Tawalbeh[2]
[1]Department of Chemical and Biological Engineering, American University of Sharjah, UAE
[2] Sustainable and Renewable Energy Engineering Department, University of Sharjah, UAE

INTRODUCTION

Fuel cells represent a groundbreaking technology for clean and efficient energy solutions. Among the various types of fuel cells, Proton Exchange Membrane Fuel Cells (PEMFCs) stand out for their exceptional performance and versatility. PEMFCs operate by converting chemical energy directly into electrical energy through electrochemical reactions, utilizing a polymer electrolyte membrane as the core component. This membrane is crucial for facilitating proton transport and maintaining gas separation, ensuring high energy conversion efficiency[1,2]. In this study, a hybrid material comprising WO_3, and graphene was employed, with PVDF serving as a supporting matrix for high-temperature PEM-fuel cell usage.

EXPERIMENTAL/THEORETICAL STUDY

Two mixtures were prepared. The first one was a 10 wt.% PVDF/DMSO solution. It was prepared by blending PVDF and DMSO for 2 hours at 120℃. The second one was a WO_3/graphene/DMSO mixture. Varying amounts of WO3/graphene, ranging from 5 wt.% to 15 wt.%, were blended with DMSO. After that, the two mixtures were mixed at room temperature for around 10 minutes. Finally, the solution was cast onto a glass petri dish and dried in the oven for 5 hours at 70℃. The synthesized membranes were then peeled off and stored in plastic zipper bags for further characterization.

RESULTS AND DISCUSSION

The unmodified PVDF/DMSO membrane exhibited a proton conductivity of 4 x 10^{-4} S/cm. However, the conductivity increased to 8 x 10^{-2} S/cm with the addition of 15 wt.% WO_3/graphene. Figure 1 presents the Nyquist plot for the PVDF/DMSO membrane with the optimal amount of WO_3/graphene added.

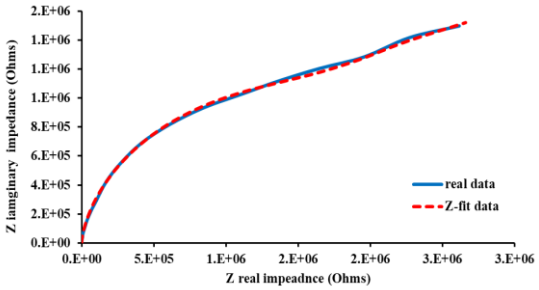

Figure. 1 Nyquist plot of 15 wt.% WO_3/graphene in PVDF/DMSO membrane.

CONCLUSION

Different mass percentages of WO_3/graphene were integrated into the PVDF/DMSO composite membranes for high-temperature fuel cell applications. The results revealed a significant enhancement in the proton conductivity by two orders of magnitude of the PVDF/DMSO membranes upon the addition of 15 wt.% WO_3/graphene hybrid material. This improvement is likely due to the increased proton transfer pathways.

REFERENCES

1. A. Selim et al., “Polymers. MDPI., 14(12):2492, (2022).
2. I Vázquez-Fernández et al., “Journal of Energy Chemistry., V (53), P: 197-207, (2021).

ACKNOWLEDGMENTS

The authors would like to acknowledge the financial support provided through AUS graduate program and Petrofac endowed chair funds.

Commented [wa1]: Dear professor, please modify this.

Catalytic Evaluation of Nickel Ceria Solid Solutions Prepared by Combustion Method for CO_2 Conversion by Dry Reforming of Methane

Parisa Ebrahimi, Mohammed Al-Marri, and Anand Kumar*
Department of Chemical Engineering, Qatar University, Doha, P O Box 2713, Qatar, presenting author
* Corresponding author (akumar@qu.edu.qa)

INTRODUCTION

There has been remarkable progress toward the development of green alternative energy sources due to an increase in energy demand and the rapid depletion of fossil fuels[1]. A dedicated approach to addressing these issues is dry reforming of methane (DRM), which involves converting carbon dioxide and methane into syngas[2]. Due to the use of methane and carbon dioxide in this process, it is a more environmentally friendly method of producing syngas than other approaches[3]. Ni-based catalysts have been extensively studied in the past decades since they are much cheaper and exhibit similar activity to noble metals. A major drawback of Ni catalysts is that they become inactive during DRM due to heavy carbon deposits[4]. However, coke formation can be highly affected by the choice of support and preparation method. The present study measured the activity, selectivity, and amount of carbon deposition during DRM on Ni/CeO_2 catalysts, calcined at different temperatures, as well as CeO_2, both synthesized and commercial, without an active metal.

EXPERIMENTAL/THEORETICAL STUDY

The solution combustion synthesis (SCS) method was used to prepare 1wt.% Ni catalyst supported on CeO_2 at a fuel-to-oxidizer ratio of 1:1 (φ=1). The resulting powders were calcined for 1 h at 400 °C, 600 °C and 800 °C and then reduced for 2 h at 600 °C with 50 SCCM of H_2 flow. The DRM was conducted in a tubular flow reactor with a CO_2/CH_4 ratio of 1 to 1 and N_2 as the carrier gas at temperatures ranging from 100 to 700 °C. Various techniques, such as XRD, TPR, SEM/EDX, and TEM, were used to examine the morphological properties and the effect of reaction, calcination and active metal on the catalysts' surface.

RESULTS AND DISCUSSION

Using the data obtained from the gas chromatograph (GC), the overall CO_2 and CH_4 conversion rate was calculated. According to the results, the 1 wt.%Ni/CeO_2 calcined at 800 °C had the highest CH_4 conversion rate, achieving nearly 89% conversion at 700 °C and negligible carbon deposition. A TPR study was also conducted to understand the dispersion of Ni sites, which is considered a considerable factor in catalytic performance of the Ni/CeO_2 catalysts.

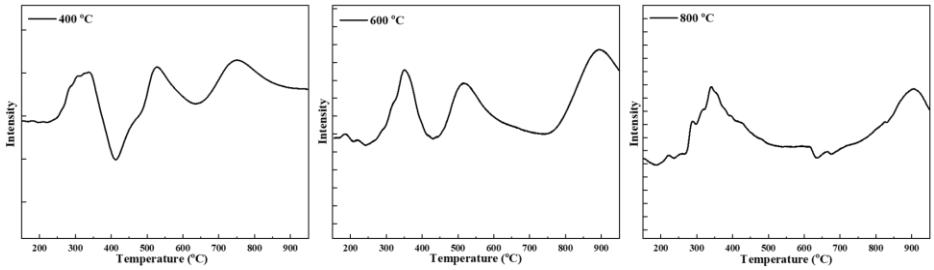

Fig. 1 H_2-TPR profiles of the 1wt.%Ni/CeO_2 catalysts at different calcination temperatures

CONCLUSION

According to TPR, catalyst reducibility changes with calcination temperature and it seems that the sample calcined at 800 °C goes through a phase transition as indicated by a broad peak in Fig. 1. On the other hand, considering both commercial and combustion-synthesized CeO_2, it is evident that combustion synthesis generates excess surface oxygen that can be readily reduced.

REFERENCES

References must be numbered. Keep the same style.

1. A. Kumar, Catalysts. 8(10), 481 (2018).
2. Y. H. Ahmad et. al, RSC Adv. 11(53), 33734-33743 (2021).
3. V. Danghyan et. al, Appl. Catal. B . 273, 119056 (2020).
4. Y. H. Ahmad et. al, Int. J. Hydrogen Energy. 47(97), 41294-41309 (2022).

Energy Decarbonisation through Direct-biogas Solid Oxide Fuel Cell and Microalgae Technology

Ousmane Wane[1], Ana A. Navarro[1], Rita X. Valenzuela[1], Beata Bochentyn[2], Araceli Fuerte[1]*
[1] Energy Department, CIEMAT, Madrid, Spain. Ousmane Wane (ousmane.wane@externos.ciemat.es)
[2] Advanced Materials Center, Gdańsk University of Technology, Gdańsk, Poland
*Corresponding author (araceli.fuerte@ciemat.es)

INTRODUCTION

The world energy strategy for the next decade is a shift towards efficient energy sources with a low carbon footprint and based on renewable energy sources to achieve sustainable development, avoiding greenhouse gas emissions and environmental damage which are leading to disquieting climate change. Solid Oxide Fuel Cells (SOFCs) can be considered as the most flexible energy converter in terms of fuel selection. In contrast with other types of fuel cells, SOFCs can use fossil and biogenic fuels[1]. Nevertheless, the use of hydrocarbon fuels entails the unavoidable formation of CO_2 in the anodic chamber that could be captured by microalgae bio-fixation.
In this context, the present work aims to evaluate the performance of a SOFC, provided of a novel impurity-tolerant ceria-based anode, directly fueled with algae biogas. The exhaust gas composition of the biogas fueled SOFCs has been analysed to quantify the CO_2 content and this data has been used to modelling its capture and recycling processes using microalgae. In the case of CO_2 capture by microalgae cultivated in a High Rate Algae Pond (HRAP)[2], it is useful to identify an optimal site for the implementation of this system and have advanced knowledge about the climate patterns in-situ.

EXPERIMENTAL/THEORETICAL STUDY

A $MCeO_2$/SDC/LSM single cell was galvanostatically operated at 1023 K for 862 h under humidified hydrogen and biogas. To quantify the concentration of CO_2 in the exhaust gas of the SOFCs, reactants and products were analysed on-line by gas chromatography. Numerical modelling and simulation applied to wastewater treatment (WWT) is a complementary tool to understand, a priori, the impact of meteorological parameters and others nutrients (substracts) such as carbon dioxide (CO_2) on productivity under limiting environmental conditions or even to guide decision-making to more relevant objectives. The Monod model was used to simulate the growth and biomass production of microalgae combined with the removal of nutrients present in wastewater and the capture of CO_2 from the SOFC enriched with air supplied in the batch culture medium.

RESULTS AND DISCUSSION

The capability of the novel impurity-tolerant ceria-based anode to operate in humidified algae biogas at 1023 K has been demonstrated. The maximum power density running on algae biogas was 74 mW/cm^2. The GC analysis shown that SOFC exhaust gas was composed by CH_4, CO_2, H_2 and CO; less than 2 mol. % of CO_2 was detected. After applying some criterious to select a suitable site to implement the system, a Typical Meteorological Sequence (TMS) for each climatic season of the year was determinated. The TMS and classical Monod[3] was used to modelize the metabolism of microalgae in the presence of nutrients in WWT.

CONCLUSION

Algae biogas is a good alternative fuel for SOFCs. The possibility to capture the CO_2, emitted by the operation of the direct-algae biogas SOFC, by biofixation using microalgae opens the opportunities to obtain an effective and non-polluting energy conversion system in the context of a circular economy.

REFERENCES

1. Zhang W et al., Adv. Energy Mater. 12 (2022) 47, 2202928.
2. Solimeno A., Parker L., Lundquist T., García J., Sci. Total Environ., 601–602 (2017) 646–657.
3. Eze V.C. et al., Algae Res. 32 (2018) 131-141.

ACKNOWLEDGMENTS

The authors acknowledge financial support from MCIN/AEI/10.13039/501100011033 and the European Union "NextGenerationEU"/PRTR (TED2021-130366B-I00), Gdańsk University of Technology (grant DEC-6/1/2022/IDUB/II.1a/Au) under the Aurum Supporting International Research Team Building programme and Programa Iberoamericano de Ciencia y Tecnología para el Desarrollo (CYTED) (RED RENUWAL 320rt0005).

Development of Low-cost Combinatory method for nanomaterial assembly and control

Ancin Maria Devis[1], Aliaksandra Rakovich[1*]

Department of Physics, King's College London, UK

Introduction

Organizing nanoparticles on surfaces in an ordered manner is crucial for their use as active components in functional devices[1]. However, patterning colloidal nanoparticles into a predefined structure with nanometre precision and scalability remains a significant challenge[2]. Our work presents a combinatory approach that is fast, reliable, and scalable to solve this issue by forming ordered patterning of nanomaterials on the substrate. We form a metallic nanostructure using nanosphere lithography as the master substrate and trap the nanoparticles above it using Dielectrophoretic. Here, the formation of the master substrate and a simulation study to demonstrate the trapping ability of the aforementioned method is presented.

Experimental and Theoretical study

The process of creating the master substrate involves two steps, as shown in Figure 1. Dielectrophoretic (DEP) traps use the interaction of dielectric particles with the medium in a non-uniform electric field to produce forces. The experimental setup for DEP trapping is a top-bottom electrode with 10 µm gap applied by an AC field. The master substrate, which is formed from NSL, serves as the bottom electrode while a plane ITO substrate is the top electrode (as shown in Figure 2). In the simulation study, the Maxwell Stress Tensor method (MST) is used to calculate the time-averaged DEP force acting on a spherical particle.

Results and Discussions

After analysing the simulation results, it was found that the gold triangle's corners are capable of trapping particles due to the stronger trapping force in that area. Also, according to the graph (Figure 2c & 2d) the trapping force magnitude increases with voltage. However, in Figure 2e, it is observed that only particles positioned very close to the gold nanotriangles can be trapped with the current experimental setup. Further research is required to ascertain how changes in the size of the triangle and the polymer can influence the trapping potential and force.

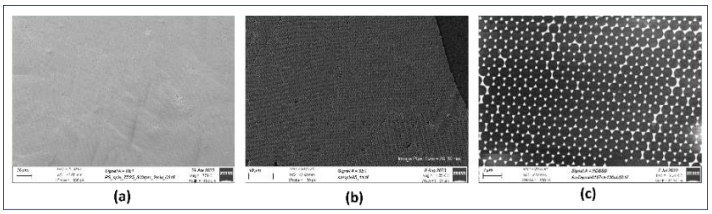

Figure 1: Formation of polymer mask using monodispersed colloidal polystyrene beads of size 600 nm using (a) drop casting (b) convective assembly (c) Hexagonal nanotriangles formed by the thermal evaporation of 40 nm gold over the substrate.

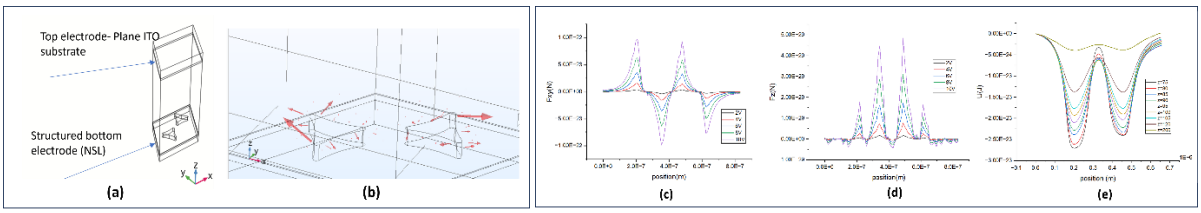

Figure 2: (a) Top-Bottom electrode model used for the simulation study (b) shows the direction and strength of the DEP trapping force on a spherical particle at z = 75 (10V, 1 MHz AC field) (c) and (d) shows the variation of force fxy (x-y plane) and fz force acting on the particles with voltage (d) Variation of potential energy with height of the particle from the surface of the substrate (10V, 1 MHz AC field).

Conclusion

A combinatory approach that is fast, reliable, and scalable by combining NSL and Dielectrophoresis to form ordered arrangement of nanoparticles is presented here.

Reference

[1] G. Petit et.al, Colloids and Interfaces **7**(1), (2023).
[2] X. Xing et.al, Nat Commun **11**(1), 1–8 (2020).

Hydrogen Production Using Al-4Mg-1Sn(-1Fe) [wt.%] Alloys: Influence of Microstructural Features and Insights for the Recycling of Al Alloys

Andre Barros (Barros) * [1*], Camila Konno (Konno) [2], Cássio Silva (Silva) [2], Andrei de Paula (de Paula) [2], Amauri Garcia (Garcia) [2], Noé Cheung (Cheung) [2]

[1*]Department of Manufacturing and Materials Engineering, University of Campinas, Brazil, presenting and corresponding author (a212042@dac.unicamp.br)

[2] Department of Manufacturing and Materials Engineering, University of Campinas, Brazil

INTRODUCTION

Hydrogen (H_2) production faces the challenge of developing cost-effective methods with low or zero carbon emissions[1]. In this context, the H_2 generated through the reaction of water with Al alloys emerges as a promising solution for portable applications, such as those supported by proton exchange membrane fuel cells[2]. However, to enhance the viability of this approach, recycled Al alloys are desirable, particularly when they no longer meet structural applications. Al-Mg-Sn alloys are practical structural materials[3], but after recycling, they contain an increased Fe content, which may limit their usage due to compromised mechanical behavior. Hence, the primary novelty of this work lies in evaluating the potential of these alloys for H_2 production, both before and after recycling. The main objective is to investigate the H_2 production behavior of the Al-4Mg-1Sn and Al-4Mg-1Sn-1Fe [wt.] alloys immersed in an alkaline medium, with a focus on the influence of microstructural characteristics.

EXPERIMENTAL STUDY

For both studied alloys, samples with various microstructural length scales were produced using a directional solidification technique. Next, a comprehensive microstructural characterization was carried out. H_2 evolution tests were conducted on small, thin samples (approximately 4x4x0.3 mm), weighing around 10 mg. These tests were based on a gravimetric approach [4], using a 2M NaOH solution.

RESULTS AND DISCUSSION

Fig. 1a illustrates the typical dendritic microstructure observed for the studied alloys. Fig. 1b and 1c show that the microstructural refinement accelerates the H_2 generation, particularly for the Fe-containing alloy. Fig. 1d demonstrates the positive effects of refined microstructures on average H_2 generation rates and H_2 yields.

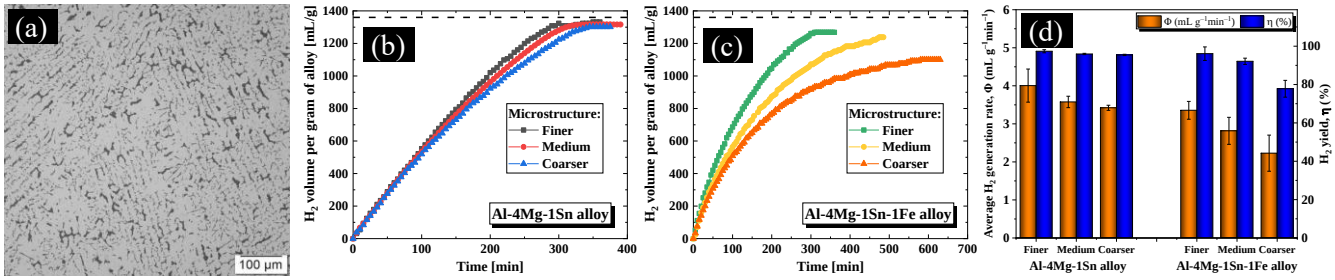

Fig. 1 – Characteristic finer microstructure (a), typical H_2 evolution curves (b and c), and (d) H_2 generation rate and yields.

CONCLUSION

The addition of 1wt.%Fe to the Al-4Mg-1Sn [wt.%] alloy increased the microstructural sensitivity of H_2 production characteristics reducing the average H_2 generation rate and H_2 yield. Microstructural refinement is shown to be favorable in mitigating this deleterious impact of Fe addition. These findings offer a direction to prevent the disposal of valuable Al alloys as waste, presenting an opportunity to leverage them for H_2 production.

REFERENCES

1. H. Ishaq et. al, Int. J. Hydrog. Energy 47, 26238-26264 (2022)
2. Y. Liu et. al, Int. J. Hydrog. Energy 42, 10943-10951 (2017)
3. B. Yang et. al, Mater. Sci. Eng. A 825, 141901 (2021)
4. M. Curioni, Electrochim. Acta 120, 284-292 (2014)

ACKNOWLEDGMENTS

Authors acknowledge FAPESP - São Paulo Research Foundation (Grants: 2021/11439-0; 2023/01422-8; 2023/12535-8).

Measuring Physical and Chemical Properties of Single Nanofibers – Possibilities and Limits

Tomasz Blachowicz [1] and Andrea Ehrmann [2]*
[1] Institute of Physics—Center for Science and Education, Silesian University of Technology, 44-100 Gliwice, Poland
[2] Institute for Technical Energy Systems (ITES), Bielefeld University of Applied Sciences and Arts, 33619 Bielefeld, Germany; andrea.ehrmann@hsbi.de

INTRODUCTION

Nanofibers can be produced by various techniques, such as a broad range of electrospinning techniques to produce nanofiber mats from different polymers or polymer blends, often filled with metallic or semiconducting nanoparticles, or by different nanotechnological bottom-up or top-down methods [1,2]. Usually, their physical or chemical parameters are measured by averaging over a fiber bundle or a part of a nanofiber mat [3].

LITERATURE STUDY

A literature review was performed, taking into account mainly studies published in the last five years, dealing with measuring different physical and chemical properties of single nanofibers, nanowires and nanotubes.

RESULTS AND DISCUSSION

Measurements of single nanofiber properties are more complicated than investigations of fiber bundles or whole nanofiber mats and thus less often found in the literature (Fig. 1). After a fast increase in such investigations between 2001 and 2009, the numbers of respective studies are now stagnating. This review thus aims at making the different possibilities more visible for a broader scientific audience by giving several examples, based on atomic force microscopy (AFM) and other broadly available techniques. The focus of this review is on technologies which reveal more information than the pure surface morphology of nanofibers or nanowires, such as tensile properties [4], thermal or electrical conductivity [5,6].

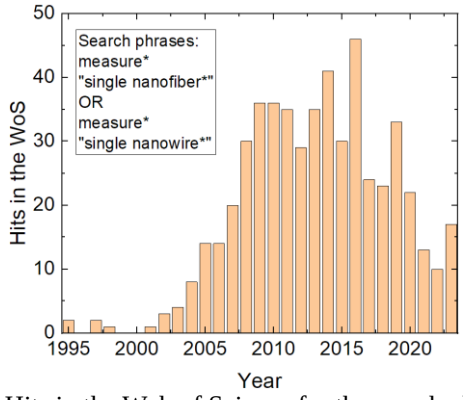

Fig. 1 Hits in the Web of Science for the search phrases given in the inset. Data taken on April 09, 2024.

CONCLUSION

This review gives an overview of different methods to test not only morphological, but also electrical, thermal, optical, chemical and other properties of single nanofibers, that have been reported in the last two decades.

REFERENCES

1. I. Alghoraibi, S. Alomari. In: A. Barhoum *et al.* (eds) Handbook of Nanofibers. Springer, Cham (2018)
2. R. G. Hoobs, N. Petkov, J. D. Holmes, Chem. Mater 24, 1975-1991 (2012)
3. S. V. Langwald, A. Ehrmann, L. Sabantina, Membranes 13, 488 (2023)
4. L. Y. Wan, H. B. Wang, W. D. Gao, F. Ko, Polymer 73, 62-67 (2015)
5. M. T. Fujii *et al.*, Phys. Rev. Lett. 95, 065502 (2005)
6. H. H. Henrichsen *et al.*, Organic Electronics 8, 540-544 (2007)

Evaluating the Impact of Solvent Vapor Annealing in Organic Thin Films Through Transfer Matrix Method

Juscelino Valter Barbosas Júnior[1], Eduardo Henrique dos Santos Rosa[1], Juan C. González[3], Amanda Louise Machado[2], Wilson José da Silva[2], Roberto Mendonça Faria[2,4], Andreia Gerniski Macedo[2]

[1]Department of Physics – Universidade Tecnológica Federal do Paraná – Curitiba – PR - Brazil
[2]Graduate Program in Physics and Astronomy (PPGFA) – Department of Physics – Universidade Tecnológica Federal do Paraná – Curitiba – PR – Brazil
[3]Department of Physics – Universidade Federal de Minas Gerais
[4]Grupo de Polímeros - Instituto de Física da Universidade de São Paulo – São Carlos – SP - Brazil

INTRODUCTION

In this work, the solvent vapor annealing procedure (SVA)[1] was used to improve the optical and adhesion features of a conjugated copolymer:molecule acceptor film. The power dissipation was simulated along the structure of organic photovoltaic device devices considering the interference occurring in stacked thin films under normal incidence by using the transfer matrix method (TMM)[2,3]. Therefore, the monitoring through ellipsometry and TMM modeling contributes to understanding the behavior of the electromagnetic wave inside the device, providing insights about proper optimizations that can be performed to increase the G(x) rate and the Jsc parameter. This model takes into account the experimental values of refractive index n and extinction coefficient k acquired from the D:A film to simulate the spatial distribution of the electric field and provide valuable information about photovoltaic parameters.

EXPERIMENTAL/THEORETICAL STUDY

PBDTTT-CT:PDI-DPP-PDI solution was prepared in chloroform (1:1.5 wt:wt, 20 mg/mL) upon magnetic stirring for 24 hours at room temperature. Then, 100 µL of this solution was spin-cast onto a cleaned glass substrate (1x1 cm^2) using the rotation of 1500 rpm upon nitrogen atmosphere. These films were dried at room temperature and then, exposed to vapor of chlorobenzene for 10 minutes inside a closed petri dish. The resulting thin films were characterized by UV-IS spectroscopy in a Kasuaki spectrometer (model IL-592) and by VASE using a J. A. Woollam M-2000 Ellipsometer equipment. Morphology was analyzed by AFM using a Shimadzu microscope (model SPM 9700-HT) in dynamic mode. The refraction index and attenuation coefficient were used in the TMM model to simulate the electric field distribution versus thickness along the organic solar cell.

RESULTS AND DISCUSSION

The results pointed out that the SVA-treated films presented distinct refraction index curves, as well as improved electric field distribution when compared with cast films, see Figure 1.

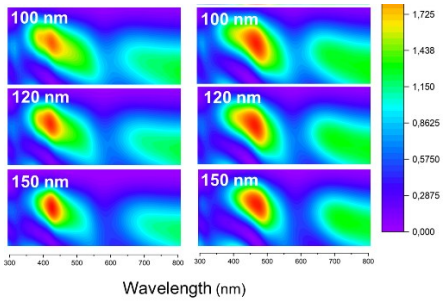

Fig. 1. Spatial electric field distribution at the PBDTTT-CT:PDI-DPP-PDI active layer with variable thickness from 100 nm (top), 120 nm, and 150 nm (bottom)

CONCLUSION

TMM simulation pointed out that the spatial electric field distribution and the exciton generation rate are dependent on the film thickness, and both parameters are impacted by the SVA treatment.

REFERENCES

1. T. R. Casagrande, et. al, Phys. Chem. Chem. Physics 25, 25280 (2023)
2. A. E. X. Gavim et. al, Solar Energy. 247, 286(2022)
3. E. H. dos Santos Rosa, et. al, Solar Energy 221, 487 (2021)

ACKNOWLEDGMENTS

This work was financially supported by Fundação Araucária (NAPI-Eletrônica Orgânica), Conselho Nacional de Desenvolvimento Científico e Tecnológico (CNPq, grants PQ2 309907/2021-7, Instituto Nacional de Eletrônica Orgânica (INEO), and Serrapilheira Institute (Grant number Serra-1709-17054).

Study of Copper-based Solutions for Neuromorphic Computing

Andreia V. Silva[1*], Catarina Dias[1], Ana T. Brandão[2], Carlos M. Pereira[2] and João Ventura[1]
[1]IFIMUP, Departamento de Física e Astronomia, Faculdade de Ciências, Universidade do Porto, Portugal ([*]andreia.silva@fc.up.pt)
[2]CIQUP, Departamento de Química e Bioquímica, Faculdade de Ciências, Universidade do Porto, Portugal

INTRODUCTION

The miniaturization of electronic components has increased exponentially in the past years, leading to its limits regarding Moore's law. In consequence, new forms of computing have emerged, such as neuromorphic computing[1]. Neuromorphic computing is brain inspired, meaning that its aim is to emulate how the complex networks of neurons and synapses work in the human brain. For that, key electronic components are needed, with memristors being the main candidates. Memristors are electronic devices that possess resistive switching (RS), a behavior that emulates synaptic dynamics[1]. Moreover, memristors can be fabricated with different types of materials, with solid-state ones taking the spotlight. However, solid-state materials are expensive, hard to produce, rigid and consume more power than what is desired. Liquid-state materials seem to overcome these issues by having RS with low to ultralow power consumption, easiness and cheapness of production, flexibility, and adaptability[2]. So, here, we propose the study of different liquid memristors based on different solutions and configurations for the future fabrication of neuromorphic computing hardware.

EXPERIMENTAL/THEORETICAL STUDY

The vertical RS devices are composed of a grounded copper (Cu) bottom electrode, a top electrode, and a solution in between. The top electrode material and electrode spacing were studied. Furthermore, two solutions were tested: $CuSO_4$ dissolved in water and in glyceline, a deep eutectic solvent (DES). Their concentrations were varied for performance assessment. Finally, a planar configuration of the device was also tested for different electrode materials [Cu and tungsten (W)] and spacing.

RESULTS AND DISCUSSION

Both configurations presented RS switching, with the vertical stack leading to the most satisfactory results. For the aqueous solution, ultralow operation voltage, high endurance, data retention and neuromorphic properties such as potentiation, depression, spiking-time-dependent plasticity (STDP) and paired-pulse facilitation (PPF) were found. By modifying the solvent, improved stability, and a change in behavior, from non-volatile to volatile, was seen. Neuromorphic properties were found as well, which is not reported in literature for volatile devices.

CONCLUSION

The emulation of synaptic behavior in the devices was attained under low voltages. Furthermore, by using liquids, advantages such as adaptability and flexibility arise, with the addition of different temporal order behaviors being obtained with the change in solvent. Such neuromorphic and temporal order characteristics are key to mimic the human brain and reach the so desired neuromorphic computing hardware network.

REFERENCES

1. Q. Wan et al., Adv. Mater. Technol., 4(4), 1–34 (2019).
2. D. Kim et al., Nanoscale, 11, 9726-9732 (2019).

ACKNOWLEDGMENTS

This work was financially supported by FCT through project PTDC/NAN-MAT/4093/2021 and "La Caixa" Foundation within project CCO 204197.

Effects of doping in alkali-metal-decorated SnC monolayers and its application to H_2 storage

Ángel R. Montoya[1], María I. Iturrios[2], Álvaro Miranda[1], Luis A. Pérez[3], Miguel Cruz-Irisson[1]
[1] ESIME Culhuacán, Instituto Politécnico Nacional, México,
[2] CECYT 8 Narciso Bassols Instituto Politécnico Nacional, México
[3] Instituto de Física, Universidad Nacional Autónoma de México, México
*Corresponding author: amontoyag1400@alumno.ipn.mx

INTRODUCTION

Hydrogen is the most common element in the universe and today it is a subject whose research is growing owing to its high energy density. However, one significant problem surrounding its use as an energy source is its storage, which must be investigated to contribute to a global transition towards a society free of carbon emissions. Several studies indicate that using two-dimensional (2D) solid-state materials such as graphene and graphene-like carbides such as SiC and GeC, and most recently, SnC, can be good options to store hydrogen due to their large surface area. Additionally, several studies have shown that the doping and functionalization of these monolayers improve their molecular adsorption capacity [1]. A. Marcos et al. [1,2] reported H_2 adsorption capacities of K- functionalized 2D-SnC and, in this work, the results of B-, Al- and Ga- doped 2D-SnC decorated with Li and K atoms are presented.

THEORETICAL STUDY

Fifty-atom 5×5 SnC supercells further doped, functionalized and with different number of adsorbed H_2 molecules adsorbed were considered and their structural and energetic properties were obtained using the density functional theory (DFT) formalism, with the GGA-PBE exchange-correlation functional. The van der Waals interactions were considered by using the DFT-D2 method of Grimme. Norm-conserving pseudopotentials were employed together with a grid of 4×4×1 k-points for the geometric relaxations and a 24×24×1 mesh for the calculation of electronic properties. The geometric coordinates of all atoms and the cell dimensions were optimized, using the conjugate gradient method, until the Hellmann-Feynman forces between atoms were less than 0.01 eV/Å.

RESULTS AND DISCUSSION

The most energetically favorable doping configuration of 2D-SnC monolayers corresponds to a Sn atom replaced by Al, B, and Ga ones. The numerical results indicate that the resulting monolayer further decorated with K and Na atoms can store up to six and five H_2 molecules per adsorption site (Figure 1), respectively, with a mean adsorption energy of 0.21 eV. These results suggest that doped and functionalized 2D-SnC could be useful as a medium for solid-state hydrogen storage, which could contribute for the development of more efficient and sustainable technologies for the storage and use of hydrogen as a source of energy.

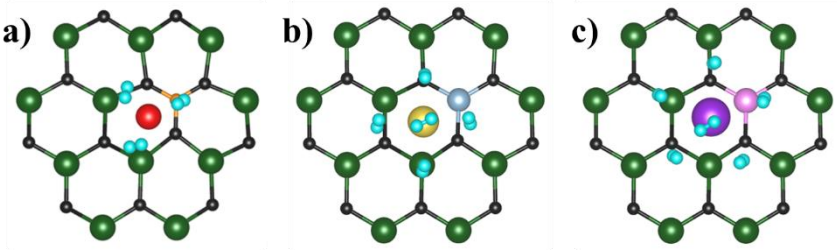

Fig. 1 Hydrogen molecules adsorbed on monolayers displaying the calculated maximum storage capacity per adsorption site: a) B-2D-SnC + Li + $3H_2$. b) Al-2D-SnC Al + Na + $5H_2$. c) Ga-2D-SnC + K + $6H_2$.

CONCLUSION

In this work, the adsorption of hydrogen molecules on alkaline-metal-decorated doped SnC monolayers were investigated. The monolayers doped with Ga and decorated with Ga adsorb the largest number of H_2 molecules per adatom with adsorption energies suitable for the hydrogen reversible storage.

REFERENCES

[1] A. Marcos et al, Mater. Lett. **298**, 130030 (2021).
[2] A. Marcos et al, Int. J. Hydrogen Energy **47**, 41329-41335 (2022).

ACKNOWLEDGMENTS

This work was partially supported by multidisciplinary project IPN-SIP 2023-2274,-2079, PIIF-UNAM and UNAM-PAPIIT IN102923. Computations were performed at Miztli supercomputer of DGTIC-UNAM (Project LANCAD-UNAM-DGTIC-180, 381). A.R.M. would like to thank CONACYT and BEIFI-IPN for their financial support.

AB-initio study on the hydrogen storage in transition-metal-decorated 2D-SnC doped with B, Al, Ga

Ángel R. Montoya[1], María I. Iturrios[2], Álvaro Miranda[1], Luis A. Pérez[3], Miguel Cruz-Irisson[1]
[1] ESIME Culhuacán, Instituto Politécnico Nacional, México,
[2] CECYT 8 Narciso Bassols Instituto Politécnico Nacional, México
[3] Instituto de Física, Universidad Nacional Autónoma de México, México
*Corresponding author: amontoyag1400@alumno.ipn.mx

INTRODUCTION

Theoretical studies have shown that 2D-SnC decorated with alkaline- and transition-metal atoms can store hydrogen molecules [1,2]. Furthermore, dopant species may be able to bind metal adatoms more strongly and prevent their diffusion over the surfaces. In this work we study the hydrogen storage capacities 2D-SnC doped with B, Al, Ga atoms and functionalized with transition-metal atoms. The results of the doped and transition-metal decorated 2D-SnC show a further improvement in the adsorption capacity of hydrogen molecules.

THEORETICAL STUDY

Fifty-atom 5×5 SnC supercells further doped, functionalized and with different number of adsorbed H_2 molecules adsorbed were considered and their structural and energetic properties were obtained using the density functional theory (DFT) formalism, with the GGA-PBE exchange-correlation functional. The van der Waals interactions were considered by using the DFT-D2 method of Grimme. Norm-conserving pseudopotentials were employed together with a grid of 4×4×1 k-points for the geometric relaxations and a 24×24×1 mesh for the calculation of electronic properties. The geometric coordinates of all atoms were optimized, using the conjugate gradient method, until the Hellmann-Feynman forces between them were less than 0.01 eV/Å.

RESULTS AND DISCUSSION

The most stable doping configurations of 2D-SnC monolayers are those where Al, B, and Ga atoms replace a Sn one of the monolayer. Likewise, on these doped SnC monolayers, the transition metal atoms tend to settle above the Sn one. The results show that the systems functionalized with Sc store up to three H_2 molecules, while Ti-, V-, and Cr-functionalized systems can store up to four molecules with adsorption energies around 0.21 eV.

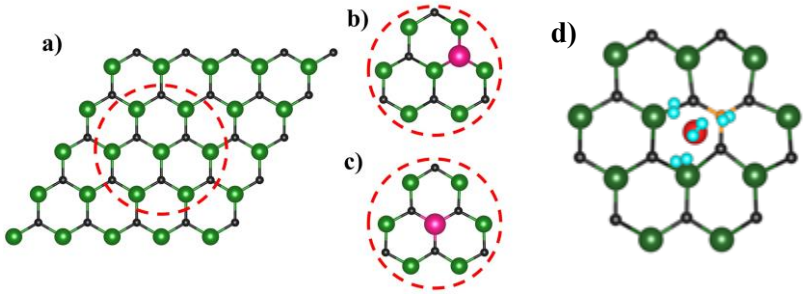

Fig. 1 a) 2D-SnC b) 2D-SnC with a doping atom replacing C c) 2D-SnC with a doping atom replacing Sn and d) 2D-SnC dB + Cr with 5 H_2 molecules adsorbed.

CONCLUSION

The interaction of hydrogen molecules with the doped and functionalized supercells is controlled by van der Waals-type forces with energies close to 0.2 eV. Moreover, the gravimetric capacities of hydrogen storage were analyzed, and the boron-doped and Ti- and Cr-decorated nanosheets may exceed 5.5 wt%, which is the goal suggested for hydrogen storage devices by the U.S. DoE. Therefore, doped SnC monolayers decorated with transition metals can be used to store hydrogen.

REFERENCES

[1] A. Marcos et al, Mater. Lett. **298**, 130030 (2021).
[2] A. Marcos et al, Int. J. Hydrogen Energy **47**, 41329-41335 (2022).

ACKNOWLEDGMENTS

This work was partially supported by multidisciplinary project IPN-SIP 2023-2274,-2079, PIIF-UNAM and UNAM-PAPIIT IN102923. Computations were performed at Miztli supercomputer of DGTIC-UNAM (Project LANCAD-UNAM-DGTIC-180,381). A.R.M. would like to thank CONACYT and BEIFI-IPN for their financial support.

Formation of porous metals with nano- and microsized structural elements under near-equilibrium condensation conditions

Anna Kornyushchenko [1,2], Vyacheslav Perekrestov[2] and Gerhard Wilde[2]

[1]Institute of Materials Physics, University of Muenster, Germany
[2]Laboratory of Vacuum Nanotechnologies, Sumy State University, Ukraine

INTRODUCTION

It is known, that porous structures depending on morphology can possess unique physical properties which can determine areas of their application.

EXPERIMENTAL/THEORETICAL STUDY

In the proposed work a new technique for synthesizing metal porous micro- and nanostructures has been developed that is based on direct current magnetron sputtering in high-purity argon. This approach is based on the phase transition of sputtered substances into the condensed state under conditions close to thermodynamic equilibrium.

RESULTS AND DISCUSSION

The low dimensional metal systems (Cr, Zn, Cu, Ti, Ni, Al) have been obtained in the different morphological forms, such as network structures, nanowires, agglomerations of weakly-bound crystals, columnar structures consisting of prolonged crystals with approximately identical habitus, etc. The results confirm the important new opportunities for size, shape and physical property tuning of nanostructured materials that are given by deposition near thermodynamic equilibrium conditions.

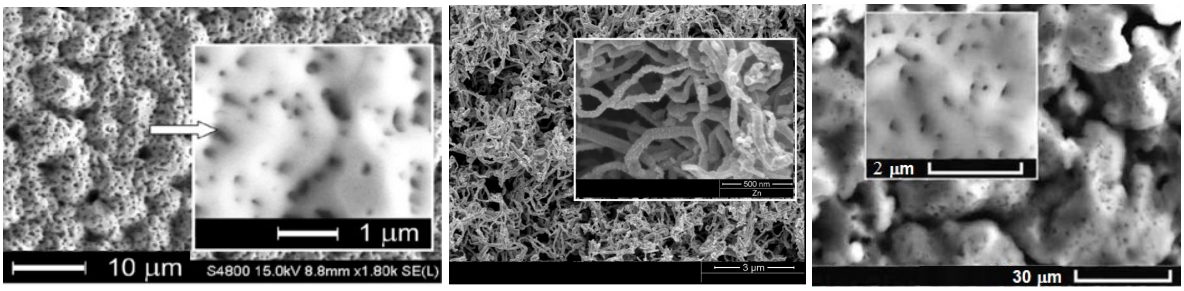

Copper **Zinc** **Aluminium**

Fig. 1 Morphology of Cu, Zn and Al layers obtained under near-equilibrium conditions

CONCLUSION

It has been established that the growth mechanism under conditions close to thermodynamic equilibrium possesses principally new peculiarities and possibilities in comparison with traditional methods of condensation from vapor state and consequently can contribute to a new zone in the structure zone model.

REFERENCES

1. A. Kornyushchenko, et.al. J. Nano- Electron. Phys. 13, 02034 (2021).
2. A. Kornyushchenko, et.al. J. Electron. Mater. 50, 2268 (2021).

ACKNOWLEDGMENTS

A. Kornyushchenko would like to acknowledge support by Philipp-Schwarz Initiative Fellowship.

Heterogeneous, multi-layered conjugated polymer nanoparticles for theranostic applications

Anton Uzunoff [1], Miao Zhao[2], Yi Wang[2], Mark Green[2], and Aliaksandra Rakovich* [3*]
[1]Physics Department, King's College London, UK, presenting author
[2] Physics Department, King's College London, UK
[3*] Physics Department, King's College London, UK, corresponding author

INTRODUCTION

Conjugated polymer nanoparticles (CPNs) present as stable, photosensitive agents useful for photodynamic therapy and fluorescent imaging diagnostics[1]. This research aims to prove the possibility of combining multiple photo-activated functionalities into a single particle by synthesizing particles with two conjugared polymers, CN-PPV and PTB7-Th, separated by a shell of SiO_2, dubbed composite SiCPNs.

EXPERIMENTAL/THEORETICAL STUDY

Both conjugated polymers (CN-PPV and PTB7-Th) were used to fabricate separate CPN samples via the nanoprecipitation method, done to act as control groups. Both were then fabricated with a covering of silica, following previous work[2]. Both conjugated polymers were stabilized in aqueous solution using the amphiphilic copolymer Pluronic F127. The hydrodynamic diameter was calculated via dynamic light scattering (DLS). Absorption and emission spectra were measured for both particles. Following that, a THF solution of CN-PPV was added under sonication to an aqueous solution of PTB7-Th silica-shelled particles, and all measurements were done again.

RESULTS AND DISCUSSIONS

CN-PPV and PTB7-Th presented with very distinct absorption peaks, allowing for easy comparison and subsequent analysis of composite SiCPNs. CN-PPV@F127@SiO_2 presented an absorption peak around 463 nm, while PTB7-Th@F127@SiO_2 has two main absorption peaks at 630 nm and 696 nm. The composite SiCPNs exhibit three separate absorption peaks with no conjugation beyond a linear combination of peaks (Fig. 1 (a)). The size of PTB7-Th@F127@SiO_2 was 88.9 nm with PDI=0.114, while after the addition of CN-PPV the diameter of the composite SiCPN was 101.6 nm and PDI=0.11.

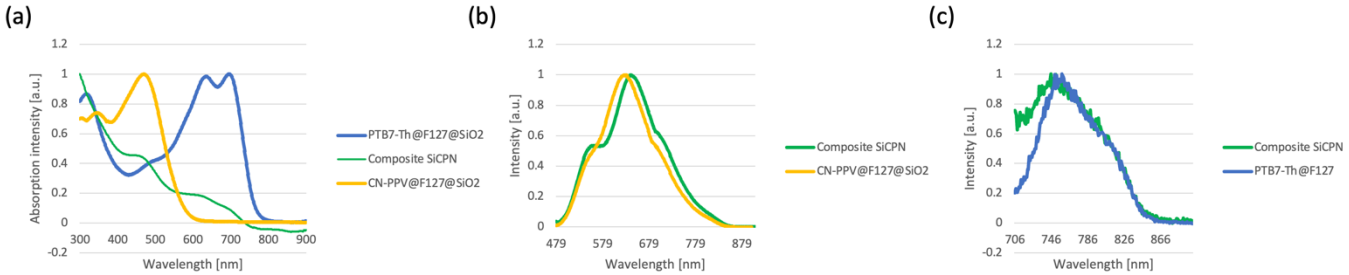

Fig. 1. Composite SiCPN spectra (a) Absorption of the two conjugated polymers on their own, as well as the composite SiCPN absorption, (b) 463 nm (CN-PPV) excitation emission and (c) 696 nm (PTB7-Th) excitation emission spectra.

CONCLUSIONS

Photophysical response shows spectra only from the specific polymer excited, no mixing of energy states visible, with the possible conclusion that conjugated polymers can be layered freely in a particle for multiple functionalities.

REFERENCES

1. Zhao, M. *et al.* Theranostic Near-Infrared-Active Conjugated Polymer Nanoparticles. *ACS Nano* **15**, 8790–8802 (2021).

2. Struan, B. *et al.*, ***Sens. Diagn.***, 2022,**1**, 1185-1188.

Nanomembranes and Urban Vehicles: A Simple Way to Minimize Urban Noise

Antonio Avila [1] and Elvis Monteiro [2]
[1]Mechanical Engineering Department, Universidade Federal de Minas Gerais, Brazil, presenting author, corresponding author (avila@ufmg.br)
[2]Research and Development Department, Stellantis Brazil

INTRODUCTION

According to Liu et al. [1], urban noise originates from sources such as road traffic and background noises. Highway traffic noise, for example, results from a combination of factors, including tire-pavement interaction, aerodynamic factors, and vehicle components. As discussed by McBride et al. [2], the dominant spectral content of the tire-pavement interaction source falls between 500 and 1500 Hz. Potin et al. [3] reported a frequency range of urban noise generated mainly by traffic, both ground and air, between 1–4 kHz.

The problem with urban noise lies in the various diseases associated with long-term exposure. Bus and cab drivers are more susceptible to hearing loss and cardiovascular diseases (hypertension and stroke) due to prolonged exposure to traffic noise. To mitigate the effects of urban noise on such professionals, an efficient and cost-effective sound absorption material must be used in public transportation.

EXPERIMENTAL/THEORETICAL STUDY

The poly (vinylidene fluoride-co-hexafluoropropylene) (PVdF-HFP) nanomembranes were synthesized via electrospinning. Since nanomembranes are delicate nanostructures, a polyurethane foam was used as the support material. The acoustic properties were experimentally measured using an impedance tube, as in Leão et al. [4].

RESULTS AND DISCUSSION

As observed in Fig. 1A-B, not only did the nanofiber diameter vary (ranging between 100-200 nm), but the morphology (porous diameter and spatial distribution) was also influenced by factors such as polymer concentration and applied voltage. The combination of nanomembranes and PU foam formed a Helmholtz resonator. Figure 1C illustrates how the addition of the nanomembrane to PU foam altered the sound absorption coefficient. The resonator response is governed by changes in airflow within the nanomembranes.

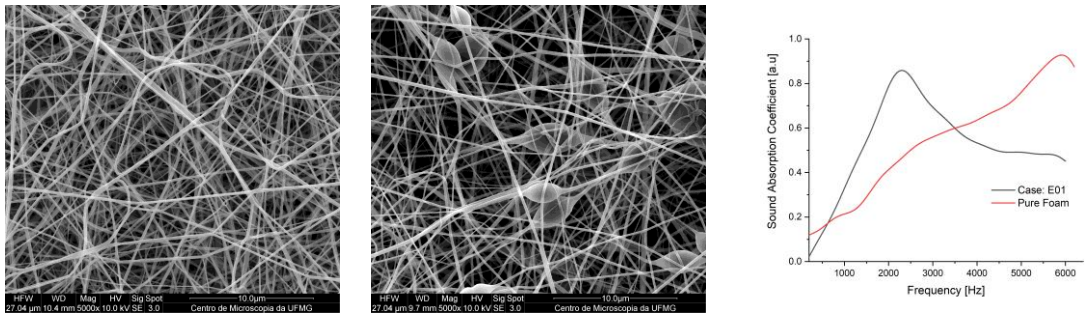

Fig. 1 Nanomembranes' morphology and sound absorption coefficient

CONCLUSION

A combination of acoustic foam and nanomembranes can function as a Helmholtz resonator with a high sound absorption capacity. The nanomembranes, with an average thickness of 5.0 nm, act as the resonator neck, while the acoustic foam, 13 mm thick, serves as the resonator cavity. The average sound absorption coefficient measures approximately 89%, with peak frequencies ranging from 2400 Hz to 4300 Hz.

REFERENCES

1. Z. Liu et al.Adv. Compos. Hybrid Mater. 4, 1215–1225 (2021).
2. S. McBride et al. Tire Sci. Technol. 49, 146–169 (2021).
3. D.A. Potvin et al Proc. R. Soc. B Biol. Sci. 278, 2464–2469 (2011).
4. S.G. Leão et al. Appl. Acoustics. 199, 109009 (2022).

ACKNOWLEDGMENTS

The authors are grateful for the financial support provided by Brazilian Research Council (CNPq) under grant 307385/2022-1, the CAPES foundation under grant 001.

The clusters formation in metal thin layers deposited by pulse arc plasma in vacuum

A.M. Zhukeshov*, A.T. Gabdullina, A.U. Amrenova and M. Mukhamedryskyzy

al-Farabi Kazakh National University, Kazakhstan.

INTRODUCTION

The study of metal layers deposited from thermal plasma is relevant due to the unusual properties and unique structure of these coatings. The purpose of our study is to trace the evolution of the structure of a copper coating deposited from the plasma of a vacuum arc in a pulsed operating mode. The practical goal is to deposit a thin layer of copper on aluminum for energy applications.

EXPERIMENTAL/THEORETICAL STUDY

The vacuum arc installation used in pulsed arc burning mode with a frequency of 10 Hz. The cathode material consist of copper 95%, the substrates for deposition - duralumin 94%, cathode diameter 50 mm. The spraying time was varied from 15 to 40 minutes. The vacuum level varied ($10^{-5} \div 10^{-6}$) Pa during the process. SEM and elemental analyses was used.

RESULTS AND DISCUSSION

From Figure 1, the evolution of the size of surface defects can be traced. First it is visible nanodust, then some spherical clusters growing in size, then dust again, but smaller. This behavior can be explained by the initial formation of the coating in layers, the gradual growth and filling of the surface with these layers. Further, under the influence of temperature, a structural transformation of dust into nanoclusters occurs. After 25 min of deposition, the spherical nanoclusters reach almost the maximum uniform size ~ 100 nm, which means this is a highly dispersed structure. The transformation process continues up to 30 minutes of spraying. After 30 min, a highly homogeneous structure was observed, and it was not possible to determine the size of the particles. The elemental composition of the surface presented by 19.98% Cu, 6,72% O_2 and Al.

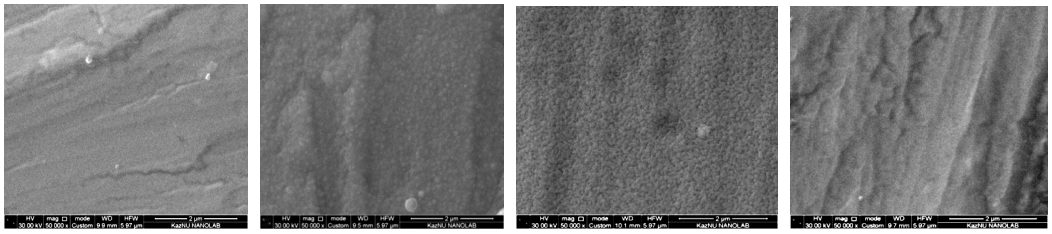

Fig. 1 Copper layer structure on aluminum substrates after 15 - 40 min deposition in vacuum

.

CONCLUSION

From the point of view of thermodynamic processes, under the action of the thermal plasma of the arc, the substrate gradually heats up to 200^0 C in first 20 min. of process [1]. Up to a certain temperature, dust forms into nanoclusters. Obviously, this occurs as a result of the fact that dust is deposited from the plasma in the form of nanoparticles. Nanoparticles were discovered in arc plasma coatings by a number of authors, for example [2,3]. The formation of nanodust from the ion component of plasma in the arc discharge region, in particular the mechanism of this process, requires additional research. The main perspective advantage of this method is good efficiency for nanomaterials fabrication and applicability for industrial produce of metal powders.

REFERENCES

References must be numbered. Keep the same style.

1. A.M. Zhukeshov, et. al, Appl. Phys. A. 126, 742 (2020)
2. Y. Agawa, et. al, Adv. Mat.Res. Online: 2010-08-11
3. A.I. Ryabchikov et. al, Applied Surface Science. 305. 487–491 (2014)

ACKNOWLEDGMENTS

Authors acknowledge the Committee of Science of the Ministry of Science and high Education and of the Kazakhstan Republic for grant IRN AP19676182 support.

Ionic liquid laden MOF-based solid-state electrolytes for sodium batteries

Arkaitz Fidalgo-Marijuan [1,2*], Alexander Mirandona-Olaeta [1], Roberto Fernández de Luis [1], Carlos M. Costa [3,4,5], Eider Goikolea [2], Idoia Ruiz de Larramendi [2]and Senentxu Lanceros-Mendez [1,6]

[1*] BCMaterials, Basque Center for Materials, Applications and Nanostructures, Spain, Arkaitz Fidalgo-Marijuan

[2] Department of Organic and Inorganic Chemistry, University of the Basque Country, Spain

[3] Physics Centre of Minho and Porto Universities, University of Minho Portugal

[4] Laboratory of Physics for Materials and Emergent Technologies, LapMET, University of Minho, Portugal

[5] Institute of Science and Innovation for Bio-Sustainability (IB-S), University of Minho, Portugal

[6] Ikerbasque, Basque Foundation for Science, Spain

INTRODUCTION

Sodium batteries are receiving increasing interest as an alternative to reduce dependence on lithium based systems. Furthermore, the development of solid-state electrolytes will lead to higher performing and safer devices[1,2]. In this work, metal-organic frameworks are combined as a physical barrier to the growth of dendrites, together with 1-ethyl-3-methylimidazolium bis(trifluoromethylsulfonyl)imide ([EMIm][TFSI]) ionic liquid that provides improved mobility to sodium ions.

EXPERIMENTAL STUDY

The used physicochemical characterization techniques are FTIR spectroscopy, TGA/DSC for the thermal analysis, X-Ray diffraction and SEM microscopy. For the electrochemical characterization of the materials ionic conductivities, Na^+ transference numbers, the electrochemical stability window and galvanostatic Na stripping/plating test were performed.

RESULTS AND DISCUSSION

It is demonstrated that the incorporation of the appropriate amount of ionic liquid within the pores of the MOF produces a considerable increase in ionic conductivity, achieving values as high as $5 \cdot 10^{-4}$ S cm^{-1} at room temperature, in addition to an acceptable Na^+ transference number. Furthermore, the developed Na[EMIm][TFSI]@MOF hybrid solid electrolytes contribute to stable and dendrite-free sodium plating/stripping for more than 100 hours. Finally, a more than notable extension of the electrochemical stability window of the electrolyte has been determined, being useful even above 7 V vs Na^+/Na. Overall, this work presents a suitable strategy for the next generation of solid-state sodium batteries.

CONCLUSION

It has been determined that the combination of porous metal-organic framework with the sodium-enriched [EMIm][TFSI] ionic liquid leads to obtaining hybrid materials with potential application as solid electrolytes in sodium batteries.

REFERENCES

1. J Feng, et. al, . Pinto et. al, J. Mater. Chem. A 3, 14539 (2015)

2. E. Goikolea, et. al, Adv. Energy Mater. 10, 2002055 (2020)

ACKNOWLEDGMENTS

The authors thank the Fundação para a Ciência e Tecnologia (FCT) for financial support under the framework of Strategic Funding UIDB/04650/2020, UID/FIS/04650/2020, UID/EEA/04436/2020, and UID/QUI/0686/2020 and under projects POCI-01-0145-FEDER-028157, MIT-EXPL/TDI/0033/2021, POCI-01-0247-FEDER-046985 and PTDC/FIS-MAC/ 28157/2017 funded by national funds through FCT and by the ERDF through the COMPETE2020. This work was supported by grant PID2019-107468RB-C21, funded by MCIN/AEI/10.13039/501100011033 and Gobierno Vasco/Eusko Jaurlaritza (project IT1546-22). This study forms part of the Advanced Materials program and was supported by MCIN (with funding from European Union NextGenerationEU (PRTR-C17.I1)) and by the Basque Government (under the IKUR program and ELKARTEK programs).

Enhanced Intramolecular Charge Transfer and Near-Infrared Fluorescence in New Chalcone Derivatives through Extended Conjugation and Planarity Coupling

Balqees S. Al-Saadi and Osama K. Abou-Zied*
Department of Chemistry, College of Science, Sultan Qaboos University, Muscat, Sultanate of Oman

INTRODUCTION

The distinctive characteristics of near-infrared fluorescent organic molecules render them indispensable across diverse applications, from energy harvesting to bioimaging and sensing technologies. In this work, we continue our investigation on the chalcone derivative, 4-dimethylamino-2′-hydroxychalcone (DHC, Fig. 1), by expanding the number of central double bonds (n =2 (2DHC) and n = 3 (3DHC)). Additionally, we also synthesized the precursor chalcones lacking the OH group (DC, 2DC, 3DC) in order to obtain a comprehensive understanding of those effects on the intramolecular charge transfer (ICT). The effect of twisting around the phenyl ring was also investigated by synthesizing the molecule with a furan ring (DHCF, Fig. 1) and its analogue DCF. This study provides insight into the complex relationship between molecular structure, conjugation length, and the behavior of the excited state, offering valuable knowledge for advanced applications in photophysics and molecular design

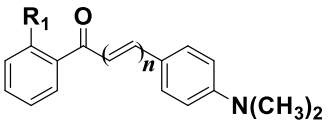

DHC: R_1=OH, n=1

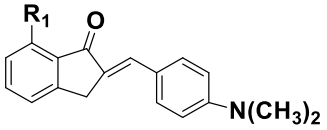

DHCF: R_1=OH

EXPERIMENTAL/THEORETICAL STUDY

The chalcone derivatives were obtained via aldol condensation reaction in basic media between aldehyde derivatives and acetophenone derivatives in (1:1) molar ratio, furnishing chalcone products. Absorption and fluorescence experiments were performed using an Agilent 8453 spectrophotometer and a Duetta spectrometer (Horiba Scientific), respectively. The femtosecond laser setups (transient absorption and fluorescence upconversion) allowed us to observe the ultrafast dynamics within the time range 100 fs – 5 ns. The samples for all spectroscopic measurements were prepared in 2 mm fused silica cuvettes and were stirred during the lifetime measurements to avoid photodegradation. For the solid samples, the crystalline form was spread on a quartz sheet.

RESULTS AND DISCUSSION

The results show remarkable bathochromic shifts in absorption and fluorescence peaks as n increases, signifying enhanced ICT and a significant increase in the excited state's dipole moment. The presence of OH groups notably amplifies these shifts due to additional electron donation. Femtosecond fluorescence upconversion and transient absoprtion techniques unraveled distinct dynamics in these derivatives, showcasing the dominance of vibrational cooling, solvation, and intramolecular motions, particularly in larger conjugated systems like 3DHC and 3DC. The observed changes in the femtosecond transinet absorption spectra suggest the existence of new active states in extended conjugation systems, indicating diverse intramolecular conformational states contributing to their relaxation dynamics. More planar confirmation in DHCF, along with more stable intramolecular hydrogen bonding, leads to a new absorption peak in the red region. Our findings demonstrate that the new structural modifications lead to a notable red shift in fluorescence, transitioning from green to the near-infrared region. The results of this study provide invaluable insights into excited-state spectroscopy, offering a roadmap for tailoring chalcone derivatives for specific applications.

CONCLUSION

In this study, we observed significant red shifts in absorption and fluorescence peaks with increasing the number of central double bonds in the parent molecule DHC, highlighting stronger ICT and higher excited state dipole moments. The presence of OH groups intensified these shifts due to an additional electron donation center. The latter, along with enforced molecular planarity, led to a new red absorption peak in DHCF. Femtosecond techniques revealed distinct dynamics, emphasizing vibrational cooling, solvation, and intramolecular motions, especially in larger conjugated systems. These findings expose diverse conformational states, guiding the customization of chalcone derivatives for targeted applications.

ACKNOWLEDGMENTS

The authors would like to acknowledge Sultan Qaboos University for its support through several research grants and PhD scholarships.

Temperature effect on adsorption properties of clay – fly ash composite nanosorbents

Barbora Dousova* [1*], Lukas Pilar [1], Miloslav Lhotka [2], Eva Bedrnova [1], Katerina Maxova [1] and David Kolousek [1]

[1]Department of Solid State Chemistry, University of Chemistry and Technology Prague, Technicka 5, 166 28 Prague 6, Czech Republic, presenting and corresponding author (dousovab@vscht.cz)

[2]Department of Inorganic Technology, University of Chemistry and Technology Prague, Technicka 5, 166 28 Prague 6, Czech Republic

INTRODUCTION

The preparation of composite sorbents from recycled and/or waste products represents a starting discipline that opens up new possibilities for obtaining broad-selective sorbents through an effective combination of all participating components[1]. Aluminosilicates (AL) in their original and modified form are widely used in adsorption technologies due to favourable physical chemical and surface properties, and for environmental and economical reasons[2,3]. In addition to other promising adsorption materials, such as carbon substances, biochar, several organic and polymeric compounds[4,5], fly ashes (FA) are of increasing professional concern in terms of finding their possible applications in industrial and environmental scale.

EXPERIMENTAL STUDY

The composite sorbents were prepared as dry mixtures of 2 AL and 3 FA (6 composites), in the weight ratio of 1:1. The suspension of each mixture with distilled water was agitated in the batch manner at 20, 40 and 70°C for 24 hours.The composites were tested for the separate adsorption of selected toxic cations (Pb^{2+}, Cs^{+}) and anions (AsO_4^{3-}, CrO_4^{2-}), and for the cation-anion co-adsorption from appropriate model solution.

RESULTS AND DISCUSSION

FA from biomass combustion arising at a low combustion temperature (to 850°C) proved to be a promising additive to AL-based composites. Cations were selectively adsorbed on both the AL and some composites, specifically: Pb^{2+} was almost quantitatively adsorbed on all AL-composites and Cs^{+} was adsorbed exclusively on the composites with zeolites[6]. The adsorption of anions on the source material and composites was ineffective, except for the AsO_4^{3-} adsorption on FA from biomass, where almost 100% efficiency was achieved.

During the co-adsorption of different ions (cation + anion) the sorption yield of a particular ion always increased due to the variability of adsorption sites and mutual affinity of oppositely charged co-adsorbed ions. In co-adsorption systems, up to 50% excess in the adsorption efficiency compared to the adsorption of particular single ion was observed.

CONCLUSION

Composite nanosorbents prepared from AL and FA confirmed the ambition to combine the adsorption properties of both components resulting in a wider selectivity to adsorbed ions and their effective removal from mixed wastewarer.

REFERENCES

1. H. Han et al, J. Hazard. Mater. 369, 780–796 (2019).
2. B. Doušová et al, J. Hazard. Mater. 165, 134–140 (2009).
3. B.K. Reeta Bhadoria et al, Desalination 254, 192–200 (2010).
4. A.S.K. Kumar et al, Ind. Eng. Chem. Res. 51, 58–69 (2012).
5. L. Chen et al, J. Clean. Prod. 156, 648–659 (2017).
6. Y. Marcus, J. Chem. Soc. Faraday Trans. 87(18), 2995–2999 (1991).

ACKNOWLEDGMENTS

This work was supported by the projects: No. TH79020001 “ABTOMAT2022 – Utilization of Aluminium Bearing Raw Materials for the Production of Aluminium Metal, Other Metals and Compounds” of the Technology Agency of the Czech Republic; No. TN02000025 “NCE II – 1. Energy conversion” of the Technology Agency of the Czech Republic.

Organic molecule Embedded Nanocomposite of $Cd_xZn_{1-x}S$ Solid Solution as a Highly Active Photocatalyst for Hydrogen Production via Water Splitting

Bashir Ahmmad*, Yuki Shizuya, Areef Billah, Anjuman Nesa Anju, and Fumihiko Hirose
Graduate School of Science and Engineering, Yamagata University, Yonezawa 992-8510, Japan
*Corresponding author's email: arima@yz.yamagata-u.ac.jp (B. Ahmmad)

INTRODUCTION

Photocatalytic water splitting is a green and sustainable process to produce hydrogen (H_2) from water. $Cd_xZn_{1-x}S$, a solid solution of CdS (Eg=2.4 eV) and ZnS (Eg=3.5 eV), is one of the widely studied materials for photocatalytic H_2 production under visible light irradiation. However, the energy conversion efficiency of this solid solution is still insufficient. Previously, we reported that the addition of organic molecule to metal sulfides can remarkably enhance their photocatalytic activity[1]. In this work, we present organic molecule (phenylalanine) embedded nanocomposite of $Cd_xZn_{1-x}S$ solid solution as a highly active photocatalyst for H_2 production.

EXPERIMENTAL

The nanocomposite of phenylalanine (PA)-embedded $Cd_xZn_{1-x}S$ (x=0.0, 0.25, 0.50, 0.75, 1.00) were synthesized by a low-temperature solvothermal technique as described in our previous report[1]. The samples were designated as C0, C25, C50, C75, C100 corresponding to the x-value and PA-embedded samples were designated as C0P, C25P, C50P, C75P, C100P, respectively. Pt was deposited on all nanocomposite samples by photo deposition method[1]. The details of the H_2 production experiment are described in our previous report[1].

RESULTS AND DISCUSSION

The FESEM images (data not shown) indicate that C0, C25, C0P, and C025P have lower particle sizes (ranging from 100 nm to 150 nm) compared to the other samples. UV-vis spectroscopy (data not shown) shows that C0, C0P samples have absorption edges in the UV region, whereas all other samples have absorption edges in the visible region. Among C0, C25, C50, C75, C100 samples, C25 exhibits the highest photocatalytic activity in terms of H_2 production from water (data not shown). This is because C25 sample has a small particle size. Fig. 1a shows the amount of produced H_2 from various samples after 2 h of irradiation. It is evident from the results that PA-embedded samples show a higher amount of H_2 production compared to non-embedded samples. It assumed that the electrons on the aromatic ring of embedded PA molecule can interact with the photogenerated holes of $Cd_xZn_{1-x}S$ and enhance charge separation, leading to a higher rate of H_2 production[1]. Fig. 1b shows the dependence of H_2 evolution on the amount of photocatalyst dispersed in the solution. It is seen that 1 mg of photocatalyst in 40 ml of sacrificial agent solution has the highest rate of H_2 production. When a large amount of photocatalyst is used, light absorption by some particles is disrupted, leading a lower rate of H_2 production. The highest rate of H_2 evolution is found to 219 mmol/g for 1.0 mg of the photocatalyst. To the best of our knowledge, this is the highest rate of H_2 production reported so far.

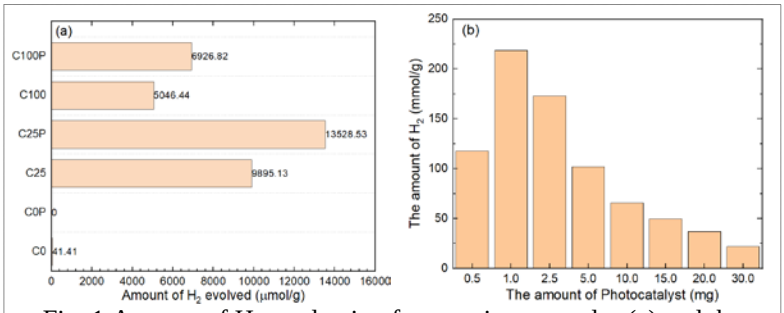

Fig. 1 Amount of H_2 production from various samples (a) and the dependence of H_2 evolution on the dose of C25P photocatalyst.

CONCLUSION

We successfully synthesized visible light active $Cd_xZn_{1-x}S$ nanocomposite for the efficient H_2 evolution via water splitting. The result suggest that our prepared material holds significant promise for practical applications in H_2 production.

REFERENCES

1. A. Billah, F. Tojo, S. Kubota, F. Hirose, B. Ahmmad, Int. J. Hydrogen Energy, vol. 46, pp. 35302-35310 (2021).

ACKNOWLEDGMENTS

This work was supported by the Sasakawa Scientific Research Grant from The Japan Science Society and Research Grant from the Foundation of Amano Institute of Technology, Japan.

Visible-light-driven Photocatalytic Oxygen Production from Water by Using $BaTiO_3$ based Ferroelectric Photocatalyst

Areef Billah, Anjuman Nesa Anju, Bashir Ahmmad* and Fumihiko Hirose
Graduate School of Science and Engineering, Yamagata University, Japan
*Corresponding author's email: arima@yz.yamagata-u.ac.jp (B. Ahmmad)

INTRODUCTION

Photocatalytic water splitting is a green and sustainable process to produce hydrogen (H_2) and oxygen (O_2) from water. For the simultaneous production of hydrogen and oxygen, hydrogen evolution reaction (HER) and oxygen evolution reaction (OER) photocatalysts are used in a system called Z-scheme. In our previous work we reported highly active CdS nanocomposite as a HER photocatalyst[1]. In this work, we report Mn and Nb co-doped $BaTiO_3$ ferroelectric material as a OER photocatalyst.

EXPERIMENTAL

$BaTiO_3$ and $BaTi_{1-x}Mn_{x/2}Nb_{x/2}O_3$ (x =0, 2.5, 5, 7.5, 10) photocatalyst materials were prepared by conventional solid state reaction method[2] and named as MN-0, MN-2.5, MN-5, MN-7.5, MN-10, respectively. The synthesized materials were analyzed by XRD, XPS, SEM, EDX, UV-visible spectroscopy, and ferroelectric tester. For the O_2 production experiment, CoO_x cocatalyst deposited photocatalysts were dispersed in $AgNO_3$ aqueous solution and irradiated under visible light.

RESULTS AND DISCUSSION

Fig. 1(a) represents that, the undoped photocatalyst MN-0 showed a negligible amount of O_2 evolution after 2 hours of irradiation, which is justifiable due to its poor absorption ability in the visible region. Surprisingly, there was a substantial increase in the rate of O_2 evolution when both Mn and Nb were co-doped into the Ti site. The MN-5 sample exhibited the highest evolution rate of O_2 evolution. Variation of the amount of CoO_x indicates that 0.5 wt% is ideal for the highest rate of O_2 evolution. It is known that spontaneous polarization in the photocatalyst materials can enhance charge separation leading to higher photocatalytic activity[3]. Ferroelectric hysteresis loop analysis (Fig. 1c) shows that MN-5 sample has higher polarization compared to the other samples. The higher polarization in MN-5 may be reason for the higher amount of O_2 evolution. Additionally, photoluminescence spectra (data not shown) reveal higher charge separation in MN-5 sample supporting this result. We also assessed the stability of MN-5 samples as an oxygen evolution photocatalyst (data not shown) and the result suggests that our prepared material holds significant promise for practical applications in oxygen evolution photocatalysis. Further research on their application in a Z-scheme system is underway at our laboratory.

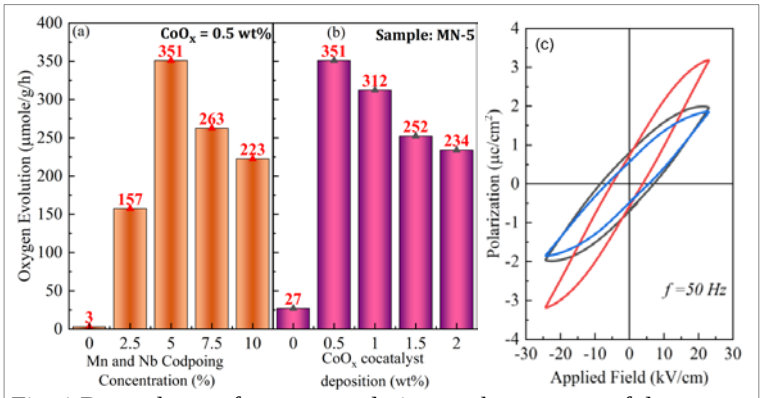

Fig. 1 Dependence of oxygen evolution on the amounts of dopants (a) and cocatalyst (b). (c) shows the results of P-E loop for various samplesN-5 sample.

CONCLUSION

We successfully synthesized visible light active $BaTiO_3$ based photocatalyst for oxygen evolution via water splitting.

REFERENCES

1. A. Billah, F. Tojo, S. Kubota, F. Hirose, B. Ahmmad, Int. J. Hydrogen Energy, vol. 46, pp. 35302-35310 (2021).
2. A. Billah, Y. Matsuno, A. N. Anju, et. al. F. Hirose, B. Ahmmad, ACS Appl. Electron. Mater. vol. 5, pp. 4261-4261(2023).
3. G. Zhang, J. Cao, G. Huang, J. Li, D. Li, W. Yao, T. Zeng, Catal. Sci. Technol, vol. 8, pp. 6420-6428 (2018).

ACKNOWLEDGMENTS

This work was supported by the Sasakawa Scientific Research Grant from The Japan Science Society and Research Grant from the Foundation of Amano Institute of Technology, Japan.

Real-data based scalable simulation model of HydroPowerPlant with Solar field and Electroyser - Slovenia case study

Boštjan Pregelj [1], David Jure Jovan [1] and Gregor Dolanc[1]
[1]Department of systems and Control, Jožef Stefan Institute, Slovenia

INTRODUCTION

Nowadays more and more cases arise, where companies are seeking ways to introduce hydrogen technologies in an economically viable way [1,2]. In Slovenia hydro-power plants (HPP) are of predominantly by-pass type, meaning the accumulation is small and can serve for daily usage variations only. With large parts of degraded areas available on the river banks, some operators recently use them to build photovoltaic fields to increase production capabilities [3]. Considering this, often excess energy is produced, that cannot be sold and has to be discarded. For these cases, an addition of power-to-gas system (P2G) seems a sensible option, However, trying to introduce it to a real system, one faces several challenges. To address them, a model has been built, described in this work.

EXPERIMENTAL/THEORETICAL STUDY

The complete model comprises HPP model, scalable PV field model and the P2G system model. The model of a HPP consists of 3 turbine-generator-model with nonlinear power-flow-height relation and accompanying accumulation lake with trapezoidal cross-section. It has been developed and tuned based on 1-year HPP operational data. The PV field model can be scaled and uses the solar data for a specified year. The P2G system model consists of a lumped nonlinear model of a commercially available electrolyser, the H_2 compression and storage model. The electrolyser nominal power as well as the storage tank can be scaled.

Beside the physical/energy side, the model comprises also economic part. It calculates the utilization rate, partial and overall efficiencies as well as hydrogen production cost considering CAPEX and OPEX for selected components.

RESULTS AND DISCUSSION

The model proves to yield results, very close to real HPP operation and can be used of dimensioning of a system. On the other hand, due to fine time scale it can also be used to study phenomena when water overflow occurs, or water is close to lower operational lever and design control for such cases. To avoid such cases, advanced controllers can be used. To this case, the water data allows also to use it as prediction variable/disturbance for use in model predictive control (MPC) design.

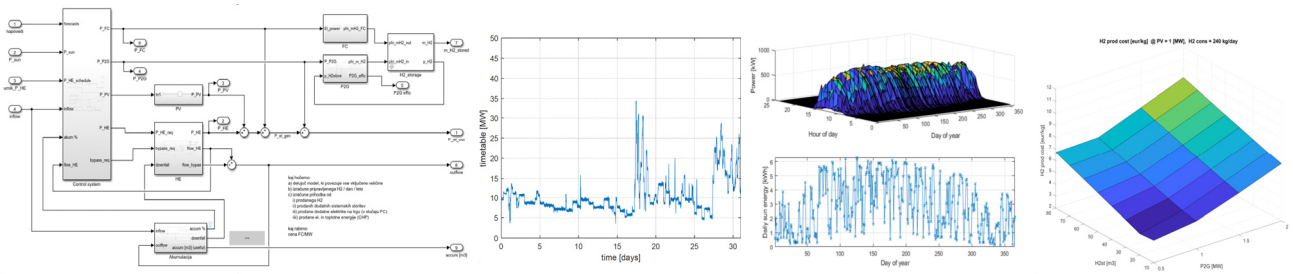

Figure: Simulink model scheme, monthly power profile, yearly solar energy profile, hydrogen production cost chart

CONCLUSION

The developed model of HPP with scalable PV and P2G can be used for macroscopic evaluation and dimensioning of a PV-P2G system setup for required demand, as well as on microscopic level, to study boundary phenomena such as accumulation limitations, rate change limitations, etc., or to test control approaches to handle them.

REFERENCES

1. A. Lewandowska-Bernat, et. al, Applied Energy, 228, pp 57-67 (2018)
2. G. Kakoulaki, et. al, Energy Conversion and Management, 228, pp 113649
3. D. J. Jovan, et. al, Energy Conversion and Management: X, 10, pp. 100081 (2021)

ACKNOWLEDGMENTS

The research leading to these results has received funding from the Slovenian Research Agency through the Research Programme P2-0001 and research projects L2-1832, L2-4456.

Understanding contact-separation triboelectric nanogenerators with nanoparticle doped materials using finite-element simulations

Carlos Callaty[1, 2*], Isabel Gonçalves[1], Cátia Rodrigues[1] and João Ventura[1]
[1]Instituto de Física dos Materiais da Universidade do Porto, Faculdade de Ciências, Universidade do Porto, Rua do Campo Alegre, s/n, 4169-007 PORTO, Portugal
[2*]Presenting author and corresponding author (carlos.callaty@gmail.com)

INTRODUCTION

Triboelectric nanogenerators (TENGs) are an attractive energy harvester for their environmental friendliness and low-cost. They can convert mechanical into electrical energy and have maritime medicine, wearables, and self-sustaining sensor applications. TENGs research focused on understanding how to improve its output, understand its working mechanism and, recently, finite-element simulations have been used to better understand TENGs. However, TENGs need enhancement in their performance and doping materials with nanoparticles has been an attractive solution to increase the relative permittivity and thus the electrical performance. The problem of tunning to the optimal nanoparticle concentration can be time and resources consuming and numerical simulations can guide the search for optimal concentration and reduce the time and resources spent.

NUMERICAL PRODECURES

In the simulations performed using time-dependent finite-element simulations with a contact-separation TENG that was modelled, according to Niu *et al.*[1], as a parallel plate capacitor with two copper electrodes and two dielectric materials (nylon and PDMS) inside an air box. In our previous work[2], we explained how to use finite-element simulations and understanding how TENG basic properties (area, material thickness) affect its performance. In here, we are continuing that work by varying the relative permittivity of one of the triboelectric materials by doping $SrTiO_3$ nanoparticles into PDMS and relating the relative permittivity with the surface charge density. The parameters to evaluate the samples performance were open-circuit voltage, short-circuit current and maximum power output.

RESULTS AND DISCUSSION

The results compared two studies: PDMS doped with $SrTiO_3$ nanoparticles and PDMS with an effective relative permittivity of nanoparticle doped PDMS. Firstly a constant charge model was tested on both cases and the evaluating parameters decreased with increasing nanoparticle concentration (effective relative permittivity), which agreed with Niu's model predictions. Due to experimental results showing that the increase in nanoparticle concentration (effective relative permittivity) led to an increase in the evaluating parameters, we concluded that the relative permittivity and surface charge are related, and we developed a correction charge model. The numerical simulation results with the charge correction showed that the evaluating parameters increased with the increase in nanoparticle concentration (effective relative permittivity) and were comparable to experimental results from other authors.

CONCLUSION

This work has shown that finite-element simulations can be used for nanoparticle doping optimization. Also, a charge correction was developed relating between the surface charge density and relative permittivity, with the results agreeing with experimental results from other researchers This opens a new way to reduce time and resources used in enhancing triboelectric materials with nanoparticles performance.

REFERENCES

1. S. Niu et al., "Theoretical study of contact-mode triboelectric nanogenerators as an effective power source," Energy Environ. Sci., vol. 6, no. 12, pp. 3576–3583, (2013), doi: 10.1039/c3ee42571a.
2. Callaty, C.; Gonçalves, I.; Rodrigues, C.; Ventura, J. Modeling the performance of contact-separation triboelectric nanogenerators. Current Applied Physics 2023,50, 100–106. doi: 10.1016/j.cap.2023.03.013.

ACKNOWLEDGMENTS

The authors acknowledge funding from projects 2022.05- 030.PTDC and UIDB/04968/2020 from FCT. FSE/POPH, FEDER, COMPETE and ON2 are also acknowledged. C. Rodrigues is thankful to FCT for grant SFRH/BD/147811/2019.

Hydrogen production through oxidative steam reforming of simulated bio-oil aqueous fraction using Co/CeSBA-15 catalysts

Carlos A. Chirinos[1], Pedro J. Megía[1], Arturo J. Vizcaíno[1], José A. Calles[1,2] and Alicia Carrero[1,2,*]
[1]Chemical and Environmental Engineering Group, Universidad Rey Juan Carlos, Móstoles, Spain
[2] Institute of Sustainable Technologies, Universidad Rey Juan Carlos, Móstoles, Spain
[*] Corresponding author (alicia.carrero@urjc.es)

INTRODUCTION

Fossil fuel prices have decreased since their 2022 peaks, yet markets continue to show tension and volatility[1]. Clean energies, particularly hydrogen-based technology, are emerging as a promising alternative for international economic growth[2]. There is a growing interest in combining fast pyrolysis of biomass with steam reforming of bio-oil aqueous phase for efficient biomass-to-energy processes. In this regard, oxidative steam reforming (OSR) is more energy-efficient than traditional steam reforming due to the exothermic partial oxidation reactions while decreasing coke deposition. Developing effective reforming catalysts is a crucial challenge to achieve both high hydrogen yield and stability. In this work, we study the effect of CeO_2 addition to Co/SBA-15 in the catalytic performance of simulated bio-oil aqueous fraction oxidative steam reforming.

EXPERIMENTAL STUDY

To be used as catalyst supports, a series of CeO_2-SBA-15 (Ce: 0-30 wt.%) were prepared by incipient wetness impregnation. Co as the active metal was later incorporated (7 wt.%) following the same procedure. All the samples were characterized by TGA, ICP-AES, DRX, H_2-TPR, and N_2 adsorption. The catalytic tests were carried out in a fixed bed reactor (Microactivity-Pro unit) at 550ºC and atmospheric pressure.

RESULTS AND DISCUSSION

In a preliminary study, the effect of CeO_2 incorporation to SBA-15 (Ce: 0-30 wt.%) was accomplished in the OSR of acetic acid as a representative compound of the bio-oil aqueous phase. The samples with 10 and 20 wt.% of Ce reached the best catalytic performance achieving high hydrogen yields, over 55%, at moderate temperatures (550 ºC). Both samples were thus tested in the OSR of acetic acid (AA), methanol (MeOH), and acetol (AC), at long-term tests reaching almost complete conversions in all cases with slightly higher hydrogen yields for Co/10CeO_2-SBA15. This sample, demonstrating a better catalytic performance, was also tested in the OSR of a mixture of AA, MeOH, and AC simulating a real bio-oil aqueous phase. The results are displayed in Fig. 1. Despite a decrease in total conversion over time, hydrogen yield was maintained at acceptable levels after 50 h time-on-stream.

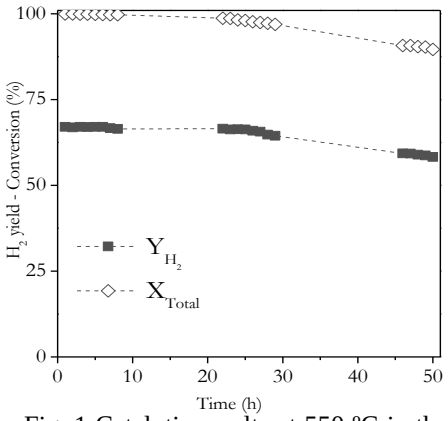

Fig. 1 Catalytic results at 550 ºC in the OSR of simulated bio-oil aqueous phase using Co/10CeO_2-SBA15.

CONCLUSION

Adding CeO_2 to Co/SBA-15 in the OSR of AA enhances hydrogen production. Specifically, the sample Co/10CeO_2-SBA-15 showed the best catalytic performance in the OSR of pure AA, MeOH, and AC, as well as in the OSR of simulated bio-oil, reaching high hydrogen yields at 550ºC.

REFERENCES

1. International Energy Agency (IEA), World Energy Outlook 2023 - IEA, World Energy Outlook 2023. (2023).

2. P.J. Megía et al., Energy and Fuels 35, 16403–16415 (2021).

ACKNOWLEDGMENTS

The authors acknowledge the financial support from the Spanish Ministry of Science and Innovation (Projects PID2020-117273RB-I00 and TED2021-131499B-I00).

The H2Excellence Project - Fuel Cells and Green Hydrogen Centers of Vocational Excellence towards affordable, secure, and sustainable energy for Europe

A.J. Gano, P.R. Pinto, M.A. Esteves, C.M. Rangel
LNEG - National Laboratory for Energy and Geology, I.P. Lisbon, Portugal

INTRODUCTION

The demand for green hydrogen (H2) and related technologies is expected to increase in the coming years mainly framed by drivers such as climate change and energy security of supply amid the European and global energy crises. REpowerEU Plan[1] called for an intensification of hydrogen delivery targets, that will bring large-scale adoption of hydrogen production and applications in various sectors, stressing the need for a skilled workforce in the emergent hydrogen markets. To that end, the Erasmus+ European H2Excellence transnational project[2] has gathered 24 partners across the EU, to establish a Platform of Vocational Excellence in the field of fuel cells and green hydrogen technologies, with an educational and training offer that will tackle identified skill gaps and implement life-long learning opportunities. The project aims to become a benchmark in training and knowledge transfer, contributing to the integration of quality employment into green hydrogen local innovative systems approaching the entire hydrogen value chain.

OBJECTIVES

The project started in 2023 and will create a set of national Centers of Vocational Excellence (CoVE's) dedicated to fuel cells and green hydrogen technologies, establishing a collaborative transnational network to bridge industry skill gaps in the field. The Portuguese partners include Inst. Politécnico de Portalegre (IPP), Inst. de Soldadura e Qualidade (ISQ), EnergyIN, and Lab. Nacional de Energia e Geologia (LNEG), which will contribute to implementing a solid collaborative education-business-research network at a pan-European scale, through an international online platform/knowledge hub for e-learning, and onsite training sharing on green hydrogen technologies. The project structure is shown in Fig. 1.

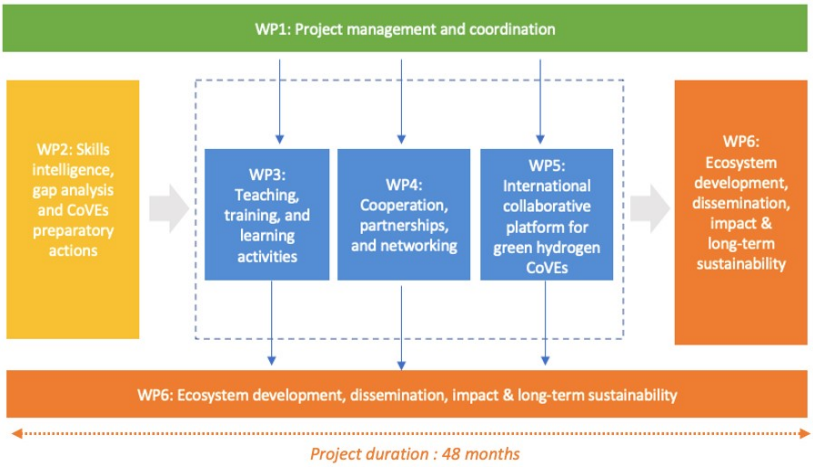

Fig 1. - Project development structure and workplan.

EXPECTED IMPACTS OF PROJECT RESULTS

During the 4 years of the project's duration, it is expected to develop and deliver custom training tools, using e-learning and onsite methodologies, and provide education and training that will upskill and reskill the hydrogen sector workforce, directed towards enforcing competencies, in line with market requirements. It will also promote collaboration and mobility of employees, supporting SME's needs across the value chain.

CONCLUSION

The Erasmus+ European H2Excellence Project's strategic and specific objectives concern the development of custom advanced training and tools for students, young engineers, and staff of companies related to the green hydrogen industry. Aims to provide alignment of those manpower skills with the market needs, fostering the key role of clean hydrogen as a building block in the energy transition and challenges of decarbonization.

REFERENCES

1. European Commission, Implementing the Repower EU Action Plan, https://eur-lex.europa.eu/legal-content/EN/TXT/PDF/?uri=CELEX:52022SC0230, 2024
2. H2Excellence - Green skills for the future workforce in fuel cells and green hydrogen sector, https://h2excellence.eu/, 2024

ACKNOWLEDGMENTS

Funded by the European Union

Funded by EU ERASMUS+ Programme. Grant Agreement n° 10110444.

Poly(2,2,6,6-tetramethylpiperidine-N-oxyl-4-vinyl ether)-impregnated carbon nanotube cluster for high-properties organic battery

Chaekyung Kim, Jae-Kwang Kim*

Department of Energy Convergence Engineering, Cheongju University, Cheongju, Chungbuk 28503, Republic of Korea
Corresponding author`s *E-mail:* jaekwang@cju.ac.kr (J.-K. Kim)

INTRODUCTION

Organic radical batteries undergo charging through a redox reaction, differing from the ion exchange mechanism employed by lithium-ion batteries. Utilizing environmentally friendly organic polymer electrode materials allow for enhanced charging and discharging rates, with further improvements achievable through the deliberate design of the active material structure. Nevertheless, challenges arise due to the dissolution of the active material in the organic electrolyte, leading to pronounced self-discharge. Additionally, the low electrical conductivity of the organic polymer necessitates a heavy reliance on conductive materials, resulting in significant capacity degradation. In this study, the active material was fabricated by incorporating an organic active material into carbon nanotube clusters through an infiltration process. It was confirmed that achieving a stable theoretical capacity in the organic radical battery was possible by reducing its dependence on conductive materials and incorporating a higher proportion of active materials. Electrochemical properties of PTVE cell are improved by enhanced electro transfer and interaction of organic active materials with the intermolecular bonding of the carbon matrix.

EXPERIMENTAL/THEORETICAL STUDY

To prepare a PTVE-impregnated carbon nanotube cluster, 0.2g of PTVE dissolved in NMP and mix with 0.05g of carbon nanotube cluster in a rotary evaporator. After concentrating at room temperature for 3 hours, the solution is heated in a heating bath at 60°C and completely dried. The dried powder is finally dried in a vacuum oven at 80°C to obtain solid active material.

RESULTS AND DISCUSSION

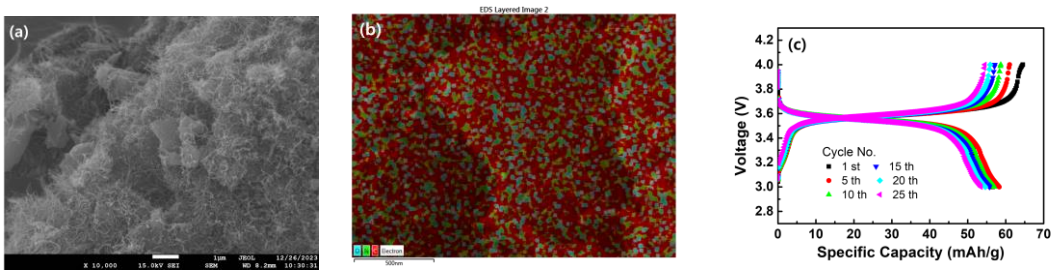

Fig 1. (a) FE-SEM image of PTVE infiltrating the inside of the carbon nanotube cluster (b) EDS Image of PTVE-impregnated-Carbon nanotube cluster (carbon, oxygen, and nitrogen) and (c) charge-discharge graph of PTVE-impregnated-carbon nanotube cluster.

CONCLUSION

FE-SEM results confirmed the successful infiltration of PTVE into the CNT cluster. EDS analysis further verified the uniform mixing and support of PTVE and CNT. The corresponding values at cycles 1, 5, 10, 15, 20, and 25 were 56.6, 58.3, 57, 55.7, 54.6, and 53.5 mAh/g. Evaluation after cell fabrication revealed that the PTVE contained within the carbon nanotube did not dissolve in the electrolyte, demonstrating effective charging and discharging performance consistent with the active material ratio.

Recycling Carbon-based Water Filters for Hydrogen Storage: a sustainable approach

Antonella Glisenti [1,2], Gabriel Merlin [1], Chiara Pierantoni [1*]
[1]Dept. of Chemical Sciences, University of Padova, Via F. Marzolo 1, Padova, Italy
chiara.pierantoni.2@studenti.unipd.it, presenting author, corresponding author
[2]ICMATE-CNR, Dept. of Chemical Sciences, Via F. Marzolo 1, Padova, Italy

INTRODUCTION

Due to its outstanding properties, hydrogen is really attractive as a replacement for the traditional polluting fossil fuels. However, in order to implement a Hydrogen Economy system based on the use of H_2 as an energy vector and fuel, advanced technologies need to be developed for its storage[1]. Among the different solutions studied, storage in solid materials stands out for being particularly safe and efficient, while also being fit for mobile applications[2]. ACs have especially shown excellent candidates for the adsorption of H_2 due to their high surface area and porosity and low weight. The aim of this work was to evaluate the hydrogen storage potential of a recycled AC material recovered from exhausted water filters, and to optimize it for this purpose by operating on its textural properties and atomic composition.

EXPERIMENTAL/THEORETICAL STUDY

Different parameters were investigated for the optimization of the spent activated carbon (SAC). First, the influence of granulometry was investigated with samples ground at different particle sizes. A chemical activation with KOH was performed to increase the SAC's specific surface area (SSA), and the resulting product was washed with two different methods, namely water and acetic acid+water, to determine the effect of an acid wash on the obtained material. Lastly, a doping process was performed to introduce N heteroatoms using urea as a nitrogen precursor. For all samples, extensive analysis of the textural parameters (SSA and Pore Size Distribution) was performed by gas adsorption with N_2 and CO_2, while hydrogen uptake measurements were performed to evaluate the material's performance in H_2 storage. Additionally, the samples were investigated via scanning electron microscopy, energy dispersive spectroscopy, elemental analysis, X-ray photoelectron spectroscopy and X-ray diffraction.

RESULTS AND DISCUSSION

The SACs were found to be highly microporous (85-100%) and impure, due to the presence of metal ions and polymeric materials used as binders for the production of water filters. No clear trend was observed for the SSA with decreasing particle size, due to the destruction of part of the microporous network that takes place with a greater comminution degree. Activation with KOH resulted in an increase of the SSA of the samples with an increase factor that ranged from 2.2-2.9, reaching over 2000 m^2/g, and enlargement of the widths of the pores present. Although washing with acetic acid did not show clear improvements of the textural properties of the material, SEM, EDS and XPS analyses showed that washing the activated sample with acetic acid effectively removes the ashes produced during the reactions with KOH, resulting in a purer product. Hydrogen storage capacities of more than 2% were reached considering measurements taken at 77 K and 1 bar. Correlation of the obtained values with different textural parameters evidenced the relevance of SSA, total pore volume and presence of ultra-micropores for the adsorption of H_2. Doping with urea resulted in the introduction of N heteroatoms (0.41% wt) and an improvement of 17% of the hydrogen storage performance of the material.

CONCLUSION

It was found that regeneration of SAC recycled from exhausted water filters results in materials with very high SSA and developed porosity, with promising hydrogen storage performances. Furthermore, the hydrogen uptake of this materials can effectively be improved through doping, using urea as a nitrogen precursor.

REFERENCES

1. P. Prachi R. et al, Advances in Energy and Power, vol. 4, no. 2, pp. 11–22 (2016)
2.P. Ramirez-Vidal et al, Int J Hydrogen Energy, vol. 47, no. 14, pp. 8892–8915, (2022)

(HE) Hydrogen Energy

Biaryl asymmetric dialdehydes and 4,4'-(((diphenylsilanediyl)bis([1,1'-biphenyl]-4',4-diyl))bis(oxy))bis(2-((2-ethylhexyl)oxy)aniline) as monomers for the preparation of silicon-containing poly(azomethine)s. Synthesis and properties

Danitza Pavez-Lizana[1], Jean Medina[1], René A. Hauyon[1], Luis E. García[1], Enzo B. González[1], Ignacio A. Jessop[2], Carmen M. González-Henríquez[3], Patricio A. Sobarzo[1], Alain Tundidor-Camba[1], Claudio A. Terraza[1]

[1] Research Laboratory for Organic Polymers (RLOP), Faculty of Chemistry and of Pharmacy, Pontificia Universidad Católica de Chile, P.O. Box. 306, Post 22, Santiago, Chile. (cterraza@uc.cl)

[2] Department of Chemistry, Universidad de Tarapacá, Arica, Chile

[3] Chemistry Department, Universidad Tecnológica Metropolitana, P.O. Box 9845, Post 21, Santiago, Chile.

INTRODUCTION

Highly π-conjugated polymers, have attracted the attention of researchers and technological companies since the discovery of conducting polymers by Shirikawa et al. due to their ubiquitous potential in industrial, technological and everyday life applications[1,2].

RESULTS AND DISCUSSION

New difunctional monomers were synthesized; four asymmetric dialdehydes and a symmetric diamine containing a tetraphenylsilane (TPS) unit as a central element. Subsequently, four silylated poly(azomethine)s were prepared by polycondensation in solution at high temperature. Structural characterization of precursors, monomers and polymers was carried out using EA, FT-IR and 1D/2D NMR techniques. The polymers were characterized according to molecular weight, solubility, thermal and electronic properties (UV-vis, PL and cyclic voltammetry) and the results allow to propose them as optoelectronic materials, active layer in solar cells for example.

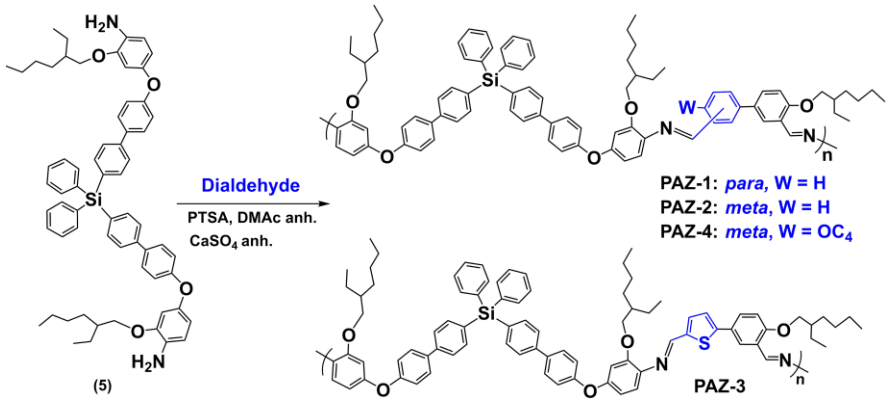

Fig. 1 Synthesis of TPS-containing poly(azomethine)s.

CONCLUSION

New silylated polymeric materials with potential applications in the opotoelectronic field were prepared and characterized. The thermal stability and bandgap values shown by the poly(azomethyl)s were in good agreement with materials for active layer in organic solar cells.

REFERENCES

1. H. Shirakawa et al., J. Chem. Soc. Chem. Commun. 578 (1977)
2. L. Ding et al. Chem. Rev. 123, 7421 (2023)

ACKNOWLEDGMENTS

This work was supported by Fondo Nacional de Desarrollo Científico y Tecnológico, FONDECYT (grant no. 1200390, 1230090).

Performance evaluation of an AEM electrolysis cell using a reinforced Sustainion® X37-50 membrane

C.Caravaca*, L. Quevedo Hernández, P. Ferreira Aparicio and J.L. Serrano
Energy Department/CIEMAT, Avda. Complutense, 40, 28040 Madrid, Spain
*Corresponding author (c.caravaca@ciemat.es)

INTRODUCTION

Hydrogen technologies play a crucial role in the challenge of reducing carbon emissions from industrial processes and economic sectors. Current methods of hydrogen production heavily rely on fossil fuels, with significant CO_2 emissions[1]. The main obstacle for the development of a sustainable renewable hydrogen energy system is the production of cost-competitive clean hydrogen at a large scale. One way to reduce these costs is to produce green hydrogen through water electrolysis using electricity from renewable sources. In recent years, Anion Exchange Membrane (AEM) electrolysers have gained popularity due to some operational and capital cost benefits[3]. This study aims to evaluate the electrochemical performance of an AEM electrolysis cell under various experimental conditions.

EXPERIMENTAL/THEORETICAL STUDY

The electrochemical performance of a 5 cm^2 anion exchange membrane (AEM) cell was evaluated using polarisation curves and electrochemical impedance spectra (EIS). The cell's behaviour during short-period electrolysis was also recorded by limiting the voltage to 2.2 V. As catalysts, commercial[4] Ni_2FeO_4 and Ni-Raney were used for the anode and cathode, respectively and using a Sustainion® X37-50 GT[4].

RESULTS AND DISCUSSION

The effect of liquid electrolyte concentration on AEM electrolysis performance was evaluated changing the concentration from 0.1 to 1.0 M KOH at 40 °C using flowrate of 26.6 mL min^{-1}. Fig. 1 A) shows the polarization curves obtained with the Sustainion® X37-50 membrane. A clear increase in the current density, and therefore in performance, is observed as the electrolyte concentration is increased, which is attributed to an increase of the ionic conductivity of the membrane. The effect of temperature on the cell performance is shown in Fig.1 B) where the highest performance is obtained at 50 °C attaining a current density of 0.23 Acm^{-2} at 2.2 V. It is also observed that except at an initial period, the current density remains quite stable along the electrolysis.

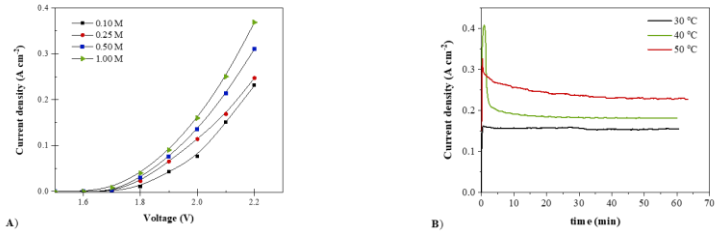

Fig. 1 A) Effect of KOH concentration on polarisation curves at 40 °C. B) Temperature effect on the current density during electrolysis at 2.2 V(0.1 M KOH). Sustainion® X37-50 AEM membrane.

CONCLUSION

This study aimed to assess the impact of various operational factors on the AEM electrolysis cell such as the increase of the KOH concentration from 0.1 M to 1.0 M that led to a 67% rise in current density. Similarly, the increase in temperature produces an increase in current densities due to an increase in the membrane's ionic conductivity.

REFERENCES

1. M. Nasser et al., Environ. Sci. Pollut. Res. 29 (58), 86994 (2022)
2. J.M. Thomas et al., J. Energy. Chem. 51, 405 (2020)
3. N. Chen et al., Energy Environ. Sci. 14(12)6338 (2021)
4. Dioxide Materials. https://dioxidematerials.com/

Modeling and technical-economic analysis of a hydrogen transport network for France

Daniel DE WOLF [1,2], Christophe MAGIDSON [2] and Jules SIGOT[2]
[1]Département Economie Gestion/TVES, University of Littoral, France, presenting author
[2]Louvain School of Management/CORE, UCLouvain, Belgium,

INTRODUCTION

This work aims to study the technical and economical feasibility of a new hydrogen transport network by 2035 in France. The goal is to furnish the charging stations for fuel cell electrical vehicles with a hydrogen produced by electrolysis of water using low carbon energy. What is new compared to previous research work on hydrogen transport (see André et al [1] or Reuß et al [2]) is the use of low-carbon electricity to produce green hydrogen.

EXPERIMENTAL/THEORETICAL STUDY

On the demand side, we assume that all drivers driving more than 20,000 km per year will switch to fuel cell electrical vehicles. This corresponds to a total demand of 100TWh of electricity for the production of hydrogen by electrolysis. To meet this demand, we primarily use surplus electricity production from wind power. This surplus will satisfy approximately 10% of demand. We assume that the rest of the demand will be produced using the surplus from nuclear power plants. We assume decentralized production, namely that 100 MW electrolyzers will be placed near the electricity production plants. Using an optimization model, we define the transport network for this hydrogen between the points of supply and the points of demand (the regions of France).

RESULTS AND DISCUSSION

Given the short distances between supply and demand, the model established that all hydrogen will be delivered by truck. The total annual cost of this network was estimated at 502 638 644€, which corresponds to €0.31€/kgH2.

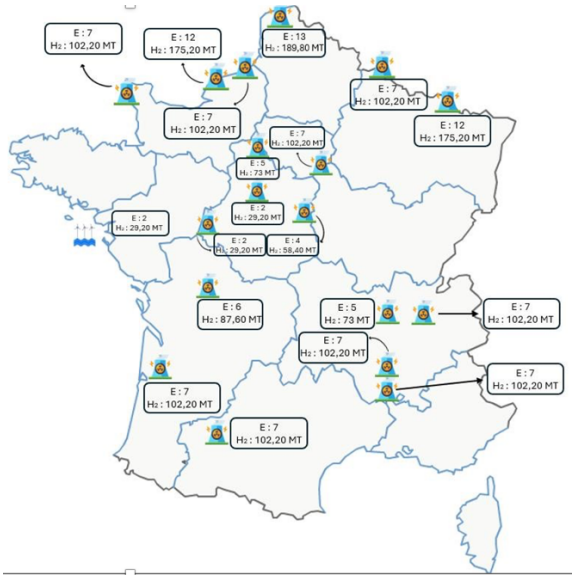

Fig. 1 Decentralized production of low carbon hydrogen

CONCLUSION

The comparison with more centralized production envisaged in Germany makes shows a reduction of a factor of 2 in this distribution cost with a decentralized production.

REFERENCES

[1] J. André, S. Auray, J. Brac, D. De Wolf, G. Maisonnier, M. Ould-Sidi, A. Simonnet, Design and dimensioning of hydrogen transmission pipeline networks, European Journal of Operational Research, Volume 229, Issue 1, 16 August 2013, pp 239-251.
[2] M. Reuß, P. Dimos, A. Léon, T. Grube, M. Robinius, and D. Stolten, Hydrogen Road Transport Analysis in the Energy System: A Case Study for Germany through 2050, Energies, vol. 14, no. 11, p. 3166, May 2021.

STRUCTURAL, OPTICAL, AND PHOTOCATALYTIC DEGRADATION OF PHARMACEUTICALS BY SINTERED Sn-ZnO COMPOSITE

Daphne Mary John[1,2], Yadhu J Nair[1,2], Lasya P[1,2], K. M. Sreekanth[*1,2], G. Sivasubramanian[1,2], K.M. Sreedhar[3],

1. Department of Sciences, Amrita School of Physical Sciences, Amrita Vishwa Vidyapeetham, Coimbatore, India-641112, Daphne Mary John.
2. Advanced Multifunctional Materials Laboratory (AMMAL), School of Engineering, Amrita Vishwa Vidyapeetham, Coimbatore, India-641112, K. M. Sreekanth (km_sreekanth@cb.amrita.edu).
3. Department of Chemistry, Amrita Vishwa Vidyapeetham, Amritapuri, Kerala, India.

INTRODUCTION

Pharmaceuticals in water is one of the growing problems of global concern, and it has been found that a greater part of the pharmaceutical wastewater produced worldwide is repudiated without any treatment [1]. Metal oxides help in the cost-effective degradation of these harmful pollutants using light, and doping makes it further effective [2]. Sintering is a method by which the powdered composite is transmuted to a strongly bonded colossal by removing inter-particle pores [3].

EXPERIMENTAL/THEORETICAL STUDY

10 grams of commercial ZnO is taken and layered in a silica crucible, and then 3 grams of Sn plates, finely scrapped into small pieces, is added over the ZnO layer. Then, 3 grams of the same ZnO is added as the top layer. The prepared composite is heated at 650^{o}C for 4 hours. The silica crucible containing the sample is allowed to cool at room temperature for 3 hours. The sample is taken out and ground in the mortar for size reduction. The sample is again heated to 650^{o}C for 6 hours, and the same procedure is repeated as above.

RESULTS AND DISCUSSION

In this work, Sn-ZnO composite was synthesized using the solid-state sintering method, and its elemental analysis, structural properties, optical properties, and morphological analysis were investigated using Energy Dispersive X-ray Spectroscopy (EDS), X-ray diffraction (XRD), UV-Vis spectrophotometer, Field Emission Scanning Electron Microscope(FESEM). Finally, the photocatalytic degradation of sulphanilamide and sulfamethazine under sunlight was studied using the UV-vis spectrum.

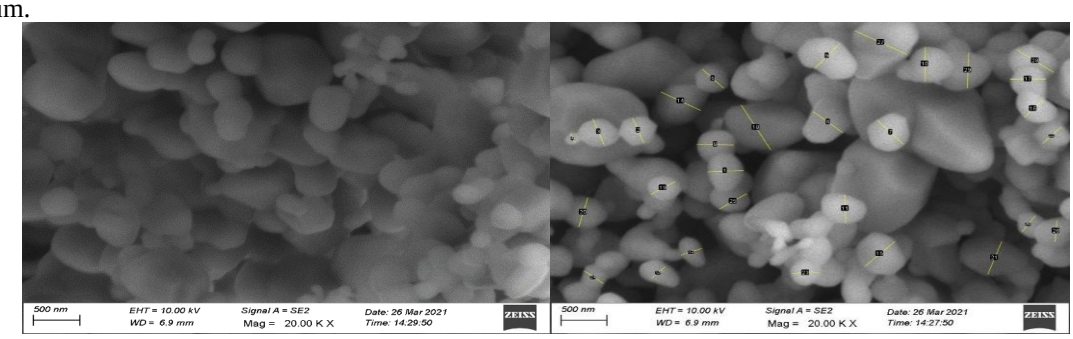

Fig. 1 FESEM image of Sn-ZnO

The size and shape of the particle can be determined by using FESEM. Figure 1 shows an agglomerated composite and the particle size is calculated to be 387.45±120 nm by image j software shown in the figure above.

CONCLUSION

Advanced and cost-effective synthesis of Sn-ZnO using the Sintering method is used to make a photocatalyst for the degradation of pharmaceuticals. The band gap of the synthesized composite is calculated from the Tauc plot. XRD determined the structural properties. FESEM shows the formation of the neck region, which helps to increase the surface area for photocatalysis. EDX plot reveals the elemental composition present in the composite. Photocatalytic degradation of sulfamethazine and sulfanilamide is due to the increase in defects with sintering, the increase in surface area due to the formation of the neck region, and also the high intensity of sunlight. So, this composite has enhanced properties that enable it to be a versatile component for industrial applications. Bandgap modification by the introduction of dopant at different concentration using solid-state sintering is a pathway to the advanced world of optoelectronics. Photocatalytic degradation of toxic elements organic dyes and pharmaceuticals using metal oxide semiconductors under sunlight is a breakthrough to green earth and good health.

REFERENCES

[1] C. Gadipelly et. al, American Chemical Society, pp. 11571–11592, (2014)
[2] J. E. Blendell and W. Rheinheimer, Elsevier, (2020)
[3] Athira Krishnan et al., Journal of Environmental Sciences, Volume 139, (2024)

Assessment of degradation effects of intermittent supply in PEM electrolyzers.

David Botana Vilanova [1,2], Araceli Fuerte[1] and Paloma Ferreira-Aparicio[1*]
[1] Department of Energy, CIEMAT, Spain
[2] Departamento de Ingeniería Química Industrial (Escuela Técnica Superior de Ingenieros Industriales), Universidad Politécnica de Madrid, España, presenting author (david.botana@ciemat.es)
[*]Corresponding author (paloma.ferreira@ciemat.es)

INTRODUCTION

The development of technologies to promote the use of clean and renewable energies able to replace fossil fuels has become an urgent issue with the aim of reducing greenhouse gas emissions. The storage of energy from renewable sources such as wind or solar energies at production peaks using energy carriers like hydrogen is of great interest due to their naturally intermittent character and highly uneven spatial distribution. Water electrolysis (WE) is one of the best methods for hydrogen production on a large scale, being proton exchange membrane (PEM) technologies, due to its characteristics, one of the most suitable options for its integration with intermittent energy sources.[1] Unfortunately, all the stack components suffer from corrosion problems to a lesser or greater extent.[2] The high manufacturing cost of PEMWE stacks and the degradation of their components are one the main barriers for wide spreading this technology. Corrosion and degradation problems are increased when the electrolyzer operates under the fluctuating conditions typically imposed by renewable energy power. This study analyzes the degradation of the materials in the internal components of PEMWE cells submitted to fluctuations of power, simulating the direct integration of WE systems with wind energy.

EXPERIMENTAL STUDY

The evaluation of a stack with state-of-the-art components under stationary and transient operation condition is carried out to analyze the problems that may arise when it is associated with intermittent energy sources. Different tests measuring voltage and current along with time are carried out. Both, in-situ characterization analysis by means of electrochemical impedance spectroscopy, and postmortem analysis of components with cross-section examination of membranes and electrodes after long-term operation and accelerated stress tests are performed.

RESULTS AND DISCUSSION

Data from the long-term operation of PEMWE cells comparing stationary and transient operation are evaluated, including accelerated stress tests. SEM analysis of cross-section of components are evaluated that provide interesting information about the effects of transient operation in PEMWE cells.

CONCLUSION

The objective of this work is studying the effects of the direct coupling of a PEM type electrolyzer to renewable energy sources, especially wind turbines, and trying to minimize the problems associated with the characteristic intermittency of this kind of energy sources. According to the proposed methodology, a single cell electrolyzer is analyzed after operation under stationary and transient regimes. Characterization of the cell during operation and postmortem analyses after operation provide valuable information about the main deactivation processes reducing the durability of the systems. This study is key to introduce adequate strategies to improve the useful life of components and systems.

REFERENCES

1. A. Mohammadi and M. Mehrpooya, “A comprehensive review on coupling different types of electrolyzer to renewable energy sources”. Energy 158, 632–655 (2018).
2. H. Kojima et al., “Influence of renewable energy power fluctuations on water electrolysis for green hydrogen production,” Int. J. Hydrogen Energy 48(12) 4572–4593 (2022).

ACKNOWLEDGMENTS

Authors acknowledge the Regional Government of Madrid and the MCIN of Spain for financing the GREENH2CM project through the Recuperation and Resilience Mechanism with NextGenerationEU funds (PRTR-C17.I1).

Optimization of Metal-Supported Intermediate-Temperature Solid Oxide Fuel Cells (MS-IT-SOFCs) for electrical energy production

Prof. Dr Didier Fasquelle

Unité de Dynamique et Structure des Matériaux Moléculaires (UDSMM)
Université du Littoral Côte d'Opale (ULCO), BP717, 62228 Calais, France

E-mail address: didier.fasquelle@univ-littoral.fr

Solid oxide fuel cells (**SOFCs**) are promising devices for energy-conversion applications due to their high electrical efficiency and eco-friendly behavior. Nowadays, commercial SOFCs are electrically efficient at high operating temperatures, typically between 800 and 1000°C. This high-temperature range restricts their real-life applications, but also their lifetime. Our basic goal deals with the objectives to reduce the operating temperature by working in the range from 500 to 700°C. Among SOFCs, metal-supported intermediate-temperature solid oxide fuel cells (**MS-IT-SOFCs**) may provide very cheap SOFC cells with increased lifetime and reduced operating temperature. In view to develop highly efficient electrodes and fuel cells, this presentation will be divided in 2 parts. The first part focuses on the physical and electrical characterizations of porous **GDC-backbones** which have been impregnated with **LSCF** sol-gel solutions and NiO solutions, for composite cathodes and anodes, respectively. The porosity of the backbone was controlled by the addition of different pore-formers. The performance of different samples was compared by studying the evolution of the electrical resistivity in function of temperature. An important effect has been demonstrated: whatever the temperature, from **500 to 700°C**, the resistivity can be tuned both by the solution viscosity and by the kind of pore-former. The second part is dedicated to the complete fabrication of **Metal-Supported Intermediate-Temperature SOFCs** (MS-IT-SOFCs). These cells were studied from **600 to 750°C**. In function of the developed structures and test conditions, we have measured values of the **power density** ranging from **150 to 520 mW/cm^2**. These highly interesting results will be presented during the conference in Aveiro.

Key Words: GDC, LSCF, pore-former, oxide, cathode, anode, MS-IT-SOFC.

Acknowledgements: We want to thank the Region Hauts de France, and the University du Littoral Côte d'Opale (ULCO) for their financial support during the PhD studies of Sarra Belakry (2018-2022).

Performance Characteristics of HfO_2/Al_2O_3 Nanolaminated Stacks for Application in Non-Volatile Flash Memorries

D. Spassov*, A. Paskaleva T. Stanchev, Tz. Ivanov
Institute of Solid State Physics, Bulgarian Academy of Sciences, 72 Tazrigradsko chaussee, Sofia, Bulgaria, *corresponding author (d.spassov@issp.bas.bg)

INTRODUCTION

The HfO_2-based stacks have recently focused the researchers' interest in terms of application in new generation non-volatile memories operating on charge trapping (CT) effect, as a replacement of the conventionally used ONO (SiO_2-Si_3N_4-SiO_2) charge trapping medium[1]. This interest is additionally strengthened by the fact that HfO_2 -based gate stacks are already used in the production of advanced microprocessors. In some recent works, we have demonstrated that nanolaminated HfO_2/AlO_3 and Al-doped HfO_2 stacks deposited by ALD possess promising application potential as charge trapping media for flash memories[2]. In the present work we report recent results on the performance (retention characteristics and speed of write/erase operations) of memory cells based on nanolaminated HfO_2/AlO_3 stacks.

EXPERIMENTAL

The test structures were MIS capacitors with Al gate and backside electrodes, in which 16.5 nm HfO_2/Al_2O_3 nanolaminated layers (5x(20cyHfO_2:5cyAl_2O_3)) were incorporated alongside with 20 nm Al_2O_3 blocking (BO) and thermal SiO_2 tunnel (TO) layers. The HfO_2/Al_2O_3 nanolaminated stacks and BO were deposited by ALD in a single low temperature technological process. Part of the samples received post deposition annealing in O_2. (More details on deposition conditions and test structures can be found in [2]). Two thicknesses of the TO – 2.4 and 3.5 nm were investigated. The retention characteristics were measured at room temperature and 85 °C. The response of the charge trapping to the width of the applied voltage pulse was investigated in the rage of $10^{-7} \div 0.3$ s at room temperature.

RESULTS AND DISCUSSION

It was found that retention characteristics were only slightly affected by the heating (Fig1a) which suggests that trapped charges reside in deep traps and the charge loss is governed mainly by tunnel effects. A noticeable electron trapping is observed at duration of the voltage pulse above 10^{-3} s (Fig.1b) and the resulting dependency is quite sharp. The program characteristics depend on the TO thickness, and available electron density in Si inversion layer. Full release of the rapped electrons was obtained at ~10^{-2} s, and for larger times positive charge builds up in the capacitors. The erase characteristics depend on TO thickness more strongly than program ones.

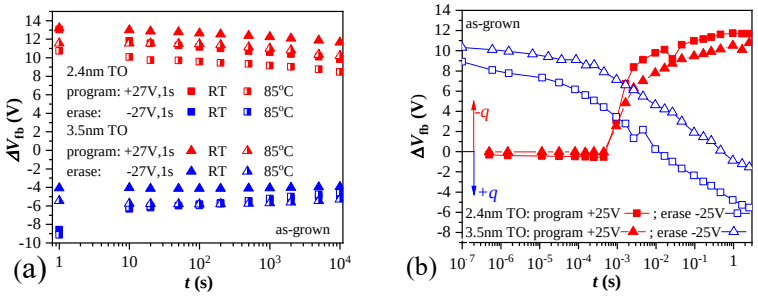

Fig. 1 Retention (a) and Program/Erase speed characteristics (b) of capacitors with as-grown HfO_2/Al_2O_3stacks.

CONCLUSION

The investigation of the performance characteristics of memory capacitors based on HfO_2/Al_2O_3 nanolaminates demonstrate their potential for flash memory applications. Additional work is required for optimization of program/erase speeds.

REFERENCES

1. C. Zhao et. al, Materials 7, 5117-5145 (2014)
2. D. Spassov, et. al, Materials 15, 6285 (2022)

ACKNOWLEDGMENTS

The work is supported by Bulgarian Science Fund under the project KP-06-H37/32.

Effect of the substrate temperature on the properties of Nb-doped TiO_2 thin films deposited by magnetron sputtering

Francisco Alfaro[1], Rafael G. Delatorre[1], Julio C. Sagás[2] and Diego A. Duarte[1]

[1] Joinville Center of Technology, Federal University of Santa Catarina, Brazil, presenting author (diego.duarte@ufsc.br)
[2] Center of Technological Sciences, Santa Catarina State University, Brazil

INTRODUCTION

Transparent conducting oxides like ITO and FTO are critical in solar cell technology due to their optical clarity and electrical conductivity[1]. Specifically, ITO typically has a resistivity in the order of 10^{-4} Ω·cm[2]. Notably, Nb-doped TiO_2 (TNO) is emerging as a competitive material for its transparency and conductive properties, crucial for optimizing the electronic structure in photovoltaic applications[3]. Advanced plasma-enhanced techniques such as magnetron sputtering are employed to finely tune material characteristics at an atomic level.

EXPERIMENTAL

TNO thin films were deposited on glass substrates using magnetron sputtering. Depositions were made at room temperature and 300°C from a 4-inch target composed of Ti with Nb inserts. The films were evaluated by two-point probe method, optical spectrophotometry (190-1600 nm range), and X-ray diffraction (XRD) analysis.

RESULTS AND DISCUSSION

Fig. 1 shows the transmittance of the samples deposited at room temperature and 300°C. Nb-doped films exhibit transmittance with averages around 76% in the visible and 62-63% in the infrared range. The resistivity for heated Nb samples was measured at about 10^{-2} Ω·cm for heated samples, contrasting with 10^{3} Ω·cm for non-heated samples. Optical bandgap values, ranging from 3.3 to 3.6 eV, were derived from Tauc plots. Analysis by XRD shows the anatase (101) phase for all samples (Fig. 2).

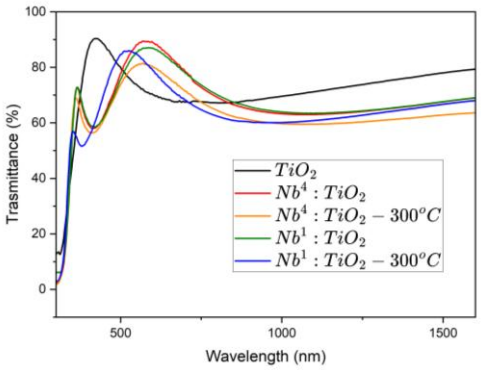

Transmittance for TiO_2 and Nb-doped TiO_2 films, deposited at 300°C and room temperature using targets with 1 and 4 Nb inserts.

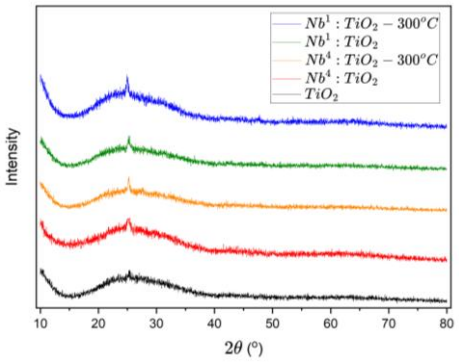

Fig. 2. X-ray diffraction (XRD) analysis for TiO_2 and Nb-doped TiO_2 films, deposited at 300°C and room temperature using targets with 1 and 4 Nb inserts.

CONCLUSION

Heat treatment significantly lowers the resistivity in Nb-doped samples, enhancing their viability for TCO applications. XRD analysis indicates a monocrystalline structure with the anatase phase. Future studies should employ grazing angle X-ray Diffraction (XRD) for a clearer understanding of the crystalline structure of these materials. Additionally, it is recommended to conduct X-ray Photoelectron Spectroscopy (XPS) and Scanning Electron Microscopy (SEM) measurements.

REFERENCES

[1] P. Basumatary, P. Agarwal. Materials Research Bulletin, 149 (2022) 111700.
[2] M.S. Farhan, et al. International Journal of Precision Engineering and Manufacturing. 14 (2013) 1465.
[3] Y. Furubayashi, et al. Applied Physics Letters, 86 (2005) 252101.

ACKNOWLEDGMENTS

The authors thank FAPESC (PAP-UDESC) and CNPq (grants nº 307408/2021-3 and 406376/2022-0).

Evaluation of Ni metallic states in Ni/Al_2O_3 catalysts obtained by chemical routes and magnetron sputtering

Diego A. Duarte[1], Augusto P. Cambunda[1], Jéssica F. Zeitoune[1], Andrey M. dos Santos[1], Maíra O. Palm[1], Teresa T. Steffen[2], Bruno F. Oechsler[1] and Rafael C. Catapan[1]

[1] Joinville Center of Technology, Federal University of Santa Catarina, Brazil, presenting author (diego.duarte@ufsc.br)
[2] Center of Technological Sciences, Santa Catarina State University, Brazil

INTRODUCTION

Supported-metal catalysts are commonly used in the chemical industry from fine chemical production to petrochemicals and generally consist of metallic particles, known as active phase, dispersed on the surface of a metallic oxide support with different geometrical formats[1,2]. They are usually produced by chemical routes that involve processes like thermal sintering in air, leading to decreasing of the catalyst activity due to the increase of metal oxides on its surface[1,2], where the production of catalysts in vacuum or inert environment such as those in magnetron sputtering systems (MS) may be an alternative to solve this issue[2]. Thus, the concentration of Ni metal states in Ni/Al_2O_3 catalysts produced by washcoating and MS was evaluated by X-ray photoelectron spectroscopy in this work.

EXPERIMENTAL

Catalysts were produced according to the experimental procedures described in previous works[1,2]. The chemical composition and electronic structure was evaluated by X-ray photoelectron spectroscopy (Thermo Scientific K-Alpha) from measurements of high-resolution spectra for the Ni2p, Al2p, O1s and C1s orbitals. The valence band was also investigated from the density of states measured between –10 and 30 eV.

RESULTS AND DISCUSSION

Fig. 1 shows the high-resolution spectra for the Ni2p orbital of the catalysts produced by washcoating and MS. The catalyst produced by MS presents a signal at 853 eV assigned to the metallic Ni^0 states and a decreasing of the signal assigned to the Ni^{2+} states at 854 eV, indicating a surface with higher concentration of metallic states.

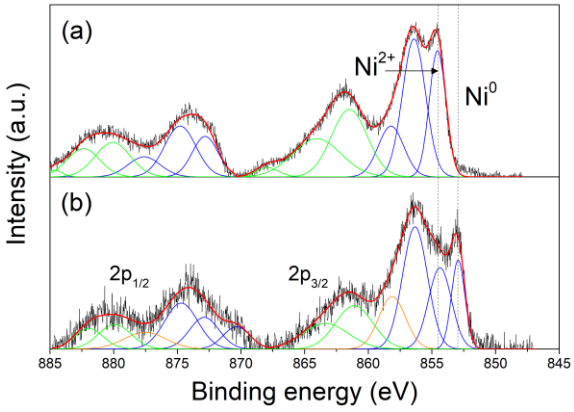

Fig. 1. High resolution spectra for the Ni2p orbital of the catalysts produced by (a) washcoating and (b) MS.

CONCLUSION

The manufacturing of Ni/Al_2O_3 catalysts by magnetron sputtering presents a higher concentration of metallic states and lower concentration of oxide compounds in comparison to catalysts produced by thermal route.

REFERENCES

1. M. O. Palm et al., Energy & Fuels 34, 2205 (2020)
2. A. M. Santos et al., Vacuum 200, 111042 (2022)

ACKNOWLEDGMENTS

Authors thank BMW Brazil Group (grant nº UFSC/2016/0110), Fundep Rota 2030 / Linha V (grant nº 27192.01.01/2020.01-00) and CNPq (grants nº 307408/2021-3 and 406376/2022-0).

Microwave-assisted hydrothermal synthesis of ZSM-5 zeolite

Camilla F.C. Nascimento[1], Jéssica Fagundes[1], Dirléia Lima[1*], Lucas Gomes[2], Isabel Tessaro1, Nilson Marcilio[1]
[1]Department of Chemical Engineering, Federal University of Rio Grande do Sul, Brazil
[2]Center for Studies in Petrology and Geochemistry, Federal University of Rio Grande do Sul, Brazil
dirleia.lima@ufrgs.br

INTRODUCTION

Zeolites are versatile materials of great interest due to their properties. ZSM-5 is widely employed in catalysis among zeolites due to its strong acidity and shape selectivity. Typically, ZSM-5 is synthesized using conventional hydrothermal methods. However, it can also be synthesized using microwave-assisted hydrothermal methods. This is because microwave (MW) results in the effective dissolution of precursors[1]. Rice husk ash (RHA) can be utilized as a silicon source in synthesizing zeolitic material, providing a cost-effective alternative to produce industrially and technologically relevant materials while mitigating pollution caused by this waste[2].

EXPERIMENTAL

Two dispersions were prepared for the synthesis of ZSM-5 zeolite. The first dispersion was obtained by adding sodium hydroxide and RHA to distilled water, and the second dispersion was prepared by adding aluminum sulfate to distilled water and sulfuric acid. After preparation, both dispersions were mixed, and the resulting dispersion was subjected to microwave treatment at powers of 260 W and 1300 W for 10 s. Afterward, the dispersion was aged for 30 minutes. Subsequently, 0.0393 mg of seed (commercial ZSM-5) was added to the mixture. The dispersion was then transferred to an autoclave reactor and placed in an oven at 190 ºC for 24 h. Afterward, the zeolite was washed with distilled water and dried at 80 ºC for 24 h. For comparison, ZSM-5 was synthesized without microwave treatment under the same conditions mentioned. The samples were characterized by X-ray diffraction, scanning electron microscopy and nitrogen physisorption analysis.

RESULTS AND DISCUSSION

According to the X-ray diffraction pattern in Figure 1, it is evident that the MW technology influences the crystallinity of the material, with an observed increase in peak intensity when employing microwave technology. Furthermore, characteristic peaks of ZSM-5 zeolite can be identified, with reflections typically at 2θ angles of 7.9º, 8.8º, 23.2º, 23.7º, and 24[1]. MW technology enhances textural properties (Table 1), suggesting that MW treatment improves the characteristics of the zeolitic material[1]. However, when evaluating only the materials obtained under the influence of MW, the increase in MW power results in a decrease in properties. This properties reduction may be related to the nucleation effect[3]; thus, at 260 W, the nucleation effects are more pronounced.

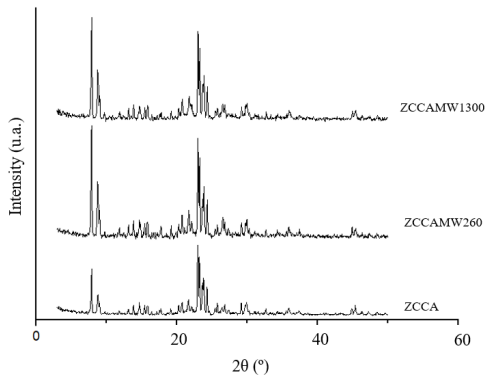

Figure 1- X-ray diffractogram

Sample	A_{bet} (m^2/g)	V_{micro} (cm^3/g)
ZCCAMW1300	292	0.094
ZCCAMW260	307	0.101
ZCCA	260	0.085

Table 1 – Textural properties of ZSM-5

CONCLUSION

The ZSM-5 zeolite was successfully synthesized using the microwave-assisted hydrothermal method and RHA. Microwave technology contributes to enhancing the properties of the zeolitic material. At a power of 260 W, a high A_{bet} of 307 m^2/g and V_{micro} of 0.101 cm^3/g were observed compared to other samples.

REFERENCES

1. S. Vichaphund et al., J Anal Appl Pyrol. 141, 104628 (2019)
2. K. Kordatos et al., Micropor Mesopor Mat. 115, 189196 (2008)
3. VICENTE, G. Síntese e propriedades da zeólita faujasita nanométrica aplicada à catálise básica (2015).

ACKNOWLEDGMENTS

To the Department of Chemical Engineering at UFRGS, CAPES, FAPERGS and CNPq for financial support.

Sustainability and innovation: CO_2 conversion by dry reforming of methane using nickel and nickel-cobalt catalysts on sustainable HZSM-5 supports

Dirléia Lima[1*], Helga Nogueira[1], Camilla Ferro[1], Isabel Tessaro[1] and Nilson Marcílio[1]
[1]Department of Chemical Engineering, Federal University of Rio Grande do Sul, Brazil
*dirleia.lima@ufrgs.br

INTRODUCTION

Among the various routes for controlling CO_2 emissions, including prevention, storage, and use, the main alternative is to use CO_2 as a raw material integrated into the CH_4 conversion process to produce syngas (H_2 + CO), known as dry reforming of methane (DRM). Syngas can be used as a feedstock for various chemical processes such as fuel cell and methanol synthesis and can be used as a feedstock for Fischer-Tropsch synthesis to produce long-chain hydrocarbons of high value. Ni-based catalysts are suitable for DRM due to their wide availability, moderate cost, and high turnover frequency[1]. However, they are prone to rapid deactivation due to the formation of carbonaceous deposits, generally of the encapsulated and graphitic type. It has been reported that adding a metal promoter influences the performance of Ni catalysts in DRM reactions. However, gasification promoters such as Ca, Co, Ce and La accelerate the oxidation of carbon deposits formed or improve the coverage of oxygenates[2]. ZSM-5 zeolite can be used as a support to improve Ni dispersion[1]. Furthermore, HZSM-5 zeolite can be synthesized using rice husk ash (RHA) as a silicon source, aiming to reduce costs and avoid using organic structure directing agents (templates) that are toxic and costly, making the most sustainable and economical process. In this context, Ni and Ni-Co catalysts were prepared supported on HZSM-5 zeolite synthesized using RHA without a template for subsequent application in the dry reforming of methane, aiming to obtain syngas.

EXPERIMENTAL

ZSM-5 zeolite was synthesized from a mixture of a basic dispersion (distilled water, NaOH and RHA), with an acidic dispersion (distilled water, aluminum sulfate and sulfuric acid). Afterward, the mixture was kept under constant stirring for 1 hour (aging stage). Next, the hydrogel was transferred to an autoclave containing the seed (ZSM-5 - CBV 2314 Zeolyst). This system was kept in an oven for 24 hours at 190 °C. Ion exchange was carried out with an ammonium nitrate solution and the sample was calcined in a muffle furnace for 2 hours at 600 °C. The catalysts were prepared using the synthesized HZSM-5 as a support. The metals (20 or 25 wt%) were impregnated by the excess solvent method using Ni and Co nitrates as precursors. Finally, they were calcined in a muffle furnace for 2 hours at 600 °C. The catalysts were characterized by X-ray diffraction. Nitrogen physisorption measurements, temperature-programmed desorption of ammonia, temperature-programmed reduction, scanning electron microscopy, thermogravimetry, and catalytic tests in the dry reforming of methane will also be realized.

RESULTS AND DISCUSSION

Figure 1 shows the X-ray diffractograms for the support (HZRHA) and the prepared catalysts. The reflection peaks characteristic of the HZSM-5 zeolite and the metallic oxides of Ni, and Co are observed, indicating that the preparation methodologies used were efficient.

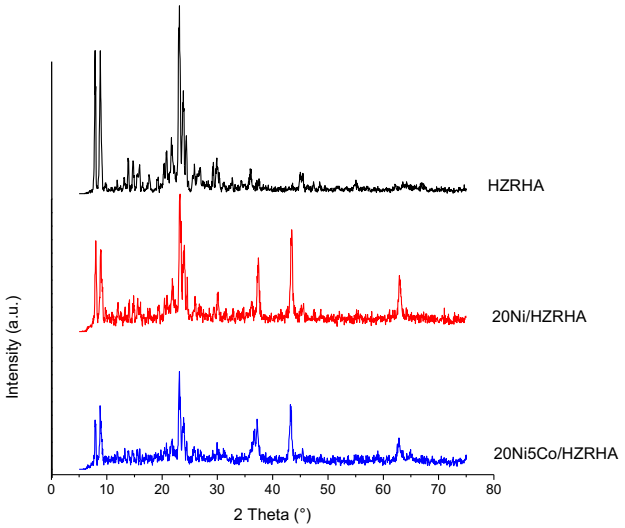

Figure 1. X-ray diffraction patterns for the prepared samples.

CONCLUSION

It was possible to obtain Ni and combined Ni-Co catalysts supported on HZSM-5 zeolite synthesized using a residue (RHA) as a silicon source and without a template.

This study highlights the importance of using greenhouse gases to generate valuable products through catalysts obtained from agro-industrial waste, contributing to a more sustainable environment.

REFERENCES

1. H.U. Hambali et. al, Chem. Eng. Sci. 227, 115952 (2020)
2. L. Zhang et. al, Fuel. 303, 121263 (2021)

ACKNOWLEDGMENTS

The authors acknowledge CAPES, FINEP, FAPERGS and CNPq for the financial support to carry out this work.

From waste to clean energy: Development of cost-effective and sustainable catalysts for hydrogen production via glycerol steam reforming

Dirléia Lima[1*], Helga Nogueira[1], Camilla Ferro[1], Robinson L. Manfro[2], Carlos A. Chagas[2], Isabel Tessaro[1] and Nilson Marcílio[1]
[1]Department of Chemical Engineering, Federal University of Rio Grande do Sul, Brazil
[2]School of Chemistry, Federal University of Rio de Janeiro, Brazil
*dirleia.lima@ufrgs.br

INTRODUCTION

Hydrogen production from the steam reforming of glycerol emerges as a promising alternative to adding value to this waste. Catalysts supported using Pt, Pd, Ru, Rh, Co, Ni, and alumina support have been studied due to their good catalytic activity and stability[1,2]. However, challenges such as catalytic deactivation due to carbon formation and sintering of metal particles are faced. To overcome these problems, doping with base metals, such as La and Mg[1], and using HZSM-5 zeolite as support can be used. Furthermore, HZSM-5 zeolite can be synthesized using rice husk ash (RHA) as a source of silicon, aiming to reduce costs and avoid the use of organic structure directing agents (templates) that are toxic and costly, aligning the process with sustainability and economic viability guidelines. In this context, the present study prepared Ni, Co, Ni-Mg, and Co-Mg catalysts supported on HZSM-5 zeolite synthesized using RHA without the use of a template for subsequent application in the steam reforming of glycerol, aiming to obtain H_2[1].

EXPERIMENTAL

ZSM-5 zeolite was synthesized from a mixture of a basic dispersion (distilled water, NaOH and RHA), which was taken to the ultrasound bath, with an acidic dispersion (distilled water, aluminum sulfate and sulfuric acid). The microwave was used on the resulting gel to dissolve the reagents better. Afterward, the mixture was kept under constant stirring for 1 hour (aging stage). Next, the hydrogel was transferred to an autoclave containing the seed (ZSM-5 - CBV 2314 Zeolyst). This system was kept in an oven for 24 hours at 190 °C. Ion exchange was carried out with an ammonium nitrate solution and the sample was calcined in a muffle furnace for 2 hours at 600 °C. The catalysts were prepared using the synthesized HZSM-5 as a support. The metals (20 or 25 wt%) were impregnated by the excess solvent method using Ni, Co, and Mg nitrates as precursors. Finally, they were calcined in a muffle furnace for 2 hours at 600 °C. The catalysts were characterized by X-ray diffraction. Nitrogen physisorption measurements, temperature-programmed desorption of ammonia, temperature-programmed reduction, scanning electron microscopy, thermogravimetry, and catalytic tests in the steam reforming of glycerol will also be realized.

RESULTS AND DISCUSSION

Figure 1 shows the X-ray diffractograms for the support (HZ) and the prepared catalysts. The reflection peaks characteristic of the HZSM-5 zeolite and the metallic oxides of Ni, Co, and Mg are observed, indicating that the preparation methodologies used were efficient.

CONCLUSION

It was possible to obtain Ni, Co, and combined Ni-Mg and Co-Mg catalysts supported on HZSM-5 zeolite synthesized using a residue as a silicon source and without a template. Applying these catalysts in the steam reforming of glycerol to obtain H_2 makes the process even more attractive, as it allows value to be added to two wastes, glycerol and RHA, and clean energy to be generated.

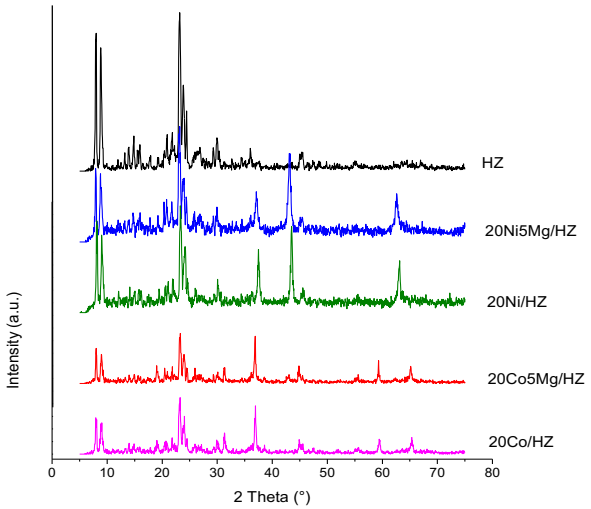

Figure 1. X-ray diffraction patterns for the prepared samples.

REFERENCES

1. D. Lima et. al, Biomass Bioenerg. 130, 105358 (2019)
2. A. Sandid et. al, Fuel Process. Technol. 253, 108008 (2024)

ACKNOWLEDGMENTS

The authors acknowledge CAPES, FINEP, FAPERGS and CNPq for the financial support to carry out this work.

Magnetic nanostructures for THz emitters with amplitude and polarization control

Elena Mishina * [1], Arseny Buryakov [1], Maksim Sapozhnikov [2] and Vladimir Preobrazhensky [1,3]
[1*]MIREA - Russian Technological University, Moscow, Russia, mishina_elena57@mail.ru
[2]Institute for Physics of Microstructures RAS, Nizhny Novgorod, Russia
[3]Prokhorov General Physics Institute of RAS, Moscow, Russia

INTRODUCTION

Over the past five years, it has become clear that to fully utilize THz radiation for spectroscopy, imaging, and other applications, it is necessary to develop a full line of devices that provide complete control of THz waves, including polarization control devices, modulators, amplifiers, and saturable absorbers[1]. Within the four main groups of THz emitters - nonlinear organic and inorganic crystals, semiconductor antennas and spintronic emitters - the latter provide the widest spectrum and the ability to control the parameters of THz waves. Here we present magnetic nanostructures with in-plane anisotropy that enable internal manipulation of THz wave amplitude and polarization solely by magnetic field strength.

EXPERIMENTAL/THEORETICAL STUDY

Two types of magnetic nanostructures were fabricated: the bilayer Co(3nm)/Pt(3nm) and spin valves Co(1,8nm)/Pt(3nm)/Co(1,8nm)/IrMn(5nm). The structures were deposited by magnetron sputtering on a glass substrate in an argon atmosphere and room temperature. The deposition process was carried out under an applied magnetic field of 400Oe, aligned in the plane of the samples. Magnetic field assisted fabrication enabled the creation of an easy magnetization axis in the same as magnetic field direction. To measure the parameters of THz generation we utilized the conventional method of THz time-domain spectroscopy (THz-TDS). For THz wave parameters control, the samples were put in an in-plane magnetic field.

RESULTS AND DISCUSSION

The Co/Pt emitters operate on the inverse spin Hall effect (ISHE), and the THz wave is generated by a charge current $\vec{j}_C$ generated in the Pt layer. The direction of polarization for THz waves $\vec{E}^{THz}$ emitted due to the ISHE is determined by the directions of the injected spin current $\vec{j}_s$ and the spin polarization of electrons $\vec{\sigma}$, which is antiparallel to magnetization $\vec{\sigma} \parallel -\vec{M}$: $\vec{E}^{THz} \propto \vec{j}_C = \theta_{ISHE}[\vec{j}_s \times \vec{\sigma}]$. Magnetization and hence THz wave polarization is controlled by the magnitude and orientation of the magnetizing field.

In the bilayer, magnetic field should be directed along the hard axis. Then by the magnetic field ramp within the anisotropy field (100 Oe for the studied samples), magnetization rotates by 180° without changing its value. It gives rise to the THz wave polarization rotation by 180° as well while its amplitude remains constant. Thus, the proposed structure is proved to be a pure polarization rotator. In the spin valve, magnetic field should be directed along the easy axis of magnetization. In this structure, antiferromagnetic IrMn layer provides pinning of magnetization direction in the neighboring Co layer. Then, for H=0, magnetization in two Co layers is directed oppositely. Then charge currents are parallel and enhances the generated THz field. When magnetic field higher than coercive field H_C, is applied to the structure, magnetizations in two Co layers become parallel. Then the charge currents from two sources, directed antiparallel, cancel each other, resulting in almost zero THz field. Modulating magnetic field in the range of 0-H_C provides modulation of THz wave amplitude with very high efficiency.

CONCLUSION

This study proposes magnetic nanostructures with in-plane anisotropy as spintronic THz emitters to control the polarization and amplitude of the THz wave, paving the way for new applications in areas such as THz imaging, sensing, and communications.

REFERENCES

1. A. Leitenstorfer et al, J. Phys. D: Appl. Phys.58, 223001 (2023).
2. A. Buryakov et al, Appl. Phys. Lett. 123, 082404 (2023).

ACKNOWLEDGMENTS

The work is supported by the Contract No. 075-15-2022-1131

PVDF-$BaTiO_3$ Nanofiber-based Piezoelectric Sensor for Wearable Applications

Qinrong He, Dagou A. Zeze and Ensieh S. Hosseini
Department of Engineering, Durham University, Durham, DH1 3LE, UK

INTRODUCTION

Piezoelectric materials have been widely applied to energy harvesters and sensing applications because of their unique properties, allowing for self-powered devices and the conversion of mechanical energy to electricity. Piezoelectric polyvinylidene fluoride (PVDF) is regarded as a good candidate for the fabrication of flexible and wearable devices with stability and biocompatibility, which has been commonly used in various biomedical applications and tissue engineering.[1,2] Electrospinning is a technique used to produce nanofibers through the application of an electric field, allowing for the production of nanofibers with diameters ranging from a few nanometers to several micrometres and simultaneous polarization of ferroelectric materials.[3] This work reports on the development of a conformal PVDF-BaTiO3 nanofibre-based piezoelectric sensor that provides good adhesion to the human body, enabling the testing of biomechanical movement for wearable applications.

RESULTS AND DISCUSSION

In this work, PVDF was mixed with $BaTiO_3$ with combined advantages of piezoelectricity from PVDF and $BaTiO_3$. Here, electrospinning was used to prepare PVDF-$BaTiO_3$ nanofibres mat under a high electrical field, which can directly align the dipole orientation to produce higher β-phase content with enhanced piezoelectric properties. Then, PVDF-$BaTiO_3$ film with copper tape as electrodes was fabricated as a flexible sensor to monitor and convert tiny vibrations and pressure into an output voltage. Figure 1a shows the output voltage of PVDF-$BaTiO_3$ sensor tested by using different vibration frequencies from 6 Hz to 18 Hz with output average voltage of 0.06 V, 0.08 V, 0.14 V and 0.28 V at 6 Hz, 10 Hz, 14 Hz and 18 Hz, respectively. Figure 1b shows the maximum output average voltage of 0.28 V at a vibration frequency of 18 Hz with the excited greatest vibration amplitude leading to the largest displacement of the device. This PVDF-$BaTiO_3$ flexible sensor holds the potential application in the fields of heartbeat, pulse and breathing monitoring for sports monitoring and health care.

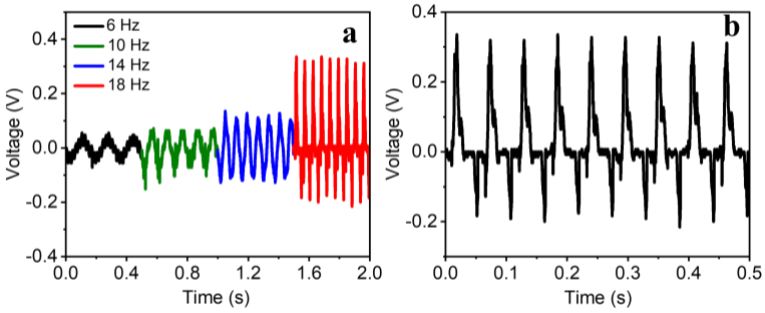

Fig. 1 (a) Output voltage signal of PVDF-$BaTiO_3$ sensor under different vibration frequencies. (b) The output voltage signal of PVDF-$BaTiO_3$ sensor at a vibration frequency of 18 Hz.

CONCLUSION

Herein, PVDF-$BaTiO_3$ electrospun film was obtained and fabricated as a flexible sensor to produce output voltage and current under different vibration frequencies and pressure, which can be used to test different impacting acceleration and monitoring biomechanical body movement possessing substantial opportunities for medical applications such as health monitoring, sports and fitness monitoring.

REFERENCES

1. C.H. Lang, et.al, Nat Commun 7 (2016).
2. G. Wang, et.al, Sensor Actuat a-Phys 280 (2018) 319-325.
3. F. Nikbakhtnasrabi, et.al, Adv. Electron. Mater 8(7) (2022)

ACKNOWLEDGMENTS

This work was supported by the Engineering and Physical Sciences Research Council (EPSRC- 933080).

Analysis of hysteretic behavior in hybrid and inorganic perovskites

Higor R. Ormonde[1], Romildo Jerônimo Ramos[1], Eralci Moreira Therézio[1]

[1]Institute of Physic, Universidade Federal de Mato Grosso, Brasil

INTRODUCTION

The advancement in the performance of perovskite photovoltaic devices has not always been accompanied by a fundamental understanding of their electronic and physicochemical properties, which can modulate the photovoltaic parameters. Hysteresis can lead to erroneous estimates of device efficiency, raising questions about its reliability during usage [1,2].

EXPERIMENTAL/THEORETICAL STUDY

Was variety the synthesis parameters that allow us to control thickness and grains (by spin-coating process), aiming to minimize electrical traps that are directly associated with the capacitive effect or charge storage. And current-voltage (I-V) measurement is used to characterize the hysteresis electrical response.

RESULTS AND DISCUSSION

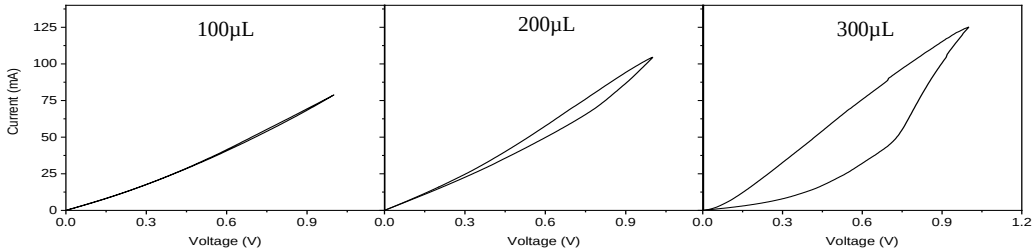

Figure 1 - I-V measurement of samples with different volume of antisolvent.

It was observed that increasing the amount of anti-solvent results in the growth of the average grain size. In Figure 1, a considerable increase in hysteresis in the I-V measurements was identified. The trapping and de-trapping processes at the grain boundaries influence the efficiency of extracting excited carriers, contributing to the occurrence of electrical hysteresis in the I-V measurements.

Group	ID	Area (u. a.)	Scan rate (V/s)	Quantity of antisolvent (μ L)
G1	Sample1	1.5741	0.04	100
		1.0788	0.1	
	Sample2	3.4336	0.04	200
		0.8901	0.1	
	Sample3	12.3866	0.04	300
		3.3029	0.1	
G2	Sample4	0.5329	0.04	100
		0.3677	0.1	
	Sample5	4.9304	0.04	200
		1.9553	0.1	
	Sample6	25.3628	0.04	300
		12.7616	0.1	

Table 1 – Area between the curves represent the intensity of hysteresis.

When it comes to the amount of anti-solvent, it is observed that the increase in the area between the curves is independent of the group or scanning rate. From the analyzed data, it can be inferred that crystallization has a significant impact on the intensity of hysteresis, where greater uniformity and smaller grain sizes are associated with reduced hysteresis effects. The samples belonging to group 2 showed increased hysteresis in the I-V measurement with the increase in the deposited anti-solvent volume.

CONCLUSION

It was demonstrated that hysteresis is an intrinsic effect of the perovskite film, originating from the interaction of charge carriers with the grains. The increase in the volume of anti-solvent during the synthesis resulted in a significant increase in the hysteresis intensity in the I-V measurements. Furthermore, by varying the rotation speed of the spin coating equipment, different film thicknesses were obtained, with thicker samples showing higher hysteresis.

REFERENCES

1. Duan, Hsin-Sheng, et al. Physical chemistry chemical physics 17.1 (2015): 112-116.
2. Elumalai, et. al. Solar Energy Materials and Solar Cells 157 (2016): 476-509.

Functional organic polymers for stretchable, healable and recyclable electronics

Fabio Cicoira [1],
[1 a] Department of Chemical Engineering, Polytechnique Montreal, Montreal, Canada

The ability of certain materials to regenerate after damage has attracted a great deal of attention since the ancient times. For instance, self-healing concretes, able to resist earthquakes, aging, weather, and seawater have been known since the times of ancient Rome and are still the object of research.

While the field of mechanically healable materials is relatively established, self-healing conductors are still rare, and are nowadays attracting enormous interest for applications in electronic skin for health monitoring, wearable and stretchable sensors, actuators, transistors, energy harvesting, and storage devices, such as batteries and supercapacitors. Self-healing can significantly enhance the lifetime of conducting materials, leading to the improved environmental sustainability and reduced costs.

Conducting polymers exhibit attractive properties, such as mixed ionic-electronic conductivity, leading to low interfacial impedance, tunability by chemical synthesis, ease of process via solution process and printing, and biomechanical compatibility with living tissues, which makes them ideal materials for bioelectronics and stretchable electronics. However, they show typically poor mechanical properties and are therefore not suitable as self-healing materials. Self-healing conductors can be achieved upon mixing with other polymers, such as poly(vinyl alcohol) (PVA) and poly(ethylene glycol) (PEG), which provide the mechanical characteristics leading to self-healing.

My talk will deal with self-healing materials obtained blending PEDOT:PSS with other materials, such as polyethylene glycol (PEG), tannic acid and polyurethane. Various self-healing modes will be presented and correlated with the electrical and mechanical properties of the materials. The use of the self-healing gels and films as epidermal electrodes will be also presented.[1-8]

REFERENCES

1. Y. Li, X. Zhou, B. Sarkar, F. Cicoira et al., *Adv. Mater*. 2108932, 2022.
2. Y. Li, X. Li, S. Zhang, F. Cicoira et al., *Adv. Funct. Mater.* 30, 2002853, 2020.
3. Y. Li, X. Li, R. N. Unnava Venkata, S. Zhang, F. Cicoira, *Flexible and Printed Electronics* 4, 044004, 2019.
4. S. Zhang, Y. Li, F. Cicoira et al. *Adv. Electron. Mater* 1900191, 2019.
5. S. Zhang, F. Cicoira, Adv. Mater. 29, 1703098, 2017.
6. X. Zhou, G. A. Lodygensky, F. Cicoira et al., *Acta Biomaterialia* 139, 296-306, 2022.
7. X. Zhou, P. Kateb, J. Fan, J. Kim, G. A. Lodygensky, B. Amilhon, D. Pasini and F. Cicoira, *Journal of Materials Chemistry C* (in press).
8. P. Kateb, J. Fan, J. Kim, X. Zhou, G. A. Lodygensky, and F. Cicoira, *Flexible and Printed Electronics*, **8** 045006, 2023.

Fluorescent nanographene-based nanocomposites: unclonable photonic microlabels for anti-counterfeiting, metrology and microsensing.

M. Reale[1], M. Cannas[1], E. Marino[1], C. M. Cruz[2], E. Macoas[3], A. G. Campaña[2], A. Sciortino[1], and F. Messina[1*]

[1]Dipartimento di Scienze Fisiche e Chimiche, Università degli Studi di Palermo, Italy
[2]Departamento de Química Orgánica, Universidad de Granada, Granada, Spain
[3]Centro de Química Estrutural, Instituto Superior Técnico, Lisboa, Portugal
*corresponding author (fabrizio.messina@unipa.it

INTRODUCTION

Nanographenes (NG) are graphene fragments displaying strong optical transitions in the visible or near-infrared range due to bandgap opening through quantum confinement on lateral sizes of a few nanometers. NGs are ideal benchmarks to study the optical response of zero-dimensional nanocarbons, sometimes showing non-trivial photophysics [1,2]. From a functional point of view, NGs can be brightly fluorescent, and their optical properties can be precisely tailored through precise structural engineering with atomic precision. Thereby, NGs are ideal building blocks of more complex nanocomposites where they behave as efficient light harvesters or light emitters.

EXPERIMENTAL/THEORETICAL STUDY

The study was mostly conducted by a combination of optical experimental methods: fluorescence microscopy, steady state, nanosecond- and femtosecond-resolved optical spectroscopy.

RESULTS AND DISCUSSION

This study focuses on a nanoribbon-shaped NG displaying visible fluorescence with very high quantum efficiency (QY=65%) [1]. We first carried out a thorough characterization of its photocycle by a combination of steady-state, nanosecond and femtosecond time-resolved optical methods. Then, we coupled these NGs with micrometer-sized polysterene spheres (NG@PS), through a simple self-assembly strategy in solution phase. The resulting NG@PS composites show unique fluorescent properties that are very different from those of the starting NGs. In fact, NG@PS fluorescence displays an entirely new set of narrow resonances (Fig. 1) due to the coupling of NG optical transitions to the whispering gallery modes of the polystyrene microsphere, acting as an optical microresonator. We argue that these NG@PS are a family of functional nanocomposites which would be potentially suitable for several applications, such as micro-sensing or micro-lasers. Besides, we show that the finely-structured spectral fingerprints displayed by NG@PS are unique for each individual microparticle, such that NG@PS can be used as luminescent unclonable labels for anti-counterfeiting applications.

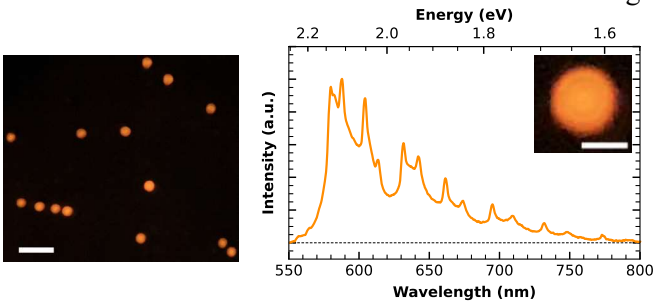

Fig. 1 Left: Fluorescence microscopy of a collection of NG@PS microcomposites (scale bar = 10 μm). Right: Fluorescence spectrum from an individual microbead (inset).

CONCLUSION

Nanographene-polysterene microcomposites are proposed as a novel family of carbon-based microresonators with several potential applications in photonics.

REFERENCES

[1] S. Castro-Fernandez et al. Angewandte Chemie 59, 7179, 2020 ; [2] M. Reale et al. Carbon 206, 45, 2023

Green Hydrogen Production via Integrated Triple Technologies: Downdraft Tower, Photovoltaic and Electrolysis

Emad Abdelsalam [1], Fares Almomani [2]*

[1] Electrical and Energy Engineering Department, Al Hussein Technical University, Amman 11831, Jordan; ayahtech@gmail.com

[2] Chemical Engineering Department, Qatar University, Qatar; Falmomani@qu.edu.qa

* Correspondence: Falmomani@qu.edu.qa

Abstract:

This work proposes an integrated structure consisting of three types of technologies to produce green hydrogen. The technologies include a downdraft tower, photovoltaic panels, and an electrolysis station. The downdraft tower is at the center of the integrated structure. The bottom of the tower is surrounded by rows of photovoltaic panels that fan out from the tower, row by row. At the base of the tower, a water pool is installed. The water pool is integrated with an electrolysis station with two pipes extending from the station to hydrogen and oxygen storage tanks outside the tower. The downdraft tower provides a jet of cool air that travels downwards from the top. The cool air interacts with a turbine located at the bottom of the tower, generating electricity that powers up the electrolysis station, producing hydrogen. Similarly, the photovoltaic panels produce electricity from solar irradiance during the daytime, combined with the electricity from the downdraft tower to power up the electrolysis station. Hence, the combined produced energy improves the production of hydrogen. The downdraft cool air helps to cool the photovoltaic panels, improving their efficiency by about 5%. Hence, improving the efficiency of the photovoltaic panels improves hydrogen production efficiency. In addition, the downdraft tower could work during the day and at night to produce electricity, depending on the weather conditions. Hence, the photovoltaic panels and the downdraft tower allow the integrated structure to produce hydrogen around the clock. The results show that the photovoltaic panels produced 463.984 MWh, and the downdraft tower produced 636.011 MWh of energy annually. The results also showed that the total energy from the system was used to produce 37161 kg of hydrogen.

Bio-Hydrogen Production from Sewage Sludge: A Sustainable Solution for Qatar's Wastewater Treatment Plants

Abstract:

Sewage sludge, a by-product of wastewater treatment, poses significant environmental challenges in Qatar due to its negative impacts on air and water quality. With the increasing population exacerbating sludge production, effective management strategies are crucial. Recent research has identified dark fermentation technology as a promising avenue for converting sewage sludge into bio-hydrogen gas, offering a sustainable solution to both waste management and energy needs. This study investigates the feasibility of bio-hydrogen production from sewage sludge in Qatar's wastewater treatment plants. Results demonstrate that optimizing substrate concentration at 5 g/L enhances hydrogen fermentation efficiency, with a maximum hydrogen yield of 47.8 mL/g-VS added and a volatile solids (VS) removal efficiency of 15.9%. However, excessive substrate concentrations (above 10 g/L) lead to the accumulation of metabolic by-products, such as lactate, acetate, and ethanol, inhibiting microbial activity and reducing hydrogen production efficiency. The findings highlight the potential of bio-hydrogen production from sewage sludge as a sustainable energy source and a means of mitigating environmental impacts. Implementing this technology in wastewater treatment plants can contribute to reducing sludge volumes, minimizing pollution, and promoting a circular economy in Qatar's wastewater management sector.

Coating of sintered Nd-Fe-B magnets used in E-motors; improving magnetic properties and corrosion resistance

Fatih DOĞAN

Assist. Prof. Dr., Munzur University, Rare Earth Elements Application & Research Center, Tunceli, Turkiye.

e-mail: fatihdogan@munzur.edu.tr

ABSTRACT

Rare earth elements are highly sensitive to oxidation and hydrogen absorption, and significant differences in the electrochemical potential of adjacent phases in humid environments lead to galvanic coupling effects. Since the microstructure of Nd-Fe-B sintered magnets is complex, their corrosion mechanisms are not yet fully understood. The Nd-rich phase may contain several phases depending on the oxygen content. Exposure of sintered Nd-Fe-B magnets to water leads to the formation of Nd-hydroxide and hydrogen, and these formations react with the Nd-rich phase between the grains and cause segregation along the grain boundaries. Commercial Nd-Fe-B magnets are often coated with different thin layers to increase corrosion resistance. Fast and reliable test methods are being developed, especially for the automotive industry. Since corrosion test methods can inadequately describe the operating conditions of the e-motor, magnets are usually only tested in the demagnetized state. Corrosion tests close to sintered Nd-Fe-B magnets e-motor application conditions have been applied. Corrosion tests for sintered Nd-Fe-B magnets are usually demagnetized and performed in aqueous solutions or vapor environments instead of organic substances such as oil. In this study, sintered Nd-Fe-B magnets have been immersed in a pre-saturated water-based salt solution, placed in gearbox oil, and subjected to temperature cycles. The test conditions have been specially selected to test the suitability of the magnets for e-motor applications (e.g. in hybrid vehicles). Through a simple high-temperature heat treatment of sintered Nd-Fe-B magnets were produced by Ni/Cu/Ni electroplating. The microstructural effect of magnetic properties and corrosion resistance on the Nd-Fe-B magnets have been systematically studied. The aim of the study; It is the realization of the coating on the sintered Nd-Fe-B magnet, which both provides high corrosion resistance and significantly reduces the thickness of the coating and ensures maximum efficiency in the use of magnets. The results of these studies are thought to play an important role in determining and optimizing the usage strategy of coated Nd-Fe-B magnets.

Keywords: Coating, NdFeB, magnetic properties, corrosion

Platinum, Palladium, and Nickel Nanomaterials for Electrochemical Energy Generation and Storage – An Overview

Gregory Jerkiewicz [1*]
[1]Department of Chemistry, Queen's University, Canada (gregory.jerkiewicz@queensu.ca)

INTRODUCTION

Electrochemistry is a fast-developing discipline due to the importance of water electrolyzers, fuel cells, and rechargeable batteries in renewable energy generation and storage. Energy-converting electrochemical processes take place at catalytically active electrode materials and in highly concentrated aqueous acidic or alkaline media. Platinum (Pt) nanomaterials are employed in polymer electrolyte membrane (PEM) fuel cells and water electrolyzers, and nickel (Ni) nanomaterials are used in alkaline water electrolyzers. In addition, micro- and nanostructured Ni materials are also used in a wide range of rechargeable batteries. Fuel cells and water electrolyzers are closely related to the *emerging hydrogen economy*, an energy generation, delivery, and utilization system in which the hydrogen gas (H_2(g)) is the energy source and carrier. If successfully realized, the hydrogen economy will replace the hydrocarbon economy and contribute to the reduction of CO_2 emissions.

EXPERIMENTAL/THEORETICAL STUDY

Experimental techniques and procedures employed in this research are as follows: water-in-oil microemulsion synthesis, thermo-gravimetric analysis (TGA), X-ray diffraction (XRD), transmission electron microscopy (TEM), scanning electron microscopy (SEM), confocal Raman spectroscopy, inductively coupled plasma-mass spectrometry (ICP-MS), cyclic voltammetry (CV), linear sweep voltammetry (LSV), potentio-dynamic polarization (PDP), and electrochemical adsorption and absorption isotherms.

RESULTS AND DISCUSSION

The contribution overviews some of our recent research on Pt-based nanomaterials for PEM fuel cells, Ni-based nanomaterials for alkaline fell cells, and palladium (Pd) and Ni nanomaterials for nickel-palladium hydride micro-batteries[1-4]. Specifically, the following nanomaterials and their materials science, electrochemical, catalytic, and/or energy storage properties are analyzed and discussed: (i) platinum-based nanoparticles (NPs), namely Pt, Pt_3Ni, and Pt_3Co; (ii) cubic and octahedral Pd NPs; (iii) β-$Ni(OH)_2$ nanoparticles and nanosheets; and (iv) composite Pd@β-$Ni(OH)_2$/C nanomaterials having different Pd and Ni loadings. The research on the Pt_3Ni and Pt_3Co NPs demonstrated that there was no Fe/Co present in their surface or near surface regions. The research on Pd NPs as hydrogen (H) storage materials showed that they adopted a *core-shell-skin structure* upon H absorption. The research on carbon-supported β-$Ni(OH)_2$ nanosheets revealed that they are suitable materials for rechargeable micro-batteries, and on the Pd@β-$Ni(OH)_2$/C nanomaterials demonstrated that they were excellent electrocatalysts for the hydrogen oxidation reaction (HOR) in aqueous alkaline media.

CONCLUSION

The applicability and broad-scale implementation of metallic nanomaterials in real-life electrochemical energy generation and storage devices depends on only on their catalytic properties and long-term stability and durability, but also on their manufacturing cost, and availability and abundance of raw materials. The outcome of our research sheds light on the applicability of Pt, Pt_3Ni, and Pt_3Co NPs in PEM fuel cells, Pd NPs and β-$Ni(OH)_2$ nanosheets in rechargeable batteries, and Pd@β-$Ni(OH)_2$/C nanomaterials in alkaline fuel cells.

REFERENCES

1. A. Zalineeva et al, Sci. Adv. 3, e1600542 (2017)
2. S. Tahmasebi et al, J. Phys. Chem. C 122, 11765 (2018)
3. S. Tahmasebi et al, ACS Appl. Energy Mater. 2, 7019 (2019)
4. S. Fujita et al, Langmuir 39, 15889 (2023)

ACKNOWLEDGMENTS

The research presented in this contribution would not be possible without talented graduate and undergraduate students and postdoctoral fellows and support from various granting agencies (the Natural Sciences and Engineering Research Council of Canada, Automotive Partnership Canada, Ontario Centres of Excellence) and private companies (e.g., Nissan Motor Co. and INCO, now VALE-INCO) that are gratefully acknowledged.

Solving the Sintering Problem in the Thermochemical CuO/Cu_2O Redox Cycle Via a Facile-One Pot Nanomaterials Synthesis Process

Hassan Agalit* [1*], Samuel D Widijatmoko [1], Gary A. Leeke [1] and Yongliang Li* [1*]
[1] School of Chemical Engineering, University of Birmingham, Birmingham, UK
*corresponding authors (h.agalit@bham.ac.uk and y.li.1@bham.ac.uk)

INTRODUCTION

The thermochemical reversible CuO/Cu_2O Redox cycle is a very promising long duration high-temperature (1000 °C) storage solution for different applications (e.g. solar thermal plants, cement manufacturing, etc.) [1]. This is due mainly to its relatively very high density (~810.2 kJ/kg). The main challenge for this storage technology is the sintering phenomenon which reduce dramatically the efficiency after several redox cycles. In this work, this problem is solved at the nanoscale via a facile-one pot synthesis process and without the use of any dopant. the cyclic energy density (~747 kJ/kg) of the obtained materials is very superior compared to the state-of the art [2].

EXPERIMENTAL/THEORETICAL STUDY

As depicted in Fig. 1, the hollow CuO microspheres were synthesized via the hydrothermal process, and performances of the obtained materials were analyzed via Scanning Electron Microscopy (SEM) and Simultaneous Thermal Analyzer (STA) apparatus.

RESULTS AND DISCUSSION

The multi-shells hollow CuO microspheres were successfully obtained as shown in the SEM images (Fig.1). This novel microstructure were subject to 10 Redox cycles in the temperature range of 900-950 °C. As depicted in the same figure, the reoxidation capacity is maintained stable after 10 cycles, which demonstrates that the sintering effect has been significantly alleviated solely due to the hollow microsphere structure of CuO, without the need for any doping agent.

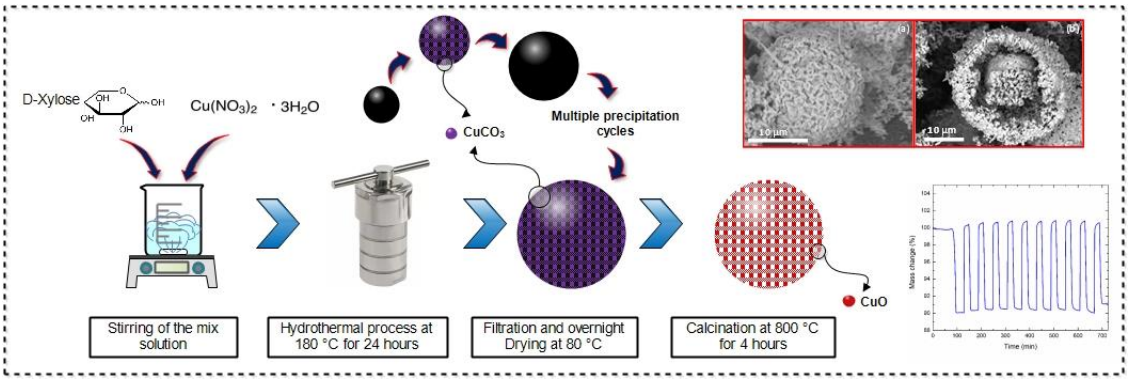

Fig. 1 Synthesis process of the Hollow CuO Microspheres for an enhanced thermochemical cyclability.

In addition to the good Redox cyclability, the synthesized materials have very high energy density (~747 kJ/kg) compared to the state-of- the art of the physically or chemically doped materials. It is actually 59% higher than that of physically doped material (~470 kJ/kg) [1], and 87% higher than that of chemically doped material (~400 kJ/kg) [2].

CONCLUSION

In summary, a novel microstructure of CuO was investigated in this work to solve the sintering problem in the thermochemical CuO/Cu_2O redox cycle. The obtained evidence demonstrate the superior storage of those materials compared to the state-of- the art in term the cyclic energy capacity. Further investigations are needed to demonstrate the same promising results over a longer number of redox cycles.

REFERENCES

1. Gigantino, M. Energy Fuels 2020, 34 (12), 16772–16782.
2. High, M. *Nat. Commun.* **2022**, *13* (1), 5109.

ACKNOWLEDGMENTS

The research leading to these results has received funding from the EPSRC, United Kingdom through the PATCH Project (EP/W027887/1).

Applications of 2D $Ti_3C_2T_x$ MXenes in neuromorphic devices

Henrique Teixeira[1*], Ihsan Çaha[2], Leonard Deepak Francis[2], Catarina Dias[1] and João Ventura[1]
[1]IFIMUP, Departamento de Física e Astronomia, Faculdade de Ciências, Universidade do Porto, Rua do Campo Alegre s/n, 4169-007 Porto, Portugal, corresponding author (research@jacteixeira.com)
[2]International Iberian Nanotechnology Laboratory, Av. Mestre José Veiga s/n, 4715-330 Braga, Portugal

INTRODUCTION

Taking inspiration from the human brain, where memory and learning occur in the same space at a low power consumption, a memristive neuromorphic computing architecture has emerged[1]. These new devices are generally composed of metal-insulator-metal stacks. However, the integration of low-dimensional materials (2D), such as MXenes, enhances the switching control, spatial and temporal reproducibility, and lower power consumption and fabrication cost[2]. In this work, 2D flakes of Ti_3C_2 MXene were chemical exfoliated from Ti_3AlC_2 precursor through an *in-situ* HF formation method, and then integrated as an heterostructure of Al_2O_3/Ti_3C_2 resistive switching stack with bottom PET/ITO flexible substrate and top W electrodes. Resistive switching behavior was obtained at low switching voltages with multi-bit capability.

EXPERIMENTAL/THEORETICAL STUDY

Ti_3C_2 flakes were synthesized with 14.78 mL of 9 M HF, 1.6 g of LiF, and 1 g of Ti_3AlC_2 powder were mixed with 5.82 mL of DI water. After stirring for 36 h at 35°C, the etched MXene was centrifuged (3500 rpm) in 30 mL of DI water for 5 min. The washing process was repeated 7 times to achieve the multilayer Ti_3C_2 solution. This suspension was sonicated for 1 h under N_2, to avoid oxidation, followed by 5 min centrifugation at 3500 rpm and the supernatant was collected. A thin-film of Al_2O_3 (5 nm) was deposited with IBD machine, followed by MXene spin-coating deposition, and lastly 75 nm W electrodes sputtered on top.

RESULTS AND DISCUSSION

Successful delamination of MXene flakes was confirmed through XRD, SEM, and TEM, achieving a dispersion-ready solution for spin-coating. The electrical properties of the fabricated stack were measured under various current stimulus, showing remarkably reliable resistive switching behaviour with high resistance ratio (10^4-10^5), as shown in Fig.1 (a), but at the same time this device is capable of multi-level resistive states with remarkable endurance [Fig.1(b)].

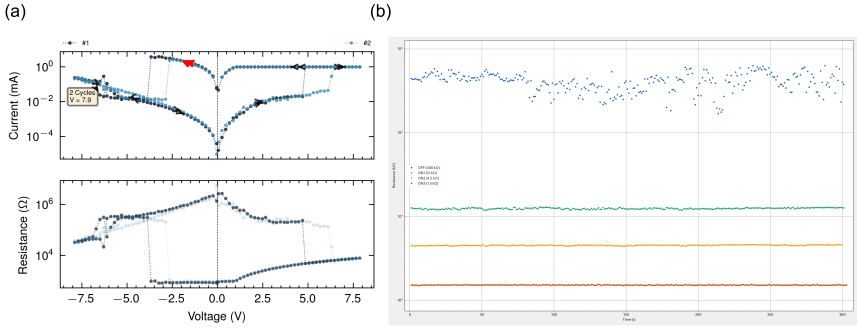

Fig. 1 (a) Resistive switching curve of PET/ITO/Al2O3/Ti3C2/W stack, (b) and it's multilevel resistance capability with high endurance.

CONCLUSION

We demonstrated the successful synthesis of 2D MXenes for integration in memristive devices, which showed remarkably high resistance ratios and multi-bit capability.

REFERENCES

1. Zhu, J. et al, Appl Phys Rev 7, 011312 (2020).
2. Y. Gong, X. et al, Small Sci1 (2021) 2100006..

ACKNOWLEDGMENTS

We thank FCT and IFIMUP, through projects PTDC/NANMAT/4093/2021, UIDB/04968/2020 and UIDP/04968/2020, and "la Caixa" Foundation within project CCO 204197.

Unveiling the role of microstructure on the electrical properties of ceria-based composites

Henrique Tidei[a], Tao Yang[b], João P. F. Grilo[a]

a Department of Materials and Ceramic Engineering – DEMaC/CICECO, University of Aveiro, Portugal

b TEMA-NRG, Department of Mechanical Engineering, University of Aveiro, Portugal

This work investigates the preparation and characterization of composite membranes for high-temperature CO_2 separation. The main objective is to elucidate the role of microstructure in terms of interfaces and surfaces characteristics and corresponding degradation limit. The composite membranes were produced through a two-step process: initial consolidation of the ceramic phase followed by impregnation with molten carbonates. Various processing conditions were optimized to achieve homogeneous and strong ceramic skeletons using organic pore forms and sintering aids. The Gd-doped ceria (CGO) is used as a ceramic oxide-ion conductor, and a eutectic mixture of Na_2CO_3 and Li_2CO_3, a carbonate-ion conductor, is used as a secondary phase in large volume (~30 vol. %). The secondary phase has a melting point at 500 ºC, temperature in which the counterflow of oxide-carbonate-ions species facilitates the desired CO_2 transport. Characterization was performed using X-ray diffraction, scanning electron microscopy and impedance spectroscopy under different atmospheric conditions. Additionally, stability test was performed both in air and CO_2. The results provide insights into the behaviour of both the isolated ceramic phase and the composite, facilitating an understanding of carbonate feature within the composites. At the typical operating temperatures (approximately 600-700°C), molten carbonates play a crucial role in ionic conduction, attributed to the relatively low ionic conductivity of the ceramic phase. After 80 hours of test at 700 ºC, materials presented moderate degradation, showing a strong impact on the total conductivity and electrode processes.

Keywords: Composite membranes; impedance spectroscopy; conductivity; Degradation.

Acknowledgement

This work was developed within the scope of the project CICECO-Aveiro Institute of Materials, UIDB/50011/2020, UIDP/50011/2020 & LA/P/0006/2020, financed by national funds through the FCT/MCTES (PIDDAC). The authors acknowledge the national funding from FCT through the PTDC/EME-REN/1497/2021project (Power Phoenix Battery-A Full Solid State Grid-scale Storage Solution).

Nanometric Structure of Adhesion Interface in Humid Environments Studied by Neutron Reflectometry

Hiroyuki Aoki [1,2]
[1]J-PARC Center, Japan Atomic Energy Agency, Japan
[2]Institute of Materials Structure Science, High Energy Accelerator Research Organization, Japan

Epoxy resins have been used as structure adhesives in various fields. The structure and physical properties of the epoxy resins is affected by the absorption of water; therefore, the effect of the water absorbed from the atmosphere on the structure of the epoxy resin at the interface with the adherend should be understood to improve the adhesion properties. This study deals with the structure analysis of epoxy resins at the interfaces with a solid substrate in high humidity. Neutron reflectometry (NR) is a powerful tool to analyze the structure of interfaces of materials at the nanometric length scale, and it can directly probe the spatial distribution of water in the epoxy resin film. Figure 1A shows the NR profiles of an epoxy resin thin film prepared by bisphenol A diglycidyl ether (DGEBA) and 1,4-bis(aminomethyl) cyclohexane (CBMA) in dry and humid atmospheres. The fitting analysis of the NR profiles provide the depth distribution of the neutron scattering length density (SLD) profile shown in Figure 1B. The SLD profiles in a humid state shows a larger peak of at the depth of 1.4 nm compared to that in a dry state. This is due to the water absorbed from the atmosphere aggregate at the interface between the epoxy resin and adhrend. The quantitative analysis of the SLD distribution showed that the condensed layer of water has a thickness of 0.6 nm. Whereas the water fraction in the bulk region was only 2-3 %, the fraction at the interface was more than 40 %. The effect of the curing condition suggested that the formation of the condensed layer is caused by the different cross-link structure of the polymer chain at the interface.

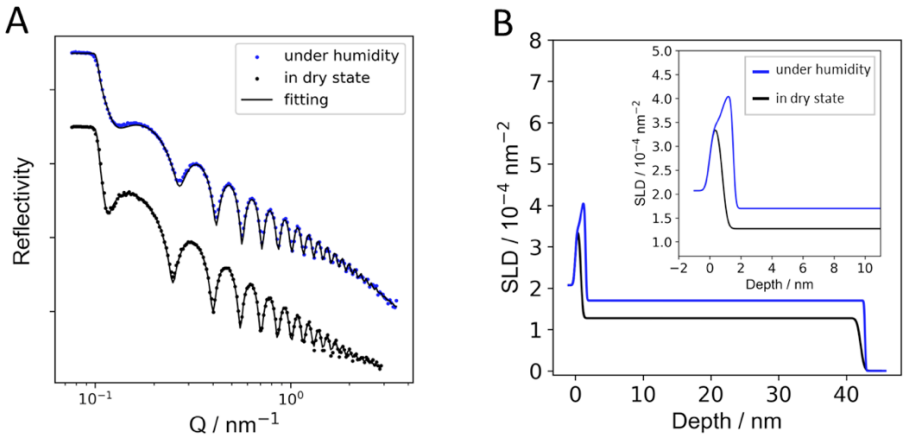

Figure 1. Neutron reflection profiles (A) and scattering length density distribution (B) for DGEBA/CBMA in dry and humid conditions. The reflection profiles are vertically shifted for visibility.

Tailoring Rapid Thermal Synthesis of Noble Metal Nanoparticles on Carbon Support for Energy Applications

Huanqing Zhang[1], Adam Elbataioui[1], Barbora Pijakova[2], Monika Stupavska[2], Lidija Rafailovic[1*], Kaikai Song[3], Jürgen Eckert[1]

[1]Department of Materials Science, Chair of Materials Physics, University of Leoben, Austria

[*](lidija.rafailovic@unileoben.ac.at)

[2]Masaryk University, Faculty of Science, Brno, Czech Republic

[3]School of Mechanical, Electrical & Information Engineering, Shandong University, China.

INTRODUCTION

In combination with carbon-based matrices, the electrocatalytical activity of noble metal nanoparticles (NPs) (e.g., Pt, Ru, Cu, etc.) are of high interest for emerging energy electrochemical applications. Our study aims to explore the stability of single and alloy NPs and their interaction at the interphase under applied potential, leveraging the synergistic effects between the carbon matrix and NPs[1]. The rapid thermal synthesis of NPs on carbon support induced by applied voltage offers versatile synthetic possibilities to engineer materials with enhanced electrocatalytic properties[2]. In this context, the composition of noble metal NPs and their alloys holds significant promise for future energy applications, driving the development of more efficient electrodes.

EXPERIMENTAL STUDY

We utilized commercially available carbon support (Toray Carbon Paper, TGP-H-60) for synthesis of single NPs and their alloys. Solution of the metal salts were loaded onto carbon paper and subjected to the rapid thermal method to heat (~1600K) to yield NPs. To gain deeper insight into the NPs electrode stability, we employ various electrochemical, microscopic and spectroscopic methods.

RESULTS AND DISCUSSIONS

Figure 1 illustrates synthesis of metal NPs and their alloys on carbon fiber support. (a) Pt NPs (~10nm) are finely distributed on the roughened fiber. (b) Compositionally complex alloy (CCA) NPs with size of ca. 10 nm are loaded on porous carbon fiber morphology. We further explore the hydrogen evolution reaction activity and stability by comparing single metal NPs and alloy combinations achieved by increasing the complexity in the fabrication of CCA systems.

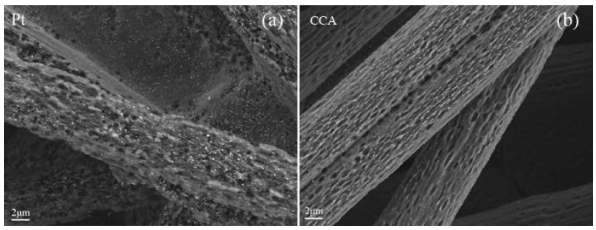

Fig. 1 Scanning electron microscopy images of fabricated Pt@C (a) and CCA (b) electrodes.

CONCLUSION

In conclusion, our study emphasizes the considerable potential of noble metal NPs integrated with carbon-based matrices for advancing energy electrochemical applications. The illustrated synthesis of metal NPs and alloys on carbon fiber support demonstrates the feasibility of finely distributed NPs and compositionally complex structures, laying the foundation for further exploration in hydrogen evolution reaction activity and stability.

REFERENCES

1. Yao, Yonggang, et al. Science 359.6383 (2018): 1489-1494.
2. Lai, Leo, et al. Small Structures 3.11 (2022): 2200112.

ACKNOWLEDGMENTS

Huanqing Zhang acknowledges the support from the China Scholarship Council (CSC, Grant No. 202206220060).

Plenary Speaker Information Form

Presentation Title:
New Paradigms in sustainable Energy solutions

Name: Ibrahim Dincer

Professor
Ontario Tech. University, Oshawa
President, Hydrogen Technologies Association
Chair, TUBA-Energy Working Group
Editor-in-Chief, Energy Storage
Editor-in-Chief, International Journal of Exergy
Editor-in-Chief, International Journal of Global Warming
Editor-in-Chief, International Journal of Research, Innovation and Commercialisation
Special Issues Coordinating Editor, International Journal of Hydrogen Energy

Biography:
Ibrahim Dincer is a full professor of Mechanical Engineering at Ontario Tech. University. Renowned for his pioneering works in the area of sustainable energy technologies he has authored/co-authored many books and book chapters, along with many refereed journal and conference papers. Dr. Dincer has chaired many national and international conferences, symposia, workshops and technical meetings. Dr. Dincer has delivered many keynotes and invited lectures. Dr. Dincer is an active member of various international scientific organizations and societies, and serves as editor-in-chief, associate editor, regional editor, and editorial board member on various prestigious international journals. Dr. Dincer currently serves as President for Hydrogen Technologies Association in Turkey and Chair for Energy Working Group in Turkish Academy of Sciences. Dr. Dincer is a recipient of several research, teaching and service awards, including the Premier's research excellence award in Ontario, Canada. During the past ten years he has been recognized by Thomson Reuters as one of the Most Influential Scientific Minds in Engineering and one of the most highly cited researchers. During the past 25 years Dr. Dincer's research and activities have been diverse and primarily focussed on sustainable energy solutions, sustainable communities and cities, district energy systems, green buildings, renewable energy technologies, energy storage technologies, hydrogen energy technologies, and waste to energy technologies. His group has developed various novel technologies for commercialization. He is known for his engineering education related talks as a committed educator.

Abstract
Humanity essentially needs to have four key things for living in a sustainable manner, namely clean air, clean water, clean food and clean energy. If energy is not clean enough, the rest of them will be affected badly. So, this makes energy really essential to achieve sustainable development which brings the need of sustainable energy solutions forefront. These solutions cover renewable energies, alternative fuels, hydrogen energy, energy storage, efficient energy utilization, and integrated energy systems and multigenerational applications, resilient community-based energy systems, but not limited to. This plenary talk will introduce the key necessities for human beings and sustainable energy solutions and discuss the paradigm changes in the way we generate, storage, convert, transport and utilize energy. It will further discuss how paradigm changes will affect the sustainable energy goals with a primary focus on hydrogen energy which requires a carbon-free energy ecosystem and a clear transformation into hydrogen economy. There is also a strong need for technologies which will be environmentally benign and sustainable.

Photoreduction of CO_2 to formic acid in a high pressure photoreactor

Simge Naz Degerli[1], Matteo Tommasi[2], Alice Gramegna[1], Gianguido Ramis[3], Ilenia Rossetti[1,2*]
[1] INSTM Unit Milano-Università, Dip. Chimica, Università degli Studi di Milano, via C. Golgi 19, Milan, Italy, presenting author, *corresponding author
[2] Chemical Plants and Industrial Chemistry Group, Dip. Chimica, Università degli Studi di Milano and CNR-SCITEC, via C. Golgi 19, Milan, Italy.
[3] Dip. DICCA, Università degli Studi di Genova and INSTM Unit-Genova, Genoa, Italy
*ilenia.rossetti@unimi.it

INTRODUCTION

The photoreduction of CO_2 is one of the most challenging uphill reactions, whose performance is limited by intrinsic catalyst efficiency features and by physical phenomena, such as CO_2 solubility in water. Nevertheless, it represents an intriguing mean to produce fuels and chemicals such as formic acid, formaldehyde, methanol and methane. In this work an innovative high pressure photoreactor is tested, operating up to 20 bar and reaching unprecedented productivity of formic acid (ca. 40 mol/h kg_{cat}) over a litre scale size. Thanks to 3D printing and in-house developed coating techniques up scaling options were studied and the possibility to mode to continuous operation was investigated. Z-scheme materials based on graphitic carbon nitride and WO_3 were tested to improve utilisation of solar light.

EXPERIMENTAL/THEORETICAL STUDY

Photocatalysts testing was carried out in a pilot scale photoreactor in stainless steel, equipped with an immersion UV lamp (365 nm maximum emission, with measured irradiance of 75 W/m^2) on 1.2 L of catalyst suspension or solution with immobilised catalytic tiles (31 mg/L) and using sodium sulphite as hole scavenger. The products were analysed both in liquid and gas phase through GC and HPLC. Testing was carried out up to 20 bar and 80°C
In this work the main photocatalyst tested is graphitic carbon nitride (g-C_3N_4). To further increase the productivity of the g-C_3N_4 a chemical treatment employing sulphuric acid was optimized and compared with exfoliation under UltraSound (US) treatment at modulated power (0-120 W). The Z-Scheme functionalization of the g-C_3N_4 exfoliated was performed using different types of metal oxides with various loadings: iron oxide, zinc oxide and tin oxide. All the catalysts have been characterized by XRD, BET and DRS analysis.

RESULTS AND DISCUSSION

Exfoliation of graphitic carbon nitride g-C_3N_4 by means of US treatment using water as a solvent was demonstrated at varying input power at constant frequency, constant amplitude and time of effective sonication. This positively contributed to the properties of the final material without critical handling or environmental issues. Exfoliation of g-C_3N_4 in water displays a strong dependence of US input power, with a slightly enhanced bandgap (2.8 eV), but most of all increased lifetime of photogenerated electrons, as observed through Diffuse Reflectance Spectroscopy (DRS) and Spectrofluorimetry data. Among all applied power (varied between 30W and 120W), 120W sufficiently exfoliated and tuned physicochemical properties of g-C_3N_4. The catalytic results demonstrate this metal free material as an efficient photocatalyst to obtain high yield of formic acid with productivities ranging from ~5100 to ~8200 mmol/kg_{cat}h at 80°C in water, which is among the highest reported in the literature.
The graphitic carbon nitride with a loading of hematite equal to 8% in weight showed the best performances among this series, with an increase of the productivity of formic acid (the main product of the photoreduction process) of 26.1% respect to the bare graphitic carbon nitride.

CONCLUSION

Significant productivity of formic acid was achieved through a high pressure photoreactor operating up to 20 bar and 80°C. Different samples of graphitic carbon nitride were compared and the best results were achieved upon exfoliation of the material, thanks to increased photocharges lifetime as determined by spectrofluorimetry and by achieving Z-scheme formulations.

ACKNOWLEDGMENTS

The authors gratefully acknowledge the financial contribution of Fondazione Cariplo through the grant 2021-0855 – "SCORE - Solar Energy for Circular CO_2 Photoconversion and Chemicals Regeneration", funded in the frame of the Circular Economy call 2021 and of MUR funding the project RIN2022PNRR "P20227LB45 - SCORE2 - Solar-driven COnveRsion of CO2 with HP-HT photorEactor" within PIANO NAZIONALE DI RIPRESA E RESILIENZA (PNRR).

Methanation of Biogas to Store and Distribute Green Hydrogen

Matteo Tommasi[1], Alice Gramegna[2], Simge Naz Degerli[2], Gianguido Ramis[3], Ilenia Rossetti[1,2*]
[1] Chemical Plants and Industrial Chemistry Group, Dip. Chimica, Università degli Studi di Milano and CNR-SCITEC, via C. Golgi 19, Milan, Italy.
[2] INSTM Unit Milano-Università, Dip. Chimica, Università degli Studi di Milano, via C. Golgi 19, Milan, Italy, presenting author, *corresponding author
[3] Dip. DICCA, Università degli Studi di Genova and INSTM Unit-Genova, Genoa, Italy
*ilenia.rossetti@unimi.it

INTRODUCTION

Biogas contains large amounts of CO_2, to be at least separated to exploit biomethane, and possibly valorised. A first option is CO_2 hydrogenation to methane, also promising to transform an energy vector that is uneasy to handle (green H_2) into a valuable and worldwide-distributed fuel and feedstock (CH_4). A "power-to-gas" framework could then help to overcome the drawbacks of H_2 as an energy storage medium and to increase the continuity and general availability of different intermittent renewable energy sources. The aim of this work is to detail aspects of the methanation of CO_2 as a method for Carbon Capture and Utilisation using green hydrogen. Different options for the efficient direct conversion of CO_2 and H_2 into CH_4 (Sabatier reaction) are here explored both experimentally and through process design.

EXPERIMENTAL/THEORETICAL STUDY

Ni-based catalysts (5-20 wt%) supported over CeO_2, SiO_2, Al_2O_3 and ZrO_2 have been prepared by impregnation and co-precipitation. Testing has been done under practically relevant conditions at pressure up to 20 bar, with a stoichiometric H_2/CO_2 feed. Process design has been accomplished with Aspen Plus process simulator, considering the Sabatier reaction for the methanation of CO_2.

RESULTS AND DISCUSSION

We considered a small delocalised plant, identified in a biogas production facility. H_2 is considered as produced from water electrolysis fed with renewable power. A key issue is the strong exothermicity of the reaction. Our research explores the use of water vapour, added on purpose to the reactor as a thermal vector and later condensed. The simplest and most economical reactor arrangement is composed of a certain number of adiabatic beds (up to five) with intercooling. Alternative arrangement has been explored designing a fluidized-bed reactor, that allow better temperature control, but this led to incomplete conversion and was difficult to scale-up.

The possibility to use the methane already present in biogas as diluent (i.e. thermal vector to control the exothermicity) was also considered, offering the additional advantage to eliminate the otherwise needed and expensive CO_2 capture step.

This option is intended to improve the CH_4 yield and to meet the purity specifications for feeding the natural gas distribution grid. Possible poisons for the methanation catalyst, such as sulphides or nitrogen containing poisons, were considered and removed by proper pretreatment. Two options were further considered, one with preliminary CO_2 separation from biogas and methanation of pure carbon dioxide, the other on with direct treatment of the biogas stream.

At least 4 reactive stages for the methanation reaction were needed to get > 75% conversion. Either adiabatic or cooled catalytic beds were compared, operating at below 400°C, with an overall size of 10^5 Nm^3/day of synthetic methane.

CONCLUSION

The results show the feasibility of a methanation reactor suitable for the direct catalytic conversion of biogas from anaerobic digestion for the delocalized production of biomethane.

ACKNOWLEDGMENTS

The authors acknowledge Task 8.4.1 of the Agritech National Research Center, funded from the European Union Next-GenerationEU (PIANO NAZIONALE DI RIPRESA E RESILIENZA (PNRR) – MISSIONE 4 COMPONENTE 2, INVESTIMENTO 1.4 – D.D. 1032 17/06/2022, CN00000022).

Hydrogen production by supercritical water gasification of alcohols and aqueous fraction of fast pyrolysis bio-oil over NiY/activated charcoal catalyst

Muhammad W. Syed[1,2], Wajahat W. Kazmi[1,2], In-Gu Lee[1,2,*]

[1]Bioenergy & Energy Resources Upcycling Research Laboratory, Korea Institute of Energy Research, Yuseong-gu Daejeon 34129, Republic of Korea
[2]University of Science and Technology, Yuseong-gu Daejeon 34113, Republic of Korea

Abstract

Recently, biohydrogen has received much attention due to the increasing demand for renewable hydrogen in chemical industry. It is important to produce biohydrogen in the same place where hydrogen is required because the transportation of hydrogen is much costly. Although biohydrogen can be produced from a wide range of feedstocks from biomethane to lignocellulosic biomass, liquid forms of biomass are relatively preferred as a feedstock for biohydrogen production because of its manageableness and low transportation cost. In this work, alcohols (methanol and ethanol) and aqueous organic fraction of bio-oil from fast pyrolysis of lignocellulosic biomass were used as feedstocks for hydrogen production. A series of catalytic gasification was carried out in supercritical water using a continuous packed-bed reactor in order to minimize the formation of coke during the gasification reaction. NiY/activated charcoal was used as a gasification catalyst and its characterization was accomplished by SEM-EDX, XRD, N_2-physiasorption isotherms, NH_3-TPD and H_2-TPR. The effect of reaction temperature, WHSV and reactant concentration was investigated to obtain optimal gasification conditions. The gaseous products mostly consist of hydrogen, carbon dioxide, and methane with maximum hydrogen contents of 60 mol% for methanol, 51 mol% for ethanol, and 47 mol% for aqueous fraction of the bio-oil at 600 ^{o}C and 250 bar. The process analysis was performed in terms of mass balance, carbon gasification efficiency, and gas yield.

Spin rotational excitations in hexagonal $LuMnO_3$

Seung Kim [1], Sang-Wook Cheong [2] and **In-Sang Yang** * [3*]
[1]Department of Physics, Ewha Womans University, Korea
[2]Rutgers Center for Emergent Materials/Department of Physics and Astronomy, Rutgers University, USA
[3*]Department of Physics, Ewha Womans University, Korea, corresponding author (yang@ewha.ac.kr)

INTRODUCTION

We have observed spin rotational excitations in $LuMnO_3$ below the Neel ordering temperatures through resonant Raman scattering. We could assign all the spin excitation peaks in terms of Heisenberg spin interaction, and found that the spin rotational angles are predominantly 60, 120, 180 degrees commensurate with the triangular lattice of the Mn-ion spins. Unlike usual spin-wave excitations, this spin rotational excitations are limited to one triangular unit cell, thus costing relatively high excitation energy (~ 0.1 eV). Optically pumped and optically detected spin rotational excitations confined in a triangular cell can be a good candidate for future spin logic/memory devices.

EXPERIMENTAL/THEORETICAL STUDY

Hexagonal $LuMnO_3$ single crystal was grown using the traveling floating zone method. Platelet sample was cleaved perpendicular to the c axis. Helium-closed-cycle cryostat was used to control the temperature of the sample from 15 to 120 K in vacuum chamber. Raman scattering spectra were obtained by Horiba LabRam spectrometer coupled with a liquid-nitrogen-cooled CCD under $z(yx)\bar{z}$ cross configuration. Excitation light source was visible red laser which has continuous 671 nm (~1.85 eV) wavelength, with the power of 40 mW on the sample chamber window.

RESULTS AND DISCUSSION

Figure 1 shows temperature-dependent Raman spectra of the hexagonal $LuMnO_3$ single crystal in cross polarization scattering geometry. The broad Raman peaks near 197, 580, and 805 cm^{-1} are non-phononic in origin, get stronger at lower temperatures below the Neel ordering temperature. These broad peaks of hexagonal $LuMnO_3$ below T_N are found to be excited through the resonance with the Mn *d-d* transition by the incident red laser (~1.85 eV).

Along with theoretical analyses of the spin-spin interaction Hamiltonian and the Raman selection rules, we could conclude that the spin excitation peaks are due to simultaneous rotation of all three Mn spins in one Mn-trimer in hexagonal *R*MnO_3 at the antiferromagnetic state. Only special-angle rotations of the three Mn spins are allowed to preserve the triangular symmetry with the antiferromagnetic ordering, thus the spin rotation angles are quantized due to the triangular symmetry of the hexagonal *R*MnO_3.[1]

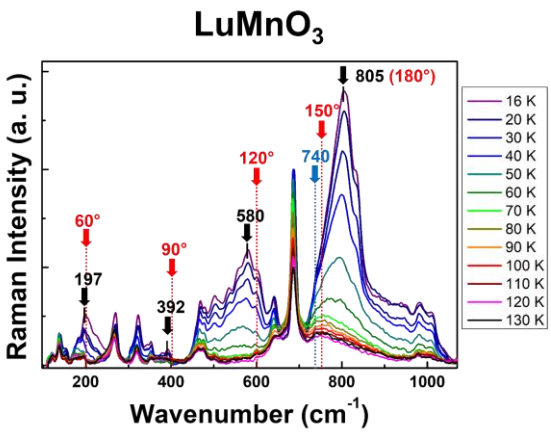

Fig. 1 Spin rotational excitation peaks are observed in hexagonal $LuMnO_3$ below T_N, The angles denoted are for the spin rotations of all three Mn-ion spins in one trimer with respect to the neighboring spins.

CONCLUSION

Spin rotational excitations in hexagonal $LuMnO_3$ are optically pumped by the incident laser (~1.85 eV) through resonance with the Mn *d-d* transition in the Raman scattering process. The observed broad Raman peaks are assigned to spin excitations corresponding to Mn-ion spin rotations by 60, 120, and 180 degrees in one triangular spin lattice. The role of Mn *d-d* transition near 1.7 eV needs to be clarified in future anti-Stokes Raman scattering measurements.

REFERENCES

1. S. Kim, J. Nam, X. Xu, S.-W. Cheong, and In-Sang Yang, Scientific Reports **12**, 2424 (2022).

ACKNOWLEDGMENTS

The measurements in this work were supported by Korea Basic Science Institute (National Research Facilities and Equipment Center) grant funded by the Ministry of Education (2020R 1A 6C 101B194). I.S.Y. acknowledges the financial support by Basic Science Research Program through the National Research Foundation of Korea (NRF) funded by the Ministry of Education (2021R1A6A1A10039823).

Computational Simulations of the Hydrogen and Methane Storage Capacities on novel MOF-521s at Room Temperature

Alejandra Granja-DelRío and Iván Cabria

Departamento de Física Teórica, Atómica y Óptica, Universidad de Valladolid, Valladolid, Spain

email: ivan.cabria@uva.es

INTRODUCTION

Lately, the intensification of global warming concerns linked to the use of fossil fuels has become more evident. An essential stride forward lies in the efficient storage of hydrogen and methane to bolster their application in electric vehicles powered by these gases. Hydrogen Fuel Cell Electric Vehicles (HFCEV) provide a carbon dioxide-free option, while Natural Gas Vehicles (NGV) contribute to reducing greenhouse gas emissions. The primary obstacle revolves around finding lightweight solid materials capable of storing hydrogen and methane gases, thereby achieving a comparable range to conventional fossil-fuel vehicles. Metal-Organic Frameworks (MOFs) represent a vast array of lightweight porous materials with numerous technological uses, including gas storage.

A recent study utilized the GPT-4 Reticular Chemistry, an AI model, to facilitate the discovery and synthesis of novel MOF-521 (Metal-Organic Framework) variants: MOF-521-H, -oF, and -mF [1]. These aluminum-based MOFs are light and possess pores with a width of approximately 10 angstroms, showing promise for gas storage applications.

THEORETICAL STUDY

Through GCMC (Grand Canonical Monte Carlo) simulations conducted at room temperature and pressures ranging from 0.5 to 35 MPa, the hydrogen and methane storage capacities, along with isosteric heats, of these innovative MOF-521s were evaluated. The simulations included calculations of total, excess, and usable storage capacities. Additionally, GCMC simulations were performed under identical conditions for classical MOFs, similar Al-based MOFs, and MOFs with comparable densities, porosities, and pore sizes as the new MOF-521s. These comparative analyses aimed to assess the capacities and isosteric heats of the new MOFs. Lennard-Jones potentials were used to simulate the interactions between the MOFs atoms and the molecules (hydrogen or methane), as well as between the molecules. The resultant data represent predictions regarding the hydrogen and methane storage capacities and isosteric heats of these innovative materials.

ACKNOWLEDGMENTS

This work was supported under MINECO research projects from Spain (Grants PGC2018-093745-B-I00).

REFERENCES

[1] Z. Zheng, Z. Rong, N. Rampal, C. Borgs, J. T. Chayes and O. M. Yaghi, Angew. Chem. Int. Ed. 62, e202311983 (2023)

Engineering New Nanostructured Hydrogel Precursors for 3D Printing of Artificial Bone Extracellular Matrices

Izabela-Cristina Stancu [1*], Elena Olăreț [1], Filis Curti [1,2], Adriana Lungu [1], Carmen-Valentina Nicolae[1], Sorina Dinescu [3,4], Alexandra-Elena Dobranici [3], Bogdan Stefan Vasile [5]
[1]Advanced Polymer Materials Group, National University of Science and Technology Politehnica Bucharest, Romania, corresponding author (izabela.stancu@upb.ro); [2]Zentiva S.A., Romania; [3]Department of Biochemistry and Molecular Biology, University of Bucharest, Romania; [4]Research Institute of the University of Bucharest (ICUB), Romania; [5]Department of Science and Engineering of Oxide Materials and Nanomaterials, National University of Science and Technology Politehnica Bucharest, Romania

INTRODUCTION

In this project we engineered new nanostructured hydrogel precursors for 3D printing, bioinspired from the nanocomposite bone extracellular matrix.

EXPERIMENTAL STUDY

The overall concept is presented in Fig. 1A. Gelatin, alginate, cellulose, and gellan gum were used to provide the hydrated matrix in which nanofillers mimicking the mineral phase of hard tissues were added. Paste-like 3D printable inks with different nanofiller loadings were formulated. Calcium carbonate from cuttle bone fragments, wollastonite and biosilica from diatomite were used for their reinfocing effect and for the potential to biomineralize. The scaffolds were characterized through swelling degree, water contact angle, stability under simulated physiological conditions, morphology evaluation, and nanoindentation. The nanocomposite nature was confirmed by scanning electron microscopy (SEM) and micro-computer tomography (micro-CT). *In vitro* biomineralization was tested. To assess scaffolds' biocompatibility and ability to support osteogenic differentiation *in vitro*, MC3T3-E1 cell line was used[1-3,4].

RESULTS AND DISCUSSION

Macroporous scaffolds with nanocomposite filaments (Fig. 1B) were obtained. Composition adjustments allowed improved deformation under controlled compression and a modulation of the bulk and surface mechanical behavior, leading to enhanced adhesion of preosteoblasts (Fig.1C). Formation of a new mineral phase was detected after cell cultures (Fig. 1D).

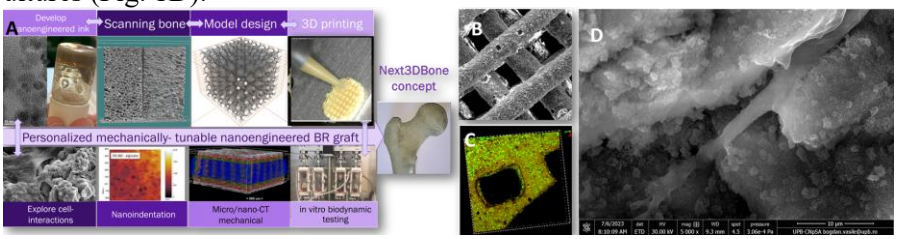

Fig. 1 (A) Methodology for the development of 3D printed scaffolds for bone regeneration (BR); (B) SEM revealing microporous nanocomposite 3D printed scaffold; (C) Preosteoblasts on 3D printed scaffold; (D) Preosteoblasts adhered and biomneralization during cell-culture (SEM).

CONCLUSION

We combined natural origin hydrogels with nanomaterials to fabricate osteoblast-responsive 3D printed scaffolds.

REFERENCES

1. F. Curti et. al, Mar. Drugs 20, 670. (2022) ; 2. S. Chiriac et al., J. Funct. Biomater., 15, 19 (2024); 3. C-V. Nicolae et al., Materials & Design 237. 112545 (2024)

ACKNOWLEDGMENTS

This work was supported from the project PN-III-P4-PCE-2021–1240, no. PCE 88/2022.

Stabilizing Interface of NCM811 Cathode Materials by Nb-oxide Coating

Jin-Sol Park[1], Jin-Hui Kim[1], Sang-Min Lee[2] and Jeom-Soo Kim[1*]
[1]Department of Chemical Engineering/BK21FOUR, DONG-A University, South Korea
[2]Graduate Institute of Ferrous & Eco Materials Technology, POSTECH, South Korea
JSenergy@dau.ac.kr

INTRODUCTION

Sulfide-based solid electrolytes exhibit ionic conductivity comparable to that of liquid electrolytes. However, their narrow electrochemical stability window results in easy decomposition, even at low voltages during electrochemical cycles. This decomposition triggers interfacial side reactions, leading to the formation of a lithium depletion layer due to the potential difference between lithium ions and the cathode. These phenomena hinder lithium ion diffusion and deteriorate the battery's electrochemical performance. Therefore, it is crucial to modify the surface of the cathode material by applying substances that suppress interfacial side reactions and facilitate the smooth movement of lithium ions.

RESULTS AND DISCUSSION

Nb-oxide coated NCM811 materials were characterized both physically and electrochemically. Samples that underwent solvent filtration after surface coating exhibited improved coating uniformity compared to those treated with solvent evaporation. SEM and EDS mapping revealed a uniform distribution of Nb. No impurity phases were detected after heat treatment at 500°C.

Nb-coated NCM811 was thoroughly evaluated using a liquid electrolyte. The sample with 0.6 mol% Nb coating achieved a discharge capacity of 215.4 $mAh \cdot g^{-1}$ and a coulombic efficiency of 94%, demonstrating the best performance among all samples in the first cycle. The Nb-oxide surface layer is believed to suppress side reactions between the cathode and electrolyte.

The effectiveness of the Nb-oxide coating was also confirmed with a solid electrolyte. The 0.6 mol% Nb-coated NCM811 showed significantly improved discharge capacity (204.5 $mAh \cdot g^{-1}$) and efficiency (94%) compared to pristine NCM811. More detailed results will be presented at the meeting.

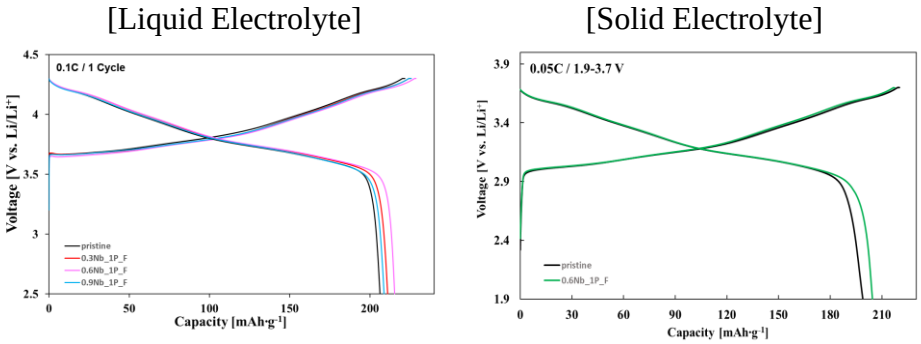

Fig. 1 Voltage profiles of 1st cycle for Nb-oxide coated NCM811 electrodes with liquid and solid electrolytes

CONCLUSION

The Nb-oxide coating is an effective method to enhance the surface stability of NCM811 cathode material by mitigating side reactions with electrolytes. To achieve optimal improvement, it is crucial to ensure coating uniformity and apply the appropriate amount of coating material. The enhancing mechanism of the Nb-oxide coating may vary with the phase of the electrolyte, which will be explored in future studies.

Optimization of Thickness for Alumina-Coated Separators for Lithium-ion batteries

Ji-Hui Oh[1,2], Jin Ae Kim[1], Dong-Won Lee[1], Weon Ho Shin[2], Min Gi Jung[3] and Jong Min Oh*[2*]
[1]Material Technology Center, Korea Testing Laboratory, KOREA, presenting author
[2*]Department of Electronic Materials Engineering, Kwangwoon University, KOREA, corresponding author (jmoh@kw.ac.kr)
[3]Department of Materials Science and Chemical Engineering, Hanyang University, KOREA

INTRODUCTION

The Study investigates the optimization of coating thickness for lithium-ion battery separators in response to the stability issues arising from the weak heat resistance of polyethylene (PE) and polypropylene (PP)[1]. Coating substrates with alumina or boehmite slurry is a common method, but variation in coating thickness impact performance. The research optimized the coating thickness of separators with excellent thermal stability through SEM, 3D profiling, and various analysis. Additionally, we conducted a comparative analysis of the characteristics of separators with single-side and double-side coating at the same thickness.

EXPERIMENTAL/THEORETICAL STUDY

To confirm the optimized single-side coating thickness, measurements of the single-side coated separator were conducted using scanning electron microscopy (SEM), surface analysis was performed using a 3D profiler, and roughness was measured. Additionally, thermomechanical analysis (TMA) was carried out to assess heat resistance, and ion conductivity performance was compared through electrochemical impedance spectroscopy (EIS).

RESULTS AND DISCUSSION

The experiment involved analyzing characteristics such as particle size and specific surface area of alumina powder and evaluating the performance of separators coated with various thicknesses. Results from the analysis of properties such as air permeability, contact angle, Puncture strength and thermal shrinkage indicated that a coating thickness of 4 ㎛ was optimal, and double-side coating exhibited superior characteristics compared to single-side coating.

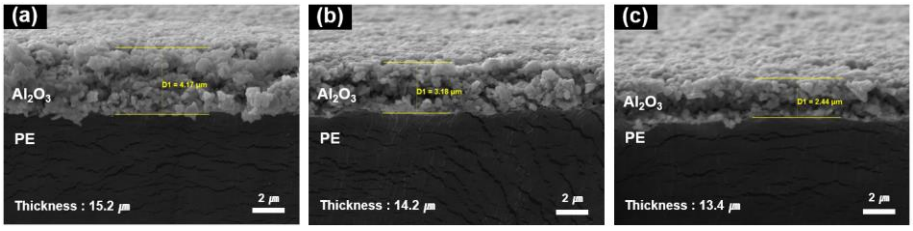

Fig. 1 Scanning electron microscopy (SEM) image of (a) 4 ㎛ (b) 3 ㎛ (c) 2 ㎛ single-side Al_2O_3 coated separators.

CONCLUSION

Among single-side coated separators with thickness of 2 ㎛, 3 ㎛, 4 ㎛ coated separator exhibited the highest thermal stability. A comparison between the single-side coating and double-side coating at the same 4 ㎛ thickness revealed an improvement in thermal stability when applying double-side coating.

REFERENCES

1. C.F. Francis, et. al. Adv. Mater. 32, 1904205 (2020)

ACKNOWLEDGMENTS

The research was supported by Korea Evaluation Institute of Industrial Technology(KEIT) grant founded by the Korea Government (MOTIE) (20012910), and the National Research Foundation grant(RS-2023-00212985) of Ministry of Science, ICT and Future Planning.

Correlation Between the Properties of ceramic-coated separators for Lithium-ion batteries and Powder Characteristics

Ji-Hui Oh[1,2], Yong-Nam Kim[1], Dong-Won Lee[1], Weon Ho Shin[2], Min Gi Jung[3] and Jong Min Oh*[2*]
[1]Material Technology Center, Korea Testing Laboratory, KOREA, presenting author
[2*]Department of Electronic Materials Engineering, Kwangwoon University, KOREA, corresponding author (jmoh@kw.ac.kr)
[3]Department of Materials Science and Chemical Engineering, Hanyang University, KOREA

INTRODUCTION

With the increasing incidents related to the safety of lithium-ion batteries, research is underway on the safety of heat-resistant separators typically made of polyethylene and polypropylene. Vulnerable to mechanical damage, these separators can lead to short circuits, increased internal temperature, explosions, and ignition. To enhance heat resistance, ceramic coating using slurries composed of ceramic particles like boehmite are widely employed[1]. This study specifically investigates the impact of ceramic particle characteristics, especially flowability, during coating on the properties of the separator.

EXPERIMENTAL/THEORETICAL STUDY

In the study, three different size of boehmite powders were used to analyze static and dynamic flowability, as well as particle size, and specific surface area. These powders were coated on PE separators using an aqueous method, and the coated separators were analyzed for thickness, porosity, contact angle, electrolyte uptake, puncture strength, and thermal shrinkage. Additionally, CR2O32-type coin cells were fabricated to evaluate the electrochemical properties.

RESULTS AND DISCUSSION

Static and dynamic flowability were excellent in the order of 0.3㎛, 0.5㎛ and 0.7㎛. Separators manufactured through aqueous coating of boehmite particles showed superior properties in various aspects, including permeability, contact angle, Puncture strength, thermal shrinkage, ion conductivitiy, and cell performance, with the 0.7㎛ particles exhibiting the best performance.

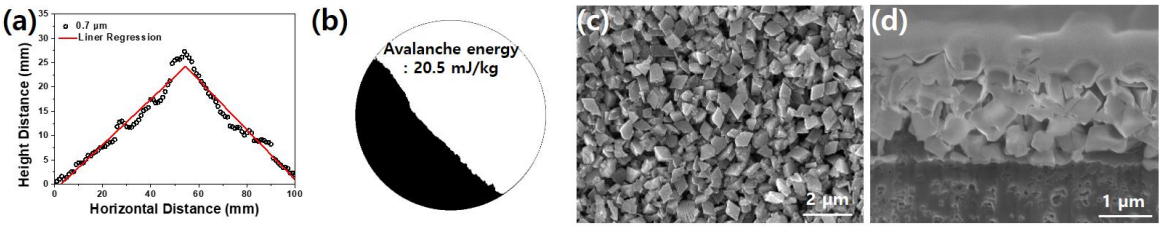

Fig. 1 Flowability measurement results of 0.7 ㎛ boehmite powder: (a) Static (b) Dynamic. SEM image of the (c)surface and (d)cross-section morphologies of the 0.7 ㎛ boehmite-coated separator.

CONCLUSION

Among boehmite powders with sizes of 0.3 ㎛, 0.5 ㎛ and 0.7 ㎛, the flowability of the 0.7 ㎛ was the most superior. The properties of the separator coated with 0.7 ㎛ boehmite powders, which demonstrated excellent flowability, were superior in the overall analysis.

REFERENCES

1. Y. Wang et. al. Ceram. Int. 47, 10153 (2021)

ACKNOWLEDGMENTS

The research was supported by Korea Evaluation Institute of Industrial Technology(KEIT) grant founded by the Korea Government (MOTIE) (20010739), and the National Research Foundation grant(RS-2023-00212985) of Ministry of Science, ICT and Future Planning.

Alginate-pectin composites: highly ordered fragments as revealed by NMR crystallography and advanced DFT calculations

Jiri Brus[1]*, Martina Urbanova[1], Jiri Czernek[1]
[1] Department of Structure Analysis, Institute of Macromolecular Chemistry, Czech Academy of Sciences, Czech Republic; brus@imc.cas.cz

INTRODUCTION

Alginate gels are outstanding biomaterials widely applicable in food and pharmaceutical industries. Although the gelation of alginate and pectin macromolecules is currently described by the *eggbox* model, when α-L-guluronic acid residues (G) in dyads (GG) are regularly complexed by Ca^{2+} ions, it has not been confirmed yet, whether alginate and pectin chains mutually interact to form hybrid eggbox dimers. Similarly, although it has been postulated that Ca^{2+} ions rapidly attack the guluronic G-blocks through electrostatic interactions, and Zn^{2+} ions interact with mannuronic M-blocks and guluronic G-blocks via coordination-covalent bonds, it is not known how the abilities to create different types of interactions affect the formation of hybrid alginate-pectin gels. This contribution thus addresses these issues and thus provides a comprehensive insight into the atomic-resolution structure of hybrid alginate/pectin co-networks double crosslinked by Ca^{2+}/Zn^{2+} ions.

EXPERIMENTAL/THEORETICAL STUDY

To obtain key information we recorded a representative set of ^{13}C CP/MAS NMR and FTIR spectra, as well as x-ray powder diffractograms that were subsequently analyzed by the approach of principal component analysis. In parallel we performed a series of high-level quantum chemical calculations by which we optimize potential local and medium-range geometries and predict corresponding NMR parameters.

RESULTS AND DISCUSSION

As a result, by using the comparative multi-dimensional factor analysis of NMR, FTIR and XRPD spectra we identified signals representing crucial structural motifs at the border between the amorphous and crystalline states, and elucidate the receptivity of different spectroscopic methods.

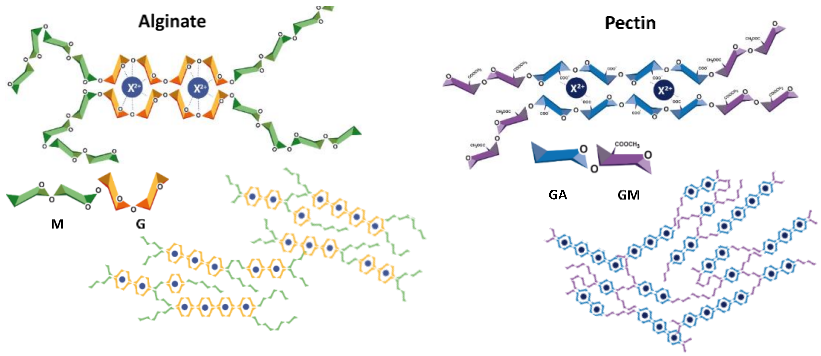

Fig. 1 Graphical representation of the currently accepted eggbox model for alginate and pectin.

CONCLUSION

In summary, by analyzing the large spectroscopic data sets in combination with large-scale NMR parameter predictions, we have uncovered the structural regularities associated with the formation and diversity of amorphous and partially ordered phases in alginate-pectin composites and hopefully found relationships between essential structural motifs and final properties.

ACKNOWLEDGMENTS

This work was supported by Czech Science Foundation (Grant No. 22-03187S and 23-05293S).

Efficient depolymerization and deoxygenation of lignins using MgNiMo/AC catalyst in supercritical ethanol

Ji-Yeon Park [1], Ishaq Kariim [2], Ghazaleh Amini [2] and In-Gu Lee [3*]
[1]Bioenergy and Resources Upcycling Research Laboratory, Korea Institute of Energy Research, Korea, presenting author
[2]Korea Institute of Energy Research, Korea
[3*]Korea Institute of Energy Research, Korea, corresponding author (samwe04@kier.re.kr)

INTRODUCTION

Depolymerization and deoxygenation of kraft, sulfuric acid, and organosolv lignins, as mechanisms to yield bio-oil, were demonstrated using the MgNiMo/activated charcoal (AC) catalyst in supercritical ethanol. Supercritical ethanol was used as both the solvent media for depolymerization and the hydrogen source for deoxygenation without additional hydrogen supply[1].

EXPERIMENTAL METHODS

An autoclave reactor of 200 mL capacity was used for the reactions. After reaction, all gas, liquid, and solid products were collected from the reactor for analysis. The characteristics of three differently produced lignins and bio-oils including elemental composition, HHV, molecular weight, FTIR, and NMR analyses, were determined.

RESULTS AND DISCUSSION

For the kraft, sulfuric acid, and organosolv lignins, bio-oil was obtained by supercritical ethanol reaction using an MgNiMo/AC catalyst. For effective depolymerization and deoxygenation of lignin, bio-oil yield, solid residue yield, oxygen content, HHV, molecular weight, gas product composition, and bio-oil composition were examined after a supercritical reaction. When the reaction time was increased from 0 to 1h in the absence of catalyst, the bio-oil yield decreased and the solid residue yield increased. The increase of the reaction time without catalyst encouraged repolymerization of depolymerized lignin. When the catalyst was applied to the supercritical ethanol system, all three lignins showed high and similar bio-oil yields. Using the MgNiMo/AC catalyst with supercritical ethanol, liquefaction of lignin was effectively performed. The catalyst promoted the depolymerization of lignin, and the ethanol media inhibited the repolymerization. The solid residue yields also decreased, and sulfuric acid lignin showed a very significant decrease. In the supercritical ethanol reaction for 0h without catalyst, the oxygen contents decreased from 27.44 to 23.12% for the kraft lignin, from 38.68 to 27.87% for the sulfuric acid lignin, and from 29.29 to 24.31% for the organosolv lignin. Without catalyst, the oxygen content decreased with reaction time. In the 1h experiment with catalyst, the oxygen content decreased again. The deoxygenation effectively occurred by reaction among ethanol, lignins, and MgNiMo/AC. The HHVs increased when the supercritical ethanol reaction was applied relative to the raw lignins, and increased with increasing time and catalyst use. For the kraft lignin, the properties of bio-oils under various conditions of time (1, 2, and 3h), temperature (300, 325, and 350˚C), catalyst dosage (2, 4, and 6 wt%), and ethanol to lignin ratio (90:10, 85:15, and 80:20 (w/w)) were compared. When the reaction time increased, the bio-oil yield increased and the solid residue yield decreased. When the reaction temperature was increased, the bio-oil yield increased and the solid residue yield decreased. When the catalyst dosage was increased, the bio-oil yield increased and the solid residue yield decreased. The bio-oil yield decreased and the solid residue yield increased relative to the case of 90:10 (w/w). The oxygen content was the lowest and the carbon content was the highest at 90:10 (w/w). Among all of the experiments, the highest HHV, 35.44 MJ/kg, was obtained at 350˚C for 3h reaction time under the 90:10 (w/w) ethanol to lignin ratio and 4wt% catalyst. The O/C value of bio-oil decreased with increasing time, temperature, and catalyst dosage for the kraft lignin. The O/C value exhibited the minimum value at the ethanol to lignin ratio of 90:10 (w/w) and 350˚C for 3h with 4 wt% catalyst.

CONCLUSION

The bio-oil yields of the kraft, sulfuric acid, and organosolv lignins under the ethanol to lignin ratio of 90:10 (w/w), 4wt% catalyst, and 1h reaction time at 350˚C and 10 bar N_2 pressure were 73.8, 75.4, and 73.0wt%, respectively. When the MgNiMo/AC catalyst was applied to the supercritical ethanol system, bio-oils were produced with high yields and low oxygen contents compared with the cases without catalyst.

REFERENCES

1. M. Zhou et al., ACS Sustainable Chem. Eng. 6, 6867 (2018)

ACKNOWLEDGEMENTS

This work was supported by the National Research Foundation of Korea (NRF) funded by the Ministry of Science and ICT (No. NRF-2022M3J1A1085377) and by the Research and Development Program of the Korea Institute of Energy Research (KIER-C4-2440).

Production of a Galinstan Based Ferromagnetic Fluid for Thermal Applications

João Maganinho*[1], Vivian Andrade[1], João Araújo[1], Daniel Silva[1], João Ventura[1], Joana Oliveira[2], André Pereira[1], Ana Pires[1] and João Belo[1]

[1]IFIMUP - Institute of Physics for Advanced Materials, Nanotechnology and Photonics, Department of Physics and Astronomy, Faculty of Sciences of the University of Porto, Rua do Campo Alegre, 687, 4169-007 Porto, Portugal

[2] FEUP – Faculty of Engineering of University of Porto, R. Dr. Roberto Farias s/n, 4200-465 Porto, Portugal

* up201904740@up.pt

INTRODUCTION

The urge for miniaturization is associated with an excessive heating which shifts smaller-scale systems' working temperature from optimal values. Galinstan's large heat conductivity and magnetic material receptiveness[1], motivated us to produce a ferromagnetic fluid with Ni particles incorporated in a Galinstan matrix suitable for applications in fluidic thermal switches, wireless and remotely controllable through application of external magnetic fields. At room temperature, these thermal control devices design and adaptability make them a promising thermal management solution[2].

EXPERIMENTAL/THEORETICAL STUDY

The ferromagnetic fluids fabricated used Galinstan batches melted in a sand bath inside a steel pan[3]. The Ni microparticles were mechanically grinded with a steel file and posteriorly subjected to orbital ball milling. The mixing of the Ni particles into the Galinstan liquid was made inside a glove bag with a four-time purged inert Ar atmosphere. The magnetic material was mixed in and alloyed into the liquid metal using an agate mortar and pestle until achieving homogeneity[3].

To test our fluid's thermal applicability, we considered the experimental setup in Fig. 1 (a), where the magnetic field is controlled by the vertical periodic movement of NdFeB magnets automated by a home-made GUI.

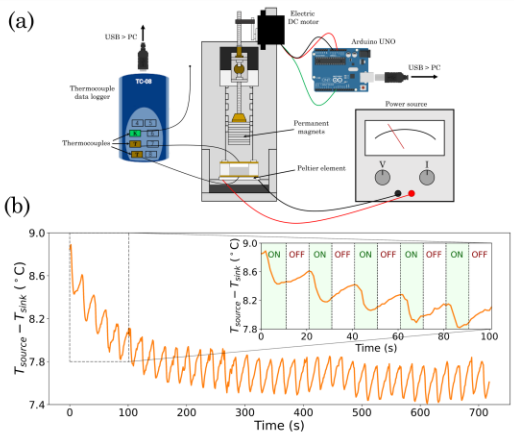

Fig. 1: (a) Experimental setup used. (b) Illustration of the temperature difference between heat source and sink during the switch actuation for a 65 % loading and a 0.05 Hz frequency.

RESULTS AND DISCUSSION

Through room-temperature SEM inspection, we found that the produced Ni particles follow a Weibull distribution with a mean particle size of (14±9) μm.

In our tests, we considered a mixture with 4 wt.% of Ni and different occupation levels of a cylindrical loading with 1 cm in height and diameter. For frequency values ranging from 0.01 Hz and 1 Hz we were able to achieve a maximum temperature span of 19.8% between heat source and sink which, combined with Fig. 1 (b), validates the device ability to control the heat flux and dissipate heat losses from the source.

CONCLUSION

We demonstrated that the produced ferromagnetic fluids are suitable for thermal management applications. Now, our focus will shift into the production of fluids with Ni nanoparticles for smaller-scale applications.

REFERENCES

1. Sen Chen, Hong-Zhang Wang, Rui-Qi Zhao, Wei Rao, and Jing Liu. Liquid metal composites. Matter, 2(6):1446-1480, jun 2020.
2. Joel B. Puga, et al. Novel thermal switch based on magnetic nanofluids with remote activation. Nano Energy, 31:278-285, 2017.
3. Isabela A. de Castro, et al. A gallium-based magnetocaloric liquid metal ferrofluid. Nano Letters, 17(12):7831-7838, nov 2017.

TiO_2/CuO_x thin film bilayers in different configurations for photoelectrochemistry

Joanna Banas-Gac[1*], Marta Radecka[2], Katarzyna Zakrzewska[1]
and Eduard Llobet[3]
[1*]Faculty of Computer Science, Electronics and Telecommunications, AGH University of Science and Technology, Poland, (jbanas@agh.edu.pl)
[2]Faculty of Materials Science and Ceramics, AGH University of Science and Technology, Poland
[3]Department of Electronic, Electrical and Automatic Engineering, Rovira i Virgili University, Spain

INTRODUCTION

Dynamics of the processes taking place in the PhotoElectroChemical cell (PEC) during green hydrogen generation[1] is considered as the most critical challenge to be faced. The key issue is to match the lifetime of photogenerated carriers to the time needed for the reaction of water splitting to occur. Therefore, it is necessary to conduct research on ensuring the most effective separation of photo-excited carriers. In the bilayer system the existence of the interface could contribute to the formation of internal electric field, similarly as in diodes, which may initiate the separation of photogenerated electron-hole pairs. The authors of this contribution will try to answer the question concerning the configuration of the TiO_2/CuO_x based heterojunctions[2] suitable for photoelectrochemical applications.

EXPERIMENTAL/THEORETICAL STUDY

Thin film multilayers were obtained by means of sequential reactive magnetron sputtering of Cu and Ti targets. X-ray diffraction (XRD) and X-ray reflectivity (XRR) were used to analyse the structural properties. X-ray Absorption Spectroscopy (XAS) and X-ray Photoelectron Spectroscopy (XPS) were performed at synchrotron SOLARIS (Poland) and Diamond Light Source (UK), respectively. Surface morphology was studied by Scanning Electron Microscopy (SEM) and Transmission Eletron Microscopy (TEM). Optical properties were determined with UV-VIS-NIR spectrophotometer. Photocurrent kinetics were measured in the PhotoElectrochemical Cell designed for this purpose.

RESULTS AND DISCUSSION

Cross-sectional HR-TEM images presented in Figures 1 a,b allow to distinguish well-defined interface between TiO_2 and CuO in two types of bilayer configuration. The comparison of X-ray absorption spectroscopy XAS in Partial Fluorescence Yield PFY and Total Electron Yield TEY modes enabled to draw conclusions regarding both volume and surface properties. The analysis includes the evolution of thin films prepared under different conditions (Fig. 1c) but also in terms of unintentional doping which occurs for TiO_2(top)/CuO bilayers, but not for inverse bilayer configuration in the form of CuO(top)/TiO_2. Photoelectrochemical measurements prove that both types of bilayers act as photocathodes and the photocurrent was found to be dependent on the thickness of TiO_2 top layer in the TiO_2(top)/CuO.

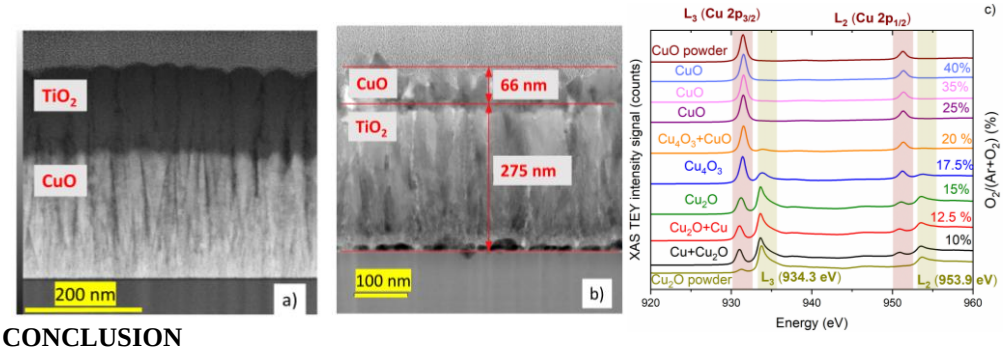

Fig. 1 *HR-TEM images of thin film TiO_2(top)/CuO (a) and CuO(top)/TiO_2 (b). XAS Cu $L_{2,3}$ spectra for CuO_x (c).*

CONCLUSION

Evaluation of the structure, optical, electronic and functional properties of TiO_2/CuO_x systems in combination with electronic band structure of the heterojunctions will be the basis for indicating type of configuration and interface properties that ensure improved photoelectrochemical properties.

REFERENCES

1. A. Kusoglu, Electrochem. Soc. 31, 47–51 (2022)
2. J. Banas-Gac et al. Appl. Surf. Sci. 616, 156394 (2023)

ACKNOWLEDGMENTS

Research supported by program „Excellence initiative – research university” for the AGH University of Science and Technology. This publication was partially developed under the provision of the Polish Ministry and Higher Education project "Support for research and development with the use of research infra-structure of the National Synchrotron Radiation Centre SOLARIS” - contract nr 1/SOL/2021/2.

Forecasting of the Steam Reforming of Ethanol for the Production of Hydrogen in a Photovoltaic Energy-Aided Packed Bed Membrane Reformer: Modelling and Simulation

Renato da Silva Pereeira[1], Jornandes Dias da Silva[*1]
[1]Polytechnic School - UPE, Laboratory of Environmental and Energetic Technology; Rua Benfica - 455, Madalena, Recife – PE, Brazil, Cep: 50750-470, Corresponding author: e-mail address:[*]jornandesdias@poli.br

INTRODUCTION

The steam reforming of ethanol (SRE) is currently considered a promising process for so-called synthesis gas (H_2 and CO). The SRE can be processed on the porous materials bed as solid open-cell foams due to high porosity and great surface area[1]. Solid open-cell foams are macroporous reticulated 3D structures constituted by interconnected cavities and made of metals (aluminum, steel), ceramics (alumina, silicon carbide etc.), or carbon materials. The Lumped-Particle Packed Bed (LPPB) Reformers have been substantially studied in the past years as a promising reformer to study the thermochemical conversion of ethanol[2]. This work has as main objective a theoretical modelling to describe the process variables of the SRE on the LPPB reformer

THEORETICAL STUDY

The mathematical modelling of the physical system is developed based on the process scheme of photovoltaic energy-driven SRE. The hybrid system can be built from solar parabolic trough, photovoltaic panels connected to battery bank, and solar heliostat. The finite volume method is used to solve the full mathematical modelling that involves mathematical models developed based on equipments of the schematic unit.

RESULTS AND DISCUSSION

Fig. (1a) shows average concentrations of H_2 and CO as a function of the operating temperature at the exit of the SRE reformer. Analyzing the syngas (H_2 and CO) as a function of the operating temperature is an important point because temperature is considered as indicator for the energy storage. As can be seen in Fig. (1a), both concentrations of H_2 and CO increase when the operating temperature raises. In view that, it is noted that H_2 has presented higher values regarding CO as the increase of the energy storage. Fig. (1b) reports the yield of H_2 as a function at different operating temperatures (573-973 K) at the exit of the SRE reformer. As results, the increase of the yield of H_2 is due to the energy thermal rise in reformer.

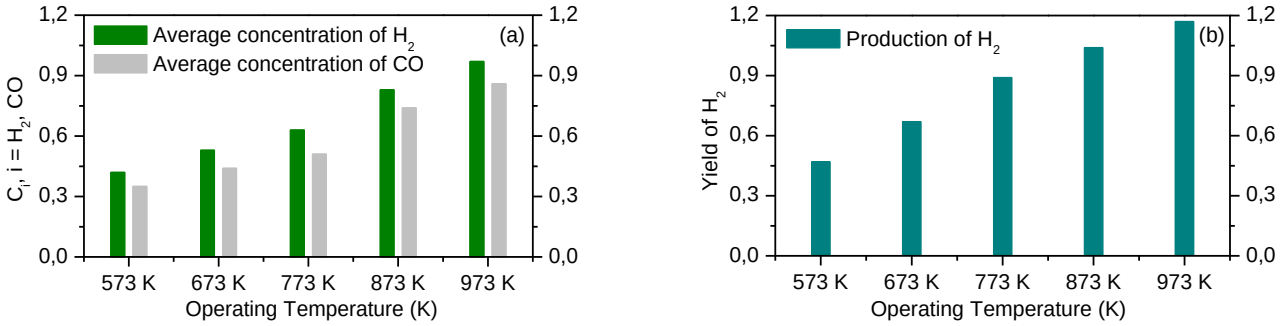

Fig. 1 (a) Average concentrations for H_2 and CO as a function of the operating temperature at the exit of the SRE reformer; (b) Yield of H_2 as a function of the operating temperature.

CONCLUSION

The solar-assisted hybrid energy systems are well-known and can be used in varying applications. The solar-driven reforming processes have become a promising technology to produce cleaner H_2. In this context, it is possible arriving the following conclusions: (1) as H_2 is considered an energy carrier, then H_2 is going to transport higher energy than CO. (2) The increase of the yield of H_2 depends on the rise of the operating temperature and, therefore, the higher yield of H_2 is at the larger operating temperature.

REFERENCES

1. V. F. Dias, J. D. Silva. An experimental investigation of gas−liquid−solid transfer and external wetting efficiency on open-cell foam in a three−phase packed bed reactor: validation and parameter estimation. Braz J Chem Eng 38, 1-18 (2022).
2. S. Anil, S. Indraja, R. Singh, S. Appari, B. Roy. A review on ethanol steam reforming for hydrogen production over Ni/Al_2O_3 and Ni/CeO_2 based catalyst powders. International J. Hydrogen Energy 47, 8177-8213 (2022).

ACKNOWLEDGMENTS

The authors of this paper would like to thank the CNPq (National Council of Scientific and Technological Development) for the financial support given (Process 56314/2021).

(HE) Hydrogen Energy

Magnetocaloric effect on nanocrystalline melt spun R_2Fe_{17} (R= Pr, Nd) ribbons

J.L. Garrido-Álvarez*[1], P. Álvarez-Alonso[1], C.F. Sánchez-Valdés[2], J.A. Blanco[1], P. Gorria[1], J.L. Sánchez Llamazares[1,3]
[1]Departamento de Física, Universidad de Oviedo, Spain
[2]Depto. de Física y Matemáticas, Universidad Autónoma de Ciudad Juárez, Mexico
[3]Instituto Potosino de Investigación Científica y Tecnológica A.C., Mexico
*presenting author: UO237413@uniovi.es

INTRODUCTION

R_2Fe_{17} intermetallic alloys, specifically those with R= Pr and Nd undergo second-order magnetic phase transition with Curie temperatures close to room temperature. These alloys exhibit a notorious broad magnetocaloric effect (MCE), rendering them exceptionally promising for diverse applications, including the burgeoning field of vibrational/mechanical energy-harvesting. The fabrication of these alloys into ribbon shape not only enhances their versatility, unlocking a spectrum of potential uses in various technological domains, but also reduces both economic and ecological processing costs by avoiding lengthy annealing processes during manufacturing.

EXPERIMENTAL/THEORETICAL STUDY

R_2Fe_{17} (R = Pr and Nd) ribbons were fabricated by melt-spinning[1]. The crystalline structure of the ribbons was determined using X-ray diffraction, while the microstructure and nanostructure of the samples were analysed using both scanning and transmission electron microscopy. Magnetic measurements were conducted in a PPMS magnetometer.

RESULTS AND DISCUSSION

The polycrystalline ribbons with the rhombohedral Th_2Zn_{17}-type crystalline structure (space group $R\bar{3}m$) consist of nanograins that form agglomerated nanocrystalline entities with an approximate average size of 15 nm. These nanograins are separated by boundaries where the crystalline order disappears. The coexistence of ordered and disordered regions gives rise to the existence of two successive magnetic phase transitions shown in the low-field magnetization vs. temperature curves. The low-temperature transition corresponds to the ferro-to-paramagnetic transition of the parent bulk alloy (290 and 326 K for R = Pr and Nd, respectively[2]); while the other one can be ascribed to occurring in the disordered boundaries (323 and 350 K for R = Pr and Nd, respectively). The contribution of the disordered phase to the MCE results in a remarkable broadening of the magnetic entropy change curve $|\Delta S_M|(T)$ accompanied by an enhanced refrigerant capacity (RC > 200 J·kg^{-1} for R = Pr at $\mu_0\Delta H$ = 5 T) in comparison with the parent bulk alloy[3,4]. Interestingly, a distinctive "table-like" behavior is also observed.

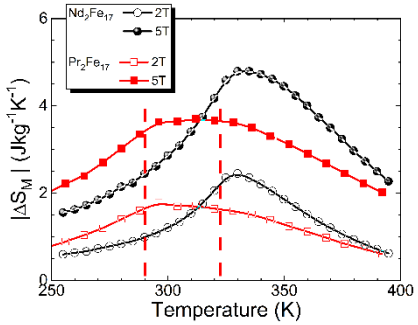

Fig. 1 Temperature dependence of the magnetic entropy changes for Pr_2Fe_{17} and Nd_2Fe_{17} melt-spun ribbons.

CONCLUSION

This work signifies progress in optimizing the magnetocaloric response at room temperature. By employing the nanostructuring of R_2Fe_{17} (R= Pr, Nd) fabricated by melt-spinning, we have successfully expanded the temperature range for the magnetic entropy change, as consequence of the existence of two successive magnetic transitions. Furthermore, we have demonstrated that a table-like behavior can be obtained under certain conditions. These findings are promising for applications such as vibrational/mechanical energy-harvesting. Our subsequent research will focus on exploring the impact of tension/pressure on the magnetocaloric effect to evaluate the performance of these ribbons in power generation from mechanical oscillations.

REFERENCES

1. Q. Johnson, D.H. Wood, G.S. Simth and A.E. Ray, Acta Cryst. B24, 274-276 (1968).
2. X.C. Kou et al., J. Magn. Mater. 177, 1002 (1998).
3. P. Gorria et al., Acta Mater. 57, 1724–1733 (2009).
4. P. Álvarez-Alonso et al., J. Appl. Phys. 115, 17A929 (2014).

ACKNOWLEDGMENTS

Work supported by Spanish MCIN/AEI/10.13039/501100011033/ and ERDF, UE (PID2022-138256NB-C21), and Principado de Asturias (SV-PA-21-AYUD/2021/51822). J.L.S.LL. acknowledges the support received from the EU-NGEU, MIU, and Plan de Recuperación, Transformación y Resiliencia (Maria Zambrano program; Ref: MU-21-UP2021-030 71741542).

Syngas production via oxidative reforming of methane and propane using a dual-phase inorganic membrane reactor

J. A. Fabián-Anguiano and J. Ortiz-Landeros *
[1]Department of Metallurgy and Materials Engineering/ESIQIE-IPN, Instituto Politécnico Nacional, México. *Corresponding author (jortizla@ipn.mx)

INTRODUCTION

It has been suggested that ceramic-carbonate membrane reactors selectively separate CO_2 at high temperatures and valorize it via a catalyzed reaction. Recently, reforming processes of hydrocarbons with CO_2 have been reinvestigated due to the potential to obtain syngas mixtures exhibiting different stoichiometric ratios of (H_2/CO). For example, dry reforming of CH_4 with CO_2 has been a case study for obtaining a low syngas ratio of about ~1[1]. As an alternative, propane (C_3H_8) reforming has recently attracted attention as a new route of decarbonization.[2]

EXPERIMENTAL/THEORETICAL STUDY

Dense membranes were obtained by uniaxially pressing $LiAlO_2$/Ag powders and the subsequent direct infiltration of the prepared supports with a eutectic ternary mixture of Li_2CO_3/Na_2CO_3/. Permeation measurements were conducted using a commercial Probostat high-temperature permeation system (NORECs) equipped with gas mixers and flow controllers.[2] Oxy-CO_2 reforming reactions into the system were performed by using a catalyst bed of 10 wt.% Ni supported on CeO_2 placed on the sweep side. In the membrane's permeate side, the sweep gas was switched from pure Ar to 7 vol % of CH_4 or C_3H_8 in Ar. Reaction products were analyzed by GC measurements.

RESULTS AND DISCUSSION

The CO_2 and O_2 permeating properties of a $LiAlO_2$/Ag-carbonate membrane are used to oxy-reform methane or propane in a membrane reactor. Operating at 725-850 °C, the membrane showed outstanding stability and permeability properties, including CO_2/N_2 and O_2/N_2 selectivity. After packing a Ni/CeO_2 catalyst, the membrane reactor produced syngas efficiently, above 800 °C. The membrane survived the long-term permeation test under working circumstances with little microstructural and permeation alterations. The membrane reactor's performance was affected by carbon deposition poisoning the catalyst during reaction testing, affecting syngas production. Thermodynamic simulations supported experimental results.

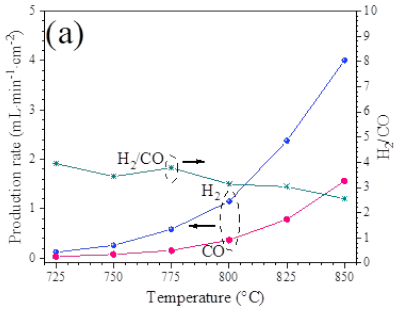

Fig. 1 Syngas production when using a sweep of C_3H_8 diluted in argon: (a) H_2 and CO production rate as a function of temperature.

.

CONCLUSION

Results are conclusive and evidence the high capability of the studied ceramic-carbonate membrane reactor to combine its perm-selectivity properties observed at 825-850 °C to perform a catalyzed reaction process such as the oxy-dry reforming.

REFERENCES

1. M. Alhassan et. al, RSC Advances, 13, 1711-1726 (2023).
2. J. A. Fabián-Anguiano et. al, Chem. Eng. Sci., 210, 115250 (2019).

ACKNOWLEDGMENTS

This work was supported by Proyectos de Investigación Científica y Desarrollo Tecnológico SIP-IPN 2024. The authors express appreciation for the SIBE-IPN, EDI-IPN, and BEIFI-IPN programs.

The Solid State Physics Programme at ISOLDE-CERN: an Important Update

Juliana Heiniger-Schell[1,2*]
[1]European Organization for Nuclear Research (CERN), CH-1211 Geneva, Switzerland
[2]Institute for Materials Science and Center for Nanointegration Duisburg-Essen (CENIDE), University of Duisburg-Essen, 45141 Essen, Germany

INTRODUCTION

ISOLDE-CERN is the worldwide reference facility for the production and delivery of radioactive ion beams of high purity. The produced beam is dedicated to many different purposes for, e.g., atomic and nuclear physics, astrophysics, material science, biophysics, and medical research. Since the late 70s the laboratory is pioneer in the use of nuclear techniques for studying local properties of materials using high-technology equipment[1].

EXPERIMENTAL TECHNIQUES

The brand-new ultra-high-vacuum implantation chamber called ASPIC's Ion Implantation chamber (ASCII)[2] decelerates the radioactive ion beam delivered at ISOLDE-CERN allowing to perform ultra-low energy ion implantations, and local measurements on the surface and interface of materials. The new MULTIPAC setup for Perturbed Angular Correlation Experiments in Multiferroic (and Magnetic) Materials[3] consists of a unique cryogenic magnetic system that simultaneously allows to measure local magnetic and ferroelectric properties of materials in magnetic fields up to 8.5 T. Last, but not least, the eMIL-Setup[4] is an advanced emission Mössbauer spectrometer for measurements in versatile conditions of several classes of materials, thanks to the emission Magnetic Mössbauer Analyzer (eMMA) extension[5].

DISCUSSION

The huge demand for innovative materials, which will be used in the new generation of "green" technology, such as motors, generators, wind power, photovoltaics, e-mobility, requires local characterization techniques. Our research program offers this possibility and is open to new ideas and collaborators and the proposals are evaluated by the ISOLDE and Neutron Time-of-Flight Experiments Committee (INTC).

CONCLUSION

This presentation introduces the new setups as powerful tools and discuss the possibilities of investigations on the frontiers of solid-state physics research, an update to the literature[6,7].

REFERENCES

1. K. van Stiphout, et al. Letter of Intent to the ISOLDE and Neutron Time-of-Flight Committee. CERN-INTC-2023-006 / INTC-I-248 (11/01/2023.
2. K. van Stiphout, L.-A. Lieske, M. Auge and H. Hofsäss, Crystals 12(5), 626 (2022).
3. J. H.-Schell et al., Letter of Intent to the ISOLDE and Neutron Time-of-Flight Committee. CERN-INTC-2023-012 / INTC-I-249 (11/01/2023).
4. D. Zyabkin et al., NIM A, 968, 163973 (2020).
5. P. Schaaf, D. Zyabkin, J Schell. Letter of Intent to the ISOLDE and Neutron Time-of-Flight Committee. CERN-INTC-2020-008 / INTC-I-211 (08/01/2020).
6. K. Johnston et al., J. Phys. G Nucl. Part. Phys. 44, 104001, (2017).
7. J. H.-Schell, CERN EP Newsletter "ISOLDE: On the frontiers of materials science for a sustainable future". Available at https://ep-news.web.cern.ch/content/isolde-frontiers-materials-science-sustainable-future (10/03/2024).

ACKNOWLEDGMENTS

Special thanks to Prof. Armandina Lopes, Dr. Joao Guilherme Correia, Prof. Vitor Amaral and Prof. Joao Pedro Araujo for their wonderful scientific contributions to our research programme. I thank the financial support received from the German Ministry of Education and Research (BMBF) under grants 05K16PGA, 05K22PGA and 05K22PGB, the Portuguese Foundation for Science and Technology (FCT, projects CERN/FIS-TEC/0003/2019 and CERN/FIS-TEC/0003/2021) and the European Union's Horizon Europe Framework research and innovation programme under grant agreement no. 101057511 (EURO-LABS).

(ANM) Advanced Nano Materials

DFT-Determined Chemi and Physisorption Degrees of Adsorption of Alkali Metals by a SnC Monolayer

Julio-Zuriel Gonzalez-Vazquez[1], Álvaro Miranda[1], Raúl Oviedo-Roa[2], Fernando Salazar[1], Miguel Cruz-Irisson[1]

[1]ESIME Culhuacán, Instituto Politécnico Nacional, México
[2*]Instituto Mexicano del Petróleo, México, México oviedor@imp.mx

INTRODUCTION

The efficiency of molecular hydrogen storage by nanostructured surfaces depends on the intensity under which the hydrogen molecules are adsorbed, which can be modulated through decorating of the adsorbing surface with adatoms. In this work we apply a methodology for determining the degree of chemisorption and physisorption [1] in order to characterize the adsorption of alkali-metal (AM) atoms from Li to Cs on hexagonal monolayers of tin carbide (SnC) [2].

THEORETICAL STUDY

The adsorption of adatoms was investigated by calculating the adsorption energy ΔE on the SnC monolayer, defined as $\Delta E = E_{\mathrm{AM:SnC}} - (E_{\mathrm{AM}} + E_{\mathrm{SnC}})$, where $E_{\mathrm{AM:SnC}}$, E_{AM} and E_{SnC} are the Density-Functional-Theory (DFT)-calculated energies for the AM-containing SnC monolayer, the free AM and the pristine SnC, respectively. In general, the energy E can be broken down as $E = E_{\mathrm{non-disp}} + E_{\mathrm{disp}}$ where $E_{\mathrm{non-disp}}$ is the non-dispersive component, originated from quantum interactions which can give rise to the formation of covalent bonds, and E_{disp} is the dispersive component due to long-range interactions. Therefore, it is defined the degree of chemisorption as $D_{\mathrm{chem}} \equiv \Delta E_{\mathrm{non-disp}}/\Delta E$ and that of physisorption as $D_{\mathrm{phys}} \equiv \Delta E_{\mathrm{disp}}/\Delta E$.

RESULTS AND DISCUSSION

The degree of chemisorption between the monolayer's Sn atom and the adatom decreases as the AM atom's radius increases from 87.34 % for Li down to 72.56 % for Cs. However, the new formed bonds among adatoms and the SnC monolayer have mainly physisorption character; *i.e.*, the net chemisorption degree results as a global effect of non-covalent bonds. Likewise, as expected, the adsorption energy goes with the chemisorption degree, validating the method for calculating the chemisorption degree. Finally, the electrons of the highest *s* atomic levels of AMs are fully transferred to the C atoms neighboring to the adsorption sites.

CONCLUSIONS

The calculation of the degrees of chemi and physisorption based on the non-dispersive and dispersive contributions to the adsorption energy allows for a quantitative measure of the adsorption character. The SnC monolayer adsorbs AM atoms mainly under a chemisorption character although individual linking bonds are non-covalent. The AM atoms size affects both chemisorption degree and adsorption energy.

REFERENCES

[1] Bermeo-Campos, R., Arellano, L. G., Miranda, Á., Salazar, F., Trejo-Baños, A., Oviedo-Roa, R., & Cruz-Irisson, M. (2023). DFT insights into Cu-driven tuning of chemisorption and physisorption in the hydrogen storage by SnC monolayers. Journal of Energy Storage, 73, 109205.

[2] Marcos-Viquez, A. L., Miranda, A., Cruz-Irisson, M., & Pérez, L. A. (2022). Tin carbide monolayers decorated with alkali metal atoms for hydrogen storage. International Journal of Hydrogen Energy, 47(97), 41329-41335.

ACKNOWLEDGEMENTS

This work was partially supported by multidisciplinary project IPN-SIP 2024-0702 and UNAM-PAPIIT IN109320. Computations were performed at the supercomputer Miztli of DGTICUNAM (Project LANCAD-UNAM-DGTIC-180). J.Z.G.V. would like to thank CONACYT and BEIFI-IPN for their financial support.

(ANM) Advanced Nano Materials

Dielectric and electrical properties of complex perovskite Nano-materials

K.D. Mandal*, Anup Kumar
Department of Chemistry, Indian Institute of Technology (Banaras Hindu University), Varanasi, UP 221005, India

* Corresponding Author E-mail: kdmandal.apc@itbhu.ac.in

Abstract

$ACu_3Ti_4O_{12}$ (ACTO, where A = Ca, $Y_{2/3}$, $Bi_{2/3}$) type of ceramics were successfully synthesized by semi-wet route. The Single phase formation of these ceramic was confirmed by powder X-ray diffraction studies. These ceramics were further characterized by dielectric and impedance studies. The dielectric constant (ε_r) was found very high for these ceramics at room temperature. The tangent loss (tan δ) value of these ceramics were found slightly high. Scientists have been working to reduce dielectric loss by doping or partial substitution of different elements at Cu and Ti sites independently or simultaneously by applying different synthesis route. The dielectric constant and tangent loss both decrease with increasing frequency in the lower frequency regions, while these are almost constant in the higher frequency regions. Impedance studies were used to see the contributions of grain and grain boundaries effect.

****

Unraveling the Mechanisms of the First-Order Phase Transition in Near-Equiatomic Fe-Rh Alloys

K. Padrón-Alemán* [1,2*], M. Rivas [1], J.C. Martínez-García [1], P. Álvarez-Alonso [1], P. Gorria [1], J.H. Belo [3], A.M. dos Santos [4], J.L. Sánchez Llamazares [5]

[1]Departamento de Física, Universidad de Oviedo, Oviedo, Spain

[2*]Institut Laue-Langevin, Grenoble, France, presenting & corresponding author (padronk@ill.fr)

[3]Departamento de Física e Astronomia, Faculdade de Ciências, Universidade do Porto, Portugal

[4]Neutron Scattering Division, Oak Ridge National Laboratory, Tennessee, USA

[5]Instituto Potosino de Investigación Científica y Tecnológica A.C., San Luis Potosí, México

INTRODUCTION

Near-equiatomic Fe-Rh alloys exhibit record-breaking giant magnetocaloric effect around room temperature. These alloys undergo a first-order phase transition (FOPT) from antiferromagnetic (AFM) to ferromagnetic (FM) and vice versa accompanied by approximately 1 % cell volume change upon heating/cooling while keeping the ordered CsCl-type crystal structure[1]. The magnetic properties of these alloys strongly depend on composition and fabrication methods[2]. Understanding the underlying mechanisms of the phase transition is, therefore, essential for guiding the material improvement for applications. In this work, we focused on two bulk alloys with close composition, $Fe_{50}Rh_{50}$ and $Fe_{49}Rh_{51}$, which display markedly different FOPT[2]. To gain insights of the magnetic and structural phase transition, we combined neutron thermo-diffraction and magnetization analysis along with temperature first-order reversal curves (T-FORC).

EXPERIMENTAL/THEORETICAL STUDY

$Fe_{100-x}Rh_x$ bulk alloys with x = 50 and 51 were prepared by induction melting and thermally annealed at 1000 °C for 48 h[2]. Neutron temperature dependent diffractogram patterns were obtained using the time-of-flight technique. Conventional and T-FORC magnetization measurements, were performed under a constant applied magnetic field $\mu_0 H$ of 2 T.

RESULTS AND DISCUSSION

The differences in the FOPT of the two alloys are fingerprinted in the T-FORC distribution (Fig. 1). Our analysis and previous works[3] suggest that the FOPT in the $Fe_{50}Rh_{50}$ alloy is governed by internal stresses that lead to coexistent domain nucleation and growth over a large range of temperatures. In contrast, the presence of an additional Rh atom compared to Fe in the $Rh_{49}Rh_{51}$ alloy can trigger sudden nucleation followed by coalescence, resulting in a very sharp magnetostructural transition. The reported change of volume of the unit cell in 1% approximately in both alloys, being abrupt in the $Fe_{49}Rh_{51}$, support the above reasoning.

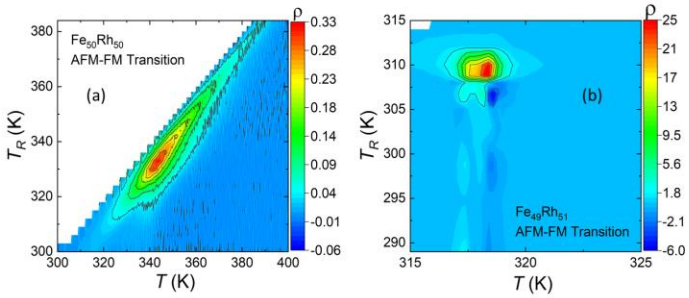

Fig. 1 T-FORC distribution for $\mu_0 H = 2$ T of the transition AFM-FM of (a) $Fe_{50}Rh_{50}$ and (b) $Fe_{49}Rh_{51}$.

CONCLUSION

The disparity between the T-FORC distribution of each alloy highlights the contrast between both phase transitions. Through close observation of the evolution of the lattice parameter, the T-FORC, and their T-derivatives, we unraveled the mechanisms of the transition in each alloy. From our study, the T-FORC analysis emerges as a valuable fingerprint for capturing typical behaviors.

REFERENCES

1. L.H. Lewis et. al, J. Phys. D: Appl. Phys. 49, 323002 (2016)
2. M.L. Arreguín-Hernández et. al, J. Alloys. Compd. 871, 159586 (2021)
3. D. J. Keavney et. al, Sci Rep, vol. 8, no. 1 (2018)

ACKNOWLEDGMENTS

Work supported by MCIU, AEI, European FEDER (MCIU-19-RTI2018- 094683-B-C52), Principado de Asturias (SV-PA-21-AYUD/2021/51822), SEP-CONACyT, Mexico (project A1-S-37066), and LINAN (IPICyT), Spain MCIN/AEI/10.13039/501100011033/, and ERDF, UE (project number: PID2022-138256NB-C21). J.L.S.LL. acknowledges for the support received from the EU-NGEU, MIU, and Plan de Recuperación, Transformación y Resiliencia (Maria Zambrano program; Ref: MU-21-UP2021-030 71741542).

The effects of surface fluorination on the sintering and electrochemical properties of oxide-based solid electrolytes (LLTO, $Li_{3x}La_{2/3-x}TiO_3$)

Kodai Sakaguchi [1], *Jae-ho Kim** [2] *and Susumu Yonezawa* [3]
[1,2,3]*Department of Materials Science and Engineering, Faculty of Engineering, University of Fukui, Japan*
[1]*presenting author*
[2*]*corresponding author (kim@matse.u-fukui.ac.jp)*

INTRODUCTION

All-solid-state batteries are a next-generation batteries with growing expectations in terms of safety and performance[1]. However, there are many challenges. The expansion and contraction of the active material causes poor interface connection (the surface where the active material and electrolyte are in contact) and cracks in the electrode, and the performance degradation due to rapid increase in interface resistance is a major issue[2]. In particular, the increasing of particle size in making process of the oxide solid electrolytes causes to a decrease in the contact area with the active material, and makes it difficult to maintain the bonding. In this study, we attempt to prepare high purity and fine particle solid oxide electrolytes (LLTO, $Li_{3x}La_{2/3-x}TiO_3$) for all solid-state batteries by various synthesis methods such as solid phase method and hydrothermal synthesis, using surface fluorination techniques

EXPERIMENTAL/THEORETICAL STUDY

The following two methods were attempted in the preparation of oxide solid electrolytes. (1) In the solid phase method, Li_2CO_3, La_2O_3, and the fluorine-modified TiO_2 were mixed in ethanol at a molar ratio of 0.33:0.56:2 (x=0.1), and sintering conditions (temperature (800~1200 °C), time (4~22 h), etc.) were changed. (2) In the hydrothermal synthesis, the specimens were prepared by mixing a solution containing Li_2CO_3 and La_2O_3 at a molar ratio of 0.33:0.56:1 (x=0.1), heating and pressurizing the mixture for 24 h at 200 °C in a sample decomposition vessel (HU-100) and then sintering the mixture for 6 h at 800 °C. A commercial product (Toho Titanium Co., Ltd.) was used for comparison.

RESULTS AND DISCUSSION

The XRD results (Fig. 1) show that high purity LLTO can be synthesized by the solid-phase method. Fig. 2 shows that LLTO can be made into finer particles than commercial samples. The improved dispersibility and reactivity of the raw material may be caused to the effects of surface fluorination.

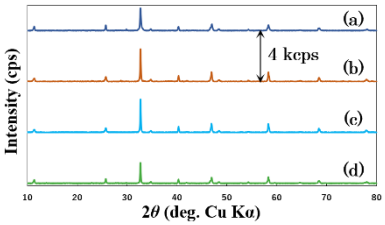

Fig.1 XRD patterns for LLTO samples synthesized at various reaction temperatures. [(a)800°C→900°C→1000°C, (b)800°C→1000°C→1100°C, (c)800°C→1100°C→1200°C, (d)commercial sample]

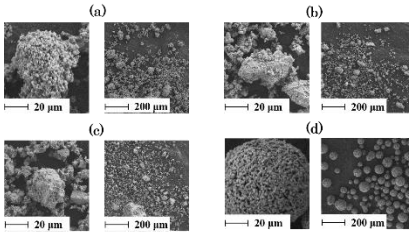

Fig.2 SEM micrographs of various LLTO samples. [(a)800°C→900°C→1000°C, (b)800°C→1000°C→1100°C, (c)800°C→1100°C→1200°C, (d)commercial sample]

CONCLUSION

In the solid-phase method, we succeeded in synthesizing high-purity and fine-particle LLTO by using surface fluorination treatment technology. In this presentation, we will report the results of XRD, FE-SEM, and particle size distribution analysis of LLTO samples synthesized by methods other than the solid phase method, as well as the electrochemical properties of solid electrolytes synthesized by the solid phase method.

REFERENCES

1) *Kun Yu et. al.*, Journal of the European Ceramic Society, 38, 4483–4448 (2018)
2) *Xinyi Zou et. al.*, Journal of Energy Storage, 74, 109483 (2023)

Magnetic field-enhanced hydrogen evolution reaction on Ni foam electrodes

Konrad Eiler* [1*], Jordi Sort [1,2] and Eva Pellicer [1]
[1]Departament de Física, Universitat Autònoma de Barcelona, Spain
[2]Institució Catalana de Recerca i Estudis Avançats, Pg. Lluís Companys 23, Barcelona, Spain

In view of the climate crisis and increasing international restrictions with respect to emissions, hydrogen and fuel cell technology is a promising candidate for future energy supply in all sectors. Research focuses on making the technology affordable for large-scale implementation, by avoiding the use of platinum group metals, nanostructuring electrocatalysts, and making the electrochemical processes for hydrogen production as energy-efficient as possible.

In recent years, the enhancement of water splitting through external magnetic fields has gained great attention from the research community. Concerning the hydrogen evolution reaction (HER), the reaction responsible for hydrogen production, its enhancement through magnetic fields is generally ascribed to magnetohydrodynamic (MHD) effects as a result of electrolyte convection due to Lorentz forces. While most studies focus on the effect of magnetic fields on sophisticated nanostructured electrodes, the physical nature of magnetic field-enhanced electrocatalysis lacks investigation.

In this work, the effect of electrolyte concentration on the activity of commercial Ni foam electrodes under the actuation of a magnetic field is studied in alkaline and neutral media. It is revealed that the effect of magnetic fields on the HER is significantly enhanced at low concentrations of the electroactive species (OH^-). During chronopotentiometry at a constant current density of –10 mA/cm^2, homogeneous magnetic fields are supplied to a miniature three-electrode electrochemical cell normal to the electric field by means of an electromagnet. 1.2 T, 0.4 T and 0.2 T are applied in the form of pulses of 20-50 s. While at electrolyte concentrations of 1.0 M KOH and 0.1 M KOH, the shift in overpotential when applying a magnetic field of 1.2 T is on the order of 10 mV (thus making the HER energetically more favourable), at an electrolyte concentration of 0.01 M KOH the enhancement in overpotential is on the order of 100 mV, both with and without KCl as a supporting electrolyte. Finally, in a neutral electrolyte containing 1 M KCl (similar to seawater conditions), the improvement in overpotential amounts to 50 mV. The studies are complemented by linear sweep voltammetries with and without an applied magnetic field.

The observed effects are related to the so-called magnetic gradient force as part of the Kelvin force, which is established in case of the existence of a gradient in the magnetic flux density B as well as a gradient in the magnetic susceptibility χ. The gradient in magnetic susceptibility is caused by a concentration gradient ∇c of the paramagnetic species OH^- through the electrolyte, which develops due to the electric field between the Ni foam and a Pt counter electrode during HER electrocatalysis, and potentiates at very low species concentrations. In addition, a gradient of B is established at the interface between the electrolyte and the ferromagnetic Ni foam in a homogeneous magnetic field. The rotational part of the Kelvin force density, f_K, responsible for a mass flow on OH^- species can be expressed as[1]:

$$\nabla \times f_K = \frac{\chi}{2\mu_0}(\nabla c) \times (\nabla B^2)$$

This work provides new insight on the fundamentals of magnetic-field enhanced electrocatalysis, and the observations made may have a significant impact on seawater catalysis at close to neutral pH, where the concentration of electroactive species are low.

REFERENCES

1. G. Mutschke et. al, Electrochim. Acta 55, 9060 (2010).

ACKNOWLEDGMENTS

This work has received funding from Generalitat de Catalunya under project 2021-SGR-00651, and the Spanish Ministerio de Ciencia e Innovación under PID2020-116844RB-C21 and associated FEDER Project.

Irradiation of nitrogen plasma on TiO_2 and ZnO nanowire arrays for organic photovoltaic solar cell applications

Bello Ladan Muhammad[a], Franscious Cummings[b], Jibrin Alhaji Yabagi[a] Maryam Mohammed[a]

[a]Department of Physics, Ibrahim Badamasi Babagida University P.M.B 11 Lapai, Niger State Nigeria
[b]Electron Microscope Unit, University of the Western Cape, Private Bag X17, Bellville 7535, South Africa.

.

Abstract

This work reports on a simple, yet unique approach to improving the opto-electronic properties of vertically-aligned arrays of rutile TiO_2 and Wurzite ZnO nanowires by means of controlled nitrogen doping during exposure to highly kinetic radio-frequency generated N_2 plasma radicals. Morphologically, the plasma treatment causes a distortion of the vertical alignment of the nanowires due to a dissociation of the weak Van der Waals force clustering the nanowires. Optical spectroscopy show that plasma treatment increases the light transmission of TiO_2 arrays from 48% to 90%, with the ZnO arrays exhibiting an increase from 70% to 90% in the visible to UV range. The as-synthesized TiO_2 array has an indirect band gap of 3.13 eV, which reduces to 3.03 eV after N_2 treatment, with the ZnO equivalent decreasing from 3.20 to 3.17 eV post plasma exposure. A study of the 3d transition metal near edge fine structure of both Ti and Zn show that the N_2 plasma treatment of the nanowires results in nitrogen doping of both TiO_2 and ZnO lattices; this is confirmed by scanning transmission electron microscopy coupled with energy dispersive spectroscopy x-ray maps collected of single nanowires, which show a clear distribution of nitrogen throughout the metal-oxide. Application of these structures in P3HT:PCBM polymer blends shows progressive improvement in the photoluminescence quenching of the photoactive layer when incorporating both undoped and nitrogen-doped nanowires.

Keywords: Hydrothermal synthesis; one-dimensional nanowire arrays; RF plasma nitrogen doping; electron energy loss spectroscopy

Chemical synthesis and electrochemical performance of Hausmannite-Mn_3O_4/rGO materials for supercapacitor applications

Lorena Cuéllar-Herrera[1], Elsa Arce-Estrada[1], Daniella Esperanza Pacheco-Catalán[2], Leonardo Vivas[3], Antonio Romero-Serrano[1]*

[1*] Instituto Politécnico Nacional-ESIQIE, UPALM, CDMX, México, C.P, 07738
[2] Unidad de Energía Renovable, Centro de Investigación Científica de Yucatán, A.C. Carretera Sierra Papacal-Chuburná Puerto Km 5, Sierra Papacal, 97302, Mérida, México.
[3] Universidad Técnica Federico Santa María, Avenida Vicuña Mackenna 3939, Santiago, Chile.

INTRODUCTION

Supercapacitors (SCs) are promising devices due to their numerous advantages. Amidst SCs with pseudocapacitance, spinel-like structured Mn_3O_4 known as Hausmannite is an encouraging material[1]. Although, Mn_3O_4 presents disadvantages[2]. For these reasons, researchers have developed SCs combining Mn_3O_4 with pure carbon materials. Graphene is an excellent choice due to its good electrical conductivity, which could enhance the electrochemical performance of Mn_3O_4. In this work, a facile approach is reported to fabricate Hausmannite Mn_3O_4/rGO composites for use in supercapacitor electrodes.

EXPERIMENTAL/THEORETICAL STUDY

Specifically, the Mn_3O_4 and rGO single phases were synthesized by only 1 hour of dry ball milling and a modified Hummer method, respectively. Subsequently, composites of different Mn_3O_4/rGO ratios were practically prepared by ultrasonic processing. The physicochemical properties of the resultant materials were characterized by SEM, XRD, Raman spectroscopy, TGA, XPS, and N_2 adsorption-desorption techniques. Moreover, the electrochemical performance of an electrode supercapacitor was tested in two different experimental configurations, i.e., a three-electrode cell and a symmetric supercapacitor-(SSC).

RESULTS AND DISCUSSION

Fig. 1 shows the CV profiles of Mn_3O_4/rGO electrodes tested in KOH (6M) electrolyte at a 5 mV s^{-1} scan rate. The CV curves are quasi-rectangular, exhibiting a nearly symmetrical shape and showing no peaks in the reduction and oxidation zones. The sample with the best electrochemical performance was MGO-3 with a Cs value of 525 Fg^{-1} in which the nanometer particle and pore sizes are features capable of providing the highest specific capacitances of the synthesized electrodes.

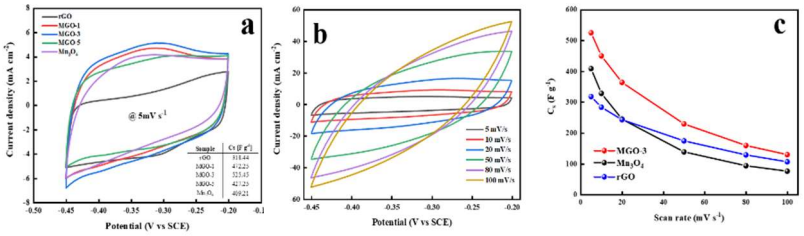

Fig. 1 a) Cyclic voltammograms for capacitance response in three-electrode cell for rGO, MGO-1. MGO-3, MGO-5 and Mn_3O_4 at 5mV s^{-1} scan rate,

CONCLUSION

Mn_3O_4/rGO materials were successfully synthesized using a facile approach. All the fabricated composites showed outstanding and superior electrochemical properties, taking their single constituents as a baseline. The highest electrochemical capacitance of 527 $F \cdot g^{-1}$ at 5 mV s^{-1} was observed for the sample MGO-3.

REFERENCES

1. Z. Huang et. al, J Alloys Compd, 830, 154637 (2020).
2. C. Nithya et. al, Nanoscale Adv, 1, 4347 (2019).

ACKNOWLEDGMENTS

The authors wish to thank the National Council for Science and Technology (CONACYT), the National Polytechnic Institute (IPN), and the Researcher National System (SNI) for the support of this research.

Synthesis and Characterization of Er-doped silica nanoparticles for biological applications

D. González-Alonso[1], L. González-Legarreta*[2]
[1] Depto de Física Aplicada, Universidad de. Cantabria, Avda. de Los Castros 48, 39005 Santander, Spain
[2*] Dept. QUIPRE, Inorganic Chemistry-University of Cantabria, Nanomedice-IDIVAL, Avda. de Los Castros 46, 39005 Santander, Spain

In recent years the research in silica nanoparticles has experienced an exponentially increased owing to their unique physical-chemical properties that confers on them a great applicability in different fields such as catalysis, adsorption of pollutants, termoelectrics, among others[1]. However, their biocompatibility and versatile functionalization along with their high surface area make them especially suitable for biomedical applications, e.g., bioimaging, drug delivery and biosensing[2,3]. This work presents the synthesis and characterization of Er-doped silica carriers by sol-gel method from tetraethyl orthosilicate as precursor of silica, cetyltrimethylammonium bromide as pore generating agent and erbium as optical active element. Nanoparticles were characterized by transmission electron microscopy (TEM), X-ray diffraction (XRD), thermogravimetry, Raman spectroscopy, Fourier transformed infrared spectroscopy and N_2 adsorption-desorption isotherms. Results show a specific surface area of 685 m^2/g with a measured pore diameter ranging within 2.5-2.8 nm. We succeed in introducing the erbium in the silica nanoparticles. As a result, the luminescent intensity of the silica nanoparticles increased, which in turn opens new perspectives of silica nanoparticles to be used as biological markers or biosensors.

REFERENCES

1 M. Vallet-Regí, Acta Biomaterialia 137, 44-52 (2022)
2 M. Vallet-Regí et. al, Chem. Soc. Rev., 51, 5365 (2022)
3 N. Benedicta Fernandes et. al, Coordination Chemistry Reviews 478, 214977(2023).

Improved shielding effective behaviour in the polypyrrole based nanocomposites by incorporation of dielectric $CaCu_3Ti_4O_{12}$ nanoparticles

Lovepreet Kaur Dhugga [1], Dwijendra P. Singh [2,*]

[1]Department of Physics and Materials Science, Thapar Institute of Engineering & Technology, Patiala, Punjab, India, presenting author

[2,*]Department of Physics and Materials Science, Thapar Institute of Engineering & Technology, Patiala, Punjab, India, corresponding author (dpsingh@thapar.edu)

INTRODUCTION

Polymers are preferred as electromagnetic interference shielding materials due to many advantages like ease of synthesis, flexibility, conductivity etc [1,2]. Different materials are considered as appropriate fillers in order to enhance electrical and magnetic properties of the polymer matrix [3]. In present work, effect of $CaCu_3Ti_4O_{12}$ (CCTO) encapsulation on microwave shielding behaviour of polypyrrole-cobalt ferrite nanocomposites was studied in X-band (8.2-12.4GHz). This is a novel and emerging material which can be utilised in various electronic applications, microwave communication and environmental safety.

EXPERIMENTAL/THEORETICAL STUDY

Initially, CCTO was synthesized by modified sol-gel auto combustion technique whereas $CoFe_2O_4$ was fabricated through hydrothermal route. Then, polypyrrole-$CoFe_2O_4$-$CaCu_3Ti_4O_{12}$ nanocomposites were prepared by *in-situ* chemical oxidative polymerization technique. The compositions of pyrrole: $CoFe_2O_4$: $CaCu_3Ti_4O_{12}$ in the nanocomposites are taken in the ratio 1:0.5:0, 1:0.5:0.1, 1:0.5:0.3 and 1:0.5:0.5 by weight fraction, and denoted as PF5C0, PF5C1, PF5C3 and PF5C5 respectively. The nanocomposites were characterized using XRD, FTIR, VSM, FESEM and VNA to determine their structural and electromagnetic properties.

RESULTS AND DISCUSSION

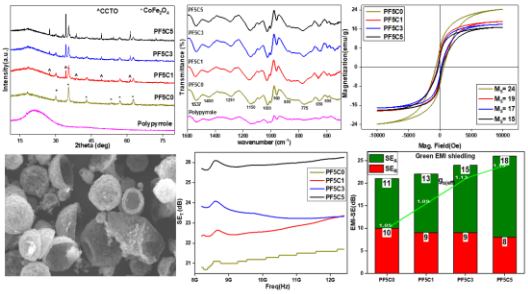

Fig. 1 X-ray diffraction graph, Fig. 2 FTIR results of nanocomposites, Fig. 3 M-H loop of nanocomposites, Fig. 4 FESEM image of PF5C5, Fig. 5 and 6 SE_T, SE_A, SE_R and $g_{S(eff)}$ of nanocomposites

XRD and FTIR confirms the formation of Polypyrrole-ferrite-CCTO nanocomposites by the presence of all the characteristic peaks of the materials in the graphs as shown. VSM reveals the decrease in saturation magnetization values of composites with the addition of CCTO as it is non-magnetic in nature. FESEM studies presents the microstructure of PF5C5 in which the CCTO and ferrite nanoparticles are attached to polymer chain results into bending of polypyrrole and formation of cup-like structures. The total shielding effectiveness (SE_T) for PF5C5 comes out to be ~ 26dB which is > 20dB fulfilling the commercial requirement. Along with this, absorption dominated shielding (SE_A~18dB) and effective green shielding index ($g_{s(eff)}$>1) makes it green and effective shielding material.

CONCLUSION

Polypyrrole provides the conductive path where the incorporation of CCTO with high dielectric constant lead to interfacial polarizations responsible for dielectric losses in the material. Moreover, presence of $CoFe_2O_4$ results into magnetic losses. This gives absorption dominated microwave shielding. Also, these investigations outline the highest effective green shielding as $g_{s(eff)}$ ~ 1.15 makes this novel composite an efficient green shielding material.

REFERENCES

[1] A. Muzaffar et. al, Polym-Plast Tech Mat vol. 59, no. 15, pp. 1667–1678 (Oct. 2020)

[2] S. Maiti et. al, ACS Appl. Mater. Interfaces. vol. 5, no. 11, pp. 4712–4724 (Jun. 2013)

[3] S. Alamri et. al, J. Magn. Magn. Mater. vol. 555 (Aug. 2022)

ACKNOWLEDGMENTS

The authors acknowledge AR&DB, DRDO for financial support in this research and DST-FIST for providing the research grant for facilities XRD and VSM, and Thapar Institute of Engineering & Technology, Patiala for the FESEM facility.

White TADF based OLED by Exciplex Principle in Wet-processed Devices

Emmanuel Moraes, José Carlos Germino and Luiz Pereira*
Department of Physics and i3N – Institute of Nanostructures, Nanomodelling and Nanofabrication, University of Aveiro, Portugal, luiz@ua.pt

INTRODUCTION

Lighting technology is changing very fast towards an enhanced area of research looking for the best solutions to get highly efficient, long-life, and architectural appellative products. Solid State Lighting technologies based on OLEDs–Organic Light Emitting Diodes, became the focus of a huge scientific research in recent years due to their unique properties. In particular, the white-OLED (WOLED) can be fabricated with a large CCT (color correlated temperature) range – from cool white to warm white – with high (up to 98) CRI (color rendering index). However, the use of thermal evaporation methos for device fabrication implies a complex and high-cost final structure. The focus of the present work is to use the unique properties of organic semiconductor electrical carrier dynamics, to develop solution deposited WOLEDs in simple device structure, following the concept of printed electronics. Further optimization can be done once a useful structure and process is established.

RESULTS AND DISCUSSION

Thermally activated delayed fluorescence (TADF) appears as a new generation of emitting for high-efficiency OLED. In the present study, we chose a blue emission TADF (DMOC-DPS) to combine with TAPC to generate white light emission by the exciplex principle. The blue emission of the DMOC-DPS and the energy combination between DMOC-DPS and TAPC results in an orange emission (complementary color to white light generation). This way, we obtained a WOLED with a color render index (CRI) of around 85, ideal for indoor application. In the trade-off between device structure simplicity (only two organic layers) and efficiency, we achieved one of the best results using DMOC-DPS, with an EQE over 5%.

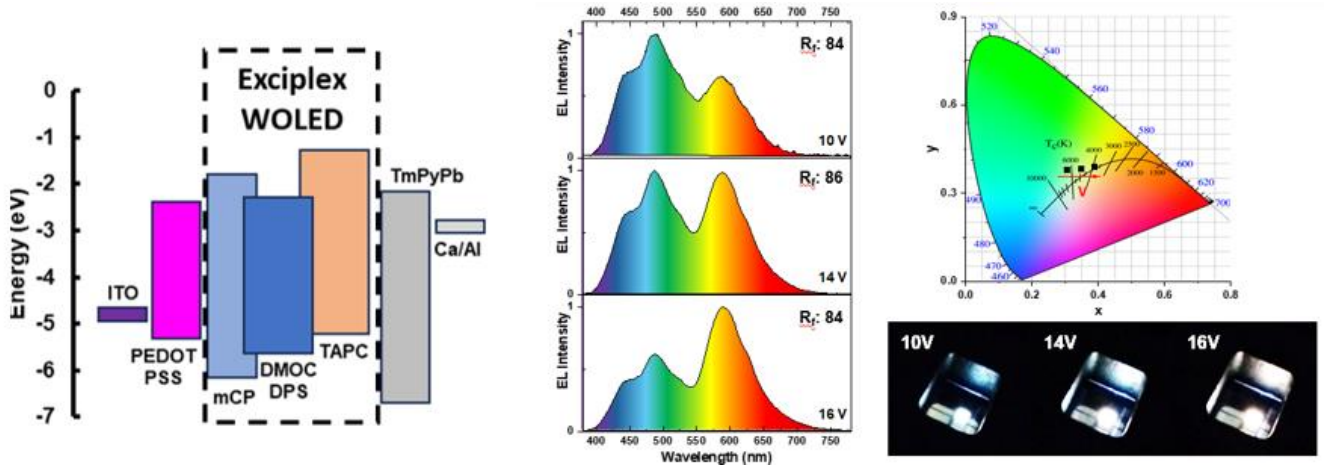

Fig. 1 Molecular structure of the materials, the energy level diagram of layers, and the exciplex formation. Electroluminescence spectra of the exciplex OLED and their respective Rf index, the x and y coordinate. Data was measured at 10, 14, and 16V and with color tuning regarding voltage

CONCLUSION

Simple WOLED structure deposited by solution process, can be obtained with a blue TADF emitter DMOC-DPS that, combined with TAPC results in an orange emission (complementary color to white light generation). This way, we obtained a WOLED with a color fidelity index (Rf) of around 85 ideals for indoor application.

ACKNOWLEDGMENTS

This work is funded by National Funds through the FCR – Fundação para a Cieência e a Tecnologia, I.P., under the scope of the projects UID/50025/2020-2023, LA/0037/2020 and 2021.02056.CEECIND.

AI-Based Multiclassification Electronic Nose for Detection of Volatile Organic Compounds

Maria Lucas, João Leça and Luiz Pereira*
Department of Physics and i3N – Institute of Nanostructures, Nanomodelling and Nanofabrication, University of Aveiro, Portugal, luiz@ua.pt

INTRODUCTION

The development of the electronic nose (e-nose) has made significant advances in the detection of volatile organic compounds (VOCs), particularly in biomedicine. However, the accuracy of such systems, particularly for very low biomarkers concentration, is currently a significant drawback. The present work explores the ability of semiconductor oxidized gas (MOX) sensors, joined with artificial intelligence methods, to enhance the pattern recognition of some biomarkers related with gastro-intestinal pathologies. The results indicate that e-nose can detect VOCs at a concentration of mg/L, something never achieved before.

RESULTS AND DISCUSSION

The eNose was made with four different gas sensors from Winsen. Tensor Flow was used to create a multiclassification Artificial Neural Network that could distinguish the compounds under study: acetic acid, acetone, isopropanol and pentane, either individually or in mixtures. The best accuracy achieved in training a neural network was 85%. In some situations, the accuracy was affected by the overfitting problem and could be easily solved with a more complete training dataset. The data acquisition was optimized (electronic part) and the dataset attempts to include collected data originated from different fluctuations in the several environment conditions for the sensor (including temperature and humidity).

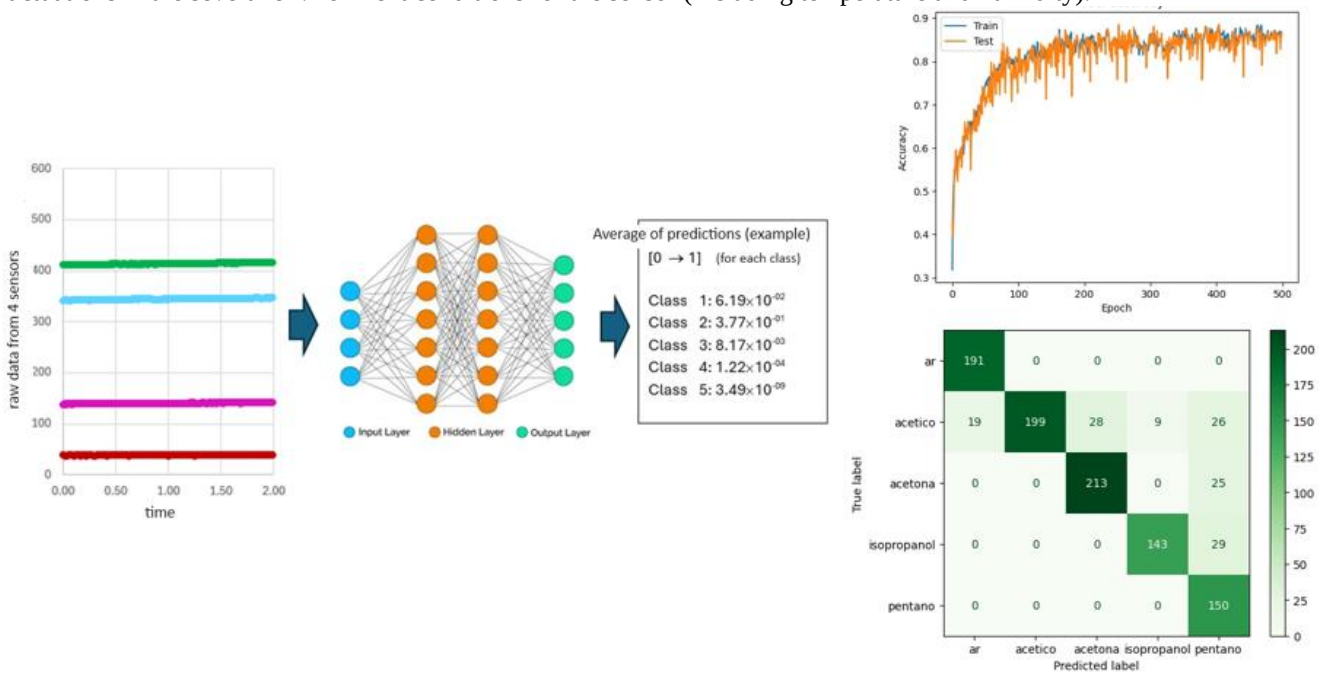

Fig. 1 Overall AI eNose structure and training / test / validation data (accuracy, loss and confusion plot)

CONCLUSION

The developed e-nose shows very promising results. The furthermore complete dataset creation should be able to increase significantly the already very good accuracy, making such a device a candidate for biomedical applications in the home care concept.

ACKNOWLEDGMENTS

This work is funded by National Funds through the FCR – Fundação para a Cieência e a Tecnologia, I.P., under the scope of the projects UID/50025/2020-2023, LA/0037/2020 and 2021.02056.CEECIND. The present study was developed in the scope of the Project "Agenda ILLIANCE" [C644919832-00000035 | Projeto n.º46], financed by PRR – Plano de Recuperação e Resiliência under the Next Generation EU from the European Union

Lithium-ion Battery State of Health Prediction from Partial Discharge Curves Using Artificial Neural Networks

Bruno Melo * and Luiz Pereira
Department of Physics and i3N – Institute of Nanostructures, Nanomodelling and Nanofabrication, University of Aveiro, Portugal, bmelo@ua.pt

INTRODUCTION

The present study presents a new machine-learning model for predicting the aging of lithium-ion batteries that combines a linear regression model with a multiclass classification model. The output result of the model gives a class prediction of the current state of health of the battery. The inference can be made from a partial discharge curve of a battery, dismissing the requirement of discharging the battery entirely to get an accurate value of its capacity.

EXPERIMENTAL/THEORETICAL STUDY

The accuracy of the model was optimized by testing different architectures of feedforward fully connected neural networks, and Random Forest machine-learning algorithms. The AI model was based on both regression / multiclassification model, employing TensorFlow as a low-level platform. The training / test / validation process shows good accuracy and a correct classification output. Optimizations made in the prediction process allows further complete regression output as well as a indicative classification prevision that can be used for any type of ion-based battery since the correspondent training was correctly made.

RESULTS AND DISCUSSION

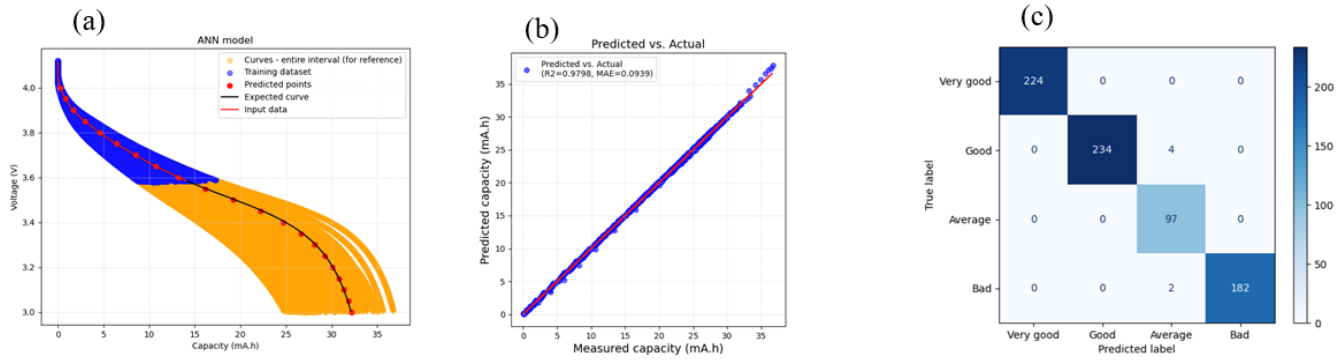

Fig. 1 Battery capacity prediction (a) and the resulting MSE (b). Confusion matrix for the test dataset predictions using the classification model (c).

The regression model used for predicting the battery capacity was found to be very effective, showing small MSE even when just a small portion of the discharge curve was used for inference. For the multiclass classification model, the model showed high accuracy, with an obtained accuracy above 99% for the test dataset.

CONCLUSION

Predictive models based on artificial neural networks were developed to determine the SOH (State of Health) of batteries. The low computational cost of these models and the ability to predict the battery capacity in reduced time allows their integration into high-performance microcontrollers to build a compact and portable characterization device for evaluating battery degradation.

ACKNOWLEDGMENTS

This work is funded by National Funds through the FCR – Fundação para a Cieência e a Tecnologia, I.P., under the scope of the projects UID/50025/2020-2023, LA/0037/2020 and 2021.02056.CEECIND. The present study was developed in the scope of the Project "Agenda NGS" [Projeto n.º58], financed by PRR – Plano de Recuperação e Resiliência under the Next Generation EU from the European Union

Rules for Designing Active Layers of Efficient Solution-deposited OLEDs Based on the host: guest Concept: from Simulations to Real Data

Luiz Pereira
[3]Department of Physics and i3N – Institute of Nanostructures, Nanomodelling and Nanofabrication, University of Aveiro, Portugal, luiz@ua.pt

INTRODUCTION

Some of the most important keys to build efficient Organic Licht Emitting Diodes (OLEDs) from solution deposited methods, that, simultaneously have simple device structure and good efficiency, are the modulation of the electrical profile of emissive layer and the consequent design of such layer based on the host: guest concept.

The best approach for the fabrication process was a hybrid approach of the solution and a thermally evaporated process, keeping the device structure with only two organic layers.

In this work, a complete overview of the methods for building OLEDs active layers employing TADF emitters (thermally activated delayed fluorescence) processed by solution, is explored. The focus is the host: guest concert, both explored by theoretical simulation of injection/transport of charge and further recombination/loss. All the hypotheses will be exemplified by experimental data.

RESULTS

With proper optimization of the device structure with two-organic layers, we can achieve higher EQE for three different emitters. In this context, OLEDs with emitters red-orange 2-[4 (diphenylamino)phenyl]-10,10-dioxide-9H-thioxanthen-9-one (TXO-TPA), green 2,5-bis(4-(10H-phenoxazin-10-yl)phenyl)-1,3,4-oxadiazole (2PXZ-OXD) and blue bis[4-(3,6-dimethoxycarbazole)phenyl]sulfone (DMOC-DPS) have been explored by doping in a mixed p-type, n-type and bipolar host system of poly(N-vinylcarbazole) (PVK) with 1,3-Bis(N-carbazolyl)benzene (mCP), 1,3-Bis[2-(4-tert-butylphenyl)-1,3,4-oxadiazo-5-yl]benzene (OXD-7), 2,2',2''-(1,3,5-Benzinetriyl)-tris(1-phenyl-1-H-benzimidazole) (TPBi) and 4,4′-Bis(N-carbazolyl)-1,1′-biphenyl (CBP). The devices were fabricated with the electron transport layer (ETL) of 1,3,5-Tri(m-pyridin-3-ylphenyl)benzene (Tm3PyPB). Furthermore, the devices were compared with different thicknesses of both ETL and an emissive layer. The red TXO-TPA exhibited EQE over 18%; sky blue OLEDs of DMOC-DPS with high EQE of near 6%; and the green 2PXZ-OXD in mCP exhibited EQE over 20%. All turn on voltage (VON) are near 3V, Numerical simulations are used to design the device structure.

Fig. 1 Two-organic layers OLEDs deposited by solution process (orange-red, green and blue emitters)

CONCLUSION

The optimization of simple OLED device structure, employing efficient emitters, can be achieved by a correct design of the active layer, that can be modulated by physical simulation. Such a process, together different host systems based on their electrical carrier properties, establishes a new framework for printed based methods for OLEDs fabrication.

Developing of Two Different Types of Polymeric Nanoparticles as Carriers of Doxorubicin

Lyubomira Radeva [1], Krassimira Yoncheva [1]
[1]Faculty of Pharmacy, Medical University of Sofia, Bulgaria

INTRODUCTION

Doxorubicin is a well-known anticancer drug which is pronouncedly used in various antitumor therapies. However, there are some major limitations to its application which are still unresolved. For instance, it possesses highly pronounced photolysis in aqueous solutions[1]. The incorporation of the drug into polymeric nanoparticles is an appropriate strategy to improve its stability[2,3]. The aim of this research is to encapsulate doxorubicin into polymeric nanomicelles and nanogels, and to evaluate their characteristics.

EXPERIMENTAL STUDY

Doxorubicin-loaded micelles were prepared with the non-toxic Pluronic P123 and F127 copolymers via film hydration method. Drug-loaded nanogels were prepared from the natural polymers chitosan and albumin via electrostatic gelation method. The mean size and polydispersity index (PDI) were determined via dynamic light scattering method (DLS) and the shape via transmission electron microscopy (TEM). The in vitro release tests were conducted via dialysis in buffers with pH 5 and 7.4. The stability of the drug in reference aqueous solution and nanoparticles was evaluated under daylight for 30 days.

RESULTS AND DISCUSSION

The loaded nanomicelles and nanogels were prepared at a ratio 1:10 between the drug and the polymers. The encapsulation efficiency of doxorubicin into the nanomicelles was found to be 96 %, while into the nanogels it was 75 %. DLS analysis revealed small mean diameters (57 nm and 29 nm for micelles and nanogels, respectively) and narrow size distribution (PDI of 0.296 and 0.223, respectively). TEM analysis showed a spherical shape and confirmed the small mean size of the nanoparticles (Fig. 1).

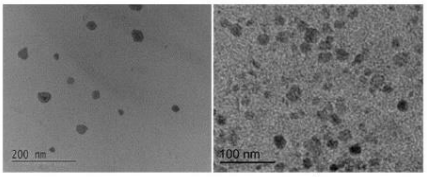

Fig. 1 TEM of the loaded micelles (a) and nanogels (b)

The in vitro release tests showed sustained release for 24 h when the drug was loaded in the micelles and 8 hours when incorporated into the nanogels, with slightly faster release in the medium with acidic pH (Fig. 2, a and b). Regarding the stability of the pure and encapsulated drug, a significant protection after its encapsulation in both types of the nanoparticles was observed. After 30 days of sunlight exposure a degradation of 33% in the reference solution, only 3% when encapsulated in the micelles and no degradation in the nanogels were detected (Fig. 2, c).

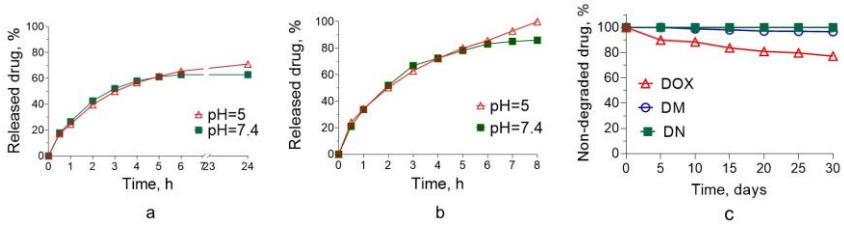

Fig. 2 In vitro release profiles of loaded micelles (a) and nanogels (b) in media with pH of 5 and 7.4, and photolysis of pure doxorubicin (DOX) and encapsulated in micelles (DM) or nanogels (DN) under daylight exposure (c)

CONCLUSION

The two types of nanoparticles developed, namely nanomicelles and nanogels, were characterized as appropriate drug delivery systems for the anticancer drug doxorubicin and significantly improved its stability.

REFERENCES

1. K. Nawara et al, J. Phys. Chem. A. 116, 4330–4337 (2012)
2. S. Bandak et al, Pharm. Res. 16, 841–846 (1999)
3. K. Kamenova et al, Polymers. 14, 3694 (2022)

ACKNOWLEDGMENTS

The research was funded by the European Union-NextGenerationEU, through the National Recovery and Resilience Plan of the Republic of Bulgaria, project No. BG-RRP-2.004-0004-C01.

Structural, Electronic and Vibrational Properties of CuScSi Half Heusler Compound: A First Principle Approach

M. M. Sinha* and Rekha Rani
Department of Physics, Sant Longowal Institute of Engineering and Technology, Longowal, Sangrur (Punjab) - 148106 (INDIA)
*Corresponding author: mm_sinha@rediffmail.com

Motivated by the excellent thermoelectric properties of half-Heusler compounds, study of structural optimization, electronic band structure and phonon dynamics of a new half Heusler compound CuScSi have been carried out by using first principle approach. The calculated results will be interpreted with the existing experimental results. It has been observed that half Heusler compound CuScSi is a semiconductor with a band gap 0.15 eV. All calculated phonon modes are found to be positive confirms its dynamical stability. The negative formation energy confirms the chemical stability of the compound.

The interplay of material from and cation ratios in multimetallic pentlandite catalysts

Maciej Kubowicz[1*], Andrzej Mikuła[1], Miłosz Kożusznik[1]
[1]Faculty of Materials Science and Ceramics, AGH University of Krakow, Poland
*kubowicz@agh.edu.pl

INTRODUCTION

In response to the current movement away from fossil fuels in the energy-oriented industry the production and utilization of hydrogen emerges as one of the more intriguing solution. Primarily derived from the processing of fossil fuels[1,2], hydrogen can be produced by environmentally friendly water electrolysis process and related hydrogen evolution reaction (HER). Currently, platinum and precious metal compounds[3,4] are the most important catalysts of the HER process in commercial applications. However, a potential alternative is represented by transition metal chalcogenides characterized by pentlandite structure TM_9Ch_8 (TM – transition metals, Ch – chalcogenides) [5,6]. Numerous studies indicate that the HER performance of these materials[4,7] can be tailored both by the catalyst form (powder anchored to metallic electrode, ingot, sintered solids) and by chemical composition affecting the so-called intrinsic materials' properties. As the next step in optimizing these materials, we want to present an assessment of the catalytic properties of pentlandites as a function of their morphology, focusing on changes in the Co, Fe, and Ni ratios in the cationic sublattice and an equimolar ratio of sulfur and selenium in the anionic sublattice ($Co_{9-x-y}Fe_xNi_yS_4Se_4$). Examining these materials as powders, ingots, and sintered pellets provide a valuable insight into the chemical composition, morphology, and catalytic performance relationships, while, examining sintered pellets acting as actual catalysts and electrode simultaneously, constitutes increased simplicity of obtaining these functional catalysts.

EXPERIMENTAL/THEORETICAL STUDY

Pentlandites were synthesized using direct reaction between elements in a tube furnace. The materials were investigated in forms of: powder catalysts anchored to the screen-printed electrodes, ingot samples cut directly after synthesis without any additional processing, and pellets sintered by means of inductive hot pressing (IHP) method. HER processing was performed in a conventional three-electrode system with pentlandites acting as working electrode, Pt + Pt black as an auxiliary, and Ag/AgCl as the reference electrode. The measuring procedure covering determination of HER activity before and after stability tests, determination of electrochemical surface active area (ECSA), and stability tests was performed accordingly to the reported electrochemical methodology using Gamry equipment.

RESULTS AND DISCUSSION

Maintaining an equimolar ratio of metals in ternary and quaternary pentlandites, a small addition of selenium translates into the highest catalytic activity as long as the surface development is significant (powder catalysts). For materials in solid form, a higher addition of selenium seems to positively influence catalytic parameters. By maintaining high concentration of selenium in the material but controlling the concentration of individual metals, it has been demonstrated that for powder catalysts, the most favorable ones have a high iron content. Conversely, with an increase in material density and a decrease in surface development (ingots, pellets), the best-performing samples are those with a high nickel concentration. The content of these two elements seems to be crucial in designing multicomponent catalysts based on pentlandites.

CONCLUSION

The study presented that multicomponent pentlandites can be successfully utilized in electrolyzers not only in powder form anchored to metallic electrodes but also as electrodes themselves in solid form. Considering Se-rich systems, it was demonstrated that nickel (similarly to selenium itself) reduces the ECSA, generating higher currents at relatively low overpotentials. The iron content is also crucial, significantly influencing the HER performance due to the attractiveness of active sites. The presence of cobalt in quaternary systems is negligible in terms of HER activity but enhances the durability of these materials under operating conditions[3].

REFERENCES

1. S. Wang et. al, Nano Converg 8, 4 (2021)
2. M. Carmo et. al, Int J Hydrogen Energy 38, 12, 4901-4934 (2013)
3. M. Smialkowski et. al, ACS Mater Au 2, 4, 474-481 (2022)
4. B. Konkena et. al, Nat Commun. 7, 12269 (2016)
5. A. Mikuła et. al, Dalt Trans. 50, 27, 9560-9573 (2021)
6. A. Mikuła et. al, J Mater Chem A. 11, 7526-7538 (2023)
7. S. Piontek et. al, ACS Catal. 8, 2, 987-996 (2018)

ACKNOWLEDGMENTS

This work was financially supported by the National Science Centre, Poland, under grant no. 2022/45/B/ ST8/03336.

Light-induced defected TiO_2 nanosheets decorated with Pt single atoms for enhanced photocatalytic hydrogen production

Majid Shahsanaei[1,2], Sina Hejazi[1,3], Nastaran Farahbakhsh[1,2], Julian Müller[4], Sadegh Pour-Ali[5], Charles Ogolla[4], Shiva Mohajernia[3], Benjamin Butz[4], Manuela S. Killian[1*]

[1] Chemistry and Structure of novel Materials, University of Siegen, Germany, presenting author, corresponding author (manuela.killian@uni-siegen.de)
[2] Department of Materials Engineering, Isfahan University of Technology, Isfahan, Iran
[3] Department of Chemical and Materials Engineering NRGMATs, University of Alberta, Edmonton, Canada
[4] Micro- and Nanoanalytics, University of Siegen, Germany
[5] Faculty of Materials Engineering, Sahand University of Technology, Tabriz, Iran

ABSTRACT

The cutting-edge field of heterogeneous catalysis is prominently influenced by single-atom decoration, which exploits the remarkable atomic-level efficiency of catalysts. Simultaneously, there is a growing interest in TiO_2 nanosheets adorned with single atoms[1], owing to their abundant surface-exposed reactive sites and strong binding affinity towards these atomic species. This intriguing development reduces catalyst costs while preserving exceptional performance in the realm of photocatalytic hydrogen (H_2) generation from water. In this study, we employ light-induced methods to create precisely defined atomic-scale defects on the surface of highly active TiO_2 nanosheets, with a predominant exposure of the (001) facet. Light-induced in situ formation of Ti^{3+} defects on TiO_2 nanosheets plays a crucial role in achieving uniform and stable dispersion of Pt single atoms (SAs), leading to high efficiency in Pt SA co-catalyzed photocatalytic H_2 production. Remarkably, we conducted experiments using identical parameters under photo-deposition conditions to facilitate a more comprehensive comparison. Surprisingly, Pt decoration on the photo-deposited samples resulted in the formation of complete nanoparticles, and the H_2 production rate was significantly lower than those prepared using light-induced methods. In the context of this research, it was observed that under UV-LED light irradiation, the oxidation of TiO_2 to Ti^{3+} is a reversible process. Upon light cessation, reduction occurs. It was found that the most favorable adsorption of Pt single atoms occurs precisely 5 minutes after light interruption (Fig 1). Any deviation from this specific duration, whether extended or reduced, results in the formation of nanoparticles, leading to a subsequent decrease in the co-catalytic efficiency for H_2 production. Thus, this study offers a straightforward method for fully harnessing the potential of noble metal catalysts by successfully forming single atoms (SAs).

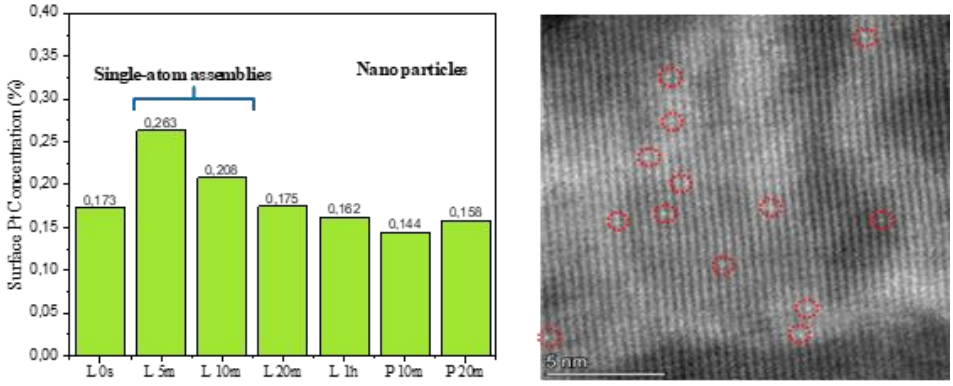

Fig. 1 deposition of Pt under various UV-exposure conditions: L describes samples where Pt-solution is added for x min after switching off the light, P denominates Pt deposition under continuous light exposure. Right: HAADF-STEM image of LI5m, showing single atoms.

REFERENCES

S. Hejazi, et al., Room-temperature defect-engineered titania: An efficient platform for Pt single atom decoration for photocatalytic H_2 evolution, Int. H. Hydrogen Energy 51 (2024) 222. https://doi.org/10.1016/j.ijhydene.2023.08.126.

ACKNOWLEDGMENTS

DFG KI2169/2-1 is acknowledged for funding

Room-temperature defect-engineered titania: An efficient platform for Pt single atom decoration for photocatalytic H_2 evolution

Sina Hejazi[1,6], Hamid Mehdi-pour[2], Charles Ogolla Otieno [3], Julian Müller [3], Sadegh Pour-Ali [4], Majid Shahsanaei [1], Saeedeh Sarabadani Tafreshi [5], Benjamin Butz [3], Shiva Mohajernia[6], Manuela S. Killian[1*]

[1] Chemistry and Structure of novel Materials, University of Siegen, Germany, presenting author, corresponding author (manuela.killian@uni-siegen.de)
[2] Faculty of Physics, University of Duisburg-Essen, Germany
[3] Micro- and Nanoanalytics, University of Siegen, Germany
[4] Faculty of Materials Engineering, Sahand University of Technology, Tabriz, Iran
[5] Department of Chemistry, Amirkabir University of Technology, Tehran, Iran
[6] Department of Chemical and Materials Engineering, NRGMATs, University of Alberta, Edmonton, Canada

ABSTRACT

Single-atom (SA) decoration represents the forefront of technological advancements in heterogeneous catalysis, harnessing the exceptional performance of catalysts at the atomic level. However, the high surface energy of isolated atoms often leads to agglomeration, resulting in the formation of nanoparticles. To address this challenge, trapping single atoms within surface defects has emerged as an effective strategy for atom immobilization. Conventional defect engineering techniques, such as high-temperature thermal reduction, suffer from adverse effects, such as sintering of the support material. In this study, we introduce a novel and facile room-temperature sonochemical method to induce well-defined atomic-scale defects on the surface of highly active TiO_2 nanosheets, predominantly exposing the (001) facet. By introducing a highly diluted Pt precursor to the ultrasonicated nanosheet slurry, isolated Pt atoms were selectively trapped within freshly formed defects. Remarkably, the resulting Pt single atom decorated samples exhibit a striking 100-fold increase in photocatalytic H_2 evolution compared to pristine TiO_2 nanosheets. Notably, we demonstrate that the density of the generated defects and the loading of Pt single atoms can be precisely tailored by adjusting the sonication time. Atomic-scale characterization, complemented by density functional theory (DFT) calculations, provides compelling evidence of the strong bonding between Pt single atoms and the defects generated via sonochemical treatment. Our findings offer a promising approach for defect engineering and SA decoration on a larger scale, underscoring the significant potential of this room-temperature technique for heterogeneous catalysis.

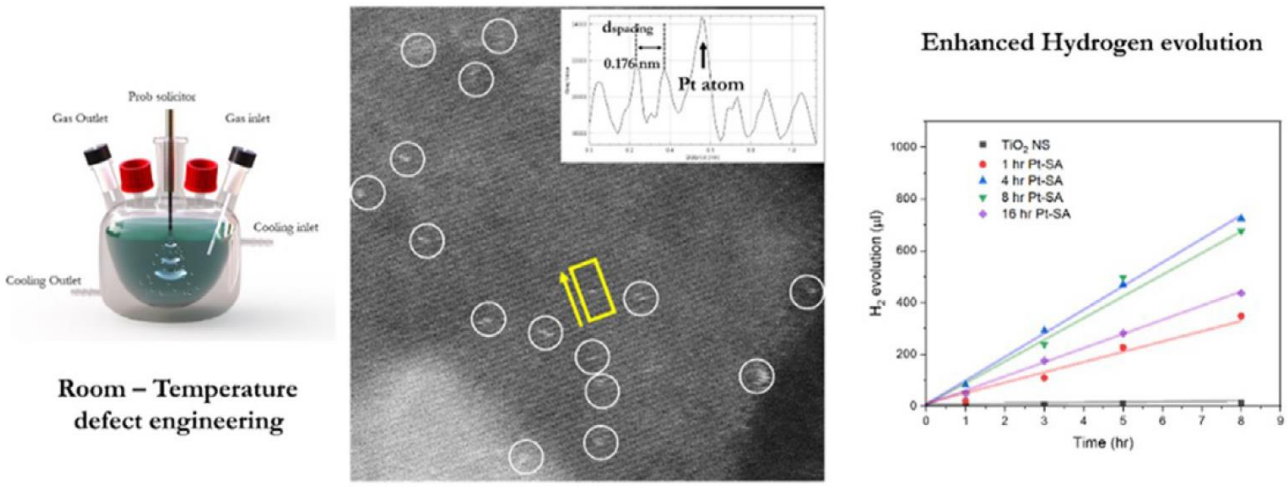

Fig. 1 Sonochemical defect formation enables room temperature defect engineering and facilitates the deposition of single atom Pt for photocatalytic hydrogen production.

REFERENCES

1. S. Hejazi, et al., Room-temperature defect-engineered titania: An efficient platform for Pt single atom decoration for photocatalytic H_2 evolution, Int. H. Hydrogen Energy 51 (2024) 222. https://doi.org/10.1016/j.ijhydene.2023.08.126.

ACKNOWLEDGMENTS

DFG KI2169/2-1 is acknowledged for funding

LCA of $La_{0.6}Sr_{0.4}Co_{0.2}Fe_{0.8}O_{3\pm\delta}$ synthesis for green hydrogen production through solar driven thermochemical cycles

David Castro-Jiménez[1], Alejandro Pérez[1], María Orfila[1], Pedro Leo[1], María Linares[1], Raúl Sanz[1,2], Javier Marugán[1,2], Raúl Molina[1], Juan Ángel Botas[1,2]
[1]Chemical an Environmental Engineering Group, Rey Juan Carlos University,
[2]Instituto de Investigación de Tecnologías para la Sostenibilidad, c/ Tulipán s/n, 28933 Móstoles, Spain
maria.linares@urjc.es

INTRODUCTION

Hydrogen (H_2) is a versatile and clean energy carrier that plays a pivotal role in addressing global energy challenges and mitigating climate change. Green H_2 production can be obtained by thermochemical cycles. In this process a metal oxide is thermally reduced using solar energy. Subsequently, it is oxidized with water (H_2O) to produce H_2. Perovskites are promising materials for this application as they are non-stoichiometric oxides with good redox properties [1]. However, it is important to ensure that the synthesis of these materials is sustainable. To evaluate this fact, the Life Cycle Analysis (LCA) can be used to assess contributions of the synthesis method to potential environmental impacts such as greenhouse gas emissions, energy consumption, or water pollution, among others [2]. So, in this work, we present two synthesis routes to obtain a $La_{0.6}Sr_{0.4}Co_{0.2}Fe_{0.8}O_{3\pm\delta}$ perovskite for green H_2 production through thermochemical cycles and the environmental evaluation of both methods through life cycle analysis, in order to determine the optimal synthesis methodology.

EXPERIMENTAL/THEORETICAL STUDY

The perovskite was synthesized by three different methodologies, conventional Pechini method (acid pH), modified Pechini method (basic pH) [3], and reactive grinding. Afterwards, they were evaluated for H_2 production through thermochemical cycles using an experimental system with a tubular furnace coupled to a H_2 and O_2 gas analyzer. The reduction step was performed at 1000 °C, while the oxidation was performed at 800 °C. Afterwards, LCA was conducted to determine the best synthesis methodology, considering various environmental aspects. The functional unit was the production of 1 cm^3 of H_2 and the methodology for comparison among synthesis methods was ReCiPe 2016 Midpoint (H) V1.07.

RESULTS AND DISCUSSION

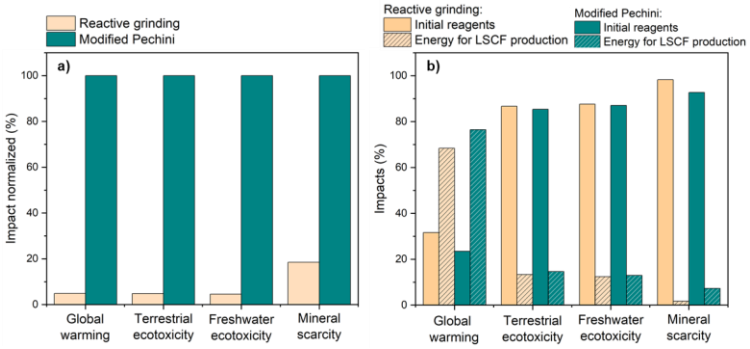

Figure 1. a) Normalized higher potential environmental impacts, and b) Contribution of the raw material extraction and energy consumption.

The results obtained for H_2 production revealed that although the three synthesis routes allow obtaining the desired perovskites, in terms of structure (XRD), the Pechini method leads to an unstable material while the rest of methodologies, modified Pechini and reactive grinding showed a stable behaviour but with different H_2 production of 1.5 and 4.5 cm^3 STP/$g_{material}$·cycle, respectively. The LCA was performed only for these last both methodologies. In Figure 1a, the higher potential impacts obtained by the Recipe LCA method are presented. As it can be seen, the reactive grinding synthesis methodology is the least harmful due to its higher synthesis yield, avoiding also the use of solvents and intermediate thermal steps. Additionally, most of the potential impacts are attributed to the extraction of raw materials, except for global warming which is mainly caused by the energy consumption of the processes, which is mostly obtained by fossil fuels according to the Spanish energy mix (Figure 1b).

CONCLUSION

Finally, it can be concluded that the $La_{0.6}Sr_{0.4}Co_{0.2}Fe_{0.8}O_{3\pm\delta}$ is a promising perovskite for green H_2 production through thermochemical cycles with an activity of 4.5 cm^3 STP/$g_{material}$·cycle. Additionally, it can be confirmed that the best synthesis methodology is reactive grinding due to the lower environmental impact and the highest H_2 production.

REFERENCES

[1] A. Bayón et al., Int. J. Hydrogen Energy, 45, 12653 (2020).
[2] D. Alique et al., Int. J. Hydrogen Energy, 51, 302-319 (2024).
[3] A. Pérez et al., Catal. Today, 390-391, 22-33 (2022).

ACKNOWLEDGMENTS

The authors thank MCIN/AEI/10.13039/501100011033 and European Union "NextGenerationEU"/PRTR for financial support through RHYDROGENALTES (TED2021-132540B-I00) project, and "Comunidad de Madrid" and Rey Juan Carlos University for their financial support to ONEHYDRO Young Researchers R&D Project (M-2733).

Nano SnO_2 and Ga_2O_3 clusters supported on zeolite Y for the exploitation of biomass into high-value chemicals

Xi Liu [1], Carmine D'Agostino [2], Degirmenci Volkan [3], and Marco Conte [4*]
[1]School of Chemistry and Chemical Engineering, Shanghai Jiao Tong University, Shanghai, 200240, P.R. China
[2]Department of Chemical Engineering and Analytical Science, The University of Manchester, Oxford Road, Manchester, M13 9PL, UK
[3]School of Engineering, University of Warwick, CV4 7AL, Coventry, UK
[4*]Department of Chemistry, University of Sheffield, Sheffield, S3 7HF, UK (m.conte@sheffield.ac.uk)

INTRODUCTION

The isomerization of sugars is a category of processes that, if harnessed, will unlock the potential of utilizing biomass for the production of high value platform chemicals.[1] This is extremely significant from an energetic balance point of view since carbohydrates make up the majority (up to 60%) of biomass-derived feedstock.[2] We have developed advanced nanomaterials based on zeolites that are capable to carry out these isomerizations.

EXPERIMENTAL/THEORETICAL STUDY

Through the utilization of characterizations such as chemisorption, XPS, XRD, NMR, HAADF-STEM, and EXAFS, we were able to establish that a simple impregnation method for creating our catalysts resulted in Sn/Y primarily consisting of small SnO_2 clusters on the outer surface of the zeolite. On the other hand, Ga/Y consisted of well-dispersed Ga species predominantly located within the zeolite pores (**Fig. 1**).

RESULTS AND DISCUSSION

This study utilizes zeolite Y as a support for synthesizing Sn and Ga-doped zeolites, with the objective of catalyzing the isomerization of glucose into fructose (**Fig. 2**). [3,4] While our materials do not react in water, they do react in alcohol media though to different extents. We could determine a reaction pathway that involves a hydride shift for converting glucose to fructose and mannose, as well as a Brønsted acid pathway that forms a methyl fructoside intermediate and then hydrolyzes it to fructose, if water is added subsequently.

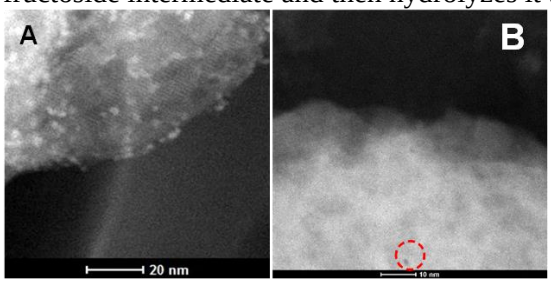

Fig. 1. (A) HAADF-STEM image of a Sn/Y catalyst and (B) of a Ga/Y catalyst prepared via wetness impregnation.

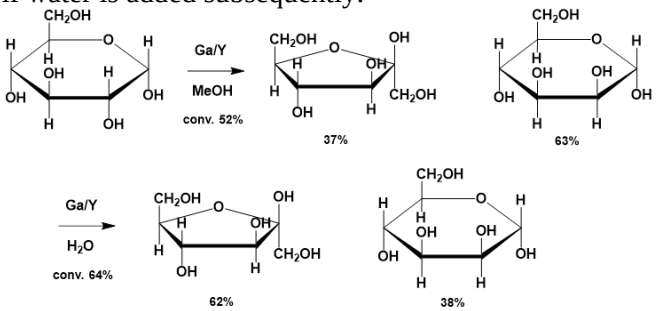

Fig. 2. Effect of methanol and water as sequential solvents using Ga/Y (and Sn/Y) catalysts.

CONCLUSION

It is rather surprising to obtain a highly dispersed metal by using a straightforward impregnation protocol, and this could have implications beyond our study. This phenomenon has been rarely observed so far, and only by using when using Fe and vacuum synthesis methods and with alkali metals as promoters.[5] As such, our study may have drastic implications on the exploitation of biomass for chemicals.

REFERENCES

1. I. Delidovich et. al, ChemSusChem 9, 547 (2016)
2. S. Dutta, ChemSusChem 5, 2125 (2012)
3. M. Kashbor et. al, Appl. Cat. A: Gen. 642, 118689, (2022)
4. L. Foster et. Al, J. Catal. 425, 269, (2023)
5. Y. Li et. al, Appl. Cat. A: Gen. 366, 57, (2009)

Lasing Properties in Self-Assembled Quantum Dot Superparticles

Marco Reale[1*], Pietro Castronovo[1], Cherie R. Kagan[2], Marco Cannas[1], Christopher B. Murray[2], Emanuele Marino[1], Alice Sciortino[1], and Fabrizio Messina[1]
[1]Department of Physics and Chemistry "E. Segrè", University of Palermo, Italy *(marco.reale@unipa.it)
[2]Department of Chemistry, University of Pennsylvania, Philadelphia, United States

INTRODUCTION

Semiconductor quantum dots (QDs) have attracted significant scientific interest due to their extraordinary optical characteristics, including size-dependent absorption and photoluminescence spectra, almost unitary emission quantum yields, combined with their solution-processability and synthetic control[1]. More recently, colloidal QDs are increasingly being used as building blocks for mesoscale assemblies known as superparticles (SPs)[2], expanding their potential for optoelectronic applications. Here, we present a systematic optical study of the lasing properties of SPs assembled from CdSe/CdS core/shell QDs with unitary photoluminescence quantum yield.

EXPERIMENTAL STUDY

We performed the study by using steady-state and time-resolved optical spectroscopies under tunable laser excitation, coupled with an optical microscope to analyze the properties at a single-SP level.

RESULTS AND DISCUSSION

The use of a source-sink emulsion process on CdSe/CdS core/shell QDs allows the production of red fluorescent SPs with 10 μm diameter[2] (Figure 1a). These SPs behave as spherical microcavities capable of lasing through the narrow whispering-gallery modes resonances associated with the circular geometry. The emission of individual SPs was studied in detail below and above the lasing threshold (Figure 1b) as a function of the excitation power and excitation wavelength. We achieve narrow single- or multi-modal lasing emission under optimized experimental conditions of optical pumping and sample choice. We show that lasing from individual SPs is spectrally tunable by the choice of excitation wavelength (Figure 1c) depending on whether the core or shell of the QDs is primarily photoexcited. While we measure the SP lasing emission to be isotropic, achieving simultaneous physical and optical coupling to an optical fiber achieves directionality, producing a microlaser that can be integrated with existing photonic technologies. Interestingly, we also demonstrate that lasing spectra are extremely sensitive to the morphology and the environment of each individual SP, representing a unique fingerprint that paves the way to applications in anticounterfeiting, random number generation, and sensing.

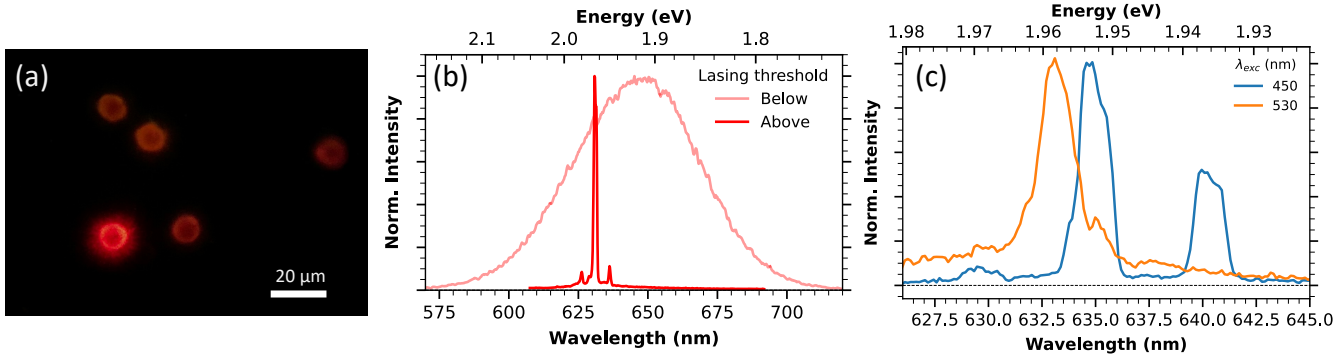

Fig. 1 (a) Microphotoluminescence image of SPs. The brightest SP is being excited above lasing threshold (b) Emission spectra of a single SP below and above lasing threshold. (c) Lasing spectra of the same SP under two different pumping wavelengths.

CONCLUSION

The unique properties of superstructures obtained by the self-assembly of core/shell QDs, behaving as tunable microlasers, are studied in detail revealing a huge potential for multiple applications in photonics and optoelectronics.

REFERENCES

1. C. B. Murray et al., J. Am. Chem. Soc. 115, 8706 (1993)
2. E. Marino et al., Chem. Mater. 34, 2779 (2022)

Production of bio-oil from grape residues over montmorillonite catalysts

Amanda R. Mallmann[1], Francieli M. Mayer[1], Arthur M. de Andrade[1], Anderson J. Schwanke[1], Dóris Ruiz[2], Maria do Carmo Rangel[1*]
[1*]Universidade Federal do Rio Grande do Sul, Brazil (maria.rangel@ufrgs.br)
[2]Universidad de Concepción, Chile

INTRODUCTION

The use of residual biomass for producing fuels follows the global trend of converting waste into high value products, avoiding the accumulation in the environment and reducing the use of fossil sources. The catalytic pyrolysis of biomass is a promising route to obtain bio-oil, which is a candidate to replace diesel. Aiming to produce high quality bio-oil, clays (montmorillonite) with different acidities were evaluated in the catalytic pyrolysis of industrial grape residues, in this work. As far as we known, there is no study about this system which offers several possibilities of applications, such as the production of several chemicals, besides biofuels.

EXPERIMENTAL/THEORETICAL STUDY

A commercial montmorillonite clay (Sigma Aldrich, CAS 1318-93-0), designated as K, was dried and dispersed in solutions of hydrochloric acid (1, 2, 4 and 6 mol L^{-1}), followed by drying at 60 °C for 48 h. The samples were named K1, K2, K4 and K6, where the numbers represent the concentration of acid solution. The solids were characterized by X-ray diffraction, textural analysis by nitrogen adsorption and acidity measurements by temperature-programmed ammonia desorption.

Sirah grape residues (skin and seeds) from a wine producer were crushed, sieved and dried in an oven at 60 °C for 24 h. For the catalytic pyrolysis experiments, biomass was mixed with the selected catalyst in a ratio of 1/1. The experiments were performed in a Py-GC/MS (Shimadzu) under nitrogen flow. The thermokinetic study was performed in TGA Q50 equipment (Universal) using 10 mg of sample at heating rates of 5, 10, 15 and 20 °C min^{-1}, under nitrogen flow. Thermokinetic parameters were determined by the isoconversional, non-isothermal methods of Flynn-Wall-Ozawa (FWO), Kissinger-Akahira-Sunose (KAS) and Friedman[1].

RESULTS AND DISCUSSION

Typical X-ray diffraction profiles of montmorillonite clay were shown by all samples and no change in specific surface area was noted, regardless the acid concentration. Only weak and moderate acidic sites were identified for K sample. After treatment, the total amount of acid sites increased for all clays, except for K2 sample, K4 showing the highest value, followed by K1> K6> K1> K2. Strong acid sites (T > 550 °C) were created in the treatment for all clays, K1 showing the highest amount, followed by K6 and K4.

The FWO method produced the best fit for experimental pyrolysis data, this method being chosen to calculate the activation energies (Ea) for the catalytic and non-catalytic reactions. As expected, the values changed during pyrolysis, due the different stages during reaction[2]. In a general trend, during cellulose and hemicellulose decomposition, 50% of biomass are converted to products, at around 277 and 344 °C, respectively. At these conditions, Ea strongly decreased for acidified catalysts, due to the activity of the acid sites in cracking, oligomerization, decarboxylation and decarbonylation[3]. The average activation energy for non-catalytic pyrolysis (75 kJ mol^{-1}) was not changed for pyrolysis over K (72 kJ mol^{-1}). However, over the acidified catalysts, the values change significantly indicating new reaction pathways to produce bio-oils with different compositions, as shown by CG/MS. The catalysts decreased the amount of oxygenates, generating high quality bio-oil.

CONCLUSION

The creation of strong acid site on montmorillonite increased its catalytic activity for cracking, oligomerization, decarboxylation and decarbonylation, leading to the production of high-quality bio-oil.

REFERENCES

1. M.E. Brown, Introduction to thermal analysis: techniques and applications, Springer, Netherlands (2001)
2. X. Hu, M. J. Gholizadeh, J. Energy Chem. 109, 39 (2019)
3. M.C. Rangel at. al, Biomass 3, 31 (2023)

ACKNOWLEDGMENTS

The authors acknowledge FINEP, CNPq and FAPERGS for the financial support.

Capturing carbon dioxide by MCM-41-supported lanthanum

Thaís Ribeiro[1], Maria do Carmo Rangel[1,2*]
Diogo da Silva[3], Julyane Solano[4], Antonio Silva[4]
[1]Programa de Pós-Graduação em Engenharia Química, Universidade Federal da Bahia, Brazil
[2]*Universidade Federal do Rio Grande do Sul, Brazil (maria.rangel@ufrgs.br)
[3]Universidade Federal de Uberlândia, Brazil
[4]Universidade Federal de Alagoas, Brazil

INTRODUCTION

As the main greenhouse gas, carbon dioxide has been extensively investigated in last years, several technologies being proposed for its capture, storage and utilization. Adsorption is recognized as a promising option to the capture, due to the simplicity and low cost. However, new efficient adsorbents are still needed to make this technology commercially viable. The combination of MCM-41 and lanthanum oxide has proven to result in promising adsorbents, because of the large pores and the high specific surface area of MCM-41, as well as of the basic character of lanthanum oxide, creating high chemical affinity to carbon dioxide[1]. Aiming to get efficient adsorbents for carbon dioxide capture, mesoporous MCM-41-supported lanthanum (x/MCM-41; x = 5; 10; 20 and 30% La) adsorbents were studied in this work.

EXPERIMENTAL/THEORETICAL STUDY

The samples were prepared by wet impregnation of lanthanum precursor on MCM-41 previously prepared. The adsorbents were characterized by X-ray diffraction, nitrogen adsorption/desorption and basicity measurements by TPD/CO_2. The adsorption capacity was evaluated by thermoprogrammed desorption. The data of adsorption kinetics were fitted using the pseudo-first order, pseudo-second order, intraparticle diffusion and Elovich models. The adsorbents were reused for ten cycles, being regenerated after each cycle.

RESULTS AND DISCUSSION

The samples showed typical X-ray diffractograms of MCM-41 ordered mesoporous hexagonal structure, regardless lanthanum incorporation. However, the lanthanum-containing samples became less ordered. All isotherms were type IV and the pore distribution curves were narrow unimodal (2-4 nm). However, the specific surface area largely decreased (from 1156 for MCM-41 to 620 $m^2\ g^{-1}$ for lanthanum-containing samples) with lanthanum increasing. The average mesopores diameter and volume were decreased by lanthanum, suggesting that some were occupied by the bulky La^{3+} ions, causing the decrease in specific surface area. In spite of this, lanthanum increased the adsorbent efficiency and stability after ten cycles of reuse. The sample with 5% La adsorved more carbon dioxide (38.8 $mgCO_2/(g\ ads)^{-1}$) than pure MCM-41 (34.1 $mgCO_2/(g\ ads)^{-1}$), followed by the solids with 10, 20 and 30% La, the first one showing a value close to MCM-41. During reuse, MCM-41 strongly deactivated, reaching values much lower than lanthanum-containg samples, the solid with 5% showing the highest vale (34.8 $mgCO_2/(g\ ads)^{-1}$). Therefore, lanthanum not only increased carbon dioxide capture but also the stability for ten cycles. The adsortion over lanthanum-poorest sample (5%), as well as over MCM-41, showed a kinetic behavior according Elovich model, indicating that chemisorption is the rate-determining step. Over the other samples, the best fit was provided by the Pseudo-First Order model, showing that adsorption capacity is proportional to the number of active sites on the adsorbent.

CONCLUSION

Lanthanum improves the capture of carbon dioxide by MCM-41 and the stability of the adsorbents for ten cycles. This can be related to the basic sites for chemisorption provided by lanthanum. For MCM-41 and 5%La/MCM-41, the adsorption kinetics is described by Elovich model, indicating that chemisorption is the rate-determining step. For the other samples, the behavior is described by PFO model, according to which the adsorption capacity is proportional to the number of active sites on the adsorbent. 5%La/MCM-41 showed the highest adsorption capacity and stability for ten cycles.

REFERENCES

1. T.R.S. Ribeiro et al. Carbon dioxide capture by lanthanum-modified MCM-41, FEZA 2021. Virtual

ACKNOWLEDGMENTS

Authors acknowledge CNPq, FINEP and Petrobras. TR acknowledges FAPESB for the graduate scholarship.

Theoretically probing structural and electronic properties of Pr-based crystals for energy applications

M. Francisca Queirós[1,2], E. Lora da Silva*[1,3]; V. M. Pereira[2]; M.C. Santos[4], Tao Yang*[5]
[1]IFIMUP, Department of Physics and Astronomy, Faculty of Science, University of Porto, Porto, Portugal, presenting author (up201805084@g.uporto.pt)
[2]CF-UM-UP, Department of Physics and Astronomy, Faculty of Science, University of Porto, Porto, Portugal
[3]High Performance Computing Chair, University of Évora, Largo dos Colegiais 2, 7004-516 Évora, Portugal
[4]CICECO, Universidade de Aveiro, 3810-1933, Aveiro, Portugal
[5]TEMA-NRG, Departamento de Engenharia Mecânica, Universidade de Aveiro, 3810-1933, Aveiro, Portugal, corresponding author (yangtao@ua.pt)

Background & Aim The Pr-based crystal $Pr_2O_2SO_4$ has recently attracted experimental interest for its potential as a high quality cathode for Solid Oxide Fuel Cells [1], [2] and as an oxygen storage material [3]. This project has the objective of theoretically exploring the structural, electronic and magnetic properties of this lanthanide oxysulfate with an oxysulfide counterpart Pr_2O2_S.

Methods We will use first-principles techniques to compute and characterize the stable crystal structures. Our calculations will be based on Density Functional Theory (DFT) [4] as implemented in the Quantum Espresso (QE) software package. We will employ exchange-correlation functionals based on the general gradient approximation (GGA) within the Perdew-Burke-Enzerhof (PBE) scheme. As a member of the lanthanoid series, Pr is a heavy element with unfilled f-orbitals, which means that special care must be taken to assess possible magnetic ground-states, as well as respective strongly correlated states. To address this we will also perform DFT+*U* calculations, which add a Hubbard term to the density functional to better capture the above mentioned effects.

Results After converging the parameters related to the basis set size and the k-mesh density, it is intended to obtain the equilibrium parameters and analyze the energetically more stable structural space group (monoclinic C2/c, orthorhombic I222 or tetragonal I-42m). The calculation of the inter-site Hubbard parameter is to be performed, and analysis of the partial density of states will aid in the assessment of the importance of the inclusion of the U parameter. The electronic band structure of this material and of the Pr_2O_2S is envisaged, in order to obtain information related to the nature of respective band gaps.

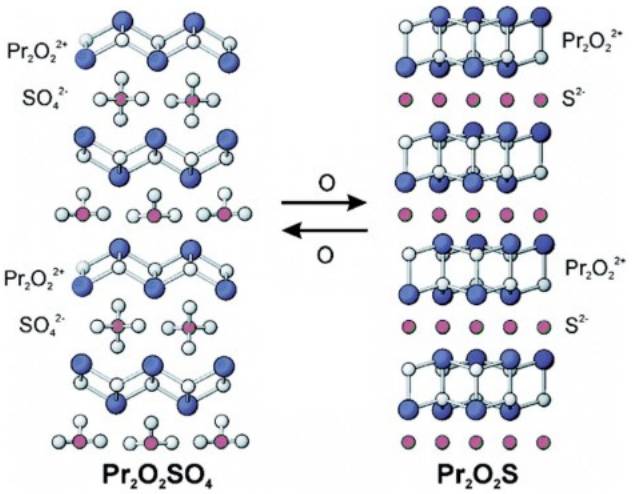

Figure 1: Crystal structure of $Pr_2O_2SO_4$ and Pr_2O_2S. This figure has been adapted from ref. [1]

Conclusions By theoretically understanding the characteristics of $Pr_2O_2SO_4$ and Pr_2O_2S, and the physics underlying the functionality of these materials, it will allow for the optimization of the required parameters for other possible applications.

References [1] F.J.A Loureiro *et al*. **J. Mater. Chem.** A 3, 12636 (2015). [2] Tao Yang *et al*. **J. Power Sources** 306, 611 (2016). [3] M. Machida *et al*. **J. Mater. Chem.** 16, 3084 (2006). [4] Richard M Martin. Electronic structure: basic theory and practical methods. Cambridge University Press, 2020.

ACKNOWLEDGMENTS The authors acknowledge the national funding from FCT through the PTDC/EME-REN/1497/2021project (Power Phoenix Battery-A Full Solid State Grid-scale Storage Solution) and computational resources through the 2022.15832.CPCA.A2 project at Univ. Évora – Oblivion.

Exploring the Integration of Mxenes in Polymers for Resistive Switching Devices

Maria Grácio*[1], Henrique Teixeira[1], Catarina Dias[1] and João Ventura[1]

[1]IFIMUP, Departamento de Física e Astronomia, Faculdade de Ciências, Universidade do Porto, Rua do Campo Alegre s/n, 4169-007 Porto, Portugal, presenting and corresponding author: *up201705000@fc.up.pt

INTRODUCTION

The As the downscaling of conventional electronic components reaches its limit, resistive switching (RS) devices have emerged as a promising novel technology, with applications ranging from non-volatile memories[1] to neuromorphic systems[2]. Metal-insulator-metal memristive devices are one of the most interesting devices in the field of memories, presenting RS and resembling properties of neural synapses, while offering the possibility of high-density integration[3]. The integration of 2D materials on RS devices has gained attention in the past years for performance enhancement. In particular, MXenes (e.g., $Ti_3C_2T_x$) are known for their excellent electrical, mechanical, and chemical properties, and their resistive switching ability has already been demonstrated[4].

EXPERIMENTAL/THEORETICAL STUDY

We have explored the incorporation of MXenes into polymeric matrices[5]. Polyvinylidene fluoride (PVDF) is known for its good electrochemical and thermal stability, as well as mechanical robustness, allowing great flexibility, toward flexible memristive architectures. By combining these materials, we can enhance the electrical response of the polymer. After exfoliating the T2C3Tx from the MAX phase, the $Ti_2C_3T_X$/PVDF composite was synthesized by dispersion of the 2D flakes in the polymer matrix, using dimethylformamide (DMF) as solvent, and by magnetic stirring under 60 ºC for 2h. The composite active layer was deposited through spin-coating, in either an ITO or W bottom electrode, and using W/Ag to define microsized circular top electrodes. The $Ti_2C_3T_X$/PVDF weight ratio was varied from 1% to 10%.

RESULTS AND DISCUSSION

We achieved resistive switching in PVDF polymer by inserting 3 wt.% $Ti_3C_2T_X$ in the polymer matrix. Bipolar resistive switching was observed in the devices, with low SET and REST voltages comprehended between -0.5 and 0.5 V, and on R_{ON}/R_{OFF} ratio around 10. Different variables involved in the variability of switching parameters were tested, such as forming voltage, switching voltage magnitude and polarity and current compliance.

CONCLUSION

We will perform studies of chemical stability of the devices and MXenes in PVDF. These results are in the path to develop more resilient memristors, towards non-volatile memories and neuromorphic systems.

REFERENCES

1. D. B. Strukov et al., Nature, 453, 80–83 (2008)
2. D. Marković et al. Nat Rev Phys 2, 499–510 (2020)
3. Yang, J. Joshua et al. *Nature nanotechnology* 8 1 (2013)
4. X. Yan et al., *Small*, 15, 1900107 (2019)
5. Y. Cao et al., *RSC Adv.*, **7**, 20494 —20501 (2017)

ACKNOWLEDGMENTS

We thank FCT and IFIMUP, through projects PTDC/NANMAT/4093/2021, UIDB/04968/2020 and UIDP/04968/2020, and "la Caixa" Foundation within project CCO 204197.

Ferroelectric and dielectric properties of P(VDF-TrFE) composites with molecular ferroelectric 2-(hydroxymethyl)-2-nitro-1,3-propanediol as filler material

Marianela Escobar-Castillo*[1], Samet Duman[1] and Doru C. Lupascu[1]

[1] Institute for Materials Science and Center for Nanointegration Duisburg-Essen (CENIDE), University of Duisburg-Essen, Germany

*marianela.escobar@uni-due.de

Abstract

Molecular ferroelectric materials have many advantages in comparison to the inorganic ferroelectrics, like moderate synthesis temperature, lower weight, high structural variability, etc. Organic ferroelectric materials that are water soluble can be embedded in organic polymers to protect it from moisture and enhance its mechanical flexibility and stability. For the application in some devices it is important that such composites preserve its ferroelectric properties. 2-(hydroxymethyl)-2-nitro-1,3-propanediol is a molecular ferroelectric material with a spontaneous polarization of 8 μC/cm^2, several polarizations directions and good piezoelectric properties (27.8 pC/N)[1]. In this work we prepared P(VDF-TrFE) composite films with the ferroelectric 2-(hydroxymethyl)-2-nitro-1,3-propanediol as filler material, and investigated the dielectric and ferroelectric properties of the flexible films. XRD results show that the crystal structure of the filler material do not change during film preparation process, and that the composites possess ferroelectric behaviour with a ferroelectric-paraelectric phase transition at around 390 K at different frequencies.

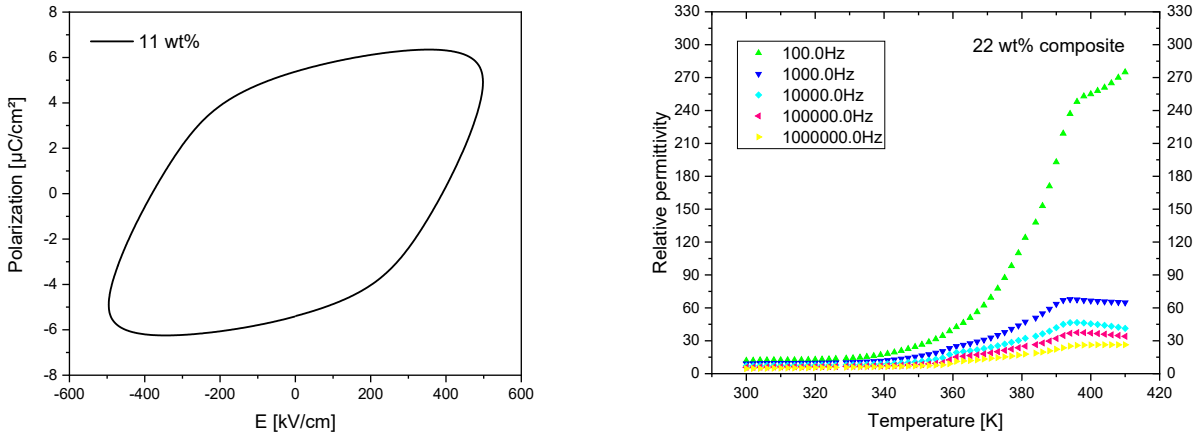

Picture 1. Ferroelectric and dielectric properties of the composites PVDF-TrFE/ Tris (hydroxymethyl) nitromethane.

[1] Yong Ai, Yu-Ling Zeng, Wen-Hui He, Xue-Qin Huang, and Yuan-Yuan Tang, Six-Fold Vertices in a Single-Component Organic Ferroelectric with Most Equivalent Polarization Directions, J. Am. Chem. Soc. 2020, 142, 13989-13995, https://dx.doi.org/10.1021/jacs.0c06936

Study of Thermal Fields Inside Pipes in Solar Collectors Working with Ionanofluids by Means of the HEATT® Platform

Mariano Alarcón[1*], Manuel Seco-Nicolás[1], Juan-Pedro Luna-Abad[2], Imane Moulfera[3] and Gloria Víllora[3]

[1]Electromagnetism and Electronics Department, International Campus of Excellence in the European context (CEIR) Campus Mare Nostrum, University of Murcia, Spain, presenting and corresponding author (mariano@um.es)

[2] Thermal and Fluid Engineering Department. International Campus of Excellence in the European context (CEIR) Campus Mare Nostrum, Technical University of Cartagena, Spain

[3]Chemical Engineering Department, International Campus of Excellence in the European context (CEIR) Campus Mare Nostrum, University of Murcia, Spain

INTRODUCTION

The fluids that work inside the tubes of the solar thermal collectors normally work in a laminar regime and are subject to asymmetric boundary conditions[1]. In recent years, various fluids, such as nanofluids and ionanofluids, have been tested in these collectors to improve or solve specific problems. The publicly accessible HEATT® platform can solve these types of problems[2].

EXPERIMENTAL/THEORETICAL STUDY

Based on bibliographic and experimental data on the characterization of ionic liquids and ionanofluids, their behavior in thermal solar collectors on the HEATT platform has been simulated. The behavior of different fluids (water, ionic liquid and graphene oxide ionanofluid) has been simulated to evaluate their use in solar collectors.

RESULTS AND DISCUSSION

HEATT provides the fluid temperature fields in the different sections of the conduit along the pipe graphically and numerically. The results allow determining the characteristic length of the process or optimal length in terms of the design of the solar collector pipes for all these fluids, as well as visualizing their temperature field, which in cases of high viscosity can be an indication of possible problems.

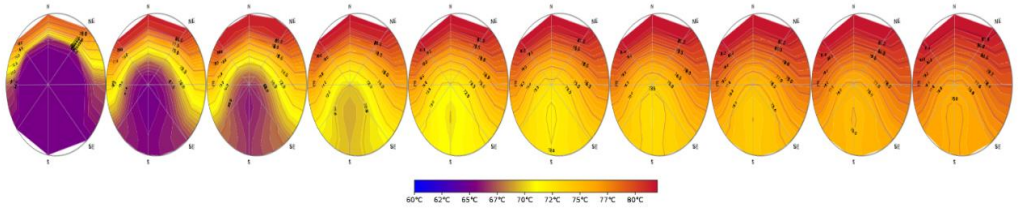

Fig. 1 Temperature field of the cross sections along the pipe in L/10, 2L/10, 3L/10 etc.

CONCLUSION

The behavior of different liquids (water, ionic liquid, and graphene oxide ionanofluid) has been modeled to evaluate their use in thermal solar collectors. It has been observed that the ionic liquid and to a lesser extent the ionanofluid present a very inhomogeneous temperature distribution in the usual lengths in flat solar collectors, requiring greater length to achieve a complete development of the thermal field inside.

REFERENCES

1. M. Seco-Nicolás, M. Alarcón, and J. P. Luna-Abad, “3D numerical simulation of laminar forced-convection flow subjected to asymmetric thermal conditions. An application to solar thermal collectors,” Solar Energy, 2021, doi: 10.1016/j.solener.2021.02.022.
2. M. Alarcón, M. Seco-Nicolás, J.P. Luna-Abad, and A.P. Ramallo-González, “HEATT,” 2022. https://heatt.inf.um.es/en/.

ACKNOWLEDGMENTS

This work has been partially supported by grants ref. TED2021-130389B-C21 financiado por MCIN/AEI/10.13039/501100011033 y por la Unión Europea “NextGenerationEU”/PRTR”, PID2020-113081RB-I00 funded by MCIN/AEI/ 10.13039/501100011033 and part of the grant ref. 22129-PI-22 funded by the research support program of the Seneca Foundation of Science and Technology of Murcia, Spain

Obtaining and Analyzing of Flexible and High Conductive Bio-based Polymers, Dopped with PANI-CNT

Marius Bodor [1], Aurora Lasagabáster-Latorre[2], M. Sonia Dopico-García[1], María-José Abad[1*]
[1]Campus Industrial de Ferrol, Grupo de Polimeros-CITENI, Universidade da Coruña, Spain
[2]Dpto Química Orgánica I, Escuela de Óptica, Universidad Complutense de Madrid, Spain

INTRODUCTION

As a continuation of previous work[1], the present study is aimed to obtain an electrically conductive 3D printable material using digital light processing (DLP), made from a bio-based resin and polyaniline/multiwalled carbon nanotube filler (PANI-CNT). The final purpose was obtaining a flexible and high electrically conductive material more environmentally friendly with the advantages given by the 3D printing, such as low cost and adaptable design.

EXPERIMENTAL/THEORETICAL STUDY

The samples were obtained through 3D printing, with the DLP technology (an ELEGOO-MARS printer was used). Different analyzing techniques were applied to the characterization of the resin formulation and the printed samples, such as rheology, UV-spectrophotometry, FTIR-spectrometry, mechanical testing and electrical conductivity measurements.

RESULTS AND DISCUSSION

The preparation of PANI-CNT was similar to the method described in Arias et al. [1]. Increasing percentages were used as filler in a resin mixture containing acrylates with around 75% bio-renewable carbon.

Table 1. Electrical conductivity of PANI-CNT filler and printed sample PANI-CNT-acrylate based resin

Sample	Thickness [mm]	Avg. for electrical conductivity [S/cm]
PANI-CNT	0.7	16
PANI-CNT-3% acrylate-based resin	1.7	$1.2*10^{-2}$

The results in Table 1 offers an insight into the performance of the printed materials related to the electric conductivity, showing the values achieved for both the filler PANI-CNT and the printed composite. This was one of the main features of the obtained samples, although other important properties were characterised, using different material analysing techniques, mentioned above. Other important results are related to the filler's suspension behaviour in the polymeric matrix, with great outcome even after more than one month. Also, the printability of the obtained mixes is manageable up to contents of 3% filler addition.

CONCLUSION

The utilization of a bio-based monomer in a resin mixture that also contained a conductive filler, enabled the obtaining of a flexible and high electrically conductive polymeric material, through 3D printing, that might be used in sensors technology.

REFERENCES

1. A. S. Goretti et. al, Adv. Electron. Mater. 8, 2200590 (2012)

ACKNOWLEDGMENTS

The authors are thankful for grant PID2020-116976RB-I00 funded by MCIN/AEI/ 10.13039/501100011033); Xunta de Galicia-FEDER (Program of Consolidation and structuring competitive research units (ED431C 2023/24); and to the Ferrol Industrial Campus programme Talento Investigador ref. 2023-CP-066 funded by the Convenio Xunta de Galicia - UDC.

Antibacterial activity of centrifugal spun fibers blended with ZnOnanoparticles for the treatment of *Acne vulgaris*

Martina Rihova[1*], Kristyna Cihalova[2], Zbynek Heger[2] and Jan M. Macak[1,3]
[1*]Central European Institute of Technology, Brno University of Technology, Purkynova 123, 61200Brno, Czech Republic, (martina.rihova@ceitec.vutbr.cz)
[2]Department of Chemistry and Biochemistry, Mendel University in Brno, Zemedelska 1, 613 00 Brno, Czech Republic
[3]Center of Materials and Nanotechnologies, Faculty of Chemical Technology, University of Pardubice, Nam. Cs. Legii, 565, 530 02 Pardubice, Czech Republic

INTRODUCTION

Acne vulgaris is a dermatological severe disease affecting large portion of the population[1]. ZnO nanoparticles (NPs) represent very efficient agent with for the treatment of *Acne* and enhanced skin compatibility, compared to antibiotics. Its antibacterial effect is attributed mainly to the eminent release of biologically active Zn^{2+} ions from nanoparticles surface and the formation of reactive oxygen species resulting in the death of bacterial cells[2]. On the other hand, the nanoparticles need to be properly dispersed on a suitable carrier, to be applicable on the skin. Fibrous materials have the potential to be great NPs carrier, owing to their unique characteristics, including high porosity, a large specific surface area, and good breathability. Combining ZnO NPs and fibers creates a very promising hybrid material, that is attractive for the treatment of *Acne vulgaris*[3-5].

EXPERIMENTAL STUDY

The GA:Pul solution with different concentrations (0,30 and 4,5 wt.%) of ZnO NPs were spun by centrifugal spinning into fibers, whose morphological and chemical analyses were carried out (SEM, ED XRF and ATB activity).

RESULTS AND DISCUSSION

The TEM demonstrates that ZnO NPs had approximately 40 nm in diameter (Fig. 1A). It can be seen ZnO NPs are attached to the fibers (Fig. 1B). SEM inspection of samples revealed that the distribution of ZnO NPs is quite uniform in all along the fibers, which confirms very good prospects of the centrifugal spinning used for fiber synthesis. Most importantly, they were characterized for their ATB activity against the acne-causing bacteria. These results will be also present.

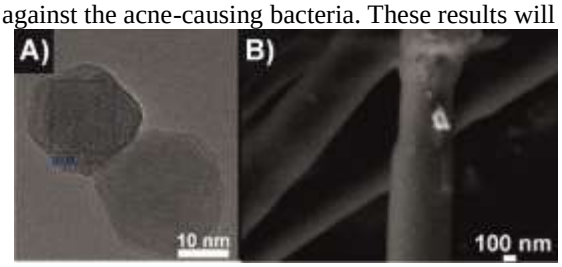

Fig. 1: A) TEM analyse of the ZnO NPs and B) high resolution SEM image of GA:Pul fibers blended with ZnO NPs

CONCLUSION

The results showed that blended fibers had antibacterial activity for as low ZnO content as 1.5 wt. %. The concept and materials in this work bear clear commercial possibilities and a very promising material for dermatologic application

REFERENCES

1. R. Balkrishnan et al., Clin. Ther. 77, 251–255 (2006)
2. A. Sirelkhatim et al., Nano-Micro Lett. 7 219–242 (2015)
3. M. Rihova et al., J. Appl Polym Sci. 168, e49975 (2021)
4. M. Rihova et al., Carbohydr. Polym. 294 119792 (2022)
5. M. Rihova et al., Appl. Mater. Today, Ms submitted.

ACKNOWLEDGMENTS

The authors acknowledge the financial support from the Ministry of Education, Youth and Sports of the Czech Republic of two large infrastructures: CEMNAT (project LM2023037) and CEITEC Nano Research Infrastructure (project LM2023051).

INTERACTIONS OF PARAMAGNETIC IONS WITH ALGINATES CHAINS AND THEIR MICROSTRUCTURE AS PROBE VERY FAST SOLID-STATE NMR SPECTROSCOPY

Martina Urbanova[1*], Libor Kobera[1], Miroslava Pavelkova[2], Jan Macku[1,2], Katerina Kubova[2] and Jiri Brus[1]

[1] Department of Structure analysis, Institute of Macromolecular Chemistry, Czech Academy of Sciences, Czech Republic; urbanova@imc.cas.cz
[2] Department of Pharmaceutical Technology, Faculty of Pharmacy, Masaryk University Brno, Czech Republic

INTRODUCTION

The metals ions cross-linked carbohydrates have attracted considerable interest due to their excellent properties such as self-healing, rapid recovery, biocompatibility and high mechanical properties combined with multi-stimulus responsiveness. Accordingly, efforts to integrate metal-coordinate cross-linking into bioinspired synthetic protein and polymer hydrogels are an increasingly active area of research. One of such polysaccharides is alginate (ALG), a naturally occurring biopolymer derived from brown seaweed. Its chemical structure contains β-D-mannuronic acid (M) and α-L-guluronic acid (G), and the segmentation of the G and M residues is responsible for its properties such as the resulting gelation and viscosity.

EXPERIMENTAL/THEORETICAL STUDY

By using a range of traditional and advanced techniques of solid-state NMR spectroscopy we monitored structural changes in alginate macromolecules induced by different types of crosslinking ions such as Fe^{3+}, Cu^{2+} and Ca^{2+}.

RESULTS AND DISCUSSION

We've successfully prepared alginate hydrogel particles cross-linked with antibacterial ions containing lactic acid suitable for vaginal administration to treat common infections using the external ionic gelation method. Unfortunately, the detailed structural data are entirely unavailable and completely lost if paramagnetic ions such as Fe^{3+}, Mn^{2+} or Cu^{2+} are used as crosslinking agents. Due to the strong paramagnetic effects of these ions including extreme signal broadening and fast coherence decay the vast majority of traditional techniques of ss-NMR spectroscopy fail (Fig.1 ^{13}C CP/MAS and MAS NMR spectra). To bridge this gap and to look into the structure of alginate systems crosslinked with paramagnetic ions we applied the recently developed an approach of very fast MAS (VF MAS) NMR spectroscopy (Fig.1 ^{13}C and ^{1}H VF MAS NMR spectra).

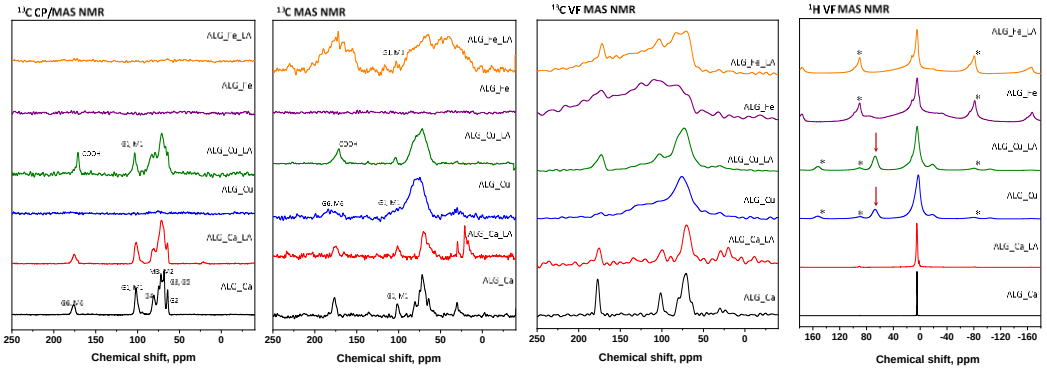

Fig. 1 ^{13}C MAS, CP/MAS and ^{13}C and ^{1}H VF MAS NMR spectra of prepared alginate particles.

CONCLUSION

The present research thus has ambitions to provide the first real experimentally confirmed insight into the complex interactions and structural transformations in alginate multicomponent systems crosslinked by paramagnetic metal ions.

ACKNOWLEDGMENTS

This work was supported by Czech Science Foundation (Grant No. 22-03187S).

Preparation and Some Properties of Polymer Films with Hierarchically Ordered Surface Structure by a Combination of Nanoimprinting and Surface-Initiated Graft Polymerization

Masahiko Minoda* and Jin Motoyanagi
Faculty of Molecular Chemistry and Engineering, Graduate School of Science and Technology,
Kyoto Institute of Technology, Japan (minoda@kit.ac.jp)

INTRODUCTION

Recently, various types of biomimicry materials have attracted much attention due to their remarkable surface functions. Polymer films with submicron-sized complex surface structures have been produced by top-down approaches (e.g. photolithography and nanoimprinting). On the other hand, surface nanostructures have also been prepared by bottom-up approaches (e.g. self-assembly formation and surface-initiated graft polymerization). In this study, we have developed a new methodology for the preparation of polymer films with hierarchically ordered surface structure by combining nanoimprinting and surface-initiated atom transfer radical polymerization (SI-ATRP), and investigated stimuli-responsive properties of the obtained surface-functionalized polymer films.

EXPERIMENTAL

To obtain the film, nanoimprinting was firstly achieved by employing polymers having both cross-linkable moieties and ATRP initiating sites and an anodically-oxidized porous alumina (AAO) as a template. After removal of AAO and cross-linking by photoirradiation, the films having vertically oriented polymer pillars on their surfaces were formed. Finally, the films were subjected to SI-ATRP of *N*-isopropylacrylamide (NIPAM) to give the target films decorated with polyNIPAM-grafted pillars (Fig. 1). Thermo-responsive change in hydrophilic nature of the obtained films were also examined by static contact angle measurement.

RESULTS AND DISCUSSION

Free radical copolymerization of coumarin-substituted methacrylate (MCMA) and α-haloester moiety-containing methacrylate (HEMA-Br) was carried out to form a precursor copolymer (M_n = 52000; M_w/M_n = 2.9; composition: [MCMA] / [HEMA-Br] = 2 / 3). Employing this polymer and AAO template (Whatman® Anodisc13), nanoimprinting was performed with Obducat Technologies AB model F-KT-254 under the condition of 130 ºC、180 s, 20 bar. After removal of AAO by immersion in 1 M NaOH aq., SEM observation indicated the formation of the film having vertically oriented polymer pillars (ca. 1000 nm length) on their surfaces. The obtained film was then photoirradiated to fix the pillar structure by intermolecular cross-linking. The resultant film was found to be insoluble in common organic solvents, and SEM analysis supported the pillar structure was maintained after photoirradiation. Finally, employing the pillar film, graft polymerization of NIPAM on the pillar surfaces was performed through SI-ATRP at 25 ºC for 5 h (conditions; [ethyl 2-bromoisobutyrate]$_0$ / [NIPAM]$_0$ / [CuCl]$_0$ / [Me_6TREN]$_0$ / [ascorbic acid]$_0$ = 1 / 100 / 1 / 2 / 1, [NIPAM]$_0$ = 50 wt%). Successful preparation of the target film with vertically oriented polyNIPAM-grafted polymer pillars on their surfaces were confirmed by FT-IR, XPS and SEM measurements. Since polyNIPAM is widely known as a representative thermo-responsive polymer, it is very interesting to investigate the thermo-responsive change in hydrophilicity and hydrophobicity of the surface of the film modified with polyNIPAM-grafted pillars. Therefore, we have also prepared the polyNIPAM-grafted counterpart from a poly(MCMA-*co*-HEMA-Br) flat film without pillar structure on its surface, and compared the thermo-responsive surface properties. As results, significant differences were observed between these polyNIPAM-grafted film samples, specifically, the film having polyNIPAM-grafted pillar structure exhibited greater hydrophilic-hydrophobic switching properties in response to temperature changes. This is presumed to be due to the synergistic effect between the surface pillar structure and the properties of polyNIPAM. Moreover, this hydrophilic-hydrophobic switching property could be repeatedly observed with increasing and decreasing temperature.

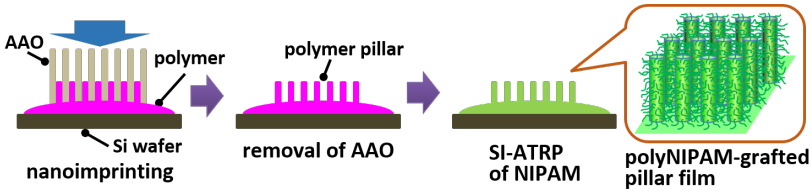

Fig. 1 Preparation of the film having polyNIPAM-grafted pillar structure.

Title: Thermochemical energy storage with Calcium Hydroxide, experimental demonstration of storage system for decentralized heat supply in buildings.

Author: Matthias Schmidt[1], Venizelos Sourmelis, Aldo Cosquillo[1], Marc Linder[1]
[1]German Aerospace Center – DLR e.V., Institute of Engineering Thermodynamics, 51147 Köln, Germany

Abstract:

The reversible reaction of Calcium Hydroxide to CaO and water vapour is very promising for thermochemical energy storage. The storage material is cheap, abundantly available and completely environmentally friendly. Energy-wise the potential lies in the loss free storage period and an energy density several times higher than conventional thermal storage technologies. For these reasons the reaction system has been investigated by several research groups over the past decade addressing different aspects on material, reactor and storage system level. Nevertheless, unfavorable material properties like cohesiveness, agglomeration tendency and large volume changes during the reaction impede the development of cost efficient and easily scalable thermochemical reactors. Our main approach to overcome these drawbacks are to work on both sides, improving the material properties on one hand and to develop reactors with improved functionality.

One outcome of our current work is a novel reactor concept based on the principle of a mechanically induced fluidized bed. The concept uses rotating shovels which induce a mechanical fluidization of the storage material inside the reactor. The principle helps to prevent agglomeration, facilitates the gas transport to and from the reacting particles and enhances the heat transfer coefficient between the particles and the heat exchanging wall of the reactor. With the operation of two different reactors based on this concept we could successfully demonstrate the energy storage process: The electrical charging of the storage material as well as the thermal discharging in kW scale. For these reactors we also developed a pilot storage system, including storage containers for a 100kWh thermal energy and automated transport of the material to and from the reactor. We integrated the pilot system in a research building environment and demonstrated the operation outside the laboratory successfully. To improve the overall systems performance and the function of sub components we also investigated different enhanced forms of the storage material: larger granules with a nanocoating for stabilization and hard compacted briquettes. This presentation will outline the operation of the storage system, characterizing the performance, efficiency and analyzing the impact and functionality of different novel forms of the storage material. We will discuss the general potential and outlook of energy storage based on Calcium Hydroxide.

Pluronic F-127 as Coating Polymer of Conjugated Polymer for PDT Application

Miao Zhao [2], Wednesday Tarhan-King [1], Bingchen Wu [1], Jumainah Abedin [1], Bingqi Li [1], Tsz Tsung Jacky Li [1] and Aliaksandra Rakovich* [3*]
[1]Physics Department, King's College London, UK
[2] Physics Department, King's College London, UK, presenting author
[3*] Physics Department, King's College London, UK, corresponding author

INTRODUCTION

Photodynamic therapy (PDT) is a promising treatment for cancer, with conjugated polymer nanoparticles (CPNs) emerging as effective agents. This study investigates the influence of Pluronic F-127 (F127) coatings on the PDT properties of CPNs to provide insights into coating polymers for developing water-soluble copolymer photosensitizers, poly[styrene-co-maleic anhydride] (PSMA) being employed as the control coating polymer, based on our previous study[1].

EXPERIMENTAL/THEORETICAL STUDY

CPNs of different conjugated polymers were fabricated using the nanoprecipitation method and then characterized in the following manner. The hydrodynamic size and stability of CPNs in aqueous solutions were assessed using dynamic light scattering (DLS) and zeta-potential measurements. Absorption and photoluminescence spectra were obtained to characterize CPNs' optical features, while fluorescence quantum yield (QY) was measured for their suitability as fluorescent probes. Singlet oxygen production by CPNs was evaluated using a spectroscopic method employing Singlet Oxygen Sensor Green (SOSG) as a chemical sensor.

RESULTS AND DISCUSSIONS

MEH-PPV@F127 CPNs exhibited a hydrodynamic size of ~127 nm and a zeta potential of ~-14.8 mV, while CN-PPV@F127 CPNs had a size of ~97 nm and a zeta potential of ~-13.1 mV, these characteristics render the CPN particles suitable for cellular uptake[2]. Optical analysis revealed characteristic absorption and photoluminescence spectra, indicating potential for bioimaging (Fig. 1(a) and (b)). CN-PPV@F127 CPNs demonstrated a QY of ~12.5%, and MEH-PPV@F127 CPNs showed a QY of ~5%, both suitable for cell imaging. Singlet oxygen generation capability was confirmed for all F127-coated CPNs (Fig. 1(c)).

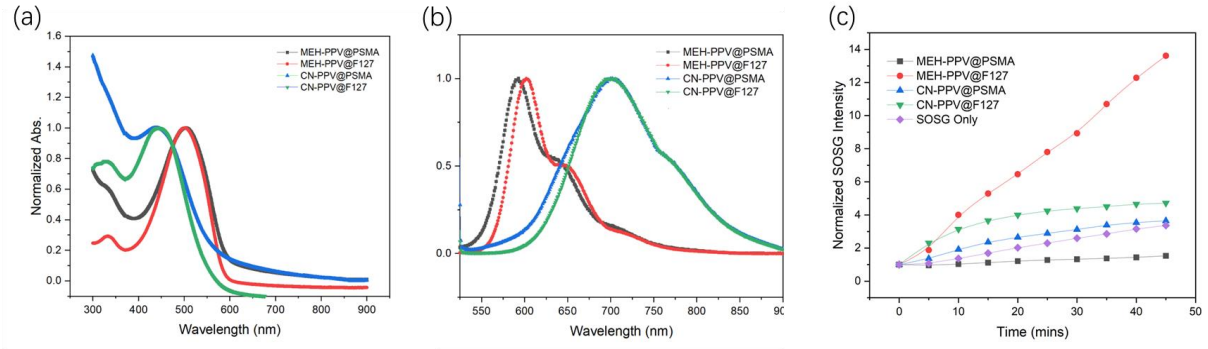

Fig. 1. Properties of CPNs. (a) Steady-state absorption, (b) steady-state emission and (c) photoinduced singlet oxygen generation of MEH-PPV@PSMA (black), MEH-PPV@F127 (red), CN-PPV@PSMA (blue), CN-PPV@F127 (green) CPNs. In panel (c), SOSG only solution (purple) was used as a control.

CONCLUSIONS

F127 is an ideal coating polymer for developing CPNs as photosensitizers. This guides the development of advanced nanomaterials in medical applications.

REFERENCES

1. Zhao, M. *et al.* Theranostic Near-Infrared-Active Conjugated Polymer Nanoparticles. *ACS Nano* **15**, 8790–8802 (2021).

2. Zhao, M., Uzunoff, A., Green, M. & Rakovich, A. *Nanomaterials* **13**, (2023).

Cyclic stability testing of Glauber's salt based composites for low-temperature applications

Veeresh Ayyagari, Amir Shooshtari, Michael Ohadi

Advanced Heat Exchangers and Process intensification Laboratory (AHXPI), University of Maryland, College Park, Maryland, USA 20740

Implementing a Thermal Energy Storage (TES) system along with heat pumps for air conditioning applications improves grid resiliency, provides monetary savings, and reduces the total carbon footprint. Organic phase change materials (PCMs) are widely used energy storage materials in TES devices due to their ease of implementation, high cyclic stability, and low supercooling. However, organic PCMs are relatively expensive and have a low thermal conductivity of ~0.1 W/m-K, increasing the payback periods and limiting the power densities of the TES devices, respectively.

Inorganic PCMs, primarily salt hydrates, are economical choice of PCMs compared to their organic counterparts, have high energy storage density and thermal conductivity and thus are a lucrative choice of PCM materials for low-cost, compact TES devices. However, salt hydrates demonstrate supercooling, which delays the crystallization and phase segregation with cycling which causes degradation in energy storage capacity with usage. Sodium Sulphate Decahydrate (SSD), also known as Glauber's salt, is one of the most inexpensive salt hydrates PCMs, melting at around 32°C. For building air conditioning applications such as peak load shifting, the PCM melting point requirement could be between 20-35 °C. However, not many composites of SSD are available in literature. The SSD's melting point could be tuned by adding low-cost melting point suppression agents. NaCl and KCl are the most popular melting point suppression agents used with SSD in the literature. While supercooling could be solved by adding Borax (a nucleating agent), phase segregation, affecting the cyclic stability remains a critical issue limiting its useful life.

Thickeners are a popular choice of additives for mitigating phase segregation, which when added to PCM increases the viscosity of the PCM, reduces the separation of phases and make them less prone to leakage. Exploring low-cost thickener is key factor to keep the cost of the salt hydrates low while enhancing its cyclic stability. Sodium Polyacrylate (SPA) is a low-cost polymer material which forms a gel like consistency when added to the PCM. Preliminary DSC studies done by authors show that when SPA and NaCl are added to SSD, the composite PCM demonstrated minimal degradation in latent heat in 10 cycles when tested using digital scanning calorimetry (DSC), with a melting point of 21 °C with a 110 kJ/kg latent heat. PCMs, when used in TES devices need to work ~ 10 years and goes through ~2000-3000 cycles. Thus, further testing was carried out to around ~500 cycles on the mixtures and their degradation of properties are presented here.

Molecular beam epitaxy growth of InAs nanowires on graphene/Si (111) substrates

Miguel González Morales[1], Máximo López López[2], Julio Mendoza Álvarez[2], José Luis Herrera Pérez[1] and Yenny Casallas Moreno*[3*]

[1] Postgraduate Department, Upiita-National Polytechnic Institute, México. (Presenting author)

[2]Physics Department, Cinvestav, México,

[3*]Conahcyt, Upiita-National Polytechnic Institute, México. Corresponding author. (ycasallasm@ipn.mx)

INTRODUCTION

Nanoscale semiconductor materials represent one of the promising technologies for the development of novel optoelectronics devices[1]. Among these materials, nanowires offer a compelling alternative due to their quantum lateral confinement of electrons, making them an alternative for the design of efficient detectors. This potential may be approached by the application of well known, highly remarkable semiconductor materials like the III-V family of compounds, with InAs standing out as a notable representative[2]. With its direct band gap and room temperature high-electron mobility, InAs is well-suited for integration into nanowire manufacturing especially for optoelectronic applications in the near to mid-infrared range[3].

In this work, we present a novel approach to fabricating InAs nanowires using molecular beam epitaxy (MBE) on Si (111) substrates coated with a few layers of graphene. This innovative substrate configuration facilitates more uniform nanowire growth, enhancing the performance and reliability of resulting optoelectronic devices.

EXPERIMENTAL/THEORETICAL STUDY

InAs nanowires were grown by MBE on Si (111) substrates coated with graphene at various temperatures, as well as on samples on Si without graphene. Structural and microscopic studies were conducted to observe the presence and distribution of the nanowires on the substrates.

RESULTS AND DISCUSSION

High-resolution X-ray diffraction (HR-XRD) analysis revealed the presence of crystalline InAs on the surface of the Si (111) substrates, exhibiting reflections corresponding to (111), (022), and (222) crystal planes. Scanning electron microscopy (SEM) micrographs provided insight into the morphology and overall distribution of the nanowires. These studies offer evidence supporting the formation of the proposed nanostructures.

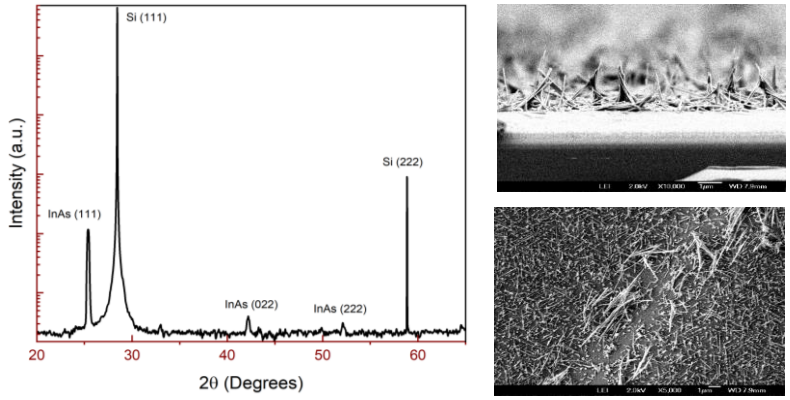

Fig. 1 (Left) HR-XR diffractograms of a sample. (Right) Sem micrograph of the surface of a growth sample.

CONCLUSION

Overall, the growth of InAs nanowires on Si (111) substrates, particularly when coated with graphene, demonstrates promising structural characteristics and distribution, affirming the feasibility of their integration into optoelectronic devices.

REFERENCES

References must be numbered. Keep the same style.

1. Liu, Junting, et al., J. Phys. Chem. Lett. 10, (2019).
2. Paladugu, Mohanchand, et al., Small 3.11 (2007).
3. Sumikura, Hisashi, et al, Nano Letters 19.11 (2019).

ACKNOWLEDGMENTS

Authors thank Conahcyt and IPN for financial support

(ANM) Advanced Nano Materials

Investigation of $WO_3/BiVO_4$ heterojunction for photoelectrochemical decomposition of organic compounds and production of hydrogen

Milda Petruleviciene[1*], Irena Savickaja[1], Jelena Kovger-Jarosevic[1], Kamila Turuta[1], Jurga Juodkazyte[1] and Arunas Ramanavicius [1,2]

[1*] Department of Chemical Engineering and Technology, Center for Physical Science and Technology, Lithuania, milda.petruleviciene@ftmc.lt

[2] Department of Physical Chemistry, Faculty of Chemistry, Vilnius University, Lithuania

INTRODUCTION

Renewable energy sources such as solar, wind, and hydropower produce no greenhouse gases compared to traditional fossil fuels. By switching to these sources, we can mitigate the effects of climate change and reduce global warming. Photoelectrochemical (PEC) systems convert light energy to chemical energy. They can be applied for simultaneous decomposition of various organic compounds *via* oxidation reactions on photoanode and production of hydrogen on cathode. The efficiency of such systems strongly depends on the nature of photoanode, because semiconductors differ greatly in terms of their valence and conduction band positions, e.g. the valence band potential of tungsten (VI) oxide corresponds to 2.8 - 3 V vs SHE (Standard Hydrogen Electrode), whereas that of bismuth vanadate is 2.4 – 2.6 V (SHE). Photo-induced WO_3 holes have much higher oxidizing power, however tungsten oxide is unstable at pH > 4. $BiVO_4$, on the contrary, is stable in neutral media, which is why the formation of $WO_3/BiVO_4$ heterojunctions has recently attracted much attention. In addition, it is known that heterojunctions facilitate the separation of charge carriers, which leads to a lower degree of recombination.

EXPERIMENTAL/THEORETICAL STUDY

$WO_3/BiVO_4$ heterojunctions were formed using hydrothermal and sol-gel synthesis. Synthesized coatings were analyzed using X-ray diffraction analysis and scanning electron microscopy. PEC properties of the coatings were characterized using cyclic voltammetry (CV), chronoamperometry (CA) and electrochemical impedance spectroscopy (EIS). Performance of heterostructured photoelectrodes in decomposition of pharmaceutical compounds with simultaneous cathodic production of hydrogen was tested.

RESULTS AND DISCUSSION

Preliminary characterization of the coatings revealed slight differences in photoelectrochemical behavior of WO_3 and $WO_3/BiVO_4$ in 0.5 M Na_2SO_4 (Fig. 1). Faradaic efficiency (FE) of PEC generation of persulfate ($S_2O_8^{2-}$) was higher in the case of heterostructured sample (Fig. 1c). Results on PEC decomposition of organic compounds coupled with H_2 evolution will be presented at the conference.

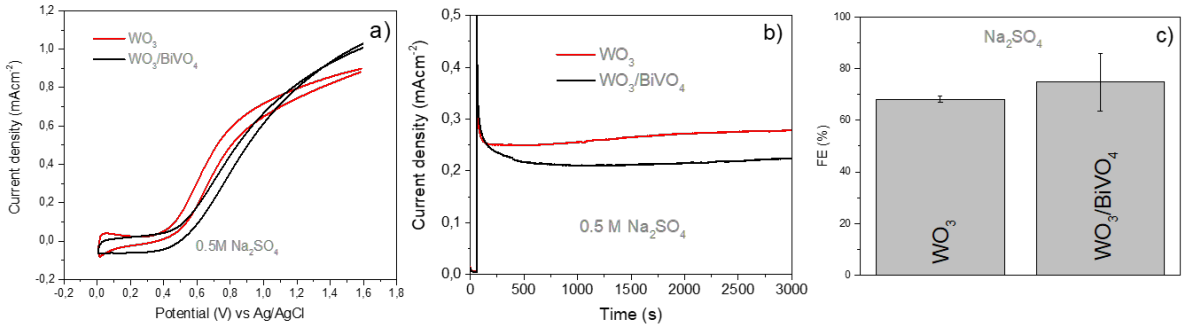

Fig. 1 CV (a), CA (b) and FE (c) of WO_3 and $WO_3/BiVO_4$ coatings. Experiments were performed in 0.5 M Na_2SO_4 under 100 $mWcm^{-2}$ illumination intensity and 1.4 V bias (vs Pt)

CONCLUSION

Initial results showed that the formation of $WO_3/BiVO_4$ heterojunction affects oxidation reactions on the surface of the photoanode. Additional experiments will be performed to investigate the mechanisms of PEC decomposition of organic compounds.

ACKNOWLEDGMENTS

This project has received funding from the Research Council of Lithuania (LMTLT), agreement No S-PD-22-2

Characterization of nanomaterials using adsorption technique

Miloslav Lhotka[1*], Barbora Dousova[2]
[1*] Department of Inorganic Technology, Faculty of Chemical Technology, University of Chemistry and Technology, Prague, Technická 5, 166 28, Prague 6, Czech Republic, presenting author, corresponding author (miloslav.lhotka@vscht.cz)
[2] Department of Solid-State Chemistry, Faculty of Chemical Technology, University of Chemistry and Technology, Prague, Technická 5, 166 28, Prague 6, Czech Republic

INTRODUCTION

One of possible definitions of the nanomaterials identifies nanomaterial as a natural, incidental or manufactured material containing particles as aggregates, agglomerates or particles in unbound state, where 50% or more of them range in the number of size distribution and one or more external dimensions are in the size range of 1 nm-100 nm. Where technically feasible and requested in specific legislation, the compliance with the definition may be determined on the basis of the specific surface area by volume (VVSA)[1]. A material can be considered falling with the definition, when the volume specific surface area of material is greater than 60 m^2 cm^{-3}. The volume-specific surface area is property of materials, which is obtained by dividing the samples external surface (S) by its solid volume (V) or by multiplying the specific surface area (SSA) by the materials skeletal density (ρ)[2].

RESULTS AND DISCUSSION

For dry powders, the volume-specific surface area can be determined via the gas-adsorption measurement of the specific surface area by nitrogen (with adsorption isotherms of type II, III or IV according to the IUPAC classification)[3], and multiplying it by skeletal density from the He-pycnometry measurement. To determine the specific surface of the nanomaterial, it is necessary to know the amount of adsorbate needed to cover the surface with the gas molecules monolayer, and to determine the area needed to adsorb one molecule of adsorbate. The knowledge of these quantities will then allow to determine the specific surface area of a solid sample of known weight. There are number of theories, but currently the BET (Brunauer-Emmett-Teller) isotherm[4] is used to calculate the specific surface area. This procedure is interesting in comparison to the size-based criterion, because it represents well-known, low-cost, standardized method, which can be applied on dry powders without further sample preparation except degassing. It is also agglomeration-tolerant, and leads to reliable results. When the volume-specific surface area method for the positive identification of nanomaterials is applied only on non-porous materials, the classification can be considered very reliable. When the particles are porous, the volume-specific surface area will be larger than expected from their outer dimensions and consequently, such materials should be excluded from the analysis, and the classification should not be done based on volume-specific surface area measurements. However, the pore surface can be separated from the outer particle surface by the detailed analysis of the full adsorption isotherm, e.g., using an appropriate t-plot method[5].

CONCLUSION

In this study the potential of the volume-specific surface area method as a classification tool was evaluated, for the identification of both nanomaterials and non-nanomaterials. For nonporous materials: When deriving the average size of the smallest particle dimension from volume-specific surface area, taking into account the approximate particle shape (sphere, fiber, plates) a good agreement with the electron microscopy results is obtained. Achieving such a good agreement is also possible for porous particles using the t-plot method (not BET method), which is capable of separating the pore surface from the external surface of particles. Platelet materials are a special case, where the volume-specific surface area approach yields a more reliable classification than conventional electron microscopy, because electron microscopy cannot always address the relevant smallest dimension of the particles.

REFERENCES

1. W. Liu, S. Song, M. Ye, Y. Zhu, Y. Zhao and Y. Lu, Nanomaterials **12** (2022) 1845
2. W. Kreyling, M. Semmler-Behnke and Q. Chaudhry, Nano Today **5** (2010) 165
3. Thommes, M.; et al. Physisorption of gases, with special reference to the evaluation of surface area and pore size distribution (IUPAC Technical Report). Pure Appl. Chem. 87 (9-10), 1051-1069, 2015
4. S. Brunauer, P. H. Emmet a E. Teller, J. Am. Chem. Soc. **60** (1938) 309.
5. B.C.Lippens, B.G. Linsen and J.H. de Boer, J.Catal. **3** (1964) 32

Theoretically-assisted evaluation of $(Fe,Ni)_3Se_4$ for water-splitting applications

Miłosz Kożusznik[1*], Andrzej Mikuła [1], Krzysztof Mars[1]
[1]Faculty of Materials Science and Ceramics, AGH University of Krakow, Poland
*mkozusznik@agh.edu.pl

INTRODUCTION

Large-scale process of hydrogen production via water-splitting faces significant operational costs, primarily attributed to the utilization of expensive electrocatalysts based on precious metals such as Pt. To overcome this problem, new groups of materials and ways to boost their electrocatalytic activity are developed. Here, we report the performance of a relatively unexplored group of materials characterized by monoclinic metal-like structure based on transition-metal chalcogenides with a general formula of TM_3Se_4 (TM = Fe,Ni). Hydrogen evolution reaction (HER) performance of TM_3Se_4 materials[1] and simplified synthesis route enhances their attractiveness for industrial applications. Additionally, *ab-initio* calculations play a crucial role in unraveling the intricate mechanism of H_2 production, by predicting the optimal chemical composition as well as providing valuable insight for further advancement in the field of TM_3Se_4-based catalysts.

EXPERIMENTAL/THEORETICAL STUDY

TM_3Se_4 materials were synthesized via annealing in tube furnace, after which they were ground and either pressed into pellets via inductive hot-pressing method or casted onto commercial screen-printed electrodes. Crystal structure, chemical composition and homogeneity were analyzed by means of X-ray diffraction and scanning electron microscopy. To gain insight into the electronic structure of examined materials, a*b-initio* calculations were performed within the density functional theory (DFT) formalism. The electrochemical performance and stability of studied materials were examined via voltametric and chronoamperometric methods, respectively.

RESULTS AND DISCUSSION

The electrochemical properties of a material are intricately tied to both its microstructure and chemical composition. The latter directly influences the electronic structure, thereby impacting H^+ adsorption processes occurring on the surface. The calculated *d*-band center presented in Fig. 1 (d_{bc}) serves as pivotal link between theoretical modeling and experimental observation. Notably, based on previous research, the Fe-Ni systems may exhibit catalytic activity similar to $(Co,Fe,Ni)_3Se_4$, which proved to be a promising electrocatalyst for HER[1]. Calculations of ΔG_{H^*} for pre-selected surfaces of the materials allow for determination of the most probable H^+ adsorption sites[2]. The microstructure also plays an important role in catalytic processes, where porosity becomes a critical factor enabling penetration of the electrolyte into deeper parts of the pellet. The synergistic approach of adjusting the chemical composition, implementing the surface engineering, and *ab-initio* modeling provide excellent ways for future development of cost-efficient and highly active electrocatalysts for water-splitting and other industrially-oriented applications.

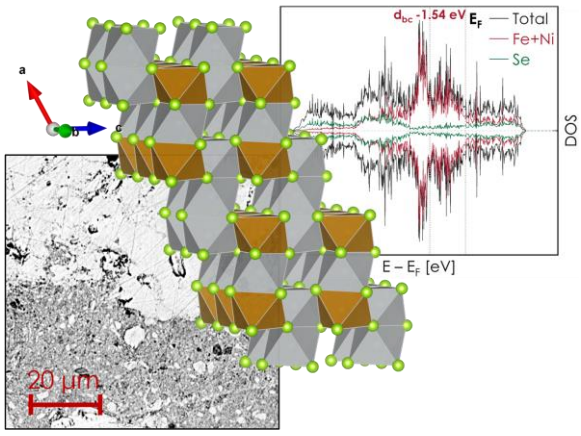

Fig. 1 $FeNi_2Se_4$ model alongside DOS plot and SEM image of the pellet surface

CONCLUSION

A group of monoclinic transition-metal chalcogenides containing Fe and Ni were synthesized, and their performance was evaluated by combining theoretical and experimental data. Future research will be focused on finding the optimal chemical composition in the $(Co,Fe,Ni)_3Se_4$ system and expanding the theoretical models to include point defects.

REFERENCES

[1] A. Mikuła et al, J. Mater. Chem. A 11 5337-5349 (2023)
[2] J. Nørskov et al, J. Electrochem. Soc. 152 J23 (2005)

ACKNOWLEDGMENTS

This work was financially supported by the National Science Centre, Poland, under grant no. 2022/45/B/ ST8/03336. We gratefully acknowledge Poland's high-performance computing infrastructure PLGrid (HPC Centers: ACK Cyfronet AGH) for providing computer facilities and support within computational grant no. PLG/2023/016825.

Integration of Silver Nanoparticle-Polymer Nanocomposite into 3D-Printed Protective Cover: a Study of Antiviral Performance

Mindaugas Ilickas[1*], Asta Guobienė[1], Karolis Gedvilas[2,3], Mantvydas Merkis[4], Brigita Abakevičienė[1,4*]
[1]Institute of Materials Science, Kaunas University of Technology, K. Baršausko St. 59, 51423 Kaunas, Lithuania
[2]Faculty of Natural Sciences, Vytautas Magnus University, Universiteto St. 10, 53361 Akademija, Kaunas distr., Lithuania
[3]Research Institute of Natural and Technological Sciences, Universiteto St. 10, 53361 Akademija, Kaunas distr., Lithuania
[4]Department of Physics, Kaunas University of Technology, Studentų St. 50, 51368 Kaunas, Lithuania
[*]Corresponding authors Brigita Abakevičienė (brigita.abakeviciene@ktu.lt) and Mindaugas Ilickas (mindaugas.ilickas@ktu.lt)

INTRODUCTION

Efforts to combat microorganisms involve surface modification and the development of antimicrobial coatings. Direct deposition of biocidal substances on surfaces enables effective modification without altering bulk properties. Recent advancements include polymer-solvent-active material nanocomposites[1], providing varied antimicrobial effects based on concentrations and compound compositions. The use of 3D scanning and printing allows to produce complex, geometrically shaped, and flexible protective coatings[2] to mitigate the spread of microorganisms on frequently touched surfaces.

EXPERIMENTAL/THEORETICAL STUDY

In this work, AgNPs synthesized through photochemical methods[3] using $AgNO_3$ and Irgacure 819 are incorporated into a PVB polymer matrix, forming an AgNP-PVB nanocomposite. This nanocomposite is applied as a thin-film coating on custom protective cover produced with Artec Space Spider 3D scanner (Artec 3D, Luxembourg) and Form 3 stereolithographic 3D printer (Formlabs, USA) using Flexible 80A resin (Formlabs, USA). The 3D model reconstruction algorithm is developed using Matlab (MathWorks, USA). To evaluate the antiviral properties, 10-well substrates were 3D printed from Flexible 80A polymer, 8 wells were coated with AgNP-PVB-A (AgNP concentration – 500 ppm), and AgNP-PVB-B (AgNP concentration – 200 ppm) nanocomposites or were left empty to assess the properties of the printed cover itself. The 8 wells are then filled with the test solution and left for 24 hours. The 9^{th} and 10^{th} wells are used as controls and are filled with the test solution for the one-step qRT-PCR analysis after 24 hours.

RESULTS AND DISCUSSION

The results of the antiviral tests using the AgNP-PVB-A nanocomposite coating show that the average cycle threshold (*Ct*) value in the test wells is 30.78 ± 2.00 compared to 25.92 ± 0.04 in the control wells. The *Ct* values decrease to 28.22 ± 0.88 (test) and 24.65 ± 0.40 (control) when using the AgNP-PVB-B nanocomposite coating. The AgNP-PVB-B control test *Ct* values are similar to those of the Flexible 80A polymer (25.27 ± 1.41 (test) and 24.61 ± 0.11 (control)), indicating the antiviral properties of the printed coating itself. The 3D printed door handle cover showed a uniform thickness with no cracks or bulges. This research contributes to the development of durable antiviral coatings aimed at inhibiting the transmission of infectious diseases in various environments.

CONCLUSION

In conclusion, this study formed different concentration (AgNP concentration – 200 ppm and 500 ppm) AgNP-PVB nanocomposite coatings on 3D printed protective cover, demonstrating effective antiviral properties, with *Ct* values of 30.78 ± 2.00 and 28.22 ± 0.88. Also, an algorithm for reconstructing the 3D model of the cover from the 3D scanned model has been developed and tested.

REFERENCES

1. G. Isopencu, et al., Coatings 12 (2022).
2. J. Wang, et al., International Journal of Pharmaceutics, 503(1–2), 207–212 (2016).
3. M. Schmallegger, et al., ChemPhotoChem, 6(12) (2022).

Effect of freeze-drying on the drying stage of silica extracted from industrial waste

Mirian D.(Fusinato)[1*], Rafael de A.(Delucis)[1],Camila O.(Calgaro)[2], Diego G.(Santos)[2], Daniel A. (Bertuol)[3] and Pedro J.S.(Filho)[2]

[1] Postgraduate Program in Materials Science and Engineering – Federal University of Pelotas, Brazil

[2] Chemical Engineering, Technical Course in Chemistry – Federal Institute Sul-Rio-Grandense, Brazil

[3] Chemical Engineering – Federal University of Santa Maria, Brazil

mirfusinato@gmail.com

INTRODUCTION

Amorphous mesoporous silicas with a high surface area have a wide range of applications in several industries. However, their large-scale manufacture is expensive due to the use of expensive raw materials, such as tetraethyl- (TEOS)[1]. Alternative sources of silica include some agricultural wastes. Rice husk (RH) is among the agricultural residues richest in silica within its composition. Due to the energy crisis and the need to produce clean energy, in addition to reducing the environmental liabilities generated by the large volume of RH, industries have been using RH to generate energy through combustion in boiler furnaces and, as a by-product, there is the generation of rice husk ash (RHA), which has around 90% of silica[2]. Sol-gel method I one of the main methods for extracting silica from agricultural wastes. This process involves obtaining a silica gel, which is then washed and dried. In this last stage, which is carried out using ovens, the gels agglomerate themselves, which can reduce both the number of pores and overall surface area. Freeze-drying is an alternative method for this drying stage. In this context, the aim of this study is to increase the surface area of the silica obtained from RHA through the sol-gel process, including freeze-drying after washing the gel[2].

EXPERIMENTAL/THEORETICAL STUDY

The RHA used as a source of silica in this study was provided by an industry from Pelotas, located in southern Brazil. The method consists of dispersing the RHA in an alkaline solution of sodium hydroxide (2.2 M), where the amorphous silica is dissolved and converted into a soluble sodium silicate; this stage takes place in an ultrasound bath, following the procedure already carried out by Fusinato et al.[2] The first silica sample was dried using a traditional way, in an oven at 100 °C for 12 hours. The second silica sample was freeze-dried, in a way that the gel is frozen in an ultrafreezer and then freeze-dried. The silicas were analyzed by BET to determine their surface area and BJH to evaluate pore volume and size, and isotherm analysis (ASAP 2020, Micromeritics).

RESULTS AND DISCUSSION

Table 1 presents a comparison between the results of the silica extracted using the ultrasound bath dried in a traditional oven and the silica extracted using the ultrasound bath and dried through freeze-drying. There was an increase of about 40% in surface area using freeze-drying.The pore size and pore volume increased after the freeze-drying, which was acompanied by a greater surface area. Figure 1 shows similar isotherms for the two silicas, corresponding to type IV hysteresis, characteristic of mesoporous materials.

Tabela 1. Surface area, pore volume and pore diameter

Sample	S_{BET} ($m^2.g^{-1}$)	$Vt(cm^3.g^{-1})$	D_{BJH} (nm)
Normal dried silica	460.03	0.91	6.67
Freeze-dried silica	645.38	0.98	7.41

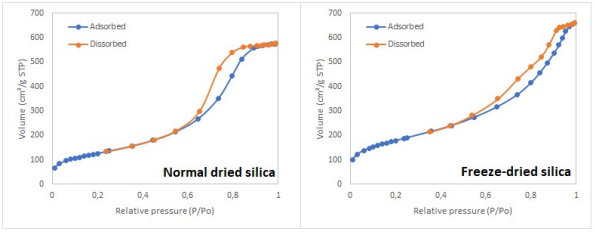

Figure 1. Isotherms of the silica samples

CONCLUSION

It was possible to obtain silica with a high surface area (645 m^2/g) from RHA generated in an industrial boiler using the ultrasound-assisted sol gel method and freeze-drying. Freeze-drying was decisive for increasing the surface area, preventing particle agglomeration.

REFERENCES

1. M. El-Sakhawy et al, Biomass Conversion and Biorefinery. 12, 4709 (2022)

2. M.D. Fusinato et al, Environmental Science and Pollution Research. 30, 21494 (2023)

ACKNOWLEDGMENTS

The authors acknowledge IFSul, IRGOVEL-Indústria Riograndense de Óleos Vegetais Ltda, FAPERGS (20/2551-0000441-4), and CNPq.

Carbon-supported Ni Nanoparticles: Synergizing of Magnetism and Adsorption for Advanced Water Decontamination

Mona Fadel*, Pablo Álvarez-Alonso , Jesus Blanco, Pedro Gorria , and Montserrat Rivas
Department of Physics, University of Oviedo, 33007, Oviedo, Spain
* Email:uo273017@uniovi.es

INTRODUCTION

Water, a fundamental life-giving resource, is frequently threatened by industrial activities. The motivation for this work is to develop an effective method for decontaminating wastewater from industries. A promising approach is to use magnetic nanoparticles (NPs) exhibiting adsorption functionalities, allowing for easily removal through magnetic separation. Nickel (Ni) NPs have excellent catalytic activity and a ferromagnetic behavior that facilitates efficient magnetic separation[1]. In this sense, coating Ni NPs with activated carbon is an ideal strategy for this purpose thanks to its low density and large porosity[2].

EXPERIMENTAL STUDY

The samples were obtained following a two-step procedure to produce Ni@C catalysts. It consists of: (i) the synthesis of nickel–imidazole MOF (NiOF) by a simple method in an aqueous medium and (ii) a thermal treatment at different carbonization temperatures to obtain a hybrid material formed by Ni NPs embedded in a carbon matrix.

RESULTS AND DISCUSSION

This work focuses on producing and analysis carbon-supported Nickel NPs derived from nickel-organic frameworks, NiOFs (see Fig. 1). The microstructure, morphology, and magnetic properties of NPs with various sizes from 5 nm to 50 nm synthesized at different carbonization temperatures (400 to 1000 ºC) were investigated. Our findings indicate that Ni NPs are surrounded by graphite-like layers, providing natural protection against oxidation. Additionally, a continuous transformation of the metastable Ni phase with hexagonal (HCP) crystal structure to the stable cubic (FCC) with raising carbonization temperature is accompanied by a rise of the value of a saturation magnetization increment from 5 to 48 emu/g-Ni. Adsorption experiments show excellent performance in the removal of noble metal (Chromium) and a dye (Methylene Blue) from water. In this presentation, I will showcase the most promising Ni NPs for water decontamination.

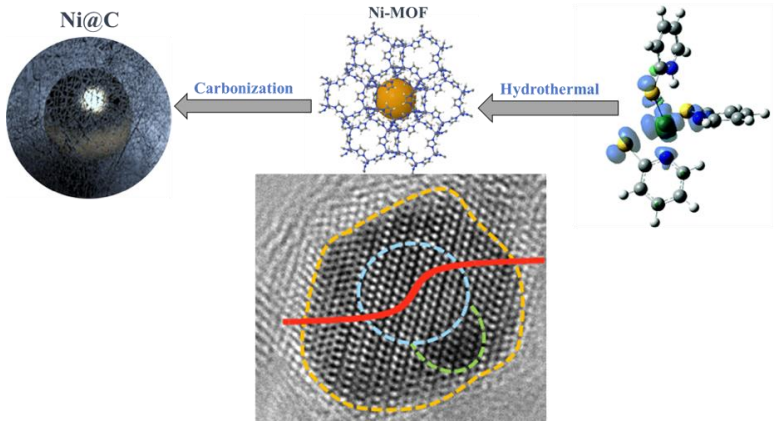

Fig. 1: Schematic of the MOF-derived fabrication of the carbon-coated Ni nanoparticles of this work.

CONCLUSION

We encompass a comprehensive investigation involving structural, microstructural and magnetic characterization of Ni NPs protected against oxidation by an ultrathin carbon coating consisting of a few atomic layers. The size, crystalline quality, and physical-chemical properties of the NPs are meticulously controlled by the carbonization temperature, a factor that determines their adsorption efficiency. By synergizing the dual properties of magnetic NPs and the porosity of the carbon matrix, we successfully demonstrated the efficiency for the removal of two common contaminants, Chromium and Methylene Blue, from water through adsorption processes.

ACKNOWLEDGMENTS

This work was financially supported by the research projects PID2022-138256NB-C21 (AEI, Spain & FEDER, EU) and AYUD/2021/51822 (Gobierno del Principado de Asturias, Spain). The authors would like to acknowledge the technical support provided by Scientific-Technical Services of the University of Oviedo, Spain.

REFERENCES

[1] F. Martin et al., J. Alloys Compd. **853** (2021) 157348.
[2] M. Fadel, et al., J. Mater. Chem. C **11** (2023) 4070.

Titanium Carbide MXenes (Ti_3C_2) with Nickel cocatalyst to Construct g-C_3N_4 Ternary Composite for Photocatalytic Green Hydrogen Production

Muhammad Tahir*
Chemical and Petroleum Engineering Department, UAE University, P.O. Box 15551 Al Ain, United Arab Emirates
Corresponding Author Email Address: muhammad.tahir@uaeu.ac.ae

INTRODUCTION

Adhering to UN sustainable development goals involves reducing greenhouse gas emissions and promoting clean energy production. Hydrogen stands out as a viable clean energy source and photocatalysis is a promising technology which utilizes renewable solar energy for green hydrogen production. Recently, 2D layered structures and noble metal-free graphitic carbon nitride (g-C_3N_4) have gained popularity for their chemical stability and solar activity and their lower efficiency can be incorporated using various cocatalysts. MXenes have recently been used as co-catalysts for photocatalytic hydrogen evolution with semiconductors such as g-C_3N_4 with the terminal functional group (-O, -OH, -Cl, and -F) have gained significant consideration [1]. Titanium carbide (Ti_3C_2) is a typical MXenes material with an accordion-like form, good conductivity, wide specific area, hydrophilicity, and great absorption of visible light [2]. The efficiency of Ti_3C_2/g-C_3N_4 can be further increased by producing TiO_2 NPs and coupling with metals like nickel as a co-catalyst[3]. In this work, 2D Ti_3C_2F MXenes with in-situ grown TiO_2 to construct Ni/g-C_3N_4/Ti_3C_2@TiO_2 S-scheme heterojunction loaded with single atom Ni was designed and tested for enhancing photocatalytic green H_2 production.

EXPERIMENTAL

The graphitic carbon nitride was synthesized using melamine as a precursor by heating it at 550 ºC for two hours followed by ultrasonication to get a 2D layered structure. On the other hand, Ti_3C_2 with in-situ grown TiO_2 quantum dots were synthesized by using HF etching of Ti_3AlC_2 under a controlled environment of time, temperature and oxygen. The heterojunction of Ti_3C_2@TiO_2 with g-C_3N_4 was developed through an ultrasonic approach followed by a self-assembly approach to attach nickel to construct the final composite. The materials were characterized using various characterization techniques to identify phase structure, morphology and visible light absorbance. All the experiments of hydrogen production were conducted using a slurry phase continuous photoreactor system.

RESULTS AND DISCUSSION

Fig. 1 (a) shows the morphology of Ni-Ti_3C_2@TiO_2/g-C_3N_4, in which, a good interface interaction of all the materials could be observed. The TEM results in Fig. 1 (b) further confirm the existence of all the components with their good distribution. The performance of the pure and the composite materials was further conducted in a slurry photoreactor under visible light and the results are presented in Fig. 1 (c). It could be seen that when Ti_3C_2 was coupled with g-C_3N_4, hydrogen production was significantly increased. However, a tremendous increase in H_2 production was observed when Ni as a cocatalyst was added to the composite. This significant improvement was due to the synergistic effect, which provides more active sites, enables more visible light absorbance and promotes charge carrier separation [4].

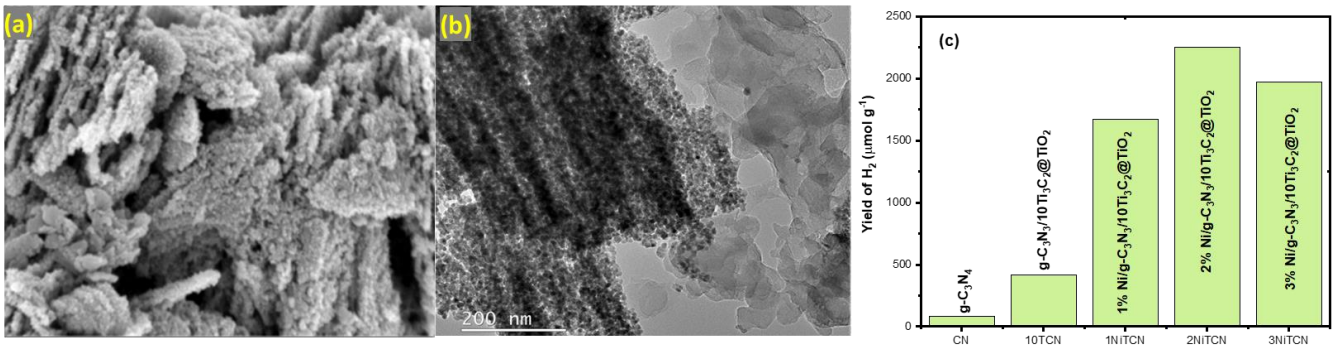

Fig. 1 (a) SEM image of Ni-Ti_3C_2@TiO_2/g-C_3N_4, (b) TEM image of composite, (c) photocatalytic activity of g-C_3N_4, Ti_3C_2/g-C_3N_4 and Ni-loaded Ti_3C_2/g-C_3N_4 composite for hydrogen production.

CONCLUSION

Utilizing an HF-etching-assisted ultrasonic approach, we successfully created the highly efficient Ni-Ti_3C_2@TiO_2/g-C_3N_4. The inclusion of Ti_3C_2 and Ni as cocatalysts shows promise in maximizing hydrogen production. The in-situ grown TiO_2 nanoparticles were promising to construct S-scheme heterojunction, resulting in significantly H_2 production.

REFERENCES

1. Tahir, M.,. *Chem. Eng. J.* **2023,** *476*.
2. Zhu, X.; Pan, Z.; Lu, W., *Int. J. Hydrogen Energy* **2023,** *48* (69), 26740-26756.
3. Tang, R.; Wang, H.; Dong, X.; Zhang, S.; Zhang, L.; Dong, F., *J Colloid Interface Sci* **2023,** *630* (Pt B), 290-300.
4. Tahir, B.; Tahir, M.; Kumar, N.,. *Int. J. Hydrogen Energy* **2023,** *48* (41), 15504-15521.

Collagen/Chitosan Membranes for PEM Fuel Cell Application

Amaal Abdulraqeb Ali[1], Muhammad Tawalbeh[2*], and Amani Al-Othman[3]
[1]Department of Chemical and Biological Engineering, American University of Sharjah, UAE
[2*]Sustainable and Renewable Energy Engineering Department, University of Sharjah, UAE
[3]Department of Chemical and Biological Engineering, American University of Sharjah, UAE

INTRODUCTION

Proton exchange membrane fuel cells (PEMFCs) are promising and sustainable alternatives to the finite and environmentally incompatible energy sources such as fossil fuels [1]. However, PEMFCs are limited by the high cost and inadequate performance at high temperatures of their gold standard proton exchange membrane (PEM), Nafion. Therefore, although highly conductive and chemically stable, there is an urgent need to replace Nafion [2]. This study reports the development of a PEM based on the sustainable natural, marine polymers collagen and chitosan modified with the highly conductive and sustainable ionic liquids (ILs). The proton conductivity of the developed membranes was evaluated and compared to those of Nafion and other natural polymer PEMs.

EXPERIMENTAL/THEORETICAL STUDY

The membranes were prepared using the solution casting procedure in which 0.1 g collagen was mixed with 0.1 g chitosan in 3% acetic acid at 45ºC for 30 mins. The additive, IL ([DEMA][OMs]), was then added to the solution in the desired amount and left mixing for 1 hour at 45ºC. The solution was poured into a petri dish and left to dry at 45ºC. The proton conductivity of the formed membrane was then evaluated using electrochemical impedance spectroscopy (EIS).

RESULTS AND DISCUSSION

While the amount of collagen and chitosan were fixed at 0.1 g each, the amount of IL incorporated was increased gradually from 0.1 g to 0.5 g with 0.1 increments. As expected, with the increase in IL content, the conductivity increased from 2.4×10^{-5} S/cm for the pure collagen/chitosan to 5.8×10^{-3} S/cm for the collagen/chitosan membrane with the highest IL content as shown in Fig. 1 below. Compared to Nafion, the collagen/chitosan/IL membrane had comparable conductivity to Nafion 212 but lower than Nafion 117. The collagen/chitosan/IL also had comparable or higher conductivity than other natural polymer-based PEMs in the literature as shown in Table 1.

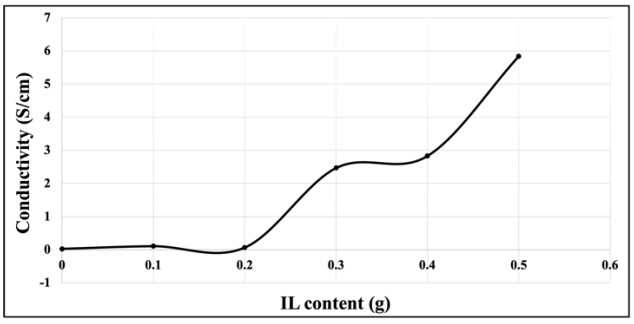

Fig. 1 Effect of IL content of the conductivity of the collagen/chitosan membranes

Table 1. Comparison of conductivities of collagen/chitosan/0.5 g IL with Nafion and other natural polymer PEMs

Composition	Conductivity (S/cm)	Ref
Collagen/chitosan/ 0.5 g IL	5.8×10^{-3}	This study
Chitosan/MoS2 & chitosan/[DEMA][OMs]	2.18×10^{-3} – 2.92×10^{-3} 2.53×10^{-3} – 11.05×10^{-3}	3,4
Nafion 212 and 117	6.94×10^{-3} and 9.8×10^{-2}	3,5

CONCLUSION

Sustainable PEMs can be developed based on marine collagen and chitosan. To compensate for the membrane's low conductivity, the sustainable and high conductive IL is incorporated. Incorporating IL increased the conductivity proportionally to IL content. The obtained conductivities were comparable to some types of Nafion and other natural polymer-based PEMs.

REFERENCES

1. Alekseenko et al..*Appl Surf Sci* **631**, 157539 (2023).
2. Okonkwo et al. *Int J Hydrogen Energy*. **46** 27956–27973.
3. Divya et al. *Carbohydr Polym* **208**, 504–512 (2019).
4. Hassan et al *Int J Hydrogen Energy* **53**, 592–601 (2024).
5. Munavalli et al. *Polymer (Guildf)* **142**, 293–309 (2018).

Lignin/Nanocellulose composite membranes for polymer electrolyte membrane fuel cells

Muhammad Tawalbeh[1*], Wessam Nimir[2], Amani Al-Othman[2], and Fares Almomani[3]
[1*]Sustainable and Renewable Energy Engineering Department, University of Sharjah, UAE
[2]Department of Chemical Engineering, American University of Sharjah, Sharjah, UAE
[3]Department of Chemical Engineering, Qatar University, Qatar

INTRODUCTION

Proton exchange membrane fuel cells (PEMFCs) are clean energy devices that convert chemical energy directly into electrical energy through electrochemical reactions. The performance of PEMFCs is heavily reliant on the membranes, which are essential for facilitating proton transport and maintaining gas separation to ensure optimal energy conversion efficiency[1]. Recently, the utilization of biopolymer materials in membranes for PEMFCs has become increasingly attractive due to their biocompatibility, renewability, and tunable properties[2]. Hence, in this study, lignin and nanocellulose were investigated for high-temperature fuel cell applications. They were synthesized using the gel casting technique, with polyvinylidene fluoride serving as a supporting matrix. The proton conductivity was measured at both room temperature and high temperature. In addition, water uptake and thermal stability were evaluated.

EXPERIMENTAL/THEORETICAL STUDY

Initially, a 25 wt.% PVDF/DMAC solution was prepared by blending PVDF and DMAC for 30 minutes at 60°C. Then, varying amounts of lignin, ranging from 4 to 24 wt.%, were added. After that, nanocellulose was introduced in different mass percentages, ranging from 9 to 37 wt.%. The mixture was then stirred at room temperature for around 10 minutes. Finally, the solution was cast onto a glass petri dish and dried in the oven for one hour at 85°C. The synthesized membranes were then peeled off and stored in plastic zipper bags for further characterization.

RESULTS AND DISCUSSION

The lignin membrane has shown a proton conductivity of 6.08×10^{-3} S/cm at 16 wt.% at room temperature. However, the introduction of 22 wt.% of nanocellulose has led to a tenfold increase in proton conductivity (1.2×10^{-2} S/cm) by enhancing proton pathways as can be seen in Figure 1. The membranes exhibited a slight decrease in proton conductivity (10^{-3} S/cm) at 150°C, indicating notable thermal stability and improved water retention. In addition, TGA data showed that the membranes are thermally more stable by maintaining ~ 90% of their weight at temperatures higher than 300◦C.

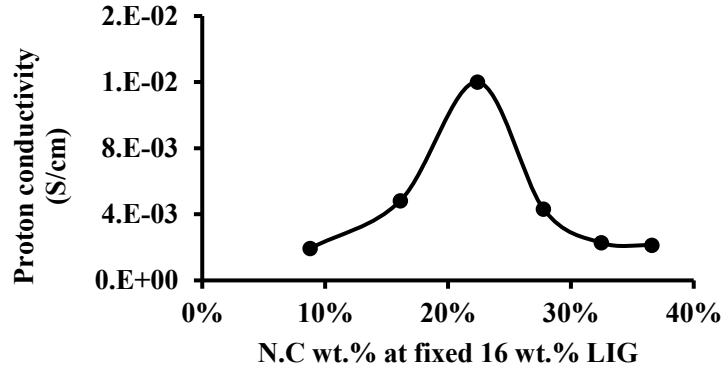

Figure 1: proton conductivity of PVDF/16 wt. LIG membrane at different nanocellulose mass percentages.

CONCLUSION

Lignin was integrated into the PVDF matrix at varying mass ratios, followed by subsequent modification of the membranes with nanocellulose. The addition of nanocellulose significantly enhanced the proton conductivity of lignin membranes by a factor of ten, attributed to the augmentation of hydrogen transfer pathways within the membrane matrix. The highest proton conductivity, reaching 1.2×10^{-2} S/cm, was attained with the incorporation of 22 wt.% nanocellulose.

REFERENCES

1. M. M. Tellez-cruz et al., “Polymers. MDPI., pp. 1-45, 3064, (2021)
2. A. J. Samaniego et al., “Green Chem. Lett. Rev., 15:1, 251-273 (2022)

Proton Conductivity Studies of H-ZSM-5 /PVDF Composite Membranes for PEM Fuel Cells

Muhammad Tawalbeh[1*], Ahmad Ka'ki[2], Amani Al-Othman[2], and Fares Almomani[3]
[1*]Sustainable and Renewable Energy Engineering Department, University of Sharjah, UAE
[2]Department of Chemical Engineering, American University of Sharjah, Sharjah, UAE
[3] Department of Chemical Engineering, Qatar University, Qatar

INTRODUCTION

Proton exchange membrane fuel cells (PEFMCs) are electrochemical devices that convert chemical energy into electricity. The performance of a PEMFC is usually determined by the efficiency of its polymer membrane (PEM) as it plays a crucial role in the overall functioning of the fuel cell. The most important role of PEM is to facilitate the proton transfer between the electrodes[1]. In this work, Nano H-ZSM-5 zeolite with Si/Al ratio of 100 along with two different ionic liquids were used as proton conductors[2]. The additives were combined with polyvinylidene fluoride as the polymer matrix. The proton conductivity and water uptake of the synthesized membranes were evaluated.

EXPERIMENTAL/THEORETICAL STUDY

The 10 wt.% PVDF solution was prepared by mixing PVDF and DMSO for 30 minutes at 60℃. Then, different amounts of zeolite ranging from 5 wt.% to 100 wt.% were mixed with 8 wt.% to 24 wt.% of ionic liquids for about 10 minutes at room temperature. Next, the two mixtures were mixed for about 5 minutes at room temperature. Finally, the mixture was casted slowly over a glass petri dish, then dried for around 5 hours at 85℃. The prepared membrane was then peeled off and kept in a plastic bag for further investigation.

RESULTS AND DISCUSSION

The amounts of both ionic liquids were fixed at 8 wt.% while H-ZSM-5 zeolite content was varied from 5-25 wt.%. As it can be noticed from Figure 1 that the membrane with IL1 gave the highest proton conductivity at 5 wt.% of H-ZSM-5 zeolite. The conductivity is enhanced by one order of magnitude compared to the (PVDF + 8% IL1), from 1.19×10^{-3} S/cm to 3.91×10^{-2} S/cm. The addition of IL2 gave the highest proton conductivity at 10 wt.% of H-ZSM-5 zeolite which is higher by 30% compared to the (PVDF + 8% IL2) membrane. Moreover, both ILs gave higher proton conductivity than the pristine PVDF with no additives.

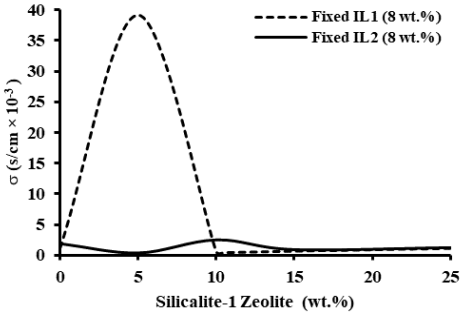

Fig. 1 Effect of H-ZSM-5 zeolite content on the conductivity of the reference membrane at fixed 8 wt.% of IL1 and IL2.

CONCLUSION

H-ZSM-5 was incorporated into the PVDF polymer matrix in different compositions. The membranes were modified with two hydrophilic ionic liquids. It was found that increasing H-ZSM-5 zeolite content caused a noticeable drop in the proton conductivity due to particle agglomeration. Moreover, both ionic liquids seemed to enhance the proton conductivity with IL1 giving the highest value of 3.91×10^{-2} S/cm at 5 wt.% H-ZSM-5 zeolite content.

REFERENCES

References must be numbered. Keep the same style.
1. E. Qu et al., J. Power Sources, 533, 231386, (2022)
2. Y. Wang et al., "Polym. Compos., 93, 223–284 (2023)

Chitosan doped membranes for electrochemical devices

Naima Naffati[1]*, Fátima C. Teixeira[1], António P. S. Teixeira[2], C. M. Rangel[1]*
[1] Laboratório Nacional de Energia e Geologia, I.P., Lisboa, Portugal.
*carmen.rangel@lneg.pt, naima.naffati@lneg.pt
[2] Departamento de Ciências Médicas e da Saúde, ESDH & LAQV- REQUIMTE, IIFA, Universidade de Évora, Évora, Portugal

INTRODUCTION

The development of new proton exchange membrane (PEM) for electrochemical devices, such as fuel cells and electrolyzers, have attracted researcher's attention in the pursuit for more sustainable and cost-effective technologies for clean energy production, being extensive those for CO_2 reduction and conversion[1,2]. To this end, in the present work, new modified chitosan (CS) membranes doped with ionic liquids (ILs) were developed to perform as PEM at those electrochemical devices, as an alternative to widely used commercial Nafion, with several advantages such as wider availability, lower cost, biodegradability and thermal stability. These modified membranes for use in electrochemical devices are expected to show suitably enhanced ion conductivity and also improved mechanical strength associated to a decrease in water uptake.

EXPERIMENTAL

The chitosan powder (CS) (medium molar mass and 75–85% deacetylation degree) and glycerol (Gly), used as a plasticizer agent, were purchased from Sigma-Aldrich. Membranes were prepared by casting chitosan/IL solutions with 50% and 33% of [EMIM][OTf], 33% of [EMIM][NTf_2], and 10% of [MIMH][HSO_4] (Fig.1). Characterization was done by ATR-FTIR spectroscopy (Perkin Elmer spectrometer) and proton conductivity was evaluated by electrochemical impedance spectroscopy (EIS) (Solartron 1250 FRA), using a BekkTech conductivity cell under controlled temperature and relative humidity (RH) conditions.

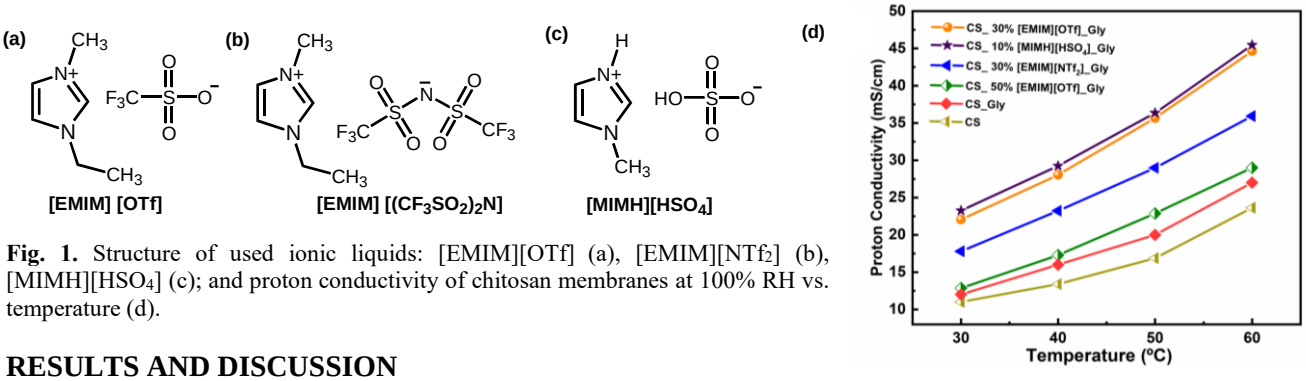

Fig. 1. Structure of used ionic liquids: [EMIM][OTf] (a), [EMIM][NTf_2] (b), [MIMH][HSO_4] (c); and proton conductivity of chitosan membranes at 100% RH vs. temperature (d).

RESULTS AND DISCUSSION

New chitosan membranes were prepared by casting with the incorporation of ILs as dopants, and analyzed by ATR-FTIR. EIS assessment of the doped membranes indicated that the incorporation of IL modifies their proton conduction. At 100% RH, all doped membranes showed a significant increase in the proton conductivity, which rises with the increase of temperature, compared to the pristine CS membrane. The best proton conductivity, 45 mS/cm, was observed for membrane CS_[MIMH][HSO_4]_Gly with 10 wt% of loading at 60 ºC (Fig. 1).

CONCLUSION

New modified chitosan membranes were obtained by casting with ILs as dopants, showing higher proton conductivity than pristine chitosan membrane at 100% RH. Results confirm that these membranes are a promising material for electrochemical devices.

REFERENCES

1. N. Naffati, M. Fernandes, V.Z. Bermudez, M.F. Nsib, Y. Arfaoui, A. Houas, J.L. Faria, C.G. Silva, M.M. Silva, Iran. Polym. J. 31, 1197-1208 (2022).
2. F.C. Teixeira, A.P.S. Teixeira, C.M. Rangel, Renew. Energy 196, 1187-1196 (2022).

ACKNOWLEDGMENTS

This work was financed by national funds through FCT – Fundação para a Ciência e a Tecnologia, I.P., within the scope of the projet PTDC/EQU-EPQ/2195/2021-CO2RED, and LAQV-REQUIMTE, project UIDB/50006/2020 and UIDP/50006/2020.

Ru modified MCM-41 mesoporous material extrudate shaped catalysts for synthesis of menthol: Design of catalytic active sites, physico-chemical characterizations and reaction mechanism

[1]Zuzana Vajglova, [*1]Narendra Kumar, [2]Markus Peurla, [1]Kari Eränen, [1]Päivi Mäki-Arvela, [1]Dmitry Yu. Murzin

[1]Åbo Akademi University, Laboratory of Industrial Chemistry and Reaction Engineering, Faculty of Science and Engineering, Henriksgatan 2, FI-20500 Turku/Åbo, Finland,

[2]Institute of Biomedicin, FI-20500 Turku, Finland, presenting author, e-mail: narendra.kumar@abo.fi

Shaped heterogeneous acidic and metal modified catalysts in the forms of extrudates, sphere, stars and cylinders are applied in several petro-chemicals, fine and speciality chemicals. Separation of heterogeneous catalysts from liquid phase reactions, regenerations and reuse are some of the important advantages as compared to the use of catalytic materials in powder forms. Menthol is one of the most valuable aroma compound used in pharmacueticals, medicinial molecules, drug discovery and additives in food ingredients. The demand for industrial production of menthol using green process technology is increasing. Synthesis of menthol from citronella using metal modified heterogeneous catalysts is the most efficient, environmental friendly and productive technology. Catalytic active metals such as Ru, Pt, Pd, Cu, Zr, Ni, Zn and Ir supported on Al_2O_3, SiO_2, SBA-15 and H-Beta zeolite have been studied for production of menthol from citronellal. Na-MCM-41 mesoporous material was synthesized in an autoclave and transformed to H-MCM-41 by ion-exchange with NH_4Cl solution for 24 h. NH_4-MCM-41 was washed with distilled water, dried at 100 ^{0}C and calcined at 450 ^{0}C in a muffale oven to obtain H-MCM-41 powder catalyst. H-MCM-41extrudate was prepared by mixing powder H-MCM-41 with colloidal silica binder Bindzil-50/80. 2 wt % Ru modified H-MCM-41 extrudate catalyst was prepared using $RuCl_3$ aqueous solution by evaporation impregnation method. The extrudates were dried at 100 ^{0}C and calcined at 400 ^{0}C for 3 h. The physico-chemical characterizations of the extrudate shaped catalysts were carried out using TEM (Figure 1), SEM-EDS (Figure 2), XRD, N_2-Physisorption and FTIR-Pyridine. Synthesis of menthol from citronellal, isopulegol and citronellal experiments over H-MCM-41and Ru-H-MCM-41 extrudate shaped catalysts were carried out for 3 h in a fixed-bed reactor at reaction temperature 70 ^{0}C and pressure 10 bar of H_2. The highest conversion of citronellal and yield of methanol was obtained for Ru-H-MCM-41 extrudate catalysts. Catalytic activity results in menthol synthesis and characterization of Ru-MCM-41 extrudate shaped catalysts will be discussed during the presenation in conference.

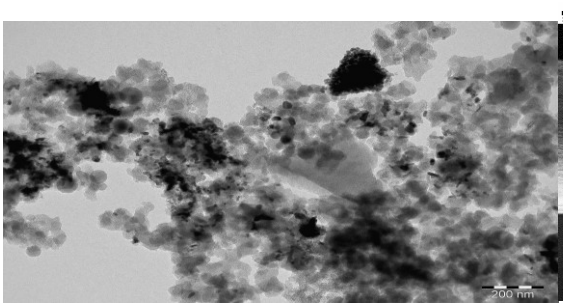

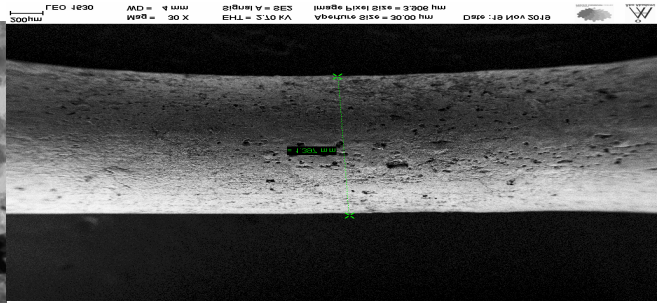

Figure 1. TEM Ru-MCM-41 extrudate. Figure 2. SEM Ru-MCM-41 extrudate.

Design and Fabrication of One-Dimensional Nanostructured Nickel Suboxides for Improved Oxygen Evolution Reaction

Nastaran Farahbakhsh[1,2], M.H. Enayati[2], S.M. Monirvaghefi[2], Sina Hejazi[1,3] , Majid Shahsanaei[1,2], Patrick Hartwich[1], Shiva Mohajernia[3], Manuela S. Killian[1*]

[1] Chemistry and Structure of novel Materials, University of Siegen, Germany, presenting author, corresponding author (manuela.killian@uni-siegen.de)
[2] Department of Materials Engineering, Isfahan University of Technology, Isfahan, Iran
[3] Department of Chemical and Materials Engineering, University of Alberta, Canada

INTRODUCTION

Defect engineering is a promising approach in catalysis research, as it can significantly enhance the specific activity and selectivity of catalytic reactions. Anodic NiO was shown to yield enhanced potential for photocatalytic applications compared to nanoparticle NiO electrodes[1]. This study uses a two-step electrochemical anodization method on nickel foil substrates to fabricate highly porous one-dimensional nanostructured nickel suboxides and evaluates the OER potential for electrodes prepared under varying annealing conditions.

EXPERIMENTAL

By applying defect engineering through annealing in different environments (Air, Ar, ArH_2 at 450°C for 12 hours), a high defect density can be created (as revealed by Mott–Schottky and X-ray photoelectron spectroscopy), leading to improved electrocatalytic activity for the oxygen evolution reaction (OER).

RESULTS AND DISCUSSION

It was found that the nanostructured NiO/NiOOH, obtained through annealing in an ArH_2 environment, shows high-efficiency electrocatalysis for OER. The nanostructured NiO/NiOOH exhibited low overpotentials (291 mV at 10 mA cm^{-2}) and maintained excellent stability over 1000 cycles. Furthermore, the electrochemical analysis, coupled with X-ray photoelectron spectroscopy (XPS), X-Ray diffraction analysis (XRD), and field emission scanning electron microscopy (FESEM), revealed that the induced structural evolution of the electrochemically active sites and defects resulted in a significant improvement of the electrocatalytic activity. Overall, the most optimized NiO_x electrode exhibited a Tafel slope of 67.7 mV dec^{-1} in 1.0 M KOH, which is significantly lower than that of conventional reference RuO_2 electrodes (with a slope of 116.2 mV dec^{-1}) , reference Ni foil (229.6 mV dec^{-1}) and NiO powder (262.9 mV dec^{-1}).

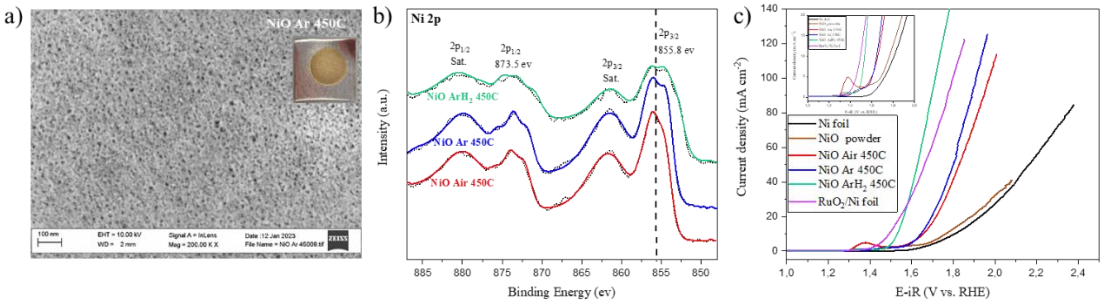

Fig. 1 a) Anodic NiO nanosponge annealed in Ar environment, SEM and optical image; b) XPS showing differences in the Ni oxidation states upon annealing in various environments; c) LSV polarization curves of anodic NiO annealed in different conditions, RuO_2/Ni foil, blank Ni foil and NiO powder (as references) in 1.0 M KOH at a sweep rate of 10 mV s^{-1}.

CONCLUSION

These findings demonstrate the capability of defect engineering and one-dimensional nanostructured nickel suboxides in developing high-performance electrocatalysts for water-splitting applications and can potentially be combined with existing NiO_2 base electrode technologies for alkaline electrocatalysis.

REFERENCES

1. U. Sultan, et al., A High-Field Anodic NiO Nanosponge with Tunable Thickness for Application in p-Type Dye-Sensitized Solar Cells, ACS Appl. Energy Mater. 3 (2020) 7865. https://doi.org/10.1021/acsaem.0c01249.

ACKNOWLEDGMENTS

DFG KI2169/2-1 and HYT Siegen are acknowledged for funding

Design and Fabrication of One-Dimensional Nanostructured Nickel Suboxides for Improved Oxygen Evolution Reaction

Nastaran Farahbakhsh[1,2], M.H. Enayati[2], S.M. Monirvaghefi[2], Sina Hejazi[1,3] , Majid Shahsanaei[1,2], Patrick Hartwich[1], Shiva Mohajernia[3], Manuela S. Killian[1*]

[1] Chemistry and Structure of novel Materials, University of Siegen, Germany, presenting author, corresponding author (manuela.killian@uni-siegen.de)
[2] Department of Materials Engineering, Isfahan University of Technology, Isfahan, Iran
[3] Department of Chemical and Materials Engineering, University of Alberta, Canada

INTRODUCTION

Defect engineering is a promising approach in catalysis research, as it can significantly enhance the specific activity and selectivity of catalytic reactions. Anodic NiO was shown to yield enhanced potential for photocatalytic applications compared to nanoparticle NiO electrodes[1]. This study uses a two-step electrochemical anodization method on nickel foil substrates to fabricate highly porous one-dimensional nanostructured nickel suboxides and evaluates the OER potential for electrodes prepared under varying annealing conditions.

EXPERIMENTAL

By applying defect engineering through annealing in different environments (Air, Ar, ArH_2 at 450°C for 12 hours), a high defect density can be created (as revealed by Mott–Schottky and X-ray photoelectron spectroscopy), leading to improved electrocatalytic activity for the oxygen evolution reaction (OER).

RESULTS AND DISCUSSION

It was found that the nanostructured NiO/NiOOH, obtained through annealing in an ArH_2 environment, shows high-efficiency electrocatalysis for OER. The nanostructured NiO/NiOOH exhibited low overpotentials (291 mV at 10 mA cm^{-2}) and maintained excellent stability over 1000 cycles. Furthermore, the electrochemical analysis, coupled with X-ray photoelectron spectroscopy (XPS), X-Ray diffraction analysis (XRD), and field emission scanning electron microscopy (FESEM), revealed that the induced structural evolution of the electrochemically active sites and defects resulted in a significant improvement of the electrocatalytic activity. Overall, the most optimized NiO_x electrode exhibited a Tafel slope of 67.7 mV dec^{-1} in 1.0 M KOH, which is significantly lower than that of conventional reference RuO_2 electrodes (with a slope of 116.2 mV dec^{-1}) , reference Ni foil (229.6 mV dec^{-1}) and NiO powder (262.9 mV dec^{-1}).

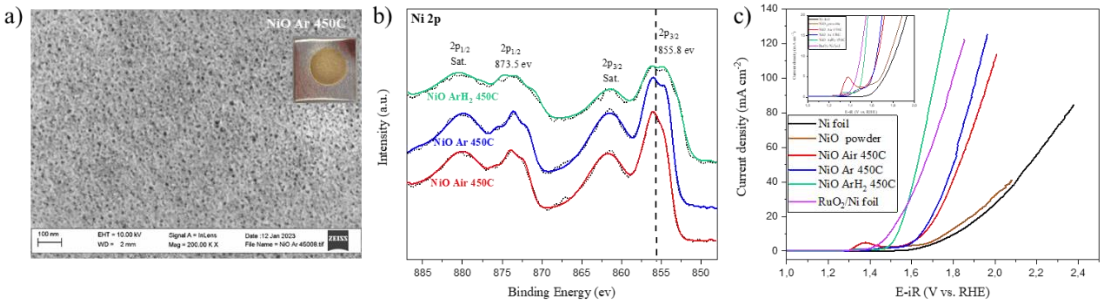

Fig. 1 a) Anodic NiO nanosponge annealed in Ar environment, SEM and optical image; b) XPS showing differences in the Ni oxidation states upon annealing in various environments; c) LSV polarization curves of anodic NiO annealed in different conditions, RuO_2/Ni foil, blank Ni foil and NiO powder (as references) in 1.0 M KOH at a sweep rate of 10 mV s^{-1}.

CONCLUSION

These findings demonstrate the capability of defect engineering and one-dimensional nanostructured nickel suboxides in developing high-performance electrocatalysts for water-splitting applications and can potentially be combined with existing NiO_2 base electrode technologies for alkaline electrocatalysis.

REFERENCES

1. U. Sultan, et al., A High-Field Anodic NiO Nanosponge with Tunable Thickness for Application in p-Type Dye-Sensitized Solar Cells, ACS Appl. Energy Mater. 3 (2020) 7865. https://doi.org/10.1021/acsaem.0c01249.

ACKNOWLEDGMENTS

DFG KI2169/2-1 and HYT Siegen are acknowledged for funding

Van der Waals Epitaxy-Assisted Growth of GaSb Nanowires on Graphene Monolayers

Nayeli Colin Becerril[1], José de Jesús Cruz-Bueno[1], Manolo Ramírez López[1], José Luis Herrera Pérez[1], Julio Mendoza Álvarez[2], Yenny Lucero Casallas Moreno[3*]
[1]UPIITA, National Polytechnic Institute, Mexico, presenting author
[2]Physics Department, Cinvestav, Mexico
[3*]Conahcyt-UPITA National Polytechnic Institute, Mexico, corresponding author (ycasallasm@ipn.mx)

INTRODUCTION

Semiconductor compounds from the antimonide family provide a good alternative to be applied in the fields of microelectronics and optoelectronics due to their electrical, structural, and optical properties, including high electron mobility and a direct band gap[1]. Recently, there has been an increased interest in improving the crystal quality of III-V semiconductors, leading to the study of coupling III-V materials alloys with 2D materials such as graphene (G)[2]. Highlighting the possible influence of graphene on the growth of nanowires of GaSb heterostructures, offering innovative perspectives for the design and fabrication of advanced optoelectronic devices[3].

EXPERIMENTAL/THEORETICAL STUDY

In this work, we employed the close space vapor transport (CSVT) technique to couple GaSb heterostructures onto graphene. GaSb films were deposited by CSVT for 10 min, at different temperatures from 510°C to 610°C, under a constant flow of H2. The substrates used were G/Si (111).

RESULTS AND DISCUSSION

The samples were characterized by Raman, scanning electron microscopy (SEM), and X-ray photoelectron spectroscopy (XPS).

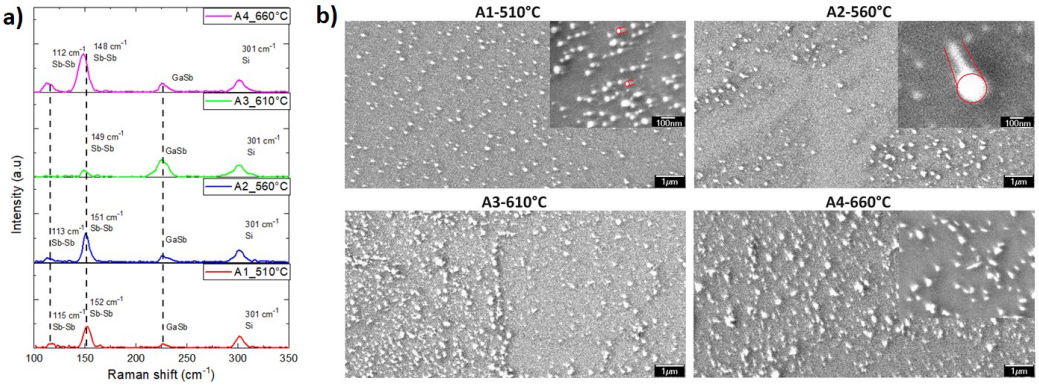

Fig. 1 a) Raman spectra and b) SEM of the GaSb/G/Si heterostructures at different temperatures.

Raman measurements confirmed the growth of GaSb on the mentioned substrates, evidencing the LO and TO phononic modes. Additionally, a cluster of GaSb islands on graphene, which could well be composed of nanocolumns were found by SEM.

CONCLUSION

It was possible to grow GaSb on G/Si (111) substrates with a technique different from conventional techniques. The development of this work will allow finding the optimal conditions to achieve the controlled growth of GaSb nanowires.

REFERENCES

1. Y.L. Casallas-Moreno et. al, Journal of Alloys and Compounds, 808, 151690 (2019)
2. Y. Alaskar et al, Adv. Funct. Mater., vol. 24, 42 (2014)
3. A. Mazid Munshi et. al, Nano Letters, 12, 9 (2012)

ACKNOWLEDGMENTS

To Conahcyt and IPN for financial support
(ANM) Advanced Nano Materials

Hydrogen detection and electrical properties of perovskite $TiSiO_4$ Schottky diode

[1]Lutfi Bilal Tasyurek, [2*]Necmettin Kilinc
[1]Depertment of Opticians, Malatya Turgut Ozal University, 44700 Malatya, Türkiye
[2]Department of Physics, Faculty of Science & Arts, Inonu University, 44280, Malatya, Türkiye

INTRODUCTION

$TiSiO_4$ perovskite is a promising potential material whose structural, electrical, mechanical and optical properties are under investigation[1] and whose sensor sensitivities have not been sufficiently investigated. Therefore, the results of hydrogen (H_2) sensing and electrical properties of $TiSiO_4$ perovskite will provide an important contribution to the literature for the investigation of other sensor applications of $TiSiO_4$ material.

H_2, is a renewable energy source and has various technological applications such as chemical production (petroleum refineries, ammonia production, fertilizer production, metal refining …), fuel cell technology to produce electricity, fuel for transportation, fuel for rocket engines, etc[2]. But, there are the some disadvantages of H_2 such as H_2 cannot be detected by human senses and H_2 is non-toxic, the lightest element, colorless, odorless, tasteless, flammable, and explosive above 4% concentrations in any ambience. Therefore the detection of H_2 is crucial and H_2 sensors are used for leak detection, safety issue, and real-time quantitative analysis[3,4]. The present study focus on fabrication of $TiSiO_4$ perovskite Schottky diode for H_2 sensor application.

EXPERIMENTAL/THEORETICAL STUDY

To fabricate of Pt/$TiSiO_4$/p-Si devices, a commercially available p-Si wafer was used and RCA1 cleaning procedure was applied[5]. The matte surface of the cleaned p-Si wafer was coated with 100nm aluminum (Al) metal by DC sputter method as a back contact. $TiSiO_4$ was coated on the glossy surface of the p-Si wafer by RF sputter method as an interface. Finally, platinum (Pt) point contacts for electrical measurements were coated by DC sputtering. I-V and C-V measurements of the fabricated Pt/$TiSiO_4$/p-Si devices were performed depending on tempereature and H_2 gas. Figure 1a shows the schematic diagram of the fabricated Pt/$TiSiO_4$/p-Si device.

RESULTS AND DISCUSSION

Figure 1b shows the I-V characteristics of the Pt/$TiSiO_4$/p-Si device measured in the range 300-473 K in 20 K steps. As can be seen from the graphs, the Pt/$TiSiO_4$/p-Si device exhibited Schottky behaviour at low temperatures near RT. However, it exhibited ohmic behavior as the temperature increased. Figure 1c shows the H_2 sensor tests of the Pt/$TiSiO_4$/p-Si device. The I-V variations of the device at room temperature in dry air and 1% H_2 flow are given. As can be seen from the figure, the Pt/$TiSiO_4$/p-Si device showed sensitivity to H_2 gas.

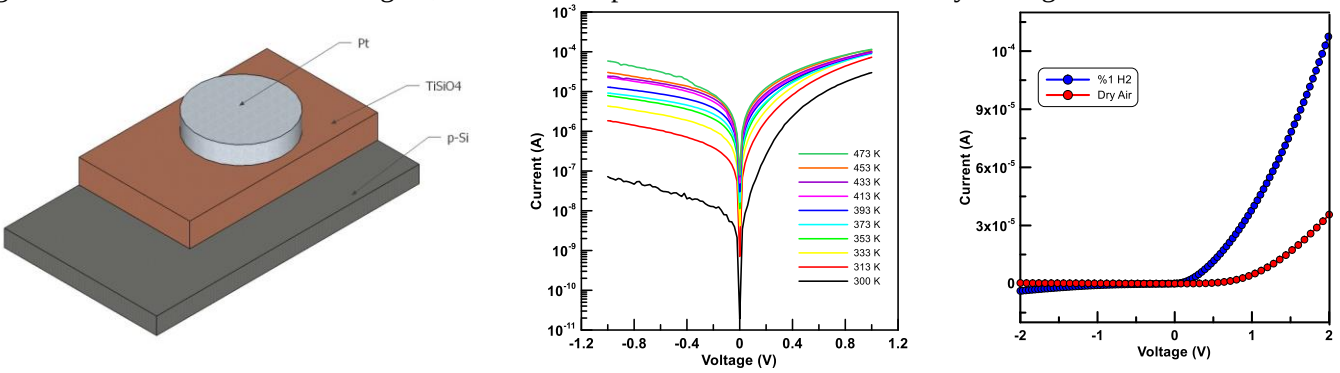

(a) **(b)** **(c)**

Figure 1. (a) Cross-sectional representation of Pt/TiSiO4/p-Si device, T **(b)** emperature dependent changes of I-V graphs with 20 K steps between 300-473 K and **(c)** Variation of I-V graphs at room temperature, under dry air and 1% H_2 flow

CONCLUSION

I-V measurements showed Schottky behavior at low temperatures and ohmic behavior as the temperature increased. According to the gas tests, the device showed sensitivity to H_2 gas.

REFERENCES

1. H. Liu, Z.-T. Liu, J. Ren, Q.-J. Liu, Solid State Communications, 251, 43-49 (2017)
2. L.M. Das, Hydrogen Energy: Production, Safety, Storage and Applications, Wiley, 2023.
3. O. Sisman, M. Erkovan and N. Kilinc, in Towards Hydrogen Infrastructure (Elsevier, 2024), pp. 275-314.
4. T. Hubert, L. Boon-Brett, G. Black and U. Banach, Sensors and Actuators B-Chemical 157 (2), 329-352 (2011)
5. L.B. Taşyürek, Ş. Aydoğan, M. Sevim, Z. Çaldıran, J Alloy Compd, 914, 165140 (2022).

ACKNOWLEDGMENTS

This study was partially funded by TUBİTAK (Project Number: 121C433) and Inonu University (Project Number: FBA-2024-3421).

Fast response and highly sensitive hydrogen sensing of Pt-Pd alloy thin films on flexible substrate

Necmettin Kilinc
Department of Physics, Faculty of Science & Arts, Inonu University, Malatya, Türkiye

INTRODUCTION

Hydrogen is the lightest element, the most abundant in the universe and a future clean energy source[1]. Additionally, hydrogen is used in a wide range of industrial applications, including chemical, glass, plastic, food, transportation, and semiconductor industries. On the other hand, hydrogen has a lower explosion limit of 4% in air and it is colorless, odorless, and tasteless and cannot be detected by the human senses. Therefore, accurate and fast hydrogen detection is very important. Hydrogen sensors are used for especially safety issues, real-time quantitative analysis and leak detection during the use of hydrogen in various industrial applications[2,3]. Among the various hydrogen sensors depending on the physico-chemical detection mechanism, the resistive metallic hydrogen sensor is one of the best performing. In general, palladium (Pd), platinum (Pt), and their alloy are used as a sensitive materials for metallic resistive hydrogen sensors[4]. In this study, the structural and resisitive hydrogen sensing properties of Pt-Pd alloy thin films prepared on a flexible substrate at different ratios were investigated.

EXPERIMENTAL STUDY

The Pt_xPd_{1-x} (x =0.25, 0.50 and 0.75) thin films were prepared by using the co-sputtering technique from pure Pt and Pd onto a flexible polyamide substrate. The thicknesses of the films were approximately 2 nm and simultaneously measured with a QCM sensor from Inficon in the PVD system. Structural characterization of the film was done by scanning electron microscopy, Energy Dispersive X-ray spectroscopy (EDX) and X-ray photoelectron spectroscopy (XPS) techniques. Two silver electrodes are coated on the PtPd alloy films by using thermal evaporation system with a shadow mask to obtain resistive sensor devices. The hydrogen sensing properties of PtPd alloy thin films were tested depending on temperature, hydrogen concentration, and the alloy composition.

RESULTS AND DISCUSSION

Fig. 1a shows the schematic diagram of the sensor device. The sensor response of $Pt_{0.50}Pd_{0.50}$ alloy thin film at the 50°C for various hydrogen concentration is shown in Fig. 1b and the hydrogen exposure causes a decrease in the resistance for the measured concentration. This behavior is similar to pure Pt based resistive hydrogen sensor and could be explained with surface charge scattering phenomenon[4-6]. Fig. 1c shows the repeatability of PtPd alloy thin film sensors exposure to 1% hydrogen at 50°C. The hydrogen sensing properties PtPd alloy thin film depending on temperature, concentration and composition rate will be discussed in detail.

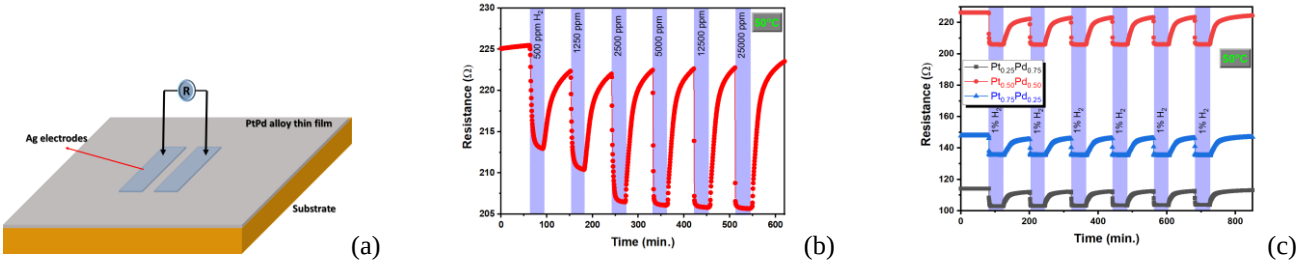

Fig. 1 A schematic diagram of the sensor device (a), sensor response of $Pt_{0.50}Pd_{0.50}$ sample (b) and the repeatability of all samples (c).

CONCLUSION

PtPd alloy thin film based resistive hydrogen sensor devices showed high sensitivity, fast response, low working temperature even at room temperature and could be used in leak detection applications.

Acknowledgment: This study was supported by Inonu University (P. no:FBA-2024-3421) for participating in the conference

REFERENCES

1. S. A. Sherif, D. Y. Goswami, E. L. Stefanakos and A. Steinfeld, Handbook of hydrogen energy. (CRC press, 2014)
2. O. Sisman, M. Erkovan and N. Kilinc, in Towards Hydrogen Infrastructure (Elsevier, 2024), pp. 275-314.
3. T. Hubert, L. Boon-Brett, G. Black and U. Banach, Sensors and Actuators B-Chemical 157 (2), 329-352 (2011)
4. N. Kilinc, Nanoscience and Nanotechnology Letters 5 (8), 825-841 (2013).
5. F. Yang, K. C. Donavan, S. C. Kung and R. M. Penner, Nano Lett 12 (6), 2924-2930 (2012).
6. N. Kilinc, J Mater Sci-Mater El 32 (5), 5567-5578 (2021).

A Loosely Bonded Polymer-A Better Host for Synthesis of Flexible Economical, Environment Benign and Easy to Handle Polymer-In-Salt Electrolyte (PISE)

Neelam Srivastava
Department of Physics (MMV Section), Banaras Hindu University, Varanasi-221005, India
neel@bhu.ac.in

INTRODUCTION

Since the inception, in 1970s, of polymer electrolytes, it has been recognized that low salt concentration polymer electrolytes (Salt-In-Polymer-Electrolytes-SIPEs), where the ion transport is through polymer segmental motion, have two limitations i) low cationic transport number and ii) slow ion transport. The formation of ion-pairs at high salt concentration puts a control on the highest possible salt concentration. In 1990s, Angell and coworker demonstrated that if the salt concentration is further increased beyond a threshold value these ion-pairs/clusters are connected throughout the lattice and then it leads to the change of ion-dynamics. Now the ion-transport is decoupled from polymer segmental motion resulting in ion diffusion through the ion-cluster. This leads to faster ion transport and improved cationic transference number. These materials are classified as Polymer-In-Salt-Electrolytes (PISEs). PISEs could not reach to commercial stage because of unavailability of good host which can accept required large amount of salt and keep it in dissociated form along with maintaining the flexible morphology required for device fabrication. Theoretically it has been predicted that the host with loosely bond chemical structure and having the possibilities of hydrogen bonding may be a good candidate. To address the problem of salt recrystallization, a new concept of adding the diluent is used to maintain a specific distance between aggregates. Another prevailing concept in the field of polymer electrolytes is stabilizing the water molecules in the electrolytes, it is an effort to have aqueous electrolyte type behavior in solid state, this concept is classified as 'Water-in-Polymer-Salt-Electrolyte' (WiPSE).

EXPERIMENTAL/THEORETICAL STUDY

Using the two concepts (addition of diluents and WiPSE) along with nature of starch-salt where the addition of salt breaks the starch (changing covalent bonds to hydrogen bonds i.e., enhancing loosely bonded structure), our group has developed a novel protocol to synthesize flexible, economical, ecofriendly and easy to handle PISE. High probability of hydrogen bonding in starch and salt also favors our selection of starch for PISEs synthesis. Adding up a novel step of exposing the synthesized PISE to high humidity (~99%) for long hours (~24 hours), the PISE behavior have been changed and now it is quite independent of ambient changes and its resistance is stabilized at lower value of resistance. Same protocol has been successfully used with many starches (namely arrowroot, rice, corn, potato, wheat etc.) with different sodium and magnesium salts.

RESULTS AND DISCUSSION

These PISE/WiPSE have low resistance (<5 Ω and sometimes going b below 1Ω), wide electrochemical stability window (>2.5V) and low resistance. They are economical and can be synthesized using a simple protocol. These PISE/WiPSE are successfully explored for supercapacitor fabrication and capacitance up to few hundreds of F/g with columbic efficiency above 97%.

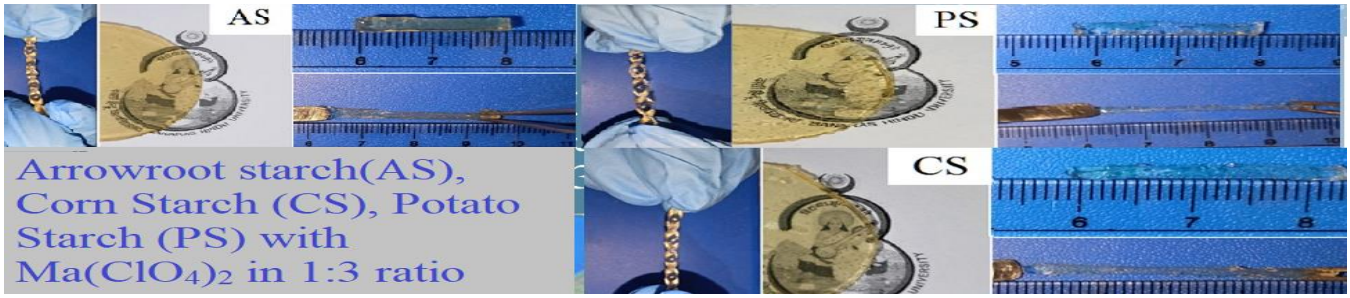

Raman Response of Gold Nanodisk Arrays

Neha Sardana (Sardana)[1*], Gaurav Pal Singh (Singh)[1], and Joerg Schilling (Schilling)[2]
[1*] Department of Metallurgical and Materials Engineering, Indian Institute of Technology Ropar, Rupnagar, 140001, India, presenting author, corresponding author (nsardana@iitrpr.ac.in)
[2] Centre for Innovation Competence SiLi-nano®, Martin-Luther-University of Halle-Wittenberg, Karl-Freiherr-von-Fritsch-Str. 3, 06120 Halle (Saale), Germany

INTRODUCTION

Periodic nanostructures are used to increase the Raman signal by electromagnetic hotspots created at the resonance modes, this technique is known as Surface enhanced Raman spectroscopy (SERS).

EXPERIMENTAL AND THEORETICAL STUDY

An optimal SERS substrate was selected among substrates of various periods fabricated using Laser interference lithography (LIL). Its practical use was tested by sensing various chemicals used in the agricultural sector. LIL was used to fabricate gold nanodisk arrays of varying periods on a glass substrate. The period to diameter ratio of the nanodisk arrays was close to 2 and the thickness was about 50 nm.

RESULTS AND DISCUSSION

The Raman response of nanodisks of varying periods was compared using the chemical Pyridine. The 300 nm period displayed the highest SERS enhancement among the LIL substrates. Experimental transmission measurements and their finite element method (FEM) simulations were performed to understand the optical response of the LIL substrates. The average enhancement factor of the 300 nm period substrate was calculated. The detection limit of various commercially used agrochemicals was tested on the optimal substrate.

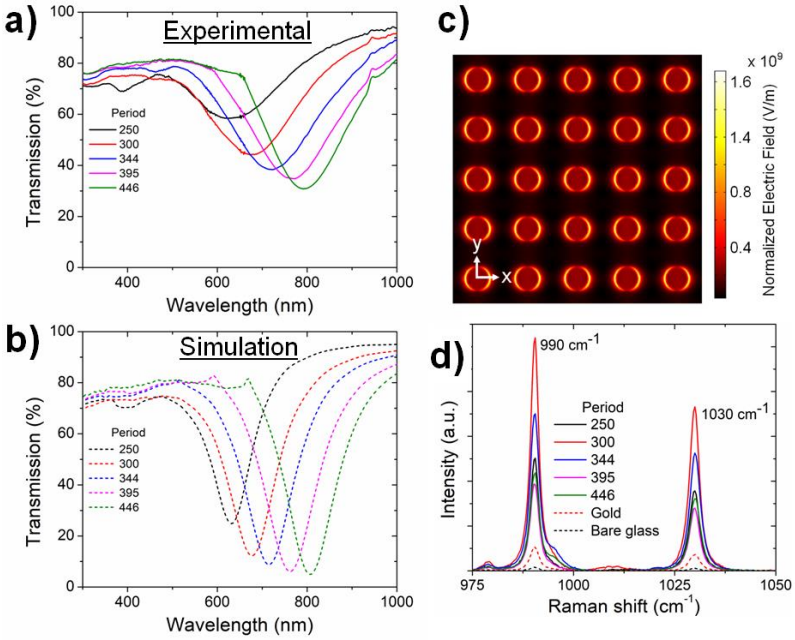

Fig. 1 (a) Experimental and (b) simulated transmission spectrum of the LIL substrates of various periods. (c) Simulated normalized electric field for the 300 nm period substrate at the resonance wavelength. (d) Response of the LIL substrates of various periods to the chemical Pyridine.

CONCLUSION

The 300 nm period substrate displayed the highest enhancement because of the vicinity of its plasmonic peak to the excitation source wavelength and also to the target molecule peak. To verify its practical use as a SERS substrate, the Raman response of varying concentrations of commercially used agrochemicals was measured on the optimal substrate.

ACKNOWLEDGMENTS

N. Sardana is thankful to Department of Science and Technology (DST), for funding through Scheme for Young Scientists and Technologists (SYST) SP/YO/2021/2098 grant.

SYNTHESIS OF THE SYSTEM SiO_2-Gd_2O_3-Eu_2O_3 AND RESEARCH OF THE ACID-BASE PROPERTIES, KINETICS OF PARTICLE FORMATION IN THE SYSTEM

Niftaliev S.I., Kuznetsova I.V., Tran Nhat Anh*

Abstract: The three-component systems SiO_2 : Gd_2O_3 : Eu_2O_3 can be used in medicine, catalysis, optics. For different applications it is necessary to characterize the surface properties of the synthesized solid phases. The surface properties can be investigated by different methods: IR-, UV- and visible spectroscopy, adsorption-chemical, the Hammett indicator adsorption method.

Purpose of work: Determine the kinetics of the synthesis of the SiO_2 : Gd_2O_3 : Eu_2O_3 system under tetraethoxysilane hydrolysis conditions in water, calculate the activation energy, and compare the effects of metal ion concentration on the formation of the SiO_2 : Gd_2O_3 : Eu_2O_3 system and researching acid-base properties of samples obtained from TEOS, europium and gadolinium nitrate solutions using different solvents: citric acid, ethanol.

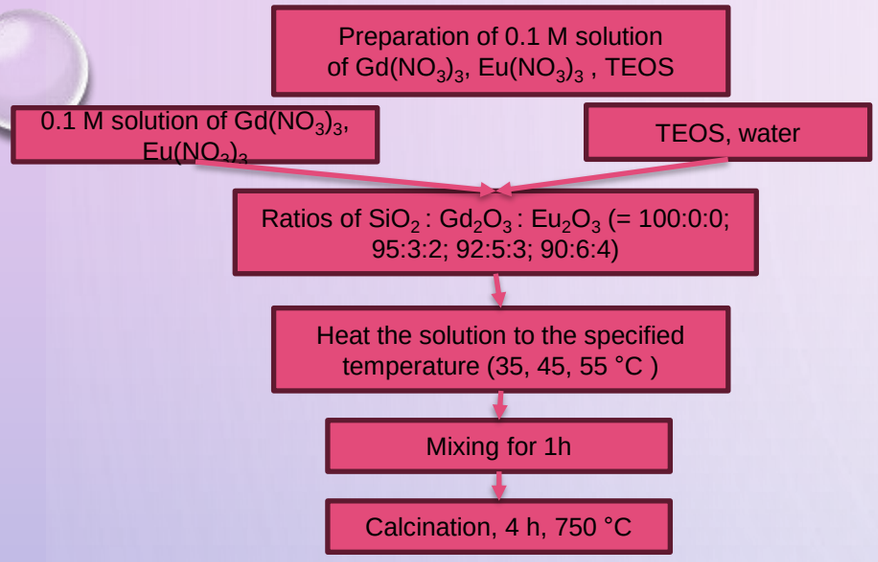

We calculated the activation energy of the hydrolysis process of the system for each ratio of components by the formula:

$$LnK_o = LnK_t - (\frac{E}{R}.\frac{1}{T})$$

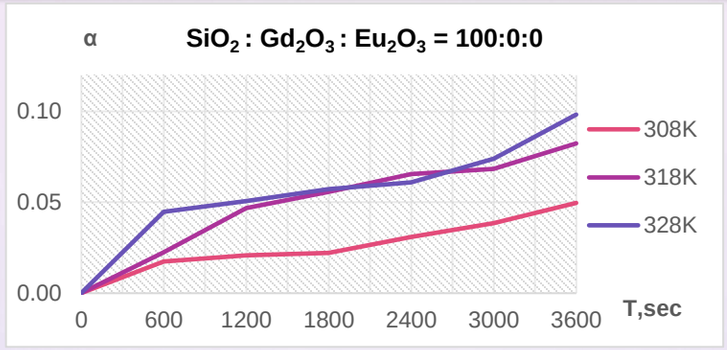

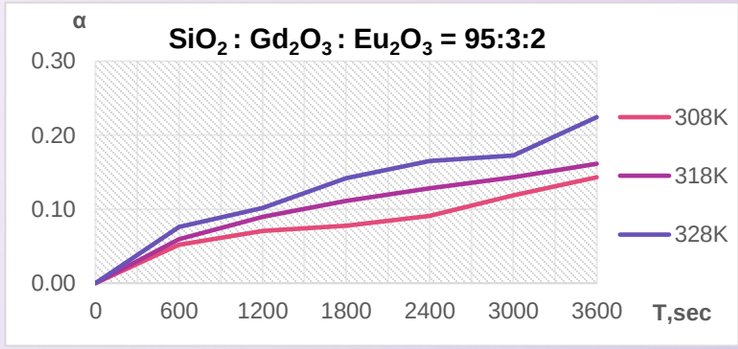

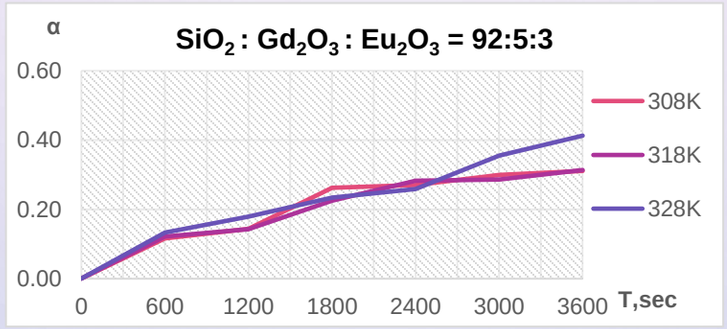

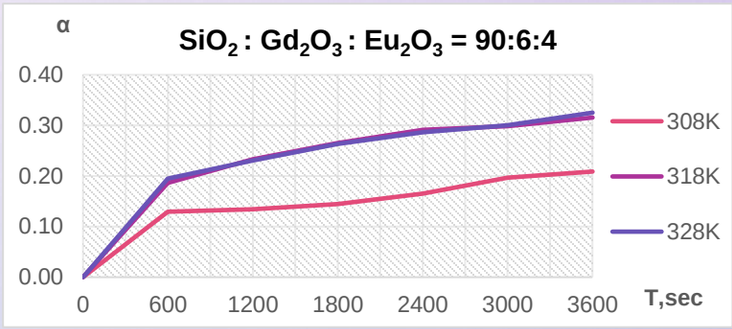

Three samples were obtained from solutions TEOS, europium and gadolinium nitrate using different solvents: citric acid, ethanol.
Sample 1: Method with citric acid after Lyophilic drying.
Sample 2: Method with ethanol after Lyophilic drying.
Sample 3: Method with ethanol, natural air drying.
The calculation of the specific adsorption g (mol/g) was performed using the formula:

$$g = \frac{c.V}{D_o}.\left|\frac{|D_o-D_1|}{a_1} \pm \frac{|D_o-D_2|}{a_2}\right|$$

where *c* is the indicator concentration, mol/dm^3; *V* is the sample volume, dm^3; D_0 is the optical density of the initial indicator; D_1 is the optical density of the indicator after sorption by the sample; D_2 is the optical density of the blank sample (solvent + material sample); a_1, a_2 are sample weights, g.

No p/p	Indicator	Specific adsorption, g ·10^5, mol/g		
		Sample 1	Sample 2	Sample 3
1	Fuchsin basic,pKa=2.1; λ=540 nm	-	0,05	0,20
2	Methyl orange,pKa=3.46; λ=464 nm	0,40	1,00	0,30
3	Bromthymol blue, pKa=7.4; λ=440 nm	0,57	0,30	0,05
4	Neutral red, pKa=9.4; λ=430 nm	2,01	6,50	0,40

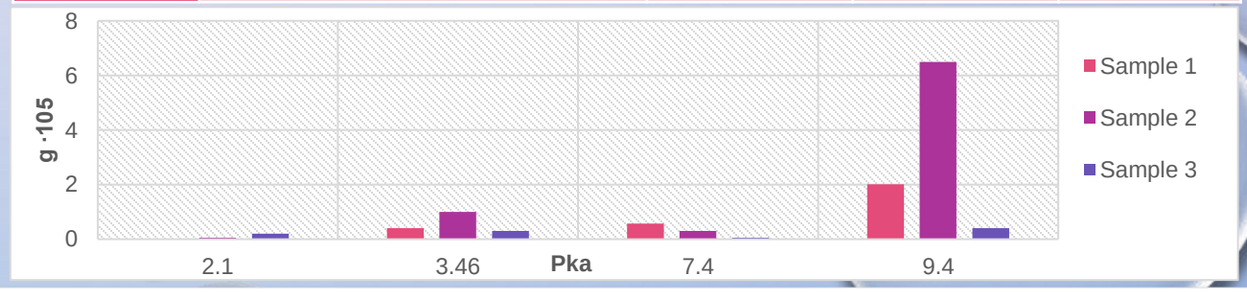

CONCLUSIONS: The activation energy of the hydrolysis process depends on the concentration of Gd_2O_3 - Eu_2O_3 oxides and varies in the range of 17.65-6.03 kJ/mol The maximum value of the activation energy is 17.65 kJ/mol for the system with the absence of rare earth elements (SiO_2 : Gd_2O_3 : Eu_2O_3 = 100:0:0). The addition of Gd^{3+} and Eu^{3+} ions reduces the activation energy of silicon oxide formation from tetraethoxysilane. So these ions play the role of catalysts. The response degree of α stage of hydrolysis increases from 2% to 20% with increasing concentration of Gd_2O_3 - Eu_2O_3. Therefore, the rate and completeness of hydrolysis increases with increase in rare earth elements oxide content. The degree of response α stage of polycondensation also increases with increasing the content of Gd_2O_3 - Eu_2O_3, but does not reach 100%, this is due to the fact that in the process of transformation hydrated gadolinium and europium ions are located on the surface of silicon oxide particles and shield them from further deposition. That is, in the process of heterogeneous hydrolysis, a layered structure was obtained: in the center the $Si(OH)_4$ nucleus, then a polymer layer ≡ Si - O - Si ≡, then a layer of hydrated metal ions, which after firing turn into oxides Gd_2O_3 and Eu_2O_3.
The concentration of major activity centers differs markedly when using different drying and synthetic methods. The best results are obtained using Lyophilic drying method and synthetic system

Reduced graphene oxide - based electrodes for energy storage

Olena Okhay[1,2*], Tao Yang[1] and Alexander Tkach[3]
[1]TEMA-Center for Mechanical Technology and Automation, Department of Mechanical Engineering, University of Aveiro, 3810-193, Aveiro, Portugal
[2]LASI - Intelligent Systems Associate Laboratory, Portugal
[3]CICECO-Aveiro Institute of Materials, Department of Materials and Ceramic Engineering, University of Aveiro, 3810-193 Aveiro, Portugal

INTRODUCTION

Energy conservation is an important topic of scientific research today. Supercapacitors and batteries can help store electrical energy obtained from other sources. Carbon-based materials (i.e. activated carbon, etc.) were used to make battery electrodes[1]. At the same time, reduced graphene oxide (rGO) is a promising material for improving the structural and electrochemical properties of capacitive electrodes used in supercapacitors and batteries[2].

EXPERIMENTAL

Graphene oxide was obtained by Hummer-based method. Freestanding rGO membranes were prepared by vacuum filtration of GO without binders with the following heat treatment. rGO-based electrodes on substrates were prepared by mix rGO aerogel with polymer binder and covering onto different substrate. Different electolytes were used for the experiment: KOH, H_2SO_4, etc.

RESULTS AND DISCUSSION

rGO aerogel, which has a large specific surface area, is a more promising material for energy storage in comparison to freestanding rGO membranes obtained by vacuum filtration without binder or prepared by simple hand-made-pressing with binder. Thus, the preparation process of rGO-based electrodes, as well as composite materials based on rGO, plays a significant role in the properties of final material.

REFERENCES

1. P. Simon et al, Electrochem. Soc. Interface 17, 38 (2008)
2. O. Okhay et al, Nanomaterials 11, 1240 (2021)

ACKNOWLEDGMENTS

O.O. thanks for support the projects PTDC/EME-REN/1497/2021 “Power Phoenix Battery - A Full Solid State Grid-scale Storage Solution”; UIDB/00481/2020 and UIDP/00481/2020 - Fundação para a Ciência e a Tecnologia, DOI 10.54499/UIDB/00481/2020 (https://doi.org/10.54499/UIDB/00481/2020) and DOI 10.54499/UIDP/00481/2020 (https://doi.org/10.54499/UIDP/00481/2020); CENTRO-01-0145-FEDER-022083 - Centro Portugal Regional Operational Programme (Centro2020), under the PORTUGAL 2020 Partnership Agreement, through the European Regional Development Fund.

(AEM) Advanced Energy Materials

Nanometric $BiVO_4$ Coating Grown by Directed Assembly on CuO-Sb_2O_5-SnO_2 Ceramics for Photoelectrochemical Water Splitting

Alexander N. Bondarchuk*[1], Frank Marken[2], Iván Corrales-Mendoza[1], Luis Á. Arellanes-Mendoza[1], Akalya Karunakaran[2]

[1*]Universidad Tecnológica de la Mixteca, México (alexbondua@yahoo.com)

[2]Department of Chemistry, University of Bath, UK

INTRODUCTION

$BiVO_4$ is a semiconductor exhibiting n-type conductivity and photocatalytic properties, with promising potential for practical applications in water purification and solar-driven hydrogen production[1]. For these applications, a high-performance and cost-effective photoelectrode with a large area of active surface is required. Such photoelectrodes can be formed on conductive and porous CuO-Sb_2O_5-SnO_2 ceramics, which act as a free-standing substrate to host the photocatalytic coating[2]. In the presented work, we report on $BiVO_4$ photoelectrodes grown through the 'directed assembly' of charged multilayers of precursors on the surface of CuO-Sb_2O_5-SnO_2 ceramics. To the best of our knowledge, this work reports for the first time on obtaining a $BiVO_4$ coating onto a CuO-Sb_2O_5-SnO_2 substrate using the 'directed assembly' method. This method could be applied for the controlled molecular-level engineering of grain surfaces in tin dioxide ceramics.

EXPERIMENTAL

Conductive CuO–Sb_2O_5–SnO_2 substrates were obtained and prepared as previously reported[2]. Subsequently, the substrate was immersed alternately for 60 seconds in: (a) a solution containing Bi^{3+} ions, prepared by dissolving 0.388g of $Bi(NO_3)_3 \cdot 5H_2O$ in 0.5mL of HNO_3 and 25mL of deionized water; (b) deionized water for rinsing; and (c) a solution containing VO_4^{3-} ions, prepared by dissolving 0.0936g of NH_4VO_3 in 25mL of 0.1 M HNO_3. Repeated application of this treatment cycle led to the formation of charged multi-layers on the host surface, consisting of Bi^{3+} and VO_4^{3-} ions. The formation of the $BiVO_4$ coating was achieved through heat treatment in air at 600°C for 1 hour.

RESULTS AND DISCUSSION

The FESEM micrographs of the obtained structures are presented in Fig. 1(a)-(c), while confirmation of the $BiVO_4$ coating, provided by the Raman spectra, is shown in Fig. 1d. The $BiVO_4$ photoelectrodes exhibit a

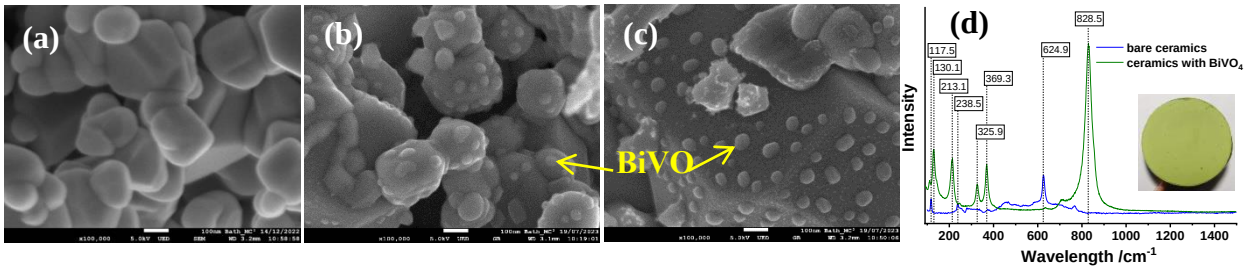

Fig. 1. FESEM micrographs and Raman spectra for (a) bare CuO–Sb_2O_5–SnO_2 ceramics and (b-d) those with a $BiVO_4$ coating obtained after 30 treatment cycles. The inset in (d) showcases the $BiVO_4$ photoelectrode.

photocurrent of approximately 8.8 mA/cm² at 1.23V vs RHE under blue LED radiation (Thorlabs M365LP1; 365 nm) in 1M NaOH electrolyte. This observed photo-response is primarily attributed to the presence of the $BiVO_4$ coating, given that the photocurrent of the bare substrate under the same LED is approximately 0.5 mA/cm² at 1.23V vs RHE.

CONCLUSION

The directed assembly method has been successfully employed to modify the grain surfaces of CuO–Sb_2O_5–SnO_2 ceramics with a nanometric functional $BiVO_4$ coating. The simplicity and monolayer precision of this method make it a promising approach for engineering the sensory and photoelectrochemical properties of SnO_2-based ceramics.

REFERENCES

1. P. Mane et. al, Int J Hydrogen Energy 47, 39796 (2022)

2. A.N. Bondarchuk et. al, Catalysis Communications 174, 106593 (2023)

ACKNOWLEDGMENTS

A.N.B. acknowledges the financial support of this study provided by CONACYT (Mexico), the grant number A1-S-20353.

Prominence of Ni Substitution in $Ni_xCo_{3(1-x)}O_{4-\delta}$ on CO_2 Methanation activity

Ch. H. Suharika[1], I. Sreedhar[1], Patrick da Costa[2,*], Satyapaul A. Singh*[,1]
[1]Department of Chemical Engineering, BITS Pilani, Hyderabad Campus, Hyderabad 500078, India
[2]Institut Jean le Rond d′Alembert, Sorbonne Université, CNRS UMR 7190, 2 place de la gare de ceinture, 78210 Saint Cyr l′Ecole, France
*Corresponding Author Email: patrick.da_costa@sorbonne-universite.fr, satyapaul@hyderabad.bits-pilani.ac.in

INTRODUCTION

Stating the constant increase in anthropogenic CO_2 emission to the atmosphere and resulting from it dynamic growth of carbon dioxide concentration, other efficient ways for utilization of this gas are necessary to develop[1]. Catalytic processes designed for this purpose are gaining popularity, among which CO_2 hydrogenation to methane is especially promising[2]. Most popular catalyst for CO_2 methanation, due to its cost-effectiveness, availability, and satisfactory price-performance ratio, is Ni/Al_2O_3 [3]. However, this material easily undergoes deactivation to various factors such as coking and sintering [4]. Those setbacks may be partially overcome by enriching the catalyst in proper promoter and application of synthesis route that can provide stronger metal-support interaction. Cobalt seems to be advantageous material, due to its high performance in steam reforming of methane [5] or Fischer-Tropsch synthesis on CO_2-rich gases [6]. Likewise, it reduces coke formation and tend to form alloy with nickel in Ni-Co bimetallic catalyst, which improves electron transfer [7]. In this work we proposed to use Co_3O_4 and Ni-substituted Co_3O_4 catalysts for CO_2 methanation.

EXPERIMENTAL/THEORETICAL STUDY

In this work, Co_3O_4 and Ni-substituted Co_3O_4 catalysts were synthesized by a single-step solution combustion method [8]. These catalysts were characterized by XRD, XPS, SEM, TEM, BET, ICP-OES and H_2-TPR analysis in order to know the physical, structural, morphological, elemental and redox properties of the materials. The catalytic activity studies were performed in a fixed bed quartz reactor with 4mm ID. Catalyst loading of 200 mg was taken in the reactor in the form of pellets with 60/80 mesh size and it was diluted with silica gel in order to maintain the consistency of 1.5 cm bed length for all the materials and the catalyst was packed between the quartz wool plugs. The catalyst was reduced with H_2 for 1 h at 400°C with a flowrate of 30 ml/min. After the completion of the reduction step, the catalyst was subjected with the feed stream with a flowrate of 100 ml/min in which the CO_2 flowrate was 2 ml/min, H_2 flowrate was 8 ml/min and the remaining was N_2 within a temperature range of 175-450°C with an increment of 25°C. The gas outlet was connected to the gas chromatography (GC) in order to measure the composition.

RESULTS AND DISCUSSION

The XRD patterns of the catalysts Co_3O_4, Ni-Co_3O_4, NiO were matched with the reference files of Co_3O_4 (JCPDS file: 00-043-1003), NiO (JCPDS file: 00-001-1239). A separate NiO phase was observed in 20%Ni-Co_3O_4 and 25% Ni-Co_3O_4 at 2θ value of 45°. This indicates the possibility of effective lattice substitution at a high Ni loadings. ICP-OES results further confirmed the accuracy of Ni loading in Co_3O_4 lattice. The H_2-TPR studies were done in order to know the reducing nature and the oxygen vacancies of the catalysts. Interestingly, the reduction ability of the catalysts was enhanced with Ni loading by shifting the rection peak maxima to lower temperature with increase in loading. Among all catalysts, 20% Ni-Co_3O_4 was found as the best material with 78% of CO_2 conversion and 98% of methane selectivity at 375°C. The synergy between NiO and Co_3O_4 is improving the catalyst performance. However, beyond 375°C, a drop in CO_2 conversion was observed due to thermodynamic limitations. DFT simulations further validated the role of oxygen vacancies for the better catalytic performance.

CONCLUSION

In this work, we successfully induced Ni substitution in lattice up to 15% loading. The role of oxygen vacancies on the catalytic activity was correlated with H_2-TPR and DFT simulations. The elemental composition was further confirmed with ICP-MS analysis. All Ni-doped catalysts offered decent performance, however, the highest performance of 78% CO_2 conversion and more than 98% CH_4 selectivity was achieved with 20%Ni-Co_3O_4.

REFERENCES

1.R. Lindsey, Climate Change: Atmospheric Carbon Dioxide, online access
2. F. D. Meylan et. al, J. Energy Storage, 11, 16–24 (2017)
3. G. Garbarino et. al, Int. J. Hydrogen Energy, 39, 11557–11565 (2014)
4. C. H. Bartholomew, Appl. Catal. A Gen., 212, 17–60 (2001)
5. D. Li, et. al, Appl. Catal. A Gen., 552, 21–29 (2018)
6. C. G. Visconti et. al, Appl. Catal. A Gen., 355, 61–68 (2009)
7. J. Liu et. al, Green Energy Environ., DOI:10.1016/j.gee.2020.10.011.
8. S.A. Singh, G. Madras, Appl. Catal. A Gen., 504, 463-475 (2015)

Comparative Analysis of Scientific Papers on LCA Applied to Building Materials

Marco Antonio Sánchez-Burgos [1*], Begoña Blandón-González [2], Esperanza Conradi-Galnares [3], Paula Porras-Pereira [4], Pilar Mercader-Moyano *[5]

[1] Department of Building Construction I, Higher Technical School of Architecture, University of Seville, Spain, presenting author

[2, 3, 4] Department of Building Construction I, Higher Technical School of Architecture, University of Seville, Spain

[5*] Department of Building Construction I, Higher Technical School of Architecture, University of Seville, Spain, corresponding author (pmm@us.es)

INTRODUCTION

Notwithstanding the myriad reported advantages of nanomaterials across diverse sectors, it is imperative to acknowledge the latent health and environmental hazards that accompany their evolution and implementation, a realm yet to be comprehensively explored[1]. The predominant focus of nanomaterial research has predominantly fixated upon their distinctive functionalities across various disciplines and applications, often at the expense of a comprehensive evaluation of the potential environmental ramifications spanning their entire life cycle[1]. There is also concern about the environmental sustainability of nanomaterials pathways contributing to environmental problems[2]. A comprehensive approach such as life cycle assessment (LCA) can provide a better understanding of the potential environmental problems of nanomaterials, guaranteeing the environmental viability of their application.

EXPERIMENTAL/THEORETICAL STUDY

The starting point of the research has been identifying nanoparticles and nanoparticles containing materials employed within the construction industry. For this purpose, an exhaustive exploration of relevant literature was undertaken employing a diverse set of terms encompassing nanoparticles and nanotechnology, coupled with keywords specifically denoting LCA in the construction domain. Subsequently, the investigation extended to the identification of standards governing impact categories in LCAs, along with the discernment of existing LCA databases pertinent to the construction sector. Furthermore, to execute a comprehensive comparative analysis across the reviewed literature, a set of indicators compiling impacts categories were summarized. Finally, a comparative analysis revolves around the following four aspects: LCA methodology in use, analyzed impact categories, site boundaries and scope of assessment.

RESULTS AND DISCUSSION

Nowadays, there is a significant lack of information regarding the fate of nanoparticles emissions once they have been released to the environment, and its consequences for human health and ecosystems quality. Currently available products databases do not include specific data regarding nanoparticles, therefore emissions throughout the whole life cycle of the nanoproducts must be informed specifically for each study. Finally, as impacts associated to nanoparticles emission cannot be calculated nowadays, it advisable to include in LCA studies information about predicted emissions and risk assessment for the nanoparticles involved.

CONCLUSION

As a result of the aforementioned information scarcity, LCA cannot be fully applied to the study of nanoproducts. Methods that can evaluate the impacts for human health and ecosystems quality, considering nanoparticle emissions, must be implemented. Due to the current importance of nanoparticles, obtaining reliable and robust results from nanoparticles LCA is valuable to improve existing methods and databases.

REFERENCES

1. I. Khan and K. Saeed, “Nanoparticles: Properties, applications and toxicities,” Arabian Journal of Chemistry, vol. 12, no. 7, pp. 908-931, 2019.
2. J. Lee, S. Mahendra and P. J. J. Alvarez, “Nanomaterials in the Construction Industry: A Review of Their Applications and Environmental Health and Safety Considerations,” ACS Nano, vol. 4, no. 7, pp. 3580-3590, 2010

ACKNOWLEDGMENTS

The results of this article derive from the project Educational platform for life cycle analysis of treatments based on nanoparticles applied to the construction industry project (code 2022-1-ES01-KA220-HED-000089985), an Erasmus+ project co-funded by the European Union. This publication reflects the views only of the author, and the Commission cannot be held responsible for any use which may be made of the information contained therein.

Characteristics of vanadium pentoxide added magnesium hydride as active Li conversion material in a Li ion battery

D. Pukazhselvan* [1,2], Ihsan Çaha[3], Francis Leonard Deepak[3] and Duncan Paul Fagg[1,2]
[1]Department of Mechanical Engineering, TEMA - Centre for Mechanical Technology and Automation, University of Aveiro, Aveiro 3810-193, Portugal
[2]LASI - Intelligent Systems Associate Laboratory, Guimarães 4800-058, Portugal
[3]Nanostructured Materials Group, International Iberian Nanotechnology Laboratory (INL), Avenida Mestre Jose Veiga, Braga 4715-330, Portugal

INTRODUCTION

Recent studies suggest that the promising lightweight binary hydride, MgH_2, can serve as an active anode material for Li-ion batteries through the following reversible reaction: $2Li+MgH_2 \leftrightarrow Mg+2LiH$ (1) [1]. The theoretical capacity of this reaction is 2038 mAh/g, which is more than five times the capacity of natural graphite, i.e. 372 mAh/g. However, the electrochemical reaction (1) is kinetically slow when pure MgH_2 is utilized, for instance, the forward conversion efficiency is < 10%, and the reversible conversion efficiency is < 5%. On the other hand, as per our previous observations upon using MgH_2 as a hydrogen storage material, it is possible to improve it kinetically by incorporating suitable additives [2]. In the literature metal oxides were identified to be promising for enhancing the Mg-H interaction at lower temperatures. Our recent experiments with V_2O_5 as an additive for MgH_2 shown promising improvements as a hydrogen storage system [2]. With these inputs, for the current study our interest is to use MgH_2-V_2O_5 composite as a Li conversion material in a Li ion coin cell battery.

EXPERIMENTAL

The 5 wt.% V_2O_5 added MgH_2 was prepared through mechanical milling technique (Retsch PM200). Structural characterizations were performed by X ray diffraction technique (Rigaku diffractometer, λ=1541 Å). CR2032 coin cells were prepared using MgH_2 as anode (carbon mounted on Cu as current collector), Celgard 3501 as separator, Li as counter electrode, $LiPF_6$ in 1M EC/DMC as electrolyte.

RESULTS AND DISCUSSION

It is found that a Li ion battery with the current anode active material (5% V_2O_5 added MgH_2) delivers ~600 mAh/g in the first cycle and restores 180 mAh/g. The reversible capacity decreases and no observable conversion occurs after 5 cycles. Nonetheless, it is also clear that V_2O_5 added MgH_2 performs better than the pure MgH_2 as the latter does not restore Li under the testing conditions employed in the current study. With this observation, our further interest is to explore the interaction between V_2O_5 and MgH_2. For this, we have reviewed 8 different samples, $xMgH_2+V_2O_5$ (x=1, 2, 3, 4, 5, 6, 7 and 8). Through these studies we have observed that the interaction between MgH_2 and V_2O_5 ends up with the formation of a V dissolved MgO rock salt, typified by $Mg_xV_yO_{x+y}$.

CONCLUSION

The current study suggests that V_2O_5 is a better additive to promote the electrochemical reaction of Li with MgH_2. The cyclic stability of the MgH_2-V_2O_5 employed battery remains an issue to be solved but it is clear that only after the incorporation of additive (V_2O_5) reversible storage of Li is possible in the current study. The detailed sample characterization study proves that the additive V_2O_5 and MgH_2 interact chemically and ends up with the formation of V dissolved MgO. From this we believe that the in-situ generated V doped MgO promotes the conversion interaction between MgH_2 and Li.

REFERENCES

1. Pukazhselvan, D., et al. Journal of Magnesium and Alloys 12.3 (2024): 1117-1130.D.
2. Pukazhselvan, D., et al. International Journal of Hydrogen Energy 59 (2024): 755-763.

ACKNOWLEDGMENTS

This article was supported by the projects UIDB/00481/2020 and UIDP/00481/2020 - Fundação para a Ciência e a Tecnologia, DOI 10.54499/UIDB/00481/2020 (https://doi.org/10.54499/UIDB/00481/2020) and DOI 10.54499/UIDP/00481/2020 (https://doi.org/10.54499/UIDP/00481/2020). D. P acknowledges FCT, Portugal for the financial support with reference CEECIND/04158/2017. The authors are also grateful for the financial support granted by the Recovery and Resilience Plan (PRR) and by the Next Generation EU European Funds to Universidade de Aveiro, through the Agenda for Business Innovation "NGS - Next Generation Storage" (Project no 02/C05-i01.01/2022 with the application C644936001-00000045).

Hydrogen storage characteristics of TiB_2 incorporated LiH/MgB_2 nanocomposite

D. Pukazhselvan* [1,2], Sergey M. Mikhalev [1,2], and Duncan Paul Fagg[1,2]
[1]Department of Mechanical Engineering, TEMA - Centre for Mechanical Technology and Automation, University of Aveiro, Aveiro 3810-193, Portugal
[2]LASI - Intelligent Systems Associate Laboratory, Guimarães 4800-058, Portugal

INTRODUCTION

The USDOE hydrogen storage capacity target for a hydrogen powered fuel cell electric car is 6.5 wt.% H_2. To reach this capacity, several classes of solid-state metal hydrides were tested, for example, intermetallic hydrides, complex hydrides and binary hydrides, however it is not yet possible to optimize a suitable hydrogen storage material as per the targets. To date, the best observed experimentally reproducible capacity is 6 wt.% H_2 by MgH_2 system (theoretical capacity: 7.6 wt.% H_2), however when we consider at least a 20% weight contribution from the tank, the 6 wt.% capacity comes down to 4.8 wt.% which is lesser than the USDOE target for hydrogen vehicles. In this context we need to develop other high-capacity hydrogen storage materials and our interest in the current study is a promising reactive hydride composite (RHC) system $2LiH+MgB_2$. The reproducible H_2 capacity of this RHC is 10.3 wt.%, however, there exist kinetic restrictions and high temperature/pressure operational constraints. To address these, in the current study, we have incorporated a small quantity of additive TiB_2 in place of MgB_2 and tested the hydrogen storage capacity of the $LiH/MgB_2/TiB_2$ nanocomposite and interesting results were achieved.

EXPERIMENTAL

All the samples in the current study ($2LiH + (1-x)MgB_2 + xTiB_2$) were prepared by mechanical milling technique using a planetary milling facility Retsch PM200. Hydrogen storage characteristics were tested by Sieverts volumetric technique and structural characterization were performed by X ray diffraction facility (Rigaku).

RESULTS AND DISCUSSION

Initially we ball milled a mixture $2LiH + (1-x)MgB_2 + xTiB_2$, where x=0, 0.25, 0.5, 0.75 and 1, for 5h and hydrogenated this mixture at the pressure of 70 bars H_2 at 370 °C for 5h reaction time. For knowing the changes occurred due to this treatment the as-prepared and the hydrogenated samples were studied by XRD technique. We have identified that the expected hydride phases, $LiBH_4$ and MgH_2 can be observed between x=0-0.5, especially between x=0.05-0.15. For instance, in the case of x=0.5 and 0.15, we have observed 9.2 wt.% H_2, that can be consistently reproduced (rapid kinetics upto 3 wt.%, and thereafter a slow kinetics is observed till the end of the reaction: dehydrogenation conditions, 406 °C/5 bar H_2). In fact, two step desorption is observed for all values of x and we believe that the first step may be due to the separate dehydrogenation of MgH_2. As far as the reaction kinetics in the second step is concerned, as compared to the case where no TiB_2 was added, all the TiB_2 added samples provided better kinetics. Another noteworthy observation is that the phase abundance of hydride phases ($LiBH_4$ and MgH_2) during repeated hydrogenation experiments is better only in the case of TiB_2 added samples.

CONCLUSION

The current study suggests that TiB_2 as an additive enhances the hydrogens storage performance of the reactive hydride composite $2LiH+MgB_2$. It is possible to store 9.2 wt.% H_2 through the composite $2LiH+0.95MgB_2+0.05TiB_2$ and the dehydrogenation kinetics tested at 406 °C/5 bar H_2 back pressure is better than that observed in the case of $2LiH+MgB_2$.

REFERENCES

1. USDOE, Target explanation document: onboard hydrogen storage for light-duty fuel cell vehicles, USDRIVE (2017), pp. 1-19
2. D. Pukazhselvan et al. Nanomaterials for Sustainable energy and environmental Remediation, Elsevier (2020), pp. 97-163.

ACKNOWLEDGMENTS

This article was supported by the projects UIDB/00481/2020 and UIDP/00481/2020 - Fundação para a Ciência e a Tecnologia, DOI 10.54499/UIDB/00481/2020 (https://doi.org/10.54499/UIDB/00481/2020) and DOI 10.54499/UIDP/00481/2020 (https://doi.org/10.54499/UIDP/00481/2020). D. P acknowledges FCT, Portugal for the financial support with reference CEECIND/04158/2017.

Chitosan Based Solid Electrolyte doped with New Azo-Azomethine Additive for Electric Double-Layer Capacitor (EDLCs)

Rafizah Rahamathullah[1*], Tuan Siti Fatimah Tuan Mohd Pauzi[1], QY Ang[1], Wan M. Khairul[2], Rosli M.I.[3], Artiqah Khairudin[3]

[1*]Faculty of Chemical Engineering & Technology, Universiti Malaysia Perlis (UniMAP), 02600 Arau, Perlis, Malaysia.
[2]Faculty of Science and Marine Environment, Universiti Malaysia Terengganu, 21030 Kuala Nerus, Terengganu, Malaysia.
[3]Faculty of Science and Technology, Universiti Kebangsaan Malaysia, Bangi 43600, Selangor, Malaysia

INTRODUCTION

At this modern era of technology, the utilization of electronic and electrical equipment has expanded dramatically in which underwent to electrical waste (e-waste)[1-2]. In conjunction to these alarming problems, the demands for an alternative method to design and develop new biodegradable materials with less hazardous byproducts critically needed to substitute conventional energy storage devices[3]. The involvement of renewable resource-based biopolymers as host matrix with incorporation of small additives to overcome the limitations inherent in a mixture of biopolymer electrolyte should be taken into consideration[4\]. Herein, new solid electrolyte based on chitosan polymer matrix integrate with new synthesized organic additive were prepared to enhance the ionic conduction and crystallinity properties. By considering the delocalization in π-orbital system, new hybrid derivative of alkoxylated azo-azomethine consist of azo (N=N) and imino (CH=N) moiety has been utilized to examine how far the effects of this additive could be able to improve the properties of electrolyte and consequently lead to the performance towards EDLC.

EXPERIMENTAL/THEORETICAL STUDY

All reactions and work up were carried out under an ambient environment and no special precaution steps were taken during the synthetic work. Targeted azo-azomethine additive was conducted via Schiff Base condensation reactions through equimolar of azo and alkoxylated aniline derivative in a simple Dean-Stark condenser. The synthesized additive was then characterized via selected spectroscopic analysis, thermal and theoretical approach prior further integrated as SBE. Afterwards, the targeted additive was dissolved in 1% of acetic acid and poured into chitosan biopolymer solution with constant stirring at ambient environment. The mixture was then casted followed by drying at 50℃ for 30 hours. The structural, thermal and conductivity of the new SBE were analyze using infrared (IR), X-ray diffraction (XRD), thermogravimetric analysis (TGA) and Electrical impedance spectroscopy (EIS).

RESULTS AND DISCUSSION

The utilization of additive involving 'Donor (D)-Spacer(π)-Acceptor (A)' concept which tailoring the azo moiety as spacer bridge assist the enhancement of the ionic mobility of the electrolyte. This can be seen from experimental and theoretical outcome. From the simulated data, the HOMO-LUMO gap of additive exhibit low range, 2.17 eV which showed good range for organic semiconducting materials. The frontier molecular orbital (FMO) distribution presented in Figure 1 reveal that unfilled π-orbital (LUMO) delocalized throughout the azo moiety and aromatic group indicate the flow of electron can be happen within the polymer. Moreover, the 3D plot from molecular electrostatic potential (MEP) also quantitatively reflects the resonance effects of substituents and give significant correlation between the MEP values and energy level in the system.

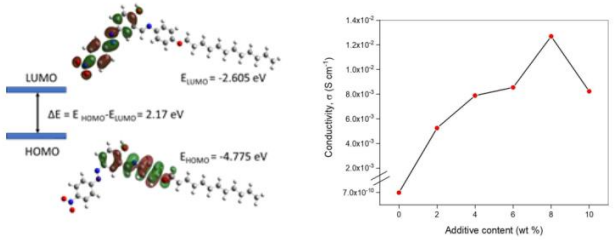

Fig.1: (a)Molecular orbital involved in the electronic transition of additive (b) conductivity of SBEs system.

The investigation of their potential as additive in SBE system has been accomplished by integrate chitosan biopolymer using solution-casting technique. A various weight ratio (2% until 10%) of synthesized additive was tested as new SBE. The highest ionic conductivity achieved was 1.27 x 10^{-3} Scm^{-1} at ambient temperature (303K) for the system containing 8 wt.% of chalcone-based additive using impedance spectroscopy (Fig.1b). While for EDLC performances, 4 wt.% reveals highest specific capacitance ~4 x10^{-5} F/g at 5 mV/s.

CONCLUSION

The preliminary outcome from simulated and experimental data indicates that utilizing appropriate substituents affect the distribution patterns of FMOs and subsequently improve in conductivity due to enhancement of ionic mobility.

REFERENCES

1. M. Shahabuddin et al., Int. J. Environ. Sci. Technol. 20(4), 4513-4520 (2023)
2. R. Nithya et al., Environ. Chem. Lett. 19, 1347-1368 (2021)
3. S. Nandy et al., Adv. Mater. Technol. 6(7), (2021)

ACKNOWLEDGMENTS

The authors would like to express gratitude to the Ministry of Higher Education, Malaysia for research grant FRGS/1/2021/STG05/UNIMAP/03/1(9003-00914).

Laser Induced Graphene-supported Cu-Ag Nanoparticle based Chemiresitive Sensor for detection of Thrombin in Human Plasma

Rahul Gupta (presenting author)[1], Tamojit Santra[2], Santosh K. Misra[2], Nishith Verma[1,3]
[1] Department of Chemical Engineering, Indian Institute of Technology Kanpur, Kanpur, 208016, India.
[2] Biological Sciences & Bioengineering, Indian Institute of Technology Kanpur, Kanpur, 208016, India.
[3] Centre for Environmental Science and Engineering, Indian Institute of Technology Kanpur, 208016, India.

Introduction

Thrombin is an important protein that can convert soluble fibrinogen to insoluble fibrin. High concentration of thrombin can cause thrombosis, while lower concentration leads to excessive bleeding. Therefore, the development of a rapid and precise sensor for thrombin detection is essential. In this study, laser induced graphene (LIG)-supported Cu and Ag bimetallic-based chemiresistive sensor is used to sense thrombin in human plasma. Chemiresistive sensors work on the principle of change in the conductivity of the sensing material on the adsorption of analyte on its surface. The precursor material for the sensing material is synthesized using suspension polymerization of phenol and formaldehyde, with the in-situ impregnation of Cu and Ag salts during gel formation step. The metal salts are directly reduced to metal nanoparticles during laser ablation. Thrombin binding aptamer (TBA) is used as the recognition element. Ag nanoparticles form a covalent bond with sulfhydryl group of TBA to which thrombin molecules attach selectively. Cu nanoparticles (NPs) enhance conductivity, and also, provide mechanical strength to the sensing material.

Materials and methods

Synthesis of Cu and Ag NPs-supported LIG (Cu-Ag/LIG)

The copper- and silver nitrate-impregnated phenol-formaldehyde co-polymeric film is synthesized using suspension polymerization[1]. Polymeric films are cut to films of 3 X 1 cm dimensions. The films are subjected to heat treatment for 4 h at 200 ^{o}C in N_2. Heat-treated films are laser ablated using fiber laser. The working parameters such as speed, power, and frequency of laser are optimized to create highly conductive Cu-Ag/LIG with surface resistance less than 50 **Ω**. No separate H_2 reduction step is required to reduce metal salts to metal NPs. The synthesized sensing material is termed Cu-Ag/LIG for reference purposes.

Fabrication of Cu-Ag/LIG chemiresistive sensor

The TBA solution is drop cast on Cu-Ag/LIG and kept at 4 ^{o}C for 12 h to form sulfhydryl linkage between Ag and TBA[2]. The films are rinsed with phosphate buffer to remove physically adsorbed TBA. The films are coated with 1% bovine albumin serum solution at 4 ^{o}C for 12 h. The coating deactivates any unreacted active site. Finally, thrombin (analyte) solution is drop cast on the modified film surface and kept at 37 ^{o}C for 30 min. The change in resistance before and after thrombin addition has been measured using novavoltmeter-2182a and ultrasensitive current source-6221, Keithley (USA).

Results and discussion

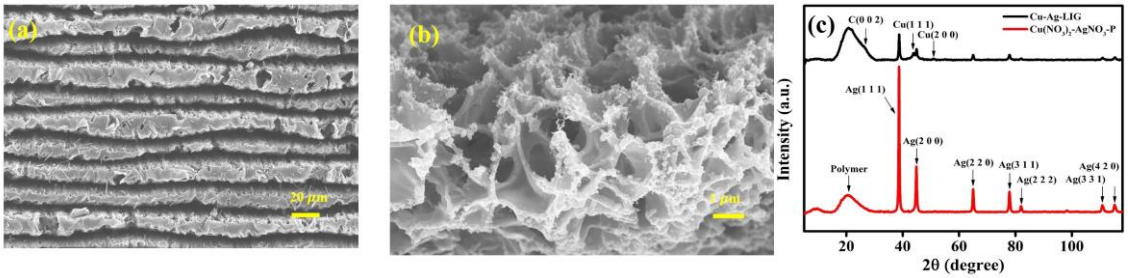

Fig. 1 (a, b) SEM images, and (c) XRD of Cu-Ag/LIG sensing chip.

Fig. 1a and 1b show the SEM images of the synthesized Cu-Ag/LIG. The grooves are formed in the direction of laser ablation (Fig. 1a). The metal NPs dispersed on the porous graphene sheet can be seen in the high magnification image (Fig. 1b). Fig. 1c shows the XRD spectra of heat-treated polymeric films before and after laser ablation. Peaks in the XRD spectra of the laser ablated films correspond to graphene plane C(0 0 2) and Cu and Ag NPs. A significant increase in the resistance of the synthesized Cu-Ag/LIG is observed on the addition of thrombin. A change in resistance is directly proportional to the concentration of thrombin added on Cu-Ag/LIG.

Conclusions

The Cu-Ag/LIG-based chemiresistive sensor for thrombin detection is developed. The laser ablation not only converts the non-conductive polymer to highly conductive graphene but also reduces metal salts to metal nanoparticles. TBA is used to selectively bind thrombin molecules on the surface of the sensing material. The significant increase in the resistance of the sensing material is observed on the addition of thrombin solution.

References

1. A. Yadav et. al, Chem. Eng. Sci., 231, 116282 (2021).
2. N. Hao et. al, Biosens. Bioelectron., 101, 14-20 (2018).

Development of Transition Metal Dichalcogenides-based nanocomposites

Transition metal dichalcogenides (TMDs) have attracted significant attention in recent years due to their unique electronic, optical, mechanical, and chemical properties. They consist of individual layers of transition metal atoms covalently bonded to chalcogen atoms. The layers are held together by weak van der Waals forces, allowing for easy exfoliation to obtain atomically thin sheets. TMDs have unique properties among other 2D materials. These properties can be tuned by varying the type of transition metal and chalcogen, as well as by altering the number of layers. This tunability offers flexibility in designing materials with specific properties of various applications.

On the other hand, TMD-based nanocomposites are of great interest. The combination of TMD with foreign materials is a widely exploited approach, and the resulted hybrid system will not only possess the unique properties of each component, but shall also feature the emergence of new properties that can potentially be used for specific applications.

Therefore, the preparation of new TMD-based nanocomposites is always an interest area of research. Since combining TMDs with foreign materials is useful, as the newly synthesized nanocomposites have the advantages of their components, and they may generate new functions due to synergistic interactions between the two different materials. Thus, studying the synthesis of new TMD-based nanocomposites is useful for exploring novel functionalized composite materials.

The work at hand presents the preparation of TMD-based nanocomposites, prepared with simple and facial methods, such as: hydrothermal, solvothermal. The resulting nanocomposites are fully characterized by XRD, SEM, TEM, FTIR. The electrochemical performance of some of the prepared nanocomposites shall be tested as candidate for Lithium ion batteries (LIBs) anode materials.

DFT-Determined Chemi and Physisorption Degrees of H_2 Adsorption on a PbC Monolayer Decorated with Alkali Metals

Ricardo Bermeo-Campos*[1], Alejandro Trejo[1], Raúl Oviedo-Roa[2] Miguel Cruz-Irisson[1]
[1]Instituto Politécnico Nacional, ESIME Culhuacán, México.
[2]Instituto Mexicano del Petróleo, México.
*Corresponding Author: rbermeoc1200@alumno.ipn.mx

INTRODUCTION

H_2 storage is a nowadays green solution for the energetic demand. The recovering of some elements and compounds from waste, like lead, allows its use as, for example, H_2-adsorbing solid materials. Lead carbide (PbC) is a compound with scarce reports for H_2 sorbing. For other carbides, as tin carbide (SnC), the alkali-metals adatoms have shown increase its H_2 storage capacity[1]. Although it is known that the ideal H_2 adsorption energy must be among 100 and 800 meV, the intensities of the chemisorption and physisorption are determinant for the H_2-storage efficiency.

THEORETICAL STUDY

In this work, we quantify the chemisorption and physisorption degrees of H_2 adsorption on the pristine and the alkali-metal-decorated PbC monolayer. Hydrogen storage was investigated through the H_2 adsorption energy (ΔE) on the PbC monolayer, defined as $\Delta E = E_{H_2:PbC} - (E_{H_2} + E_{PbC})$, where $E_{H_2:PbC}$, E_{H_2} and E_{PbC} are the Density-Functional-Theory (DFT)-determined energies for H_2-containing PbC, a free H_2 molecule and the pristine PbC, respectively. Each of these energies is composed of a non-dispersive $E_{non-disp}$ term, which reflects the quantum interactions, and a dispersive E_{disp} term, which is due to the long range interactions; *i.e.*, $E = E_{non-disp} + E_{disp}$. Therefore, their fractional contribution to ΔE give a measure for the chemisorption ($D_{chem} \equiv \Delta E_{non-disp}/\Delta E$) and physisorption ($D_{phys} \equiv \Delta E_{disp}/\Delta E$) degrees[2].

RESULTS AND DISCUSSION

According to the adsorption energies, the capacity of the pristine PbC monolayer to adsorb a H_2 molecule is similar to that of the graphene since their values are 74 and 72 meV, respectively[2]. However, in the pristine PbC monolayer there is 33.0 % chemisorption degree, in contrast to 0 % in the graphene; hence the adsorption energy is not sufficient to characterize the H_2 storage.

The presence of adatoms increases both the adsorption energy and the chemisorption degrees of a H_2 molecule in the PbC monolayer, since the adsorption energy (chemisorption degree) goes from 209 meV (98.5%) for Cs until 99 meV (26%) for K, respectively, the other adatoms having intermediate adsorption energies. With the posterior consecutive addition of H_2 molecules, some adatoms lead to better adsorption capacities, like K in which, for example, the 3rd H_2 molecule has $\Delta E = 114$ meV and $D_{chem} = 42\%$.

CONCLUSIONS

Although the alkali-metals-containing PbC could not accomplish the United States' Department of Energy requirements for low gravimetric fractions, theoretical calculations demonstrate its possible use in the efficient H_2 storing.

REFERENCES

1. A. L. Marcos, A. Miranda, M. Cruz-Irisson and L.A. Pérez, Int. J. Hydrogen Energy. **47**, 41329 (2022).
2. R. Bermeo-Campos, L. G. Arellano, A. Miranda, F. Salazar, A. Trejo-Baños, R. Oviedo-Roa and M. Cruz Irisson, J. Energy. Storage **73**, 109205 (2023).

ACKNOELEDGEMENTS

This work was partially supported by multidisciplinary project IPN-SIP 2024-0702 and UNAM-PAPIIT IN109320. Computations were performed at the supercomputer Miztli of DGTICUNAM (Project LANCAD-UNAM-DGTIC-180, 381). R.B.C would like to thank CONAHCYT and BEIFI-IPN for their financial support.

(ANM) Advanced Nano Materials

Towards sustainable epoxy based self-sensing polymer composites for high responsibility applications

R. Lima [1] P. Costa[1], J. Nunes-Pereira[2], S. Lanceros-Méndez[1,3,4]

[1] Physics Centre of Minho and Porto Universities (CF-UM-UP) and Laboratory of Physics for Materials and Emergent Technologies, LapMET, University of Minho,4710-057 Braga, Portugal
[2] C-MAST, Centre for Mechanical and Aerospace Science and Technologies, Universidade da Beira Interior, Rua Marquês d'Ávila e Bolama, 6201-001 Covilhã, Portugal
[3] BCMaterials, Basque Center for Materials, Applications and Nanostructures, UPV/EHU Science Park, 48940 Leioa, SpainBCMaterials
[4] IKERBASQUE, Basque Foundation for Science, 48013, Bilbao, Spain

The polyepoxide matrices are a class of polymers with suitable characteristics for structural and adhesive materials, showing also excellent chemical resistance. In order to reduce the ecological footprint of these materials, it is mandatory to replace petroleum-based resins with bio-based ones. In addition, these materials can be tailored to be applied by printing technologies with low temperature curing, further reducing environmental impact.

These sustainable epoxies can be tailored into multifunctional materials for advanced devices, combining their excellent mechanical properties with piezoresistive and thermoresistive sensing properties and adding conductive fillers. Carbonaceous materials present a large electrical conductivity, leading to a low percolation threshold in polymer composites. Thus, lightweight composites with mechanical and thermal sensitivity can be developed for high-performance systems, such as adhesive sensors for structural health monitoring and coating applications.

Petroleum (Araldite AW106 and AV 4076 from Huntsman) and bio-based (SR GreenPoxy 56 from GreenPoxy with 51% biobased carbons) resins were developed using carbon black, graphene, and carbon nanotubes as reinforcing materials, with a focus on sensing applications in the scope of Industry 4.0 and the Internet of Things (IoT) concepts. The effect of filler content on the mechanical and electrical properties of the different resins was evaluated for composites produced by screen-printing technique, together with their sensing properties. Bending sensing response (up to 5 mm bending) and thermoresistive behavior (up to 90 ºC) were evaluated. Both sensing characteristics demonstrate excellent sensibility and linearity between the applied stimuli and the electrical resistance response. An adhesive sensor has also been used to monitor the

temperature and bending state of structures using carbon and glass fibers as structural materials.

Acknowledgments

The authors are grateful for the support of the Portuguese Foundation for Science and Technology, I.P. (FCT, I.P.) under the R&D Units Centre of Physics of the Universities of Minho and Porto (CF-UM-UP) and C-MAST, Centre for Mechanical and Aerospace Science and Technologies (UIDB/00151/2020, https://doi.org/10.54499/UIDB/00151/2020 and UIDP/00151/2020, https://doi.org/10.54499/UIDP/00151/2020). Ricardo Lima and João Nunes-Pereira would also like to thank FCT, I.P., for the PhD grant 2020.07010.BD and the contract under the Stimulus of Scientific Employment, Individual Support (2022.05613.CEECIND, https://doi.org/10.54499/2022.05613.CEECIND/CP1746/CT0001). This study forms part of the PRR n.º 58 - NGS – New Generation Storage and Advanced Materials program and was supported by MCIN with funding from European Union NextGenerationEU (PRTR-C17.I1) and by the Basque Government under the IKUR program. Funding from the Basque Government under the Elkartek program is also acknowledged.

Influence of the synthesis method for metal-organic frameworks for CO_2 electroreduction reaction

Rodrigo Espinosa[1], Martin Trejo*[1], Maria Elena Manriquez[1] and Francisco Tzompantzi [2]
[1]Laboratorio de nanomateriales y Energías Limpias, Instituto Politécnico Nacional, Mexico, corresponding author (martin.trejo@laposte.net)
[2]Departamento de Química, Área de Catálisis, Universidad Autónoma Metropolitana Iztapalapa, Mexico.

INTRODUCTION

Metal-organic frameworks (MOFs) have proven to be suitable materials for CO_2 electrochemical reduction reaction (CO_2RR), however, the synthetic method is key for an enhanced electrocatalytic activity. In this work, we synthesized two zinc-based MOFs from 2,5-dihydroxyterephthalic acid and citric acid, respectively. The synthetic methods were muffle-assisted method and microwave-assisted method, both of them solvothermal-assisted methods.

EXPERIMENTAL/THEORETICAL STUDY

X-ray diffraction (XRD) analysis was conducted in order to elucidate the crystalline structure of each material, according to its synthetic method. Electrochemical impedance spectroscopy (EIS) studies were conducted after cyclic voltammetry (not shown here) in order to check out the resistive behaviour in CO_2-saturated 0.1 M KOH electrolyte.

RESULTS AND DISCUSSION

The X-ray diffraction patterns displayed in Fig. 1 a,b) show that both MOFs have the same diffraction angle peaks but with different intensities, according to the synthetic method. On the other hand, both microwave-assisted MOFs displayed a shorter semicircle in CO_2-saturated electrolyte (Fig. 1d,f) than in muffle-assisted method, which indicates a less resistive behaviour for the electron transfer process[1].

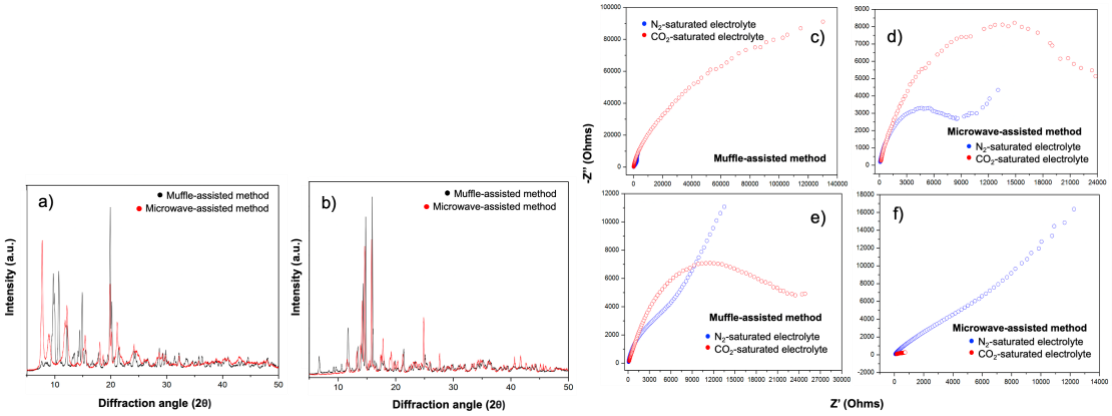

Fig. 1 Left: XRD patterns of the MOFs. a) Citric acid MOF, b) 2,5-dihydroxyterephthalic acid MOF. Right: Nyquist plots in N_2- and CO_2-saturated electrolyte c,d) 2,5-dihydroxyterephthalic acid MOF and e),f) citric acid MOF.

CONCLUSION

The microwave-assisted crystalline MOFs displayed an enhanced electrocatalytic activity during CO_2 electroreduction process than the muffle-assisted counterparts.

REFERENCES

1. Bejtka, K. et al. ACS Appl. Energy Mater., 2(5), 3081-3091 (2019).

ACKNOWLEDGMENTS

The authors thank Instituto Politécnico Nacional and CONAHCYT for the financial support.

Ni-W thin films for hydrogen evolution reaction in acidic media and optimization using machine learning: insights on electrocatalyst durability.

Roger de Paz-Castany[1], Konrad Eiler[1], Aliona Nicolenco[2], Maria Lekka[2], Eva García-Lecina[2], Guillaume Brunin[3], Gian-Marco Rignanese[3], David Waroquiers[3], Annick Hubin[4], Eva Pellicer[1]*

[1] Physics department, UAB, Spain, presenting author.

[2] CIDETEC, Spain,

[3] Matgenix, Belgium

[4] SURF, VUB, Belgium

INTRODUCTION

Hydrogen is one of the most interesting energy vectors due to its high energy density and the possibility to be produced by water electrocatalysis. Nevertheless, the most efficient electrocatalysts are platinum group metals (PGM) which are a big deterrent towards large-scale production and broad implementation due to their scarcity and economic cost. Ni-W alloys are a good alternative for three different facts. First and foremost, Ni is a common and cheap metal with high activity towards the hydrogen evolution reaction (HER)[1], and by addition of W we can increase the corrosion resistance and mechanical strength of the alloy. Finally, W acts as a catalyst activator towards HER. Our study presents a machine learning (ML) approach trained by experimentally obtained data, such as onset potential and Tafel slopes in order to predict optimized synthesis parameters with the goal to enhance the performance of Ni-W alloys towards HER in acidic media in terms of activity and durability.

EXPERIMENTAL/THEORETICAL STUDY

Ni-W alloy thin films are synthesized by electrodeposition from aqueous media from a gluconate-containing electrolyte. XRD, SEM and EDX were performed to characterize the samples.

The electrochemical activity at HER was tested in 0.5 M H_2SO_4 by 200 cycles of linear sweep voltammetry. Long-term stability tests were performed by chronopotentiometry for 7 days at a current density of $j = -10$ mA/cm^2.

RESULTS AND DISCUSSION

Electrodeposited at different current densities and varying temperatures, the W content of all Ni-W films remains constant at 12 at%. A strong variation in morphology can be observed due to the change in the deposition parameters (Fig. 1). The highest electrochemical surface area (ECSA) was obtained for deposits plated at 50 ºC and $j = -4.8$ mA/cm^2, also yielding the lowest overpotential and Tafel slope. After training of the ML model with the initial set of data, the parameters proposed by the ML algorithm (−9 mA/cm^2 at 62 ºC) led to an improved Tafel slope of 209 mV/dec (45 mV/dec after 200 cycles) and an overpotential to reach −10 mA/cm^2 (η_{10}) of 284 mV (106 mV after 200 cycles).

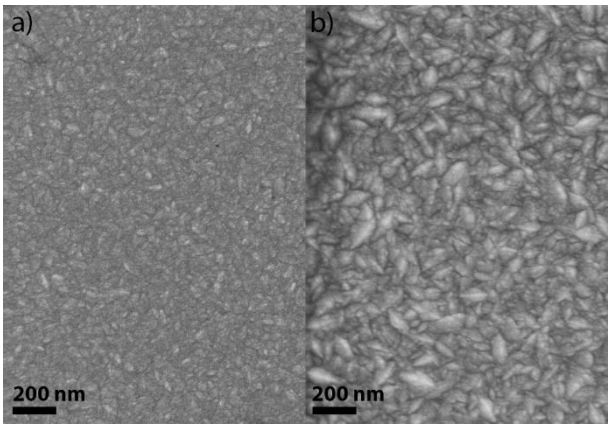

Fig. 1 SEM images of the Ni-W films electrodeposited at a fixed current density of $j = -4.8$ mA/cm^2 at (a) 25 °C and (b) 50 °C.

CONCLUSION

The implementation of a ML model enabled the prediction of optimized electrodeposition parameters for Ni-W thin films with significantly enhanced electrocatalytic activity towards HER and improved long-term stability over 7 days in acidic media.

REFERENCES

1. V. Vij et al., ACS Catal. 7 (2017) 7196-7225.
2. Y.B. Mollamahale et al., Mater Lett. 213 (2018) 15-18.

ACKNOWLEDGMENTS

This work has received funding from Horizon Europe under grant agreement No 101058076 - NICKEFFECT.

Nanostructures for the thermal and electromagnetic isolation of Space and Ground Instrumentation

L. Madueño[1], L. G. Vivas[2], D. Ramos[1], C. Martín-Rubio[1], A. Rivelles[3], A. Ruiz-Clavijo[2], A. Diaz[1], M. Schneider[4], B. Plaza[1], D. Poyatos[1], J. C. del Hoyo[1], O. Caballero-Calero[2], M. Worgull[4], S. Martin[1], B. Martín[1], M. Maicas[3], D. Navas[5], M. Martín-González[2], R. Sanz[1*]

[1]Instituto Nacional de Técnica Aeroespacial, INTA, Spain. sanzgr@inta.es
[2]Instituto de Micro y Nanotecnología, IMN-CNM, CSIC (CEI UAM+CSIC), Spain.
[3]Institute for Optoelectronics and Microtechnologies, Polythecnic University of Madrid, Spain
[4]Karlsruhe Institute of Technology, Institute of Microstructure Technology, Germany
5 Instituto de Ciencia de Materiales de Madrid, CSIC, Spain.

ABSTRACT

The thermal and electromagnetic isolation (DC to GHz range) are primary issues for space-based instrumentation and, consequently, the success of the whole space mission. This simultaneous isolation becomes critical in extremely sensitive devices as Transition Edge Sensors[1]. These type of sensors will be included in the X-IFU instrument, (ATHENA mission) that will be the next European Space Agency's space X-Ray telescope[2].

Engineered nanostructured materials may be appropriate and offer tailored responses and better performances than single-phase/component materials. However, these nanostructures must withstand harsh environments, e.g. ultrahigh vacuum and cryogenic temperatures. In addition, the synthesis of these nanostructures must be scalable to be applicable on macroscopic (m^2) areas.

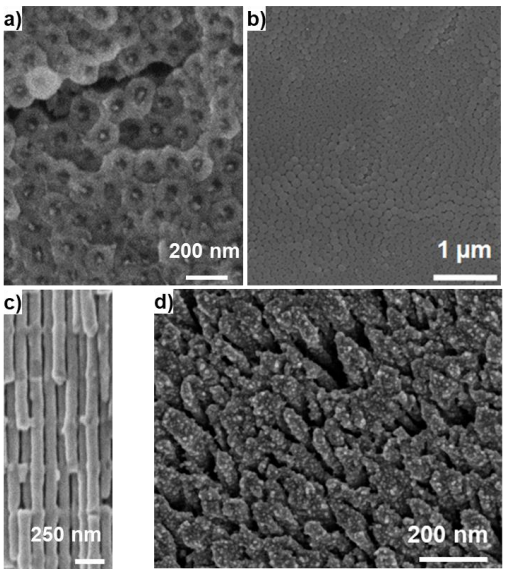

In this contribution, we will focus on the synthesized and characterized nanostructures that we propose to be included in future ground and space cryostats. We have applied two parallel synthesis approaches:

The first one bases on nanocomposite flexible films composed of Polyether-ether-ketone matrix filled with TiO_2 nanotubes, FeNi [3,4] thin films and Au/Co nanocolumns/nanoparticles (Nc/Np)[5,6] (Nanostine SL). The second one uses self-ordered three-dimensional (3D) nanonetworks of nanowires and TiO_2 nanotubes[7] obtained by electrochemical routes on aluminum and titanium[3].Each type of functional nanostructures exhibit pros and cons that will be analyzed and compared. PEEK-based nanocomposites are suitable for integration into additively manufactured PEEK structures, while 3D nanonetworks could be implemented as conformal coatings on aluminum or titanium parts. We will discuss their possible optimal application in future space cryostats.

Fig. 1 a) PEEK-TiO_2 nanocomposites b). Nanostructured FeNi surface c) 3D nanonetwork d) Nc/Np

REFERENCES

1. L. Fàbrega, et al, Proc. SPIE 9144, Space Telescopes and Instrumentation 2014: Ultraviolet to Gamma Ray, 91445P
2. https://www.the-athena-x-ray-observatory.eu/en
3. R. Sanz et al, Applied Surface Science, 399, 451-462 (2017).
4. C. Martín-Rubio et al. IEEE Transactions on Magnetics, 59, 2, 1-6 (2022)
5. G. Troncoso et al. Applied Surface Science, 526, 146699 (2020)
6. www.nanostine.com
7. A. Ruiz-Clavijo et al., Adv. Electron. Mater. 8, 2200342 (2022)

ACKNOWLEDGMENTS

This work was supported by: Karlsruhe Nano Micro Facility (KNMF), a Helmholtz Research Infrastructure at the Karlsruhe Institute of Technology, European Union (MSCA project MIDAS Grant 101107507) and grants PID2020-115325GB-C31, PID2020-117024GB-C42 and PID2020-118430GB-100 funded by MCIN/AEI/ 10.13039/501100011033.

Advanced Silicon Nanowire Fabrication and Annealing Temperature Optimization for Improving Solar Cell Efficiency

Sakti Prasanna Muduli[1], and Paresh Kale[2, *]

[1,2]Department of Electrical Engineering, National Institute of Technology Rourkela, Odisha, India, 769008

[1]*Presenting author: pinkusakti08@gmail.com*

[2,*]*Corresponding author: pareshkale@nitrkl.ac.in*

Abstract

Silicon nanowires (SiNWs) are garnering attention for potential in future photovoltaic technology. The notable features outperform conventional bulk silicon, including a large surface area, anti-reflective properties, and shorter carrier transportation paths. However, a key challenge lies in the fabrication and doping of SiNWs for p-n junction in SiNW-based photovoltaics. The work employs cost-effective pre-optimized metal-assisted chemical etching (MACE) parameters for p-type SiNW array fabrication and spin-on-doping with P_2O_5 as the P-source by phosphosilicate glass (PSG) layer formation to form an n-type emitter. A Teflon-lined stainless-steel MACE setup was used for the SiNW array fabrication to avoid the unwanted SiNW formation on the rear side of the Si substrate. The annealing temperature was optimized considering the doping diffusion depth and the oxidation layer on the inner surface of the nanopores of the SiNW tips. Annealing above 900 ºC causes oxidation on SiNW tips, leading to tip dissolution during PSG layer removal, shortening SiNW length, and widening of the bandgap. The increase in annealing temperature dissolves the surface phosphorus clusters, improving the doping uniformity with increased doping depth. The optimized annealing temperature (900 ºC) results in a bandgap of 1.57 eV, with a 42.6% improvement in ultimate efficiency. With the fabrication modification and annealing temperature optimization, the power conversion efficiency and fill factor improved by 33.7% and 37.6%, respectively, primarily due to increased shunt resistance.

Keywords: Spin-on doping; PSG layer; Phosphorus clusters; Diffusion depth; Shunt resistance

Advancing Understanding of Composite Polymer Electrolytes with LLZO Nanofibers

Sanja Tepavcevic*, Michael Counihan, Jungkuk Lee, Yuepeng Zhang Pallab Barai, Venkat Srinivasan,

Materials Science Division, Argonne National Laboratory, 9700 S Cass Ave, 60439, Lemont, IL, USA

sanja@anl.gov, +1-312-301-7957

Abstract

Ceramic Li6.55Al0.2La3Zr2O12 (LLZO) is one of the most attractive electrolyte materials for solid-state batteries that combined with metallic Li anodes holds the promise for safer and more energetically dense battery, but its performance is limited by the increases in electrolyte-electrode interfacial resistances upon cycling. The combination of Li^+-conducting ceramics and polymers offers a new pathway to create better electrolytes with both high ionic conductivity and good (electro)mechanical interfacial properties. We optimized two-step annealing processing conditions for the fabrication of cubic-LLZO nanofibers and Li_2CO_3 removal. Using industrially relevant roll-to-roll electrospinning and slot-die coating, we fabricated thin composite membranes with reproducible thickness down to 20 microns. We investigated PEO based composite polymer electrolyte (CPE) with a high, 50 wt% loading of Al-doped LLZO nanofibers in comparison with nanofiber-free PEO electrolyte. XPS measurements show that LLZO is not present at the composite electrolyte surface, and solid electrolyte interphase (SEI) formation is dictated solely by PEO and LiTFSI when reacting with Li metal. Electrochemical SEI formation, studied by cyclic voltammetry, shows SEI formation is identical with and without up to 75 wt% LLZO in the electrolyte. Galvanostatic cycling with lithium symmetric cells shows that the critical current density (CCD) can be tripled by including 50 wt% LLZO, but half cell cycling reveals this comes at the cost of CE. Varying the LLZO loading shows that even a small amount of LLZO drastically lowers the CE, from 88% at 0 wt% LLZO to 77% at just 2 wt% LLZO. Mesoscale modelling reveals that the increase in CCD cannot be explained by an increase in the macroscopic or microscopic stiffness of the electrolyte; only the microstructure of the LLZO nanofibers in the PEO-LiTFSI matrix slows dendrite growth by presenting physical barriers that the dendrites must push or grow around. This tortuous lithium growth mechanism around the LLZO is corroborated with mass spectrometry imaging. Electrochemical impedance spectroscopy (EIS) analysis showed comparable bulk ionic and interfacial resistances with and without nanofibers, indicating that PEO dominates Li^+ transport and interfacial chemistry. The total Li-ion conductivity of the composite is still governed by the polymer matrix due to high interfacial resistance between the garnet particles and the PEO/LiTFSI matrix. This work highlights important elements to consider in the design of CPEs for high-efficiency lithium metal batteries.

Enhancing Photocatalytic Water Purification through Optimized Thermal Reduction of Graphene Oxide: Synthesis and Sunlight-driven Application of rGO-TiO_2 Nanocomposites

Satam Alotibi[1*], Rana H. Al Otaibi 1, Nada F. Al-Ablan 1, Mohammed Alyami[1], Abdellah Kaiba[1], Fatehia S. Alhakami[1], and Talal F. Qahtan[1]

[1]Physics Department, College of Science and Humanities in Al-Kharj, Prince Sattam Bin Abdulaziz University, Al-Kharj 11942, Saudi Arabia

*Corresponding author: sf.alotibi@psau.edu.sa (Satam Alotibi)

INTRODUCTION

Addressing global water pollution, this study investigates the optimal thermal reduction of graphene oxide (GO) to synthesize reduced graphene oxide (rGO) and its integration with TiO_2 nanoparticles to form rGO-TiO_2 nanocomposites for sunlight-driven water purification. The process leverages in situ thermal reduction within a nitrogen atmosphere, with 240 °C identified as the optimal reduction temperature through thermogravimetric analysis (TGA) and differential scanning calorimetry (DSC)[1,2].

EXPERIMENTAL/THEORETICAL STUDY

Synthesis involved the careful thermal reduction of GO, followed by the combination with TiO_2 nanoparticles. Characterization through Raman spectroscopy, X-ray photoelectron spectroscopy (XPS), and scanning electron microscopy (SEM) confirmed the effective removal of oxygen-containing functional groups and the restoration of the graphene-like structure.

RESULTS AND DISCUSSION

The rGO-TiO_2 nanocomposites demonstrated enhanced photocatalytic efficiency in sunlight-driven degradation of methylene blue, outperforming pure TiO_2 due to their improved structural and optical characteristics. Such advancements highlight the role of these nanocomposites in sustainable water treatment, underscoring the utility of solar energy for environmental clean-up. The observed improvement is credited to the ideal thermal reduction conditions for GO that led to the reestablishment of the graphene-like configuration in rGO, thus elevating the photocatalytic performance of the nanocomposites[3,4].

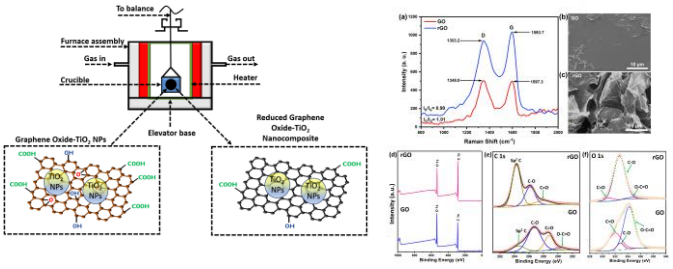

Fig. 2 (a) The Raman spectra of the GO powder and the rGO powder. (b and c) SEM images of GO powder and the rGO powder. (d-f) The XPS spectra of the GO powder and the reduced GO powder. (d) The XPS survey spectra show the presence of carbon and oxygen elements. The high-resolution C1s (e) and O 1s (f) spectra provide information on the chemical composition and electronic structure of the materials. The rGO was obtained from in situ thermal reduction by TGA at 240 °C under a nitrogen environment.

Fig. 1 Illustrates the thermal reduction of GO at 240 °C in a nitrogen atmosphere, emphasizing the removal of oxygen groups and the transformation into rGO. This figure provides a visual summary of the reduction process, underlining the methodology of the study.

CONCLUSION

This research underscores the importance of optimized thermal reduction of GO for the development of efficient photocatalytic materials. The rGO-TiO_2 nanocomposites represent a significant advance in harnessing sunlight for water purification, contributing to the field of sustainable environmental technologies.

REFERENCES

1. Romero, A., et al., Mater. Chem. Phys., 203, 284-292, 2018.
2. Singh, P., et al., Arab. J. Chem., 13, 3498-3520, 2020.
3. Afzal, M.J., et al., Environ. Technol., 40, 2567-2576, 2019.
4. Chen, Y., et al., J. Nanoparticle Res., 19, 200, 2017.

Luminescent Properties of Mix Rare Earth Ion Doped Alkali Fluoro Borate Glasses for Solid State Lighting Applications

Satish khasa[1*] and Jyoti Dahiya[1]

[1]*Department of Physics, Deenbandhu Chhotu Ram University of Science and Technology, Murthal, Haryana*

Corresponding Author e-mail: skhasa.phy@dcrustm.org

Multi-component glasses with compositions $x(La_2O_3)•(1-x)Dy_2O_3•10Bi_2O_3•30LiF•60B_2O_3$ (where La_2O_3= Eu_2O_3, Sm_2O_3) were synthesized via melt-quench technique to explore their application as LED material. X-ray diffraction profile of all the prepared compositions, confirmed the short-range order and amorphous nature of prepared samples. Their luminescent properties were studied and compared via UV-Vis-NIR and Photoluminescence studies. From UV-Vis-NIR spectroscopy the obtained direct optical band gap (E_g) values suggest semiconducting nature of prepared samples. Low values of Urbach energy indicated the presence of a smaller number of disorders and defects in the matrix. The nephelauxetic effect revealed the nature of RE-O bond in the matrix i.e., either covalent or ionic. Photoluminescence excitation and emission spectra were studied for both RE ions co-doped in the glass matrix for a variety of excitation wavelengths. The obtained colour parameters like CIE coordinates, CCT, CP% and CRI and Y/B Ratio were correlated with standard white light parameters. CIE coordinates of composition DELBB (x = 0.2) excited at wavelength 380 nm found to be (0.329, 0.342), lies closest to white light coordinates (0.333, 0.333). It has low colour purity (1.8%), high colour rendering index (58) and Y/B ratio is approaching one (1.08) which is the prime requirement.

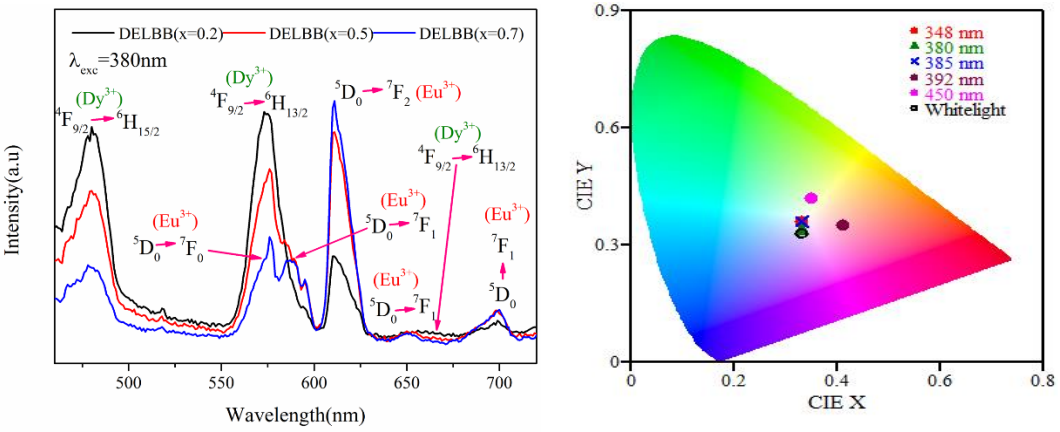

Fig.1 (a) PL spectra of Dy^{3+} and Eu^{3+} co-doped lithium bismuth borate glasses for excitation wavelength 380nm **(b)** Chromaticity Diagram of glass composition DELBB(x=0.2) excited at different excitation wavelengths

This composition is suitable for Cool WLEDs application as its CCT was evaluated as 5667K which lies in cool white region. In present work, it was observed that as an effect of co-doping of RE ions, emission colour can be tuned from cool white to **neutral** white and warm white region by varying excitation wavelengths. Thus, the prepared glasses are potential **colour tuneable luminescent materials**.

1. J Dahiya, A Hooda, A Agarwal, S Khasa, *Optical Materials*, 134,113162, 20

Development and Evaluation of Polyacrylonitrile-co-methyl acrylate (PAN-MA) Nanofiber Composite Membranes for Potential Application as Proton Exchange Membranes in Fuel Cells

Seda Köksal Yeğin[1,2*], Mualla Öner [1*] and Tomáš Remiš [3], Martin Tomáš[4], Tomáš Kovářík[5]
[1*]Chemical Engineering Department, Yıldız Technical University, Turkey, presenting author, corresponding author
[2*]Ion Membrane Company, Turkey, corresponding author
[3]Chemical Processes and Biomaterials New Technologies[3], University of West Bohemia, Czech Republic
[4]Department of Mathematics, Physics and Technology, University of West Bohemia, Czech Republic
[5]Department of Material Science and Technology, University of West Bohemia, Czech Republic

INTRODUCTION

The depletion of fossil fuels and the urgent need to address climate change has significantly increased the importance of hydrogen energy. One of the most notable advancements in hydrogen technology is the development of Proton Exchange Membrane (PEM) fuel cells, which have gained commercial availability in the market. These membranes are composed of fluorine-containing polymers based on perfluorosulfonic acid (PFSA). However, it is important to note that certain PFSAs pose risks as they are hazardous, persistent, and capable of bioaccumulation. In order to further advance hydrogen technology, it is crucial to develop PFSA-free membranes (PEMs) that are not only cost-effective but also highly efficient. In this research, a novel composite membrane based on Polyacrylonitrile-co-Methyl Acrylate (PAN-MA) was prepared using the electrospinning method. The purpose of this study was to investigate the effects of borax decahydrate and fumed silica as additives on the properties of the membrane.

EXPERIMENTAL/THEORETICAL STUDY

To characterize the membrane, several techniques were employed, including Electrochemical Impedance Spectroscopy (EIS), Thermogravimetric Analysis (TGA), and Scanning Electron Microscopy (SEM).

RESULTS AND DISCUSSION

The ionic conductivity of the composite membrane with 1% silica was measured to be 0.124 S/m at a thickness of 45 µm. Similarly, the ionic conductivity of the composite membrane with 1% borax decahydrate was found to be 0.145 S/m at the same thickness. In comparison, the PAN-MA membrane without any additives exhibited an ionic conductivity of 0.126 S/m.

CONCLUSION

Based on these results, it can be concluded that the addition of borax decahydrate as an additive in proton conductive membranes can enhance both ionic conductivity and thermal properties. This finding has important implications for the development of improved membranes for various applications in the field of proton exchange membranes and fuel cells.

REFERENCES

1. A. G. Olabi and E. T. Sayed, Energies-16, p. 2431, (2023)
2. Y. Qi, J. Liu et al, Journal of The Electrochemical Society, p. 168, (2021)
3. M. M. Tellez-Cruz, et al, Polymers, vol. 13, p. 3064, (2021)
4. S. Xiong et al., Membranes-13, p. 184, (2023)
5. E. Qu, et al, Journal of Power Sources, vol. 533, p. 231386, (2022)
6. P. Kallem et al, ACS Sustainable Chem. Eng., p. 1808−1825, 6 November 2018.
7. OECD Environment Directorate Env., Health and Safety Pub. Series on Risk Management No. 29, (2015)

ACKNOWLEDGMENTS

This work has been supported by the Research Fund of the Yıldız Technical University. Project Number: FDK-2022-4816.

ANM2022 (www.advanced-nanomaterials-conference.com) will host seven simultaneous conference sessions namely,
(ANM) Advanced Nano Materials
(AEM) Advanced Energy Materials
(AGM) Advanced Graphene Materials
(AMM) Advanced Magnetic Materials
(APM) Advanced Polymer Materials
(OLED) Organic Light Emitting Diodes
(HE) Hydrogen Energy
(SEM) Solar Energy Materials

Elucidating the Mechanisms of Water Adsorption and Release in Metal-Organic Frameworks through Simulation and Machine Learning

Serdal Kirmizialtin[1,2], Nour Alkhatib [1,2], Nakyeong Ahn[1]

1. Chemistry Program, New York University Abu Dhabi (NYUAD), P.O. Box 129188, Abu Dhabi, United Arab Emirates
2.Chemsitry Department, New York University, NY, USA

Global water scarcity has propelled the search for innovative mitigation strategies in atmospheric water harvesting, with Metal-Organic Frameworks (MOFs) emerging as a promising solution. However, the detailed atomic interactions and physical principles governing the water adsorption process in MOFs remain poorly understood. In this study, we utilize computer simulations to investigate the mechanisms of atmospheric water harvesting through recently discovered MOFs. Our simulations reveal variations in water uptake capacity under different humidity levels, in agreement with experimental data. A comparative analysis of these MOFs provides molecular insights into the thermodynamic and dynamic factors that influence the adsorption process and enable the efficient release of water upon heating. Employing machine learning for high-throughput screening, we identify novel MOFs that outperform those previously reported. We use Shapley Additive Explanations (SHAP) to rank the properties contributing to higher uptake capacity. Additionally, we explore the hydrogen bond network within MOFs using network science concepts, finding that unique network properties correlate with their water uptake and release behaviors. Our findings highlight the essential role of unsaturated water clusters for the facile release of water with temperature increase. This work elucidates the fundamental principles driving water adsorption in MOFs, guiding the design of more effective materials for atmospheric water harvesting.

Ultrafast Laser Synthesis of Nanoporous Zeolites

Mehdi Hagverdiyev [1], Meryem Merve Dogan [1], Omer Ilday [2], Serim Ilday [2], Sezin Galioglu [1*]

[1]National Nanotechnology Research Center, Bilkent University, Türkiye
[2]Faculty of Electrical Engineering and Information Technology, Ruhr University, Bochum, Germany
* Corresponding author e-mail: sezin@unam.bilkent.edu.tr

INTRODUCTION

Zeolites are a class of nanoporous materials that are used in a wide variety of scientific, technological and commercial applications. They hold the greatest commercial importance among all porous materials due to their high specific surface areas, molecular size (below 2 nm), and well-defined pore structures[1,2]. In conventional hydrothermal synthesis method, the induction period-defined as the amount of time elapsed between the achievement of a supersaturated solution and the observation of first crystals-is typically more than 15 hours or days. However, the reaction time scale of silica polymerization/depolymerization reactions is in the range of femtosecond/picosecond ranges[3,4]. This complexity arises from the challenge of analyzing more than 40 polymerization/depolymerization reactions occurring simultaneously during this extended period. Here, we propose a novel ultrafast laser synthesis method for zeolites[5]. We argue that ultrafast (femtosecond) lasers are the ideal candidates because they enable fast and high-resolution spatiotemporal energy deposition within the time scale of silica polymerization reactions. Laser-induced flows further accelerate the induction period, thereby shortening the reaction time.

EXPERIMENTAL/THEORETICAL STUDY

Silicalite-1, hierarchical ZSM-5, and Zeolite A zeolites (MFI and LTA framework types) were synthesized using an ultrafast laser with specifications of λ = 1040 nm, repetition rate: 300 fs, 9W Spectra Physics laser. Comprehensive characterizations were carried out using SEM, SEM-EDS, XRD, HR-TEM, SAED, TGA-DTA, BET, and ATR-FTIR analyses techniques. The results were compared with the zeolites synthesized via conventional hydrothermal synthesis method (control).

RESULTS AND DISCUSSION

The transparent precursor suspension ensures that multiphoton absorption occurs at 1040 nm wavelength (Fig. 1). Thanks to the steep thermal gradient and surface tension, laser induced flows are formed in the precursor suspension. Morphology and crystallinity of the zeolite crystals were characterized.

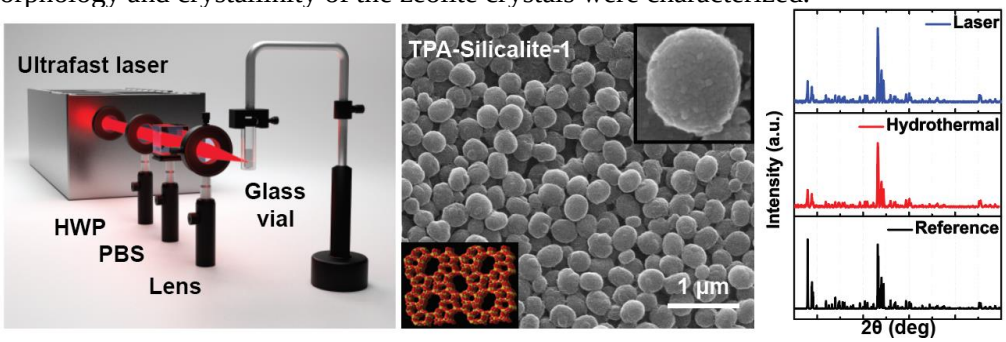

Fig. 1 Schematic of ultrafast laser zeolite synthesis set-up, and SEM and XRD images of the TPA-Silicalite-1 zeolites synthesized via ultrafast laser method.

CONCLUSION

By using ultrafast laser zeolite synthesis method, comparable crystallinity (>90%), product yield (wt.%), stability, and reproducibility, in addition to superior homogeneity and uniformity, were achieved compared to those synthesized using conventional hydrothermal method.

REFERENCES

1. G. Feng et. al, Science 351, 1188 (2016); **2.** D.J. Wales et. al, Chem. Soc. Rev. 44, 4290 (2015); **3.** X.Q. Zhang et. al, JACS 133, 6613 (2011); **4.** C.L. Schaffer et. al, J. Phys. Chem. C 112, 12653 (2008); **5.** S. Galioglu et. al, to be submitted.

ACKNOWLEDGMENTS

This work is supported by the Scientific and Technological Research Council of Türkiye (Projects: 118F115 and 120F147).

Interface and surface engineering of CIGS films to improve cell performance

Sivabalan Maniam Sivasankar [1], Carlos de Oliverira Amorim [1], Rui Ramos Ferreira e Silva [2], António F da Cunha [1],
[1]Department of Physics, i3N, University of Aveiro, Portugal
[2]Department of Materials and Ceramics Engineering, University of Aveiro, Portugal

INTRODUCTION

Solar energy is a sustainable, clean, and cost-effective source of energy. Amongst the different types of photovoltaic modules, thin-film technology is considered to be the second generation. When it comes to selecting the most cost-efficient and stable thin-film technologies, Cadmium Telluride (CdTe) and $Cu(In,Ga)(S,Se)_2$ or (CIGS) are considered to have the most potential. Thin-film technology based on the CIGS compound, is one of the most promising technologies with a band gap that can be adjusted from around 1.0 eV (CIS) to around 2.4 eV (CGS)[1].

In this article, we discuss the techniques we have implemented to produce high-quality films that are compact, have large grains, high crystallinity, and minimal defects. To achieve this, we explore various solutions such as establishing the optimum precursor order, introducing thin metal oxide interlayers, and doping alkaline impurity.

EXPERIMENTAL STUDY

The absorber precursors are deposited by the sputtering deposition technique in an in-house setup. The absorber precursors are then annealed in one of two ways, either within the deposition chamber or by Rapid Thermal Process (RTP). The absorber is then analyzed by a variety of techniques such as SEM-EDX for morphology and composition analysis, XRD for crystallinity studies, and GDOES for depth elemental composition analysis and band gap profile calculation[2].

RESULTS AND DISCUSSION

We have found that the commonly accepted bi-layer precursor approach for creating solar cell absorbers (Mo/CuGa/In or Mo/In/CuGa) may not be the best option. We discovered that using CuGa in contact with Molybdenum resulted in poorly performing cells, despite the CIGS layers being highly compact. In contrast, using Indium in contact with Molybdenum led to poor adhesion between CIGS and Mo due to void formation, resulting in rough surfaces. However, the cells made from the latter absorbers were significantly more efficient.

We found that there is a noticeable difference in the morphology of the absorber depending on whether it is annealed within the deposition chamber or with RTP. We observed that the absorber was much more compact when annealed with RTP as compared to annealing within the chamber. However, this method had the drawback of significantly increasing the chances of substrate warping or absorber damage.

We also attempted to improve the absorber effectiveness by doping with alkali metal through NaF or KF evaporation on the CIGS surface, but the results have been limited so far. On average, we observed a nominal improvement of only 1-2% between absorbers that had been treated with alkali metal and those that were not.

To analyze the depth elemental composition, we used GDOES and found that the Ga accumulation at the back of the absorber resulted in an increasing bandgap profile toward the back of the absorber.

CONCLUSION

We report here the results of our endeavor to develop high-quality, compact, and highly crystalline absorbers for CIGS solar cells.

REFERENCES

1. Turcu, M., Kötschau, I. M. & Rau, U. Composition dependence of defect energies and band alignments in the $Cu(In_{1-x}Ga_x)(Se_{1-y}S_y)_2$ alloy system. *J. Appl. Phys.* **91**, 1391–1399 (2002).

2. Bär, M. *et al.* Determination of the band gap depth profile of the penternary $Cu(In_{(1-X)}Ga_X)(S_YSe_{(1-Y)})_2$ chalcopyrite from its composition gradient. *J Appl Phys* **96**, 3857–3860 (2004).

(SEM) Solar Energy Materials

Bismuth-titan-silicate oxide glass-ceramics for energy storage

Stanislav Slavov
Department of Mathematics, University of Chemical Technology and Metallurgy, 8 Kl. Ohridski Blvd., 1756 Sofia, Bulgaria, e-mail: stanislavslavov@uctm.edu

INTRODUCTION

Storing energy in an optimal way is one of the most important problems nowadays. The synthesis of materials with improved dielectric properties is of great importance because of the possibility of their application as resistive sensors and as components of energy storage devices.

EXPERIMENTAL/THEORETICAL STUDY

The samples in the system Bi_2O_3-TiO_2-SiO_2-Nd_2O_3 was carried out by the method of supercooled melt with a cooling rate of 10^2 K/s in two stage: with temperatures respectively at 1150 °C and 1450 °C and rapid cooling to room temperature. For characterization of the resulting materials are used the following equipment: X-ray phase analysis XRD - TUR M62, Cu-Kα.,

RESULTS AND DISCUSSION

Electrical impedance measurements of selected glass-ceramics make it possible to estimate conductivity and dielectric constants over a wide temperature range from room temperature to 300 °C, for frequencies from 100 Hz to 100 kHz. The impedance and phase angle values determined for the investigated ranges are of the order of 10^8 Ohm and -90°, respectively.

CONCLUSION

Changing the starting composition of the oxide mixture allows control of the dielectric properties, such as dielectric constant and dielectric loss, and also the resulting samples have a wide range of Curie temperatures. The classical method of synthesis gives reason to obtain new dielectric materials that meet all environmental norms (using ecological raw materials) and with reduced production costs.

REFERENCES

Anirban Chakrabarti, Sreedevi Menon, Anal Tarafder, Atiar Rahaman Molla, Glass–ceramics: A Potential Material for Energy Storage and Photonic Applications, Springer, Singapore, 2022, doi.org/10.1007/978-981-19-5821-2_10

ACKNOWLEDGMENTS

The works presented in this chapter are developed as part of contract №: BG-RRP-2.004-0002-C01, project name: BiOrgaMCT, Procedure BG-RRP-2.004 „Establishing of a network of research higher education institutions in Bulgaria“, funded by BULGARIAN NATIONAL RECOVERY AND RESILIENCE PLAN and is part of an inter-academic collaboration project between the Bulgarian Academy of Sciences, the Tallinn University of Technology and the Institute of Low Temperature and Structure Research, Polish Academy of Sciences.

The Development of High-performance Electrochemical Properties with a Fine-grained Aluminium Anode for Al-air batteries

Suphitcha (Moonngam) [1] and Chaiyasit (Banjongprasert)* [1,2*]
[1]Materials Science Research Center, Faculty of Science, Chiang Mai University, Thailand
[2*]Department of Physics and Materials Science, Faculty of Science, Chiang Mai University, Thailand,
corresponding author (chaiyasit.b@cmu.ac.th)

INTRODUCTION

This study aims to develop aluminum alloys for anodes in metal-air batteries. Scientists have delved into methodologies like severe plastic deformation (SPD)[1-3], including equal channel angular pressing (ECAP), to refine the microstructure through plastic deformation[4-5]. This refinement has been demonstrated to improve electrochemical activity[4,6]. An increase in grain boundaries from grain refinement enhances the electrochemical activities of Al-Zn-In anodes, rendering them well-suited for application in aluminum-air batteries[4]. Furthermore, friction stir process (FSP) has emerged as a compelling conventional approach for microstructure refinement and the development of aluminum anodes for metal-air batteries[6-9]. The process can refine the grain structure by up to 90%[7], eliminate defects, and enhance material properties, such as improving corrosion resistance[7,9].

EXPERIMENTAL/THEORETICAL STUDY

This study explores the properties of ultrafine-grained aluminum alloy (UFG-Al) manufactured via the friction stir process, with the objective of optimizing its suitability as an anode material for metal-air batteries. The aluminum alloy underwent the friction stir process utilizing hexagonal pins in order to achieve grain refinement. Following this, heat treatment was applied at different temperatures and durations. Microstructural analysis, employing electron backscatter diffraction, was conducted to assess crystal orientation and material texture. Corrosion behavior was studied through self-corrosion tests, hydrogen evolution measurements, and electrochemical polarization tests. Battery performance tests were used to assess discharge behavior.

RESULTS AND DISCUSSION

The results indicate that aluminum alloy with an ultrafine-grained structure, manufactured through friction stirring, exhibits significant promise as a potential anode material for metal-air batteries in energy storage devices. It is possible to manipulate the heat treatment parameters, as well as the crystal orientation and texture of the alloy.

CONCLUSION

This research underscores the viability of utilizing ultrafine-grained aluminum alloys, produced through friction stir processing, as effective anode materials in metal-air battery applications.

REFERENCES

1. A.V. Volokitin et al, University of Tehran, 84–98 (2023)
2. I. Sabirov et al, Mat. Sci. Eng. A. 560, 1–24 (2013)
3. L. Fan et al, J. Power. Sources. 284, 409–415 (2015)
4. S. Linjee et al, Energy. Reports. 8, 5117–5128 (2022)
5. L Fan et al, J. Power. Sources. 299,66–69 (2015)
6. L. Zhang et al, J Power Sources. 589, 233752 (2024)
7. K. Surekha et al, Surf. Coat. Technol. 202, 4057–4068 (2008)
8. D.F. Li et al, J. Mater. Res. Technol. 18, 1763–1771 (2022)
9. X. Zheng et al, Electrochim. Acta. 354, 136635 (2020)

ACKNOWLEDGMENTS

The authors would like to thank Center of Excellence in Materials Science and Technology, and Fundamental Fund 2024. The authors acknowledge the facilities and the scientific of Chiang Mai University. This research has received funding from the NSRF via the Program Management Unit for Human Resources & Institutional Development, Research and Innovation [grant number B13F660056]

Development of tubular carbon membrane for gas separation using kaolin support

Thaís Neves[1*], João Franco[1], Nilson Marcilio[1], Isabel Tessaro[1]
[1]Department of Chemical Engineering, Federal University of Rio Grande do Sul, Brazil,
thais.tneves@gmail.com*

INTRODUCTION

Gas separation processes using membranes have attracted attention in recent years due to lower energy demand compared to conventional processes such as distillation. Carbon membranes (CM) in supported configuration exhibit high chemical, thermal, and mechanical stability, along with molecular-sized pores capable of promoting the separation of gases such as CO_2 and CH_4. The properties of the supports used in the preparation of CM, such as pore size and roughness, have a significant influence on the uniformity of the selective membrane layers. Alumina tubular supports are the most commonly used for CM preparation[1]. However, these materials come with high costs, requiring the exploration of alternative supports. Kaolin is an abundant natural ore that can be utilized in the manufacturing of ceramic materials[2]. Therefore, the innovation in this work lies in the development of carbon membranes on low-cost tubular supports manufactured from kaolin for CM application.

EXPERIMENTAL/THEORETICAL STUDY

Kaolin tubular supports were obtained from Refratarios Cumbica company (Brazil). The CMs were prepared through three coating steps of the tubes with a polymeric solution formed by the mixture of polyetherimide (PEI) and polysulfone (PES). The first coating was carried out using the vacuum method, in which the support was connected to a vacuum system and immersed in a solution with a concentration of 18% wt. The second and third coatings were performed by dip-coating, with a solution of PEI-PES 14% wt. Pyrolysis at 700 °C was carried out between each coating step. Gas permeation tests were conducted with pure gases in a stainless steel tubular permeation module, with a length of 13.5 cm. Volumetric permeate flow rate measurements were performed using a flowmeter (Agilent).

RESULTS AND DISCUSSION

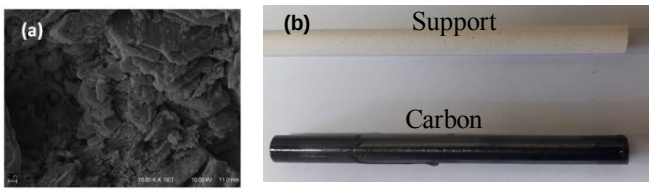

Fig. 1 SEM image of kaolin ceramic tube (a) and photographs of tubular support and tubular CM (b).

Figure 1a shows the scanning electron microscopy (SEM) image of the kaolin tubular support. The plate-like morphology of the particles is characteristic of the kaolinite phase[3]. Figure 1b displays images of kaolin support and the carbon membrane formed over the tubular structure, through the pyrolysis precursor polymer layer deposited over the kaolin tube. Despite CH_4 having a larger kinetic diameter than CO_2, according the permeation testes, the membrane permeance to CH_4 was 4418 Barrer, whereas for CO_2, it was 2503 Barrer. The higher permeance to CH_4 is associated with the entropic factor, i.e., CH_4 exhibits a structure with greater vibrational and rotational mobility compared to CO_2[4]. Replications (triplicates) demonstrated similar results. This membrane exhibits higher permeability to CH_4 and a CH_4/CO_2 separation factor of 2. Similar selectivity to CH_4/CO_2 was found in the literature[5].

CONCLUSION

This work demonstrated the feasibility of preparing carbon membranes over low-cost supports. The membranes showed potential for gas separation, with higher permeance for CH_4, which may be attributed to an entropic contribution in the permeation of methane. Other membranes are currently being prepared with a higher concentration of the precursor polymeric solution in order to achieve higher separation factors.

REFERENCES

1. Salleh et. Al, Sep. Purif. Rev. 40, 261 (2011)
2. Hubadillah et al., Ceram. Int. 44, 4538 (2018)
3. Chakraborty, A.K. Phase Transformation of Kaolinite Clay. Springer (2014)
4. Fu et al. J. Membr. Sci. 539, 329 (2017)
5. Shehu et al., J. Adv. Chem. Eng. 6 (2016)

Development of kaolin-rice husk ash support for carbon membrane application

Thaís Neves[1*], João Franco[1], Nilson Marcilio[1], Isabel Tessaro[1]
[1]Department of Chemical Engineering, Federal University of Rio Grande do Sul, Brazil
thais.tneves@gmail.com*

INTRODUCTION

Carbon Membranes (CM) are comprised of promising materials for application in gas separation processes, given their lower energy demand compared to conventional methods such as distillation. Furthermore, these membranes demonstrate potential to separate gas species with similar dimensions, such as CO_2/CH_4. CMs are typically prepared over commercial alumina ceramic supports[1]. Alternatively, supports can be obtained from low-cost materials. Kaolin (K) is a natural ore with refractory properties, primarily composed of SiO_2 and Al_2O_3[2], while rice husk ash (RHA) is an agro-industrial residue containing high SiO_2 content[3]. The combination of these materials is a cost-effective alternative for the preparation of ceramic supports. The innovation in this study is the development of low-cost ceramic supports using K and RHA for CM applications.

EXPERIMENTAL/THEORETICAL STUDY

Flat supports were prepared with different proportions of K and RHA, ranging from 10 to 50% wt., using the dry pressing technique. The materials were sintered with a heating rate of 5°C/min up to a temperature of 1400°C for 2 hours. The developed ceramic supports, with a 34 mm diameter, were coated with an 18% wt. polymeric solution of a polyetherimide and polysulfone polymer blend using the spin coating technique, followed by solvent evaporation. The supported polymeric membranes were subjected to pyrolysis at 700°C with a heating rate of 3°C/min. The carbon membranes prepared on the flat supports will be tested in the pure gas permeation process for CO_2 and CH_4.

RESULTS AND DISCUSSION

Figure 1a presents the diffractogram of K sintered at 1400°C, showing characteristic peaks of the mullite phase. According to the SEM image, mullite exhibits needle-like particle morphology[4]. In Figure 1b, the SEM image of RHA calcined at 1400°C reveals the presence of cristobalite, quartz, and tridymite phases[5]. The particles of RHA exhibit a spherical morphology with some irregularities. Figure 1c includes photographs of a flat support composed of K and 20% wt. RHA (S), a photograph of the support coated with a polymeric solution (PM), and the resulting CM after pyrolysis. It was possible to coat the flat supports with the polymeric solution, which remained on the surface of the supports, i.e., there was no intrusion into the support structure. This favors the formation of carbon membranes on alternative supports.

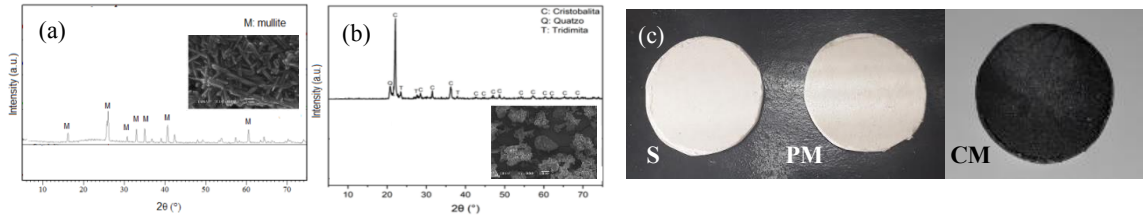

Fig. 1 Characterization of raw-materials (a) kaolin, (b) rice husk ash and (c) photographs of support (S), precursor membrane (PM) and carbon membrane (CM)

CONCLUSION

It was possible to prepare low-cost supports from K and RHA. The study introduces the potential to fabricate cost-effective supports for application in CM development. The carbon membranes are currently undergoing evaluation in the gas permeation process.

REFERENCES

1. Salleh et. Al, Sep. Purif. Rev. 40, 261 (2011)
2. Hubadillah et al., Ceram. Int. 44, 4538 (2018)
3. Foo et al. J. Colloid Interface Sci. 152, 39 (2009)
4. Fahad et al. Trans. Indian Ceram. Soc. 75, 47 (2016)
5. Kordatos et al. J. Mater. Cycles Waste Manag.15, 71 (2013)

Nanostructured Raney-Nickel electrodes for highly active and cost-efficient hydrogen evolution in alkaline media (AWE)

Timon Günther[1], Jonas Schick [1] and Richard Weihrich [1]
[1]Chair for Resource and Chemical Engineering, Institute for Materials Resource Management, University of Augsburg, Germany

INTRODUCTION

In this work we developed a cost-effective new fabrication method for highly efficient nanostructured Raney-Nickel electrode for alkaline water electrolysis (AWE) during the hydrogen evolution reaction (HER).[1] Further testing shows suitable application in the anion exchange membrane water electrolysis (AEMWE).[2]

EXPERIMENTAL/THEORETICAL STUDY

The electrodes were prepared via mechanical plating of aluminium on a nickel sheet and thermal treatment under various atmospheres to achieve leachable NiAl-phases such as Ni_2Al_3 and $NiAl_3$.[1,2] The electrochemical performance and surface area (ECSA) was determined with cyclic voltammetry (CV) and chronopotentiometry (CP) in a three-electrode and full cell setup. Electrochemical impedance spectroscopy (EIS), BET-analysis, REM-imaging and EDX-mapping were used to quantitively and qualitatively analyze the internal resistances, surface area and electrode degradation during electrolysis.[2]

RESULTS AND DISCUSSION

Current densities up to 1 A/cm² show low overpotentials of 150 – 220 mV at 100 mA/cm² at the cathode with Tafel slopes from 50 to 70 mV/dec. The “carpet-like” structure of the electrode leads to increased surface area of up to 10.9 m²/g of the Nickel catalyst and allows gas desorption and transport of hydrogen (and oxygen) without blocking inner pore structures of the electrode[3]. Long-term measurements at 1.2 to 1.8 V over 1-2 days in a full cell setup were used to study the degradation and confirm stability of the fabricated electrodes.[4]

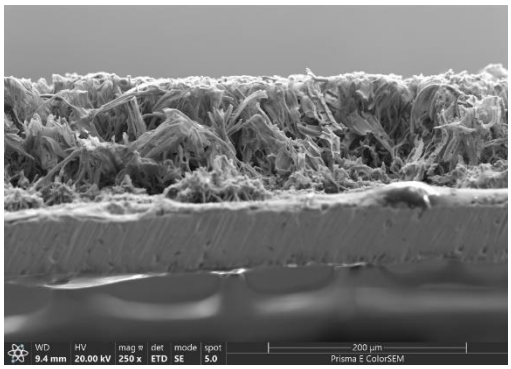

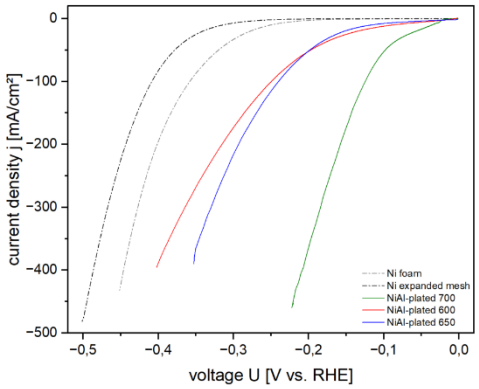

Fig. 1 SEM image of the nanostructured Raney-Nickel electrode via mechanical plating
Fig. 2 CV-curve of the fabricated Raney-Nickel electrodes during HER in 32 wt.-% KOH.

CONCLUSION

With its nanostructure and high electrocatalytically active surface area of the electrodes, this works shows a simple and cost-effective way to produce high-performing Raney-Nickel electrodes.

REFERENCES

1. C. Bernäcker et al, J. of the Electrochemical Society, 166, F357-F363 (2019)
2. E. López—Fernandez et al, ACS Catal., 10, 6159−6170 (2020)
3. C. Lee et al, Nature Energy 8, 685-694 (2023)
4. Y. Zhang et al, Int. J. of Hydrogen Energy 45 24248-24252 (2020)

Control of the photoluminescence quantum-yield of gold organometallic nanocomposites by pulsed laser driven CO_2 reduction reaction

Tommaso Del Rosso [1,*], Tahir[1], Guilherme C. Concas[1], Mariana Gisbert[1], Marco Cremona[1], Fernando Lazaro[1], Nicola Daldosso[2], Francesco Enrichi[2], Francis L. Deepak[3]

[1] Pontifical Catholic University of Rio de Janeiro, Department of Physics, Rua Marquês de São Vicente 225, 22451-900 Gávea, Rio de Janeiro, Brazil
[2] University of Verona, Department of Engineering for Innovation Medicine, Strada le Grazie 15, 37134 Verona, Italy
[3]International Iberian Nanotechnology Laboratory; Nanostructured Materials Group, Avenida Mestre Jose Veiga, Braga 4715-330, Portugal

E-mail: tommaso@puc-rio.br

Abstract: In recent years, there has been a huge interest in the CO_2 reduction reaction (CO_2RR) for the production of value-added raw materials in gas or liquid form. However, CO_2 fixation into nanoparticle systems has not yet been demonstrated. This research presents a novel approach to synthesize functional nanomaterial in colloidal form by CO_2 fixation through laser synthesis and processing of colloids (LSPC) in water [1]. These methods are historically considered as green-approaches, yielding ligand-free nanoparticles with no by-products. Our results show that carbon monoxide rich gold nanoparticles are observed after synthesis even in deionized water, while an alkaline water environment leads to C_2 and C_3 coupling, producing carboxylic acids as a typical fingerprint of the CO_2RR. Selective C_2 coupling is observed during laser processing of pre-existing gold colloids, while pulsed laser ablation of a gold target results in both C_2 and C_3 coupling to lactic acid. Remarkably, under certain conditions, photoluminescent organometallic nanocomposites are synthesized in the blue spectral region with a quantum yield of about 20% [2]. These findings open new paths to be explored in energetics, photonics, catalysis, and synthesis of functional nanomaterials at the nanoscale.

Acknowledgments:
This study was financed in part by the CAPES, FAPERJ, CNPq and AIRC.

References:
[1] D. Zhang, B. Gökce, and S. Barcikowski, "Laser Synthesis and Processing of Colloids: Fundamentals and Applications," *Chem Rev*, vol. 117, no. 5, pp. 3990–4103, Mar. 2017, doi: 10.1021/acs.chemrev.6b00468.
[2] Tahir et al.,"Pulsed laser driven CO_2 reduction reaction for the control of the photoluminescence quantum yield of organometallic gold nanocomposites", *Small Science*, 2024, https://doi.org/10.1002/smsc.202300328.

Effects of ZrO_2 addition and surface fluorination on the electrochemical properties of $LiNi_{0.5}Co_{0.2}Mn_{0.3}O_2$ cathode materials.

Tomohiro Ishikawa [1], *Jae-ho Kim*[*2] *and Susumu Yonezawa*[3]

1,2,3Department of Materials Science and Engineering, Faculty of Engineering, University of Fukui, Japan

[1]presenting author, [2]corresponding author (kim@matse.u-fukui.ac.jp)*

INTRODUCTION

Among positive electrode materials for lithium-ion batteries, Ni-rich ternary NCM ($LiNi_{0.5}Co_{0.2}Mn_{0.3}O_2$, LNCM) is drawing attention due to its high theoretical capacity (280mAh/g) and structural stability. However, there are still remained some issues which including non-uniformity in the metal composition of nickel, manganese, and cobalt, as well as significant effects of strain and cracking of the composite oxide during charge and discharge cycles. In this study, we investigated the effects of addition of fluorinated ZrO_2 in the preparation of LNCM on the sintering and electrochemical properties [1)]. Especially the surface fluorination [2)] of ZrO_2 particles can play a role to prevent aggregation between ZrO_2 particles, and it can enhance the effects of ZrO_2 addition.

EXPERIMENTAL/THEORETICAL STUDY

The surface fluorination of ZrO_2 (2μm) was conducted using fluorine gas under conditions of 25℃, 13.3 kPa,20.0 kPa for 10 min. To produce the $LiNi_{0.5}Co_{0.2}Mn_{0.3}O_2$ active material, $Ni_{0.5}Co_{0.2}Mn_{0.3}(OH)_2$ and Li_2CO_3 were mixed in a rotating and revolving mixer at a molar ratio of 2:1.05, followed by calcination in an electric furnace at 730℃ for 5 hours. After the primary calcination, ZrO_2 was added and mixed, and subjected to secondary calcination in an electric furnace at 900℃ for 8 hours. The active material ($LiNi_{0.5}Co_{0.2}Mn_{0.3}O_2$), acetylene black, and PVDF were kneaded in a mass ratio of 8:1:1, and the mixtures were coated onto an aluminum foil. It was used as a positive electrode. Lithium metal foil was used as the counter electrode, and a battery was assembled. Charge and discharge tests were conducted using this setup.

RESULTS AND DISCUSSION

The results (Fig. 1) of discharge capacities of each sample showed an increase in discharge capacity for samples with a fluorinated ZrO_2 addition. Especially Particularly the NCM sample containing ZrO_2 fluorinated with 13.3 kPa exhibited the superior discharge capacity. In this presentation, we will report on the results of the X-ray diffraction (XRD), field-emission scanning electron microscopy (FE-SEM), and X-ray photoelectron spectroscopy (XPS) analyses of each sample.

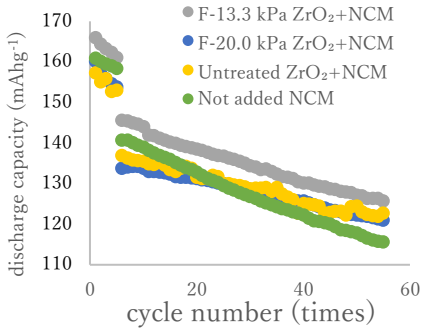

Fig.1 Cycle stability of various samples.[Below 5 cycles: 0.2C, more than 6 cycles: 0.5C]

CONCLUSION

The addition of fluorinated ZrO_2 resulted in improvements in discharge capacity and cycle performance of LNCM cathode. And the fine control of surface fluorination can especially affect the sintering and electrochemical properties of cathode materials.

REFFRENCES

1) Kai Yang, Li-Zhen Fan, Jia Guo, Xuanhui Qu, Electrochemical Acta, 63, 363-368 (2012)
2) M. Hata, T. Tanaka, D. Kato, J.H. Kim, and S. Yonezawa, Electrochemistry, 89, 223-229 (2021)

Carbon Dots-Polymer Composite Materials for WLED Application

Archana Pandey[1], Vaishali Raikwar[2]
[1,2]Physics Department, Ramniranjan Jhunjhunwala College, Ghatkopar, Mumbai-400086, India,
Presenting author: Dr. Vaishali Raikwar

Email: vaishaliraikwar@rjcollege.edu.in

Introduction:

Carbon dots (CDs) are a newly emerged nanomaterial that has unique luminescent property and their composite materials have become promising luminescent materials in a variety of applications[1]. This work describes a composite material that has a potential as white light emitting material for solid state lighting application.

Experimental:

This work uses a bottom-up procedure, for the synthesis of carbon dots, and a physical blending method is used for the preparation of composite material[2]. The polyvinyl pyrrolidone polymer matrix serves a dual purpose- surface passivation and binder.

Results and Discussion:

The effect of the concentration of carbon dots on the luminescent properties of composite material is discussed. In addition, we investigate charge transfer, energy transfer, and surface plasmon resonance impacts of the composite matrix on the luminescence of carbon dots. The composite thus formed has been applied on the UV LED chip that emits UV light of 365 nm wavelength. The white emission can be attributed to the charge transfer from the PVP matrix to the luminescence center of carbon dots.

Conclusion:

In conclusion, the carbon dots and their composite can be used in the luminescence field as a WLED (White Light Emitting Diode) source. It can be a novel source of white light.

Keywords: carbon dots, polymer, composites, WLED

References:

1. Ge, G., Li, L., Wang, D., Chen, M., Zeng, Z., Xiong, W., ... & Guo, C. (2021). Carbon dots: Synthesis, properties and biomedical applications. *Journal of Materials Chemistry B*, *9*(33), 6553-6575.
2. Du, X. Y., Wang, C. F., Wu, G., & Chen, S. (2021). The rapid and large-scale production of carbon quantum dots and their integration with polymers. *Angewandte Chemie International Edition*, *60*(16), 8585-8595

New Activation Methods for the Preparation of Carbon-based Materials from Biomass for Gas Storage Applications.

Valeria Lionetti [1,]*, Carlo Poselle Bonaventura [1], Simone Bartucci [1], Giuseppe Conte[1,2], Oreste De Luca [1,2], Giovanni Desiderio [2], Alfonso Policicchio [1,2] and Raffaele Giuseppe Agostino [1,2]

[1]Physics Department, Università della Calabria, Via P. Bucci Cubo 31C, Rende (CS), Italy.
[2]Consiglio Nazionale delle Ricerche, Istituto di Nanotecnologia (Nanotec), Italy.
*Presenting author

INTRODUCTION

The European goal of achieving decarbonization by 2050[1], coupled with the increasing global demand for energy and the impact of climate change, is propelling a shift from fossil fuels to cleaner alternatives. Hydrogen is recognized as a key element in this global transformation of the energy system, but the effective, economical, and safe storage of hydrogen presents a formidable challenge. Additional contributions can be made through processes involving carbon dioxide capture and storage, as well as the utilization of bio-methane. As a result, there is a growing interest in gas adsorption within porous materials, such as activated carbons, which are particularly advantageous due to their cost-effectiveness and efficiency. The characteristics of these activated carbons are highly contingent on factors such as the raw material, the pyrolysis process, the activation method (whether chemical or physical), and parameters like temperature and activation time[2]. This research endeavors to investigate and compare various novel methods for preparing activated carbons derived from biomass. The goal is to optimize their gas storage properties, with a specific emphasis on enhancing hydrogen adsorption performance. It has been observed that micropores (with a pore width of < 2 nm), and especially ultramicropores (< 0.7 nm), play a crucial role in the adsorption process[3].

EXPERIMENTAL/THEORETICAL STUDY

Various methods were employed to prepare activated carbons, including the pyrolysis of biomass in an inert atmosphere followed by physical or chemical activation applied to both pure biomass and pre-charred raw material. Additionally, an innovative preparation procedure involving a double activation (initially chemical and subsequently physical) was tested to enhance the porosity features of the samples. Characterization of the produced activated carbons was achieved through porosimetry analysis using the Brunauer-Emmett-Teller model (BET)[4] and Non-Local Density Functional Theory (NLDFT)[5], along with microscopy and spectroscopy techniques. The adsorption performance of gases was assessed under diverse thermodynamic conditions, and the experimental data were analyzed using the Toth model and other theoretical tools.

RESULTS AND DISCUSSION

The textural properties of the activated carbons obtained were significantly influenced by the chosen preparation method, resulting in remarkable values for specific surface area and an exceptionally high degree of microporosity. In some instances, micropores exceeded 90%, underscoring the outstanding gas storage performance achieved with a pronounced reversibility and reproducibility of the adsorption-desorption processes.

CONCLUSION

Different techniques for preparing activated carbons from biomass were formulated and evaluated. The results indicate that identifying the optimal procedures and parameters can enhance the porosity characteristics, leading to an improvement in gas adsorption capacity.

REFERENCES

1. C. Camarasa et al., Nature Communication, 13 (2022) 3077.
2. G. Conte et al., J. of Analytical and Applied Pyrolysis, 152 (2020) 104974.
3. C. Zhang et. al., International Journal of Hydrogen Energy, 38(22), 9243-9250 (2013).
4. S. Brunauer et al., J. Am. Chem. Soc., 1938, 60 (2), pp 309–319.
5. G. Kupgan et al., Langmuir 33 (42) (2017) 11138–11145.

ACKNOWLEDGMENTS

This research was supported by the National Recovery and Resilience Plan (PNRR), funded by the Italian Ministry of the Environment and Energy Security, project "Novel Materials for Hydrogen storage (NoMaH)", ID RSH2A_000035, CUP: F27G22000180006.

Nanostructured MgB_2 Plasmonic Photoanodes for Solar Water Splitting with Visible-IR Light

Vasyl G. Kravets*, Alexander N. Grigorenko
Department of Physics and Astronomy, the University of Manchester, Manchester, M13 9PL, UK
E-mail: vasyl.kravets@manchester.ac.uk

INTRODUCTION

Noble metal nanoparticles (NPs) are receiving increasing attention as photocatalysts, primarily due to their large absorption cross-sections in the visible region, resulting from their plasmon resonances. Under resonant excitation, the optical cross-sections of plasmonic nanostructures can reach ~10 times their geometric cross-sections. As a result, a large quantity of light energy is localised near the surface of plasmonic nanostructures in the form of intense local electromagnetic fields [1-3].

RESULTS AND DISCUSSION

Here we report the room temperature water splitting on magnesium diboride (MgB_2) nanostructures using visible and near IR light. We investigated the MgB_2 nanostructures, as an alternative to the noble metals nanoplasmonics, to provide the plasmonic water splitting. Note that noble-like plasmonic metals, such as Cu, Ag, Au, Pd and Pt typically exhibit low intrinsic activities with surface-adsorbed molecules due to their fully filled *d* bands. Therefore, introducing nanostructures based on non-noble metals with high intrinsic activities presents a promising strategy to efficiently harvest the solar energy. In MgB_2 nanostructures the localised surface plasmon resonances (LSPRs) are strongly coupled with interband excitations due to spectral overlap of these processes. In the our previous work we have shown that at the edges of extended surfaces of MgB_2 nanostructures can be appeared the e^-–h+ pairs which actively involve into water splitting in the photoelectochemical cells (PECs) [4].

We engineered active plasmonic nanostructures with enhanced photocatalytic performance using non-noble metallic MgB_2 high-temperature superconductor which can represent a new family of photocatalysts. Ellipsometric study of MgB_2 nanostructures demonstrated that these covalent binary metals with layered graphite-like structures can effectively absorb visible and infrared light by excitation of multiwavelengths surface plasmon modes. We demonstrated that MgB_2 plasmonic metal-based photocatalysts exhibit fundamentally different behaviour compared with semiconductors and have advantage for photovoltaics applications. Excitation of LSPRs in the MgB_2 nanostructures promotes to overcome the limiting factors of photocatalytic efficiency in the broad-band gap semiconductors due to the coupling of solar visible and infrared energy spectra to catalytic reactions in the form of enhanced local electromagnetic fields and transferring high energy carriers. The excitation LSPRs supported by intrinsic absorption in MgB_2 nanosheets can lead to achieve near full-solar-spectrum harvesting in this photocatalytic system. We show conversion efficiency of ~10% at bias voltage V_{bias} = 0.3V for MgB_2 working as a catalyst for plasmon-photoinduced seawater splitting.

This research can also support progress in new method of fabrication cheap, stable and dense packing nanostructures on flexible substrates large size for the field of photocatalysis using convenient mass production process of mechanical rolling mill procedure.

CONCLUSION

Our study demonstrates effective plasmon-induced seawater splitting on MgB_2 nanostructures. These plasmonic nanostructures consist only of metallic MgB_2 nanosheets, thus, ruling out any complications associated with semiconductor materials and their sub-bandgap absorption. Exciting the LSPRs in MgB_2 nanostructures can offer a series of unique properties and functionalities, including spectral tuneability by varying the nanostructure size and shape, size selectivity, electric field enhancement to enable a boost of photocatalytic hydrogen generation from seawater.

REFERENCES

1. Y. Kim et. al, Nature Chemistry 10, 763–769 (2018).
2. P. Christopher et. al, Nature Chemistry 3, 467–472 (2011).
3. Z. Li et. al, Acc. Chem. Res. 54, 2477−2487 (2021).
4. V. G. Kravets and A. N. Grigorenko, Opt. Express 23, A1651–A1663 (2015).

A.N.G. and V.G.K. acknowledge support of Royce ICP Round 3 project EP/X527257/1 and Graphene Flagship program, Core 3 (881603).

Tailored polymer nanocomposites for enhanced energy storage

Venkata Ramana Eskilla [1*] and M.A.Valente[1]
[1]I3N, Department of Physics, University of Aveiro, 3810-193, Aveiro, Portugal.
* Presenting author: ramana.venkata@ua.pt

INTRODUCTION

Amidst the growing energy demand and the potential impact of its production on global warming, advancing materials for energy harvesting and efficient storage is vital for sustainable progress. While batteries and supercapacitors are commonly utilized for this objective, their energy storage capacity is restricted by their low power density. Among current energy storage devices, dielectric capacitors are attractive alternatives with a stable, ultrahigh power density of the order of 10^8 W/kg and fast charge-discharge cycles, suitable for hybrid electric vehicles, wearable electronics, medical devices etc. Electroactive polymer nanocomposites (PNCs) of PVDF-family are attractive for light weight, flexible storage. Processing of PVDF plays an important role in controlling its polymorphs and breakdown. For enhanced polar phase of PVDF with higher breakdown we used multiferroic nanofillers and mechanical processing.

EXPERIMENTAL/THEORETICAL STUDY

Compression molding of solution-cast films was carried out to realize high-quality polymer nanocomposites. Ferroelectric nanofillers with $Ba_{0.7}Ca_{0.3}TiO_3$-$Co_{0.6}Zn_{0.4}Fe_2O_4$ were introduced to realize magnetoelectric (ME) PNCs. X-ray diffraction and FTIR were used to assess crystallization of PNCs while TEM and AFM were used for dimensions and morphological studies. Energy storage and breakdown analysis was performed experimentally, and results were understood via simulations.

RESULTS AND DISCUSSION

The progressive increase of nanofiller content has led to enhanced polarization (11 μC/cm^2), soft ferromagnetic properties, and enhanced ME coupling of 59 mV/cm-Oe due to switchable magnetostriction at lower saturation field of 1.2 kOe. Detailed energy storage characteristics confirm that the nanofiller inclusion up to 7.12 vol% effectively improved the recoverable energy storage density (21.2 J/cm^3) with an efficiency of 67 %. The experimental and simulation results corroborate a significantly improved breakdown strength of 617 kV/mm with reliable performance. Thus, careful processing provides viable polymer dielectrics with beneficial storage characteristics.

\

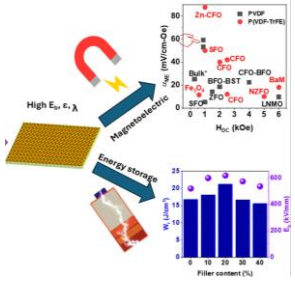

ME filler-based polymer nanocomposites for enhanced magnetoelectric and energy storage

CONCLUSION

Compression molding significantly enhanced the β-phase compared to solution-cast composites: 92.4 % for neat PVDF and 86 % for 40% filler. Local PFM and P-E experiments showed enhanced piezoelectricity and switchable polarization, consistent with the mechanically induced presence of the polar β-phase. MFM and magnetization studies revealed increased magnetization and reduced coercivity with increased filler content. PNC films exhibited ME coefficient of 59 mV/cm-Oe, with self-bias effects promising for smart wearable devices. Energy storage studies, supported by simulation, demonstrated improved breakdown strength for PVDF low filler content composites. The reduced dielectric mismatch between PVDF and BCT, facilitated by CZFO, combined with processing-induced higher P_{max}-P_r, resulted in a storage density of 21.2 J/cm^3 and an Eb of 617 kV/mm for PC20, ensuring high reliability. Overall, our study advances understanding of PVDF processing and low field ME sensing, with implications for flexible energy storage.

REFERENCES

1. E. Venkata Ramana *et al*., Surfaces and Interfaces 33 (2022) 102257.
2. E. Venkata Ramana *et al*., Journal of Energy Storage 87 (2024) 111454.

ACKNOWLEDGMENTS

This work was developed within the scope of the project 032-88- ARH/2018 (EVR) financed by FCT through DL57 law. Part of the work was supported by FCT, I.P., under the scope of the project Expl/CTM/CTM/0054/2021.

Curcumin Loading on Surface-modified Layered Zinc Hydroxide

Vera R.L. Constantino*[1], Raphael G.R. Pessoa[1] and Verônica Biselli[1]
[1]Department of Fundamental Chemistry/Institute of Chemistry, University of São Paulo, Brazil
*corresponding author (vrlconst@iq.usp.br)

INTRODUCTION

Layered metal hydroxides have been studied as nanotherapeutics for drug delivery and diagnostics[1]. Classified as particulate carriers, their bi-dimensional structure allows the intercalation of bioactive species between the layers by distinct methods in water and at ambient conditions. Focusing applications on nanomedicine, magnesium, zinc, and aluminium are the main cations chosen for investigation. *In vivo* studies demonstrated that layered hydroxides promote tissue integration, neovascularisation, angiogenesis, and stimulation of collagen formation[2]. This work chose a layered material from endogenous zinc ions to intercalate bioactive species. Layered zinc hydroxide (LZH) has layers formed by hydroxide ions coordinated to Zn^{2+} as indicated in Fig. 1a and the general formula $Zn(OH)_{2-y}(A^{x-})_{y/x}{\cdot}nH_2O$ (A is an anion of charge *x*). The naturally occurring phenols cinnamic acid and curcumin (Fig. 1b,c) were employed because of their outstanding biological properties but low chemical stability that an intercalation approach could improve. Cinnamic acid shows antioxidant, UV protection, and antimicrobial activities, while curcumin has anti-inflammatory, antiviral, and anticancer properties[3].

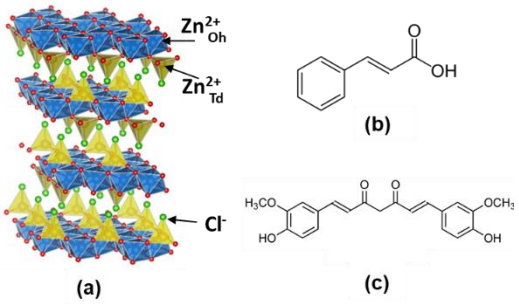

Fig. 1 Structures of LZH-Cl (a), cinnamic acid (b) and curcumin (c).

EXPERIMENTAL STUDY

LZH-Cin material was synthesised by precipitation in water at pH constant, nitrogen gas atmosphere, and using a $ZnCl_2$/Cin molar ratio equal to 2. After washing and drying, LZH-Cin was suspended in a saturated curcumin solution in ethanol and kept on a stirring table. The orange solid (named LZH-Cin-Cur) was isolated by filtration. Structural, spectroscopic, and thermal techniques were used for the materials' characterisation.

RESULTS AND DISCUSSION

X-ray diffraction (XRD) pattern showed peaks related to planes of 0.242 nm (basal spacing) and 0.271 and 0.156 nm, which attested to the formation of LZH phase and the presence of cinnamate in an interdigitated bilayer arrangement between the layers. The chemical identity of Cin was kept in the carrier system as indicated by infrared and Raman spectroscopies. The loading capacity of LZH-Cin was 35 m/m%, and the thermal stability of Cin increased 40ºC compared to cinnamic acid. The LZH-Cin-Cur particles showed uniform colour, and they were not fated after at least ten months. The basal spacing of LZH-Cin was not changed after Cur immobilisation, suggesting that the dye was on the external surface. Thermal analysis data indicated that the mass of curcumin in the LZH-CIN-CUR sample was about 24%, a highly satisfactory value for a carrier. Cur was also tentatively immobilised on LZH-Cl for comparison purposes, but the obtained material showed the deprotonated Cur's colour, which can favour dye oxidation.

CONCLUSION

An LZH carrier with a high loading capacity for cinnamate and curcumin bioactive species was obtained. The surface modification of LZH surfaces with Cin improved curcumin's chemical stability. The following studies will focus on *in vitro* assays to assess the material's biocompatibility and antioxidant properties.

REFERENCES

1. V.R.L. Constantino et al., Layered Double Hydroxides: Characterization, Biocompatibility, and Therapeutical Purposes. M. Nocchetti; U. Costantino; Eds.; 8, 413-482 (2022).
2. V.R.R. Cunha et al., Sci. Rep. 6, 30547 (2016).
3. A. Gunia-Krzyżak et al., Int. J. Cosmet. Sci. 40, 356 (2018); A. Giordano et al., Nutrients 11, 2376 (2019).

ACKNOWLEDGMENTS

Conselho Nacional de Desenvolvimento Científico e Tecnológico (CNPq), Brazil.

Structural and functional stabilization of lytic bacteriophages in biopolymeric nanoparticles: potential for biocontrol of *Pseudomonas syringae* pv. *garcae* in coffee plants

Erica Silva [1], Lucas Rodrigues [1], Marta Vila [1] and Victor Balcão *[,1,2]
[1]VBlab – Laboratory of Bacterial Viruses, University of Sorocaba, Sorocaba/SP, Brazil, presenting author, corresponding author (victor.balcao@prof.uniso.br)
[2]Department of Biology and CESAM, University of Aveiro, Aveiro, Portugal, presenting author

INTRODUCTION

Brazilian coffee production has been heavily affected by phytopathogenic bacteria that cause bacterial canker/spots and lead to serious economic losses. The treatments available for this disease are still scarce, the most common being copper derivatives and the antibiotic kasugamycin. In addition, these treatments impact crops negatively, interfering with food security and the environment. One of the most promising alternatives to the use of antibiotics is the use of bacteriophages. The aim of the present research work was to use green technology via development of a nanoparticle formulation integrating a cocktail of lytic bacteriophages with potential for the biocontrol of coffee plant bacteriosis caused by the phytopathogen Pseudomonas syringae pv. garcae (Psg).

EXPERIMENTAL/THEORETICAL STUDY

A full 3^2 factorial planning was employed to optimize nanoparticle formulation and the 9 formulations thus produced were analyzed via dynamic laser light scattering for determination of hydrodynamic size, polydispersity index and Zeta potential, together with assessment of the maintenance of phage virion lytic activity upon entrappment within the biopolymeric nanoparticle core.

RESULTS AND DISCUSSION

Entrapment of the phage virion particles in the chitosan/lecithin-coated calcium alginate biopolymeric matrix of the nanoparticles promoted structural and functional stabilization of said virions, with maintenance of their lytic viability. Maintenance of the lytic activity of the phage virion particles within the biopolymeric nanoparticles was evaluated since immobilization on different matrices can affect both their viability and availability. The process of obtaining films, coatings, and hydrogels integrating phage particles ends up exposing them to stressful conditions such as mixing, stirring, or drying. Lawns of *Pseudomonas syringae* pv. *garcae* IBSBF-158 (Psg IBSBF-158) were prepared and, on top of it, sterile filter paper disks impregnated with the nanoparticle formulations were laid. Lysis zones were observed in the lawn, surrounding the nanoparticle-impregnated filter paper disks, indicating maintenance of the lytic activity of the phage particles on the host bacteria upon immobilization within the biopolymeric nanoparticles. Hence, integration of the phage particles within the nanoparticle matrix formulations did not interfere with their lytic activity. To try to explain the lysis promoted by the entrapped phage particle cocktail when in contact with a lawn of the host (Psg IBSBF-158), a putative mechanism was put forward illustrating the putative interactions between the Ca^{2+} alginate matrix and the chitosan/lecithin coating at different pH values. Chitosan and lecithin are electrostatically bound to the surface of the Ca^{2+} alginate matrix at a lower pH (top-agar surface, pH equal to ca. 6). At a higher pH (Psg IBSBF-158 lawn surface, pH equal to ca. 9), chitosan becomes deprotonated and acquires a net negative charge, and the repulsion forces acting on the (also negatively charged) Ca^{2+} alginate matrix prevents surface rebinding. The increase in pH promotes a disentanglement of the two polymers, destructuring the nanoparticle and promoting release of the phage virions into the outer medium, where they can contact with, and infect the, bacterial host cells, promoting their lysis.

CONCLUSION

The nanoparticle formulation selected (level 0, phage cocktail at MOI 100), with ca. 561 nm in diameter and a Zeta potential of ca. +16 mV (viz. formulation #8) has, therefore, potential for utilization in the biocontrol of Psg IBSBF-158, the causal agent of bacterial halo blight in coffee plantations. With a large positive Zeta potential this nanoparticle formulation does not aggregate and, with an hydrodynamic size of ca. 561 nm, it can easily accomodate several phage virions in its core matrix.

ACKNOWLEDGMENTS

Fundação de Amparo à Pesquisa do Estado de São Paulo (FAPESP, São Paulo, Brazil) (Ref. No. 2022/10775-9, Project PsgPhageKill; Ref. No. BPE ref. 2018/05522-9, Project PsaPhageKill). Conselho Nacional de Desenvolvimento Científico e Tecnológico (CNPq, Brazil), Research Productivity fellowship PQ-2 granted to Victor M. Balcão (grant 301978/2022-0).

Photoactive Binder for Battery Use and its Potential Application for Battery Charging with Light

Elsa Briqueleur[1], Mickaël Dollé,[1] and Will Skene[3*]
[1]Department of Chemistry, Université de Montréal, Montreal, QC, Canada, w.skene@umontreal.ca

INTRODUCTION

The inert binder does not actively participate in the operation of a lithium ion battery was replaced with a photoactive polymer. Substituting the binder indeed retained its binder properties, while also being fluorescent and electroactive. The intrinsic photoactivity of the binder would be ideal to harness sunlight for charging the battery with light at the molecular level.

EXPERIMENTAL/THEORETICAL STUDY

The photoactive binder was prepared by the straightforward step-growth polymerization of a dianhydride with its complementary diamine. The polymer was confirmed by GPC and NMR.

RESULTS AND DISCUSSION

Typically, a binder in a battery plays no active role in its operation. Therefore, the binder is a dead mass whose exclusive role is to act as a molecular glue. In this role, it consolidates the active components of the battery to the current collector. Leveraging our previous results that demonstrated sunlight can be used to induce a charge transfer at the molecular level in a battery,[1, 2] we set out to develop a binder that could also sustain this effect. The design criteria of the binder was to harvest sunlight and subsequently oxidize lithium iron phosphate (LFP). The reduced dye would then inject the charge upon returning to its ground state according to the mechanism represented in Fig. 1.

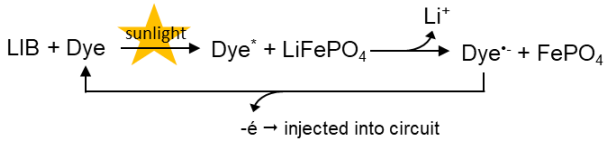

Fig. 1 General reaction scheme of sunlight induced redox reaction and subsequent dark event of LIB component and a dye at the molecular level.

The polymer developed indeed was photoactive and it retained its fluorescence. Its energy level also matched with the oxidation potential of LPF, making the light induced process exergonic. The binder further consolidated the battery components, much like a conventional binder, but with the benefit of being photoactive. Detailed post operation studies of the prepared photoactive binder were undertaken to demonstrate the binder was inert under normal charging and discharging of the battery. These detailed FT-IR spectroscopic studies also revealed the inertness of the polymer, but also demonstrated that it reacted when excited with light as designed.

CONCLUSION

An electroactive polymer was prepared that served as a binder in a lithium ion battery. The polymer was photoactive and it generated a charge upon exposure to light. The binder was integrating in an operating battery. The photoelectrode generated a charge when irradiated with light.

REFERENCES

(1) Briqueleur, E.; Shoghi, F.; Dollé, M.; Skene, W. G. Unraveling the Interfacial Electron Transfer in Various Photocathode Architectures for Advancing a Photobattery. *ACS Appl. Energy Mater.* **2023**, *6* (5), 2768-2780. DOI: 10.1021/acsaem.2c03577.
(2) Briqueleur, E.; Dollé, M.; Skene, W. G. Understanding the Light-Triggered Process of a Photo-Rechargeable Battery via Fluorescence Studies of Its Constitutional Photo- and Electroactive Components. *J. Phys. Chem.* **2022**, *126* (5), 2634-2641. DOI: 10.1021/acs.jpcc.1c09127.

ACKNOWLEDGMENTS

The Natural Sciences and Engineering Council Canada and the Canada Foundation for Innovation are acknowledged for funding and equipment, respectively. E.B. also acknowledges a graduate scholarship from UdeM and the Trottier Foundation.

Development and performance analysis of water electrolysis propulsion system with microwave igniter

Xiaodan Liu [1], Yusong Yu [1,*], Shurui Zhang [2], Jun Chen [3] and Tao Zhang [3]
[1,2] Hydrogen Energy and Space Propulsion Laboratory (HESPL), School of Mechanical, Electronic and Control Engineering, Beijing Jiaotong University, Beijing, 100044, China
[3] Beijing Institute of Control Engineering, Beijing 100190, China

INTRODUCTION

The electrolytic water propulsion system is a non-toxic, safe to launch, inexpensive and high combustion ratio impulse propulsion system. According to the current research, most of the water electrolysis propulsion systems use catalytic ignition [1-3] and spark ignition[4,5]. However, there are problems of catalyst sintering and unreliable ignition. Microwave ignition can achieve more reliable large-area ignition in space and higher ignition efficiency. Considering these aspects, the aim of this paper is to design a water electrolysis propulsion system using microwave ignition, including the microwave ignition system and thruster design.

EXPERIMENTAL/THEORETICAL STUDY

The microwave water propulsion system designed in this paper uses hydrogen and oxygen produced by a water electrolysis module and uses microwaves to ionise the hydrogen and oxygen to produce a plasma jet to assist in hydrogen combustion. According to the designed thruster model, COMSOL software is used in this study for the simulation calculation of electric field and combustion part.

RESULTS AND DISCUSSION

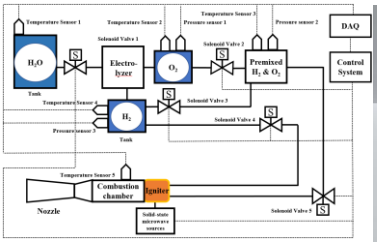

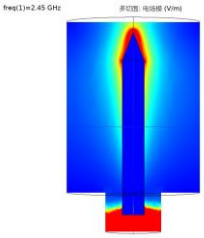

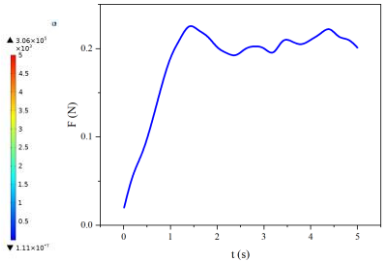

Fig. 1 The microwave water propulsion system integrates modules for electrolyzing water into hydrogen and oxygen gases.
Fig. 2 The Water electrolysis thruster incorporates a microwave ionized hydrogen gas module.
Fig. 3 The electric field distribution inside the microwave resonant cavity
Fig. 4 The transient thrust curve of the microwave water propulsion system.

In the microwave ionized hydrogen gas module, high electric field distribution occurs in the vicinity of the antenna tip, with electric field peaks reaching magnitudes of 10^5 V/m. After the ionization of hydrogen gas and its reaction with oxygen inside the thruster combustion chamber, when expelled through the nozzle, it can generate a stable thrust of approximately 0.2N. It takes about 1.3 seconds for the thrust to stabilize.

CONCLUSION

This paper presents a microwave propulsion system that integrates modules for electrolyzing water to produce hydrogen and oxygen gases. To enhance combustion performance and specific impulse, the hydrogen gas generated from water electrolysis is first passed through a microwave ionization module before entering the thruster combustion chamber to react with oxygen. Results indicate that the propulsion system achieves normal combustion and thrust output. The study will delve into the underlying mechanisms of the process.

REFERENCES

References must be numbered. Keep the same style.
1. N.E. Harmansa et. al, IAC, September 2017.
2. Ulrich Gotzig et. al, Acta Astronaut. 202, 751759 (2023)
3. Minsig Hwang et. al, Acta Astronaut. 200, 316328(2022)
4. F. Mitlitsky et. al, AIAA, September 1999
5. W.A. de Groot et. al, 33rd Joint Propulsion Conference and Exhibit, July 1997

ACKNOWLEDGMENTS

Experimental Evaluation of a Nanocomposite Gel for Water Shutoff in Oil Wells

Yalda Rokhforouz [1,*] , Ali Nakhaee [2]

[1] *Department of Petroleum Engineering, Kish International Campus, University of Tehran, IRAN, presenting author*

[2] *School of Chemical Engineering, College of Engineering, University of Tehran, IRAN*

Introduction

To overcome excessive water production in oil and gas wells, different mechanical and chemical techniques are employed. Injecting gels and polymers in the area around the wellbore is one of the promising chemical methods which potentially reduces water permeability in near-wellbore zone. Nanocomposite gels, which are polymer gels enhanced by the addition of nanoparticles, can improve some limitations of conventional polymer gels such as difficulty in controlling the gelation time, low mechanical strength, low thermal stability, and high salinity/pH sensitivity. In this research, the strength and stability of a nano-SiO_2 gel in presence of formation water is evaluated.

Materials and Methods

A nanocomposite gel was made using hydrolyzed polyacrylamide (HPAM) with a molecular weight of 5×10^6 g/mol, chromium acetate as crosslinker, and nano SiO_2 with average size of 20 nm. The mixture was stirred for 5 minutes, then heated to 100°C for gelation. Table 1 describes the Sydansk strength code that was used to assess gel strength [1].

Results

In table 2, the impact of nano SiO_2, temperature and gelation time on gel strength is summarized.

Table 1. Gel strength based on Sydansk's code

Gel Code	Description of Gel
A	No detectable gel
B	Highly flowing gel
C	Flowing gel
D	Moderately flowing gel
E	Barely flowing gel
F	Highly deformable non-flowing gel
G	Moderately deformable non-flowing gel
H	Slightly deformable non-flowing gel
I	Rigid gel

Table 2. Effect of gelation time/concentration/temperature on gel strength

gelation time (hours)	temperature (°c)	nano SiO_2 concentration (wt.%)			
		0.2	0.6	1	1.4
0.5	100	A	A	B	C
1	100	A	A	B	C
1.5	100	B	B	B	C
2	100	E	B	E	C
2.5	100	G	F	F	F
3	100	G	F	F	F
3.5	100	G	F	F	G
4	100	G	H	G	G
4.5	100	G	I	I	G
24	25	G	I	I	F
480	25	F	I	G	H

effect of nano silica composition on polymer salinity tolerance

Based on the observations, the hpam gel generated by nano silica kept its strength and structure at 100°C in salt water solutions with concentrations ranging from 40,000 to 65,000 ppm. The results indicate that the nanocomposite effectively prevents salt water penetration and is suitable for the tested salinity levels. There were no apparent signs of gel degradation or significant alterations in its properties, suggesting that the nanocomposite can withstand the salt levels. However, at a concentration of 70,000 ppm, the gel structure appears to degrade, revealing that the polymer nanocomposite is unstable at this salinity level.

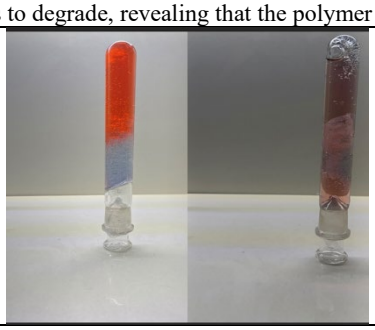

Figure 1. The effect of nano silica on the salt tolerance with a salinity of 55000 ppm
The left side features polymer- nano composite , while the right side features a polymer gel near salt water.

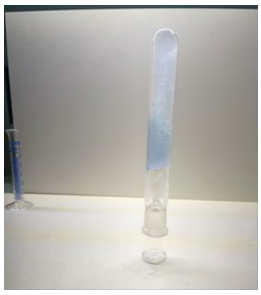

Figure2 NC gel , in distilled water with a pH level of 8.5.

Figure 3. bottle test that show efficiency of a nanocomposite polymer.

bottle test

The experiment as shown as figure 3. consisted of a glass vial filled with distilled water and heptane, followed by the addition of nanocomposite polymer into the vial. Following a four-hour period, it was noted that the polymer successfully segregated the oil phase from the water phase. This segregation was made possible by the distinctive density characteristics of the polymer. With a density higher than water but lower than oil, the polymer settled in between the two phases. This positive result indicates that when used during reservoir injection, the polymer has the potential to improve oil production efficiency by inhibiting water intrusion and enhancing reservoir sweep efficiency.

Discussion

Addition of nano-silica enhances specific qualities of the gel. While keeping the Nano-silica content low helps prevent filler aggregation and guarantees a more uniform dispersion in the polymer matrix, increasing the concentration of HPAM results in stronger gel formation and better control of liquid viscosity. In addition, the observations shows that a nanocomposite with a higher concentration of crosslinker and less than polymer demonstrates greater stability 20 days after post-curing. while HPAM gels with nano-silica exhibit stability near brine solutions (40000ppm-60000ppm). it was observed that a nanocomposite polymer successfully segregated oil from water owing to its distinct density characteristics, which could potentially improve oil recovery efficiency.

References

1. Sydansk, R. D.; Argabright, P. 1987. United States Patent.

Unleashing the Power of Hydrogen: Challenges and Solutions in Solid-State Storage

Ya-Long DU [1]and Z.Y. SUN[1,2*]

[1] Hydrogen Energy and Space Propulsion Laboratory (HESPL), School of Mechanical, Electronic and Control Engineering, Beijing Jiaotong University, China, presenting author

[2] Key Laboratory of Vehicle Advanced Manufacturing, Measuring and Control Technology (Beijing Jiaotong University), Ministry of Education, China, corresponding author (email: sunzy@bjtu.edu.cn)

INTRODUCTION

Hydrogen is considered the ultimate energy source to promote the sustainable development of global energy and achieve the goal of carbon neutrality. The storage and transportation of hydrogen is a key link connecting upstream hydrogen production and downstream hydrogen consumption, solid-state hydrogen storage is respected as the most promising storage technology for the potential of high-volume hydrogen storage density, good safety, and long storage time. However, some crucial issues, including the speed of hydrogen charging and discharging, manufacturing costs, storage efficiency, and so on, have hindered practical applications. This article will systematically analyze the current problems of solid-state hydrogen storage from the perspective of storage principles, storage materials science, application prospects, and cost evaluation.

PRINCIPLES AND TECHNICAL ROUTES OF SOLID-STATE HYDROGEN ENERGY

Solid-state hydrogen storage technology combines hydrogen with hydrogen storage materials through physical or chemical means to achieve hydrogen storage within three major principles[1]: (a) physisorption; (b) chemisorption; and (c) quasi-molecular bond storage, as demonstrated in Fig.1.

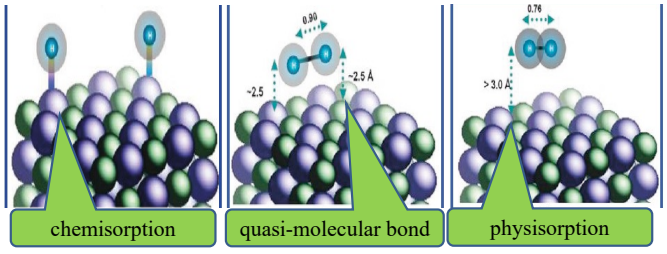

Fig. 1 Three principles of hydrogen storage in solid-state

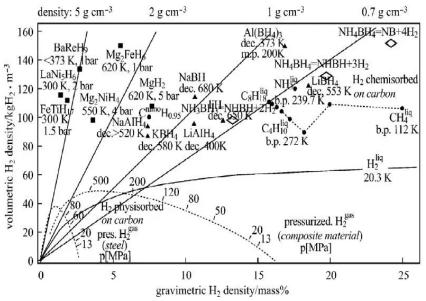

Fig. 2 Storage capability of different metal materials

Upon three principles, detailed technical routes will be summarized and comparatively discussed. Compared to the materials of physisorption (like carbon-based materials, inorganic porous materials, MOFs), metal hydrides (like LaNiH, MgH), coordination hydrides (like NaAlH), chemical hydrides (like NHBH) could provide higher storage efficiency (as shown in Fig.2) together with larger capacity albeit such materials still require modification[2], thus chemisorption should play a more important role in future.

APPLICATIONS PROSPECTS AND COST EVALUATION

Applications sections in which solid-state hydrogen and gaseous hydrogen have been comparatively discussed, solid-state hydrogen storage is believed more suitable for applications in fields like hydrogen metallurgy, seasonal energy storage, and hydrogen chemical industry rather than direction applications on vehicles. The life cycle cost of solid-state hydrogen storage is also discussed on solid-state hydrogen storage combining the technical routes and applications scenarios. Road map to hydrogen society driven by solid-state hydrogen will be raised.

CONCLUSION

Upon the systematically review and comparatively analysis on the principles, technical routes, applications prospects, and cost evaluation, the trend and research concerning solid-state hydrogen storage is concluded.

REFERENCES

1. Y. Gao et. al, Nat. Commun. 15, 928 (2024)
2. S. Liu et. al, Nat. Nanotechnol. 16, 331-336 (2021)

Combining Ni, Co, and Cu on LDH-derived catalysts for CO_2 methanation

Dirléia dos Santos Lima[1], Yan Resing Dias*[1*] and Oscar William Perez-Lopez[1]
[1*] Department of Chemical Engineering/Engineering School, Federal University of Rio Grande do Sul (UFRGS), Brazil (yan.resing@ufrgs.br)

INTRODUCTION

CO_2 methanation is a process that has recently drawn attention from the scientific community as a favorable alternative to cope with CO_2 emissions and, at the same time, uses it as a carbon source for fuels, fine chemicals, and energy production[1]. This process usually employs Ni and Al-based catalysts; however, promoting with a third metal may enhance multiple properties that improve catalytic activity and resistance to deactivation[2]. Then, this study aimed to evaluate the best composition when combining Ni, Co, and Cu on LDH-derived catalysts over their properties, activity, and resistance to deactivation for the CO_2 methanation reaction.

EXPERIMENTAL/THEORETICAL STUDY

The co-precipitation method (pH 8±0.1, 50 °C) was applied to prepare LDH-derived NiCo-, CoNi-, NiCu-, and CoCu-Al catalysts (5:1:3, mol). N_2 physisorption, XRD, H_2-TPR, CO_2 and H_2-TPD, and TPO techniques were used for sample characterization. Catalytic tests at 1 atm, 60000 mL $(g_{cat}\ h)^{-1}$, H_2/CO_2 = 4 were performed both with variable (200-400 °C) and a fixed (400 °C, 5 h) temperature[3].

RESULTS AND DISCUSSION

The activity tests (Fig. 1a) showed that, despite being almost inactive at 200 °C, the CO_2 conversion increases dramatically when reactional temperatures rise, mainly for the NiCoAl catalyst, reaching a maximum conversion of 86.1% at 350 °C and approaching the equilibrium limit. The high activity of this sample could be attributed to its higher dispersion, thus a higher number of active sites, and the improved basicity[4]. While the NiCoAl sample presents a slight decrease in activity after 350 °C, as a consequence of the RWGS reaction being favored, it continuously increases in the other samples, due to their slower activation. This could be a reflection of the low hydrogenation activity of both Co and Cu, as previously reported, despite promotion by Cu provided smaller crystallite sizes, usually linked to higher metal dispersion[5]. To the catalytic tests at a fixed temperature (Fig. 1b), neither sintering nor carbon deposition were relevant, proving their resistance to deactivation.

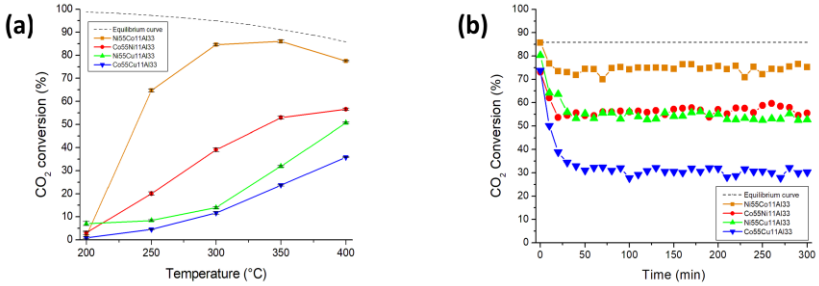

Fig. 1 (a) CO_2 conversion versus temperature and (b) time-on-stream

CONCLUSION

The different combinations of Ni, Co, and Cu on the synthesized catalysts showed that a Ni-rich Ni-Co catalyst has the highest activity for CO_2 methanation among those studied. Its better performance was attributed to a combination of more active sites due to high Ni dispersion and improved basicity, facilitating CO_2 activation and disponibility for conversion, thus corroborating a beneficial interaction between Ni and Co over the catalysts properties. The catalysts also presented high resistance to deactivation, confirming the validity of its application for CO_2 conversion in a mild temperature range.

REFERENCES

1. C. Vogt et al., Nat. Catal 2, 188-197 (2019)
2. C. Liang et al., Int. J. Hydrogen Energy 44, 8197-8213 (2019)
3. D. Lima et al., Sustain. Energy Fuels 4, 5747 (2020)
4. D. Wierzbicki et al., Int. J. Hydrogen Energy 42, 23548-23555 (2017)
5. Y. Katayama et al., Energy 22, 177-182 (1997)

ACKNOWLEDGMENTS

The authors acknowledge CAPES (PROEX program) and CNPq funding agencies for financial support.

NiAl-LDH: Effect of basic metals incorporation on methane decomposition

Morgana Rosset[1], Yan Resing Dias*[2*] and Oscar William Perez-Lopez[2]
[1] Department of Polytechnic School/Chemical Engineering, University of São Paulo (USP), Brazil
[2*] Department of Chemical Engineering/Engineering School, Federal University of Rio Grande do Sul (UFRGS), Brazil, (yan.resing@ufrgs.br)

INTRODUCTION

The catalytic decomposition of methane (CDM) offers a single-step process for producing CO_x-free hydrogen[1]. Nickel-based catalysts, though cost-effective, require modification to counter materials deactivation during the reaction[2]. Adding promoters like Pd and Cu has been explored to enhance catalytic activity and stability[3]. Layered double hydroxides (LDH) emerge as promising catalyst support, with MgNiAl-LDH demonstrating effective diffusion of carbon particles and a spinel-like structure[4,5]. The effect of metals with basic properties (Li, Mg, Ca, La) on the NiAl-LDH-derived catalyst for methane decomposition was analyzed.

EXPERIMENTAL/THEORETICAL STUDY

The Ni-Al catalyst was prepared using the co-precipitation method. In a second step, this Ni catalyst was dispersed in metal nitrate solutions following the procedure previously described to reconstruct the LDH structure[6]. Reactions were conducted at varying temperatures (550-700 °C) and at a fixed temperature of 600 °C, both heated with N_2:CH_4 (9:1). Catalyst characterization included XRD, H_2-TPR, CO_2-TPD, TPO, Raman spectroscopy, and SEM.

RESULTS AND DISCUSSION

The activity tests in different temperatures (Fig. 1a) showed that incrementing temperatures up to 600 °C positively affected the activity patterns of the La and Mg-reconstructed, and unpromoted NiAl catalysts – Li and Ca only improved until 550 °C – showing strong deactivation subsequently, mainly due to formation of carbon nanotubes, as confirmed via Raman spectra and SEM images (Fig. 1c). The La-reconstructed one had the highest activity throughout the entire temperature range (except for Li at 500-550 °C), with maximum conversion of 54.7% at 600 °C, in virtue of the presence of more active sites[7]. La incorporation slightly improved resistance to carbon deposition, whereas its low crystallite size (7.2 nm) also provided higher resistance to deactivation in the fixed-temperature test against unpromoted Ni-Al, slowing sintering (Fig. 1b).

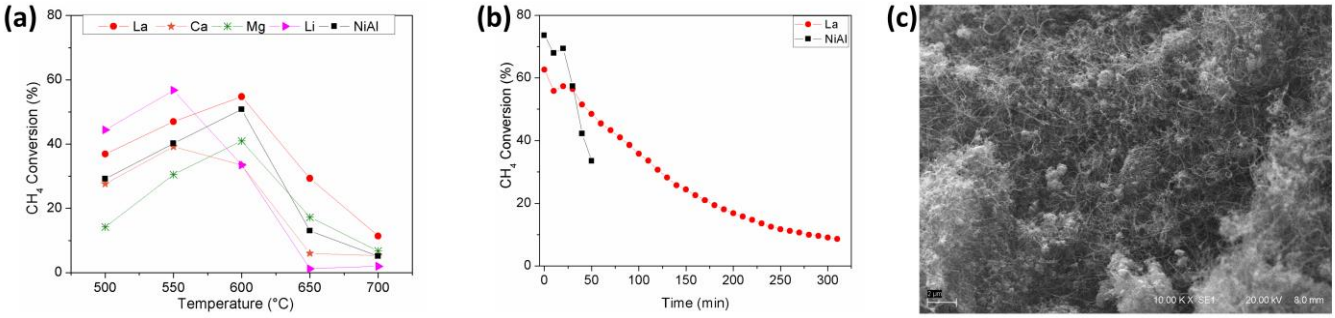

Fig. 1 CH_4 conversion versus (a) temperature and (b) time-on-stream, and SEM image of spent La-NiAl-LDH catalyst

CONCLUSION

Incorporating La in the NiAl-LDH catalyst improved the catalytic activity for CH_4 decomposition through the entire temperature range, demonstrating an increment in the number of active sites. The high activity presented without previous activation is positive, as no H_2 was spent to promote the reaction. The presence of La also lowered the crystallite size and provided basic sites, thus improving the resistance to deactivation, hindering size growth and carbon deposition.

REFERENCES

1. G. Gómez-Pozuelo et al., Fuel 306, 121697 (2021)
2. S. Karimi et al., Int. J. Hydrogen Energy 46, 20435–20480 (2021)
3. A. Rastegarpanah, Int. J. Hydrogen Energy 42, 16476–16488 (2017)
4. C. Wan et al., Int. J. Hydrogen Energy 46, 3833–3846 (2021)
5. M. Al Mesfer, Taiwan Inst. Chem. Eng. 128, 370–379 (2021)
6. M. Rosset, Catal Today. 381, 96-107 (2021)
7. B. A. Al Alwan et al., J. Indian Chem. Soc. 99, 100393 (2022)

ACKNOWLEDGMENTS

The authors acknowledge CAPES (PROEX program) and CNPq funding agencies for financial support.

Effect of Ca on LDH-derived Ni-Al catalysts for low-temperature CO_2 methanation

Yan Resing Dias*[1*] and Oscar William Perez-Lopez[1]
[1*] Department of Chemical Engineering/Engineering School, Federal University of Rio Grande do Sul, Brazil (yan.resing@ufrgs.br)

INTRODUCTION

Mitigation of carbon dioxide (CO_2) emissions and energy production are unparalleled challenges for modern society. CO_2 conversion to methane (CH_4) through methanation is a promising alternative to tackle both issues, valorizing it as a carbon feedstock for chemicals, fuels, and energy generation. As surface basicity plays an essential role in activating CO_2, this work focused on stimulating its generation in catalysts through basic-featured Ca promotion, given the lack of investigation over the effect of Ca content on Ni-Al layered double hydroxide-derived (LDH) catalysts, thus aiming to find an adequate composition that provides the best properties and, consequently, performance for low-temperature methanation[1,2].

EXPERIMENTAL/THEORETICAL STUDY

Ca-promoted (3-33 mol%) Ni-Al LDH (M^{II}/M^{III} = 2) catalysts were prepared via the co-precipitation method (pH 8±0.1, 50 °C). Extensive characterization was done through XRD, H_2-TPR, CO_2 and H_2-TPD, TPO, SEM, and TEM. Catalytic tests were performed at 1 atm, 60000 mL $(g_{cat}\ h)^{-1}$, H_2/CO_2 = 4 in stepwise (200-400 °C) and stability (250 °C, 10 h) modes[3].

RESULTS AND DISCUSSION

Except for the highest Ca-concentrated (33 mol%) sample, all synthesized catalysts presented between 65 and 80% of CO_2 conversion at temperatures as low as 200 °C, which were due to properties originating from the LDH structures, as high specific surface areas, Ni dispersion and surface area, and small crystallite sizes, leading to high availability of Ni active sites, but mainly because of improved basicity given by the Ca promotion to enhance catalytic activity in the reaction. Among the samples, the highest density of weak-medium basic sites (165.5 µmol g_{cat}^{-1}) of Ni60Ca6 catalyst can be directly linked to its highest catalytic activity of 79.4% of CO_2 conversion at 200 °C (Fig. 1a), proving that a high number of moderate basic sites improves a catalyst capacity of adsorb and activate CO_2[2,4]. The highest activity was attained by the same sample, of 86.6% at 250 °C, whereas all catalysts reached 100% of CH_4 selectivity below 300 °C (Fig. 1b). The Ni60Ca6 catalyst was also able to maintain high activity in the long-term reaction, showing resistance to sintering and carbon deposition (Fig. 1c).

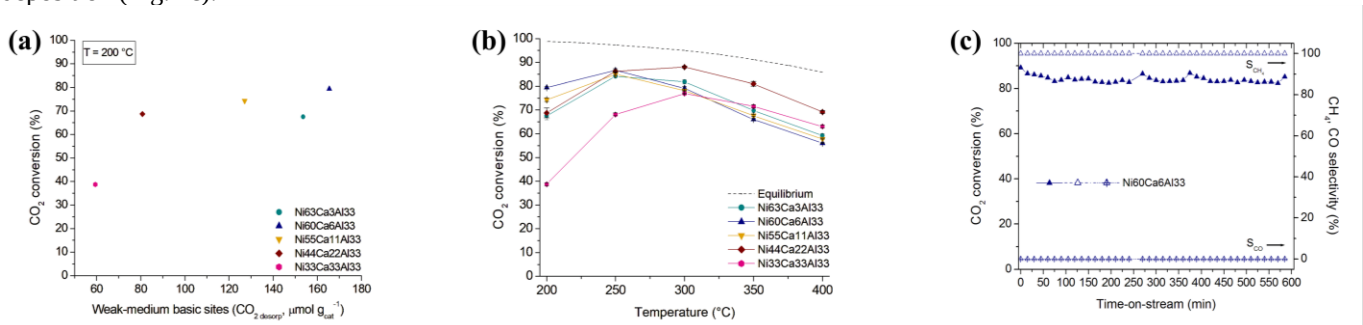

Fig. 1 (a) CO_2 conversion according to weak-medium basic sites, (b) as a function of temperature and (c) of time-on-stream

CONCLUSION

The proper composition of Ca-promoted Ni-Al LDH-derived catalysts is crucial to attain an ideal set of properties for improved low-temperature methanation. The highest number of moderate basic sites, which worked synergistically with the highest number of Ni active sites, indicated that up to 6 mol% of Ca enables outstanding performance at low temperatures, approaching the thermodynamic limit and favoring a less energy-expensive process, consequently highlighting it as an encouraging alternative to manage CO_2-related issues.

REFERENCES

1. W. K. Fan, M. Tahir, J. Environ. Chem. Eng. 9, 105460 (2021)
2. D. Wierzbicki et al., Int. J. Hydrogen Energy 42, 23548-23555 (2017)
3. Y. R. Dias et al., ChemCatChem 15, e202300834 (2023)
4. L. Xu et al., J. CO_2 Util. 21, 200-210 (2017)

ACKNOWLEDGMENTS

The authors acknowledge CAPES (PROEX program) and CNPq funding agencies for financial support.

Nanoparticle-based Scintillating Aerogels for Real-time Radioactive Gas Detection

Yannis Cheref[1,2,*], Raphaël Marie-Luce[1], Pavlo Mai[2], Frédéric Lerouge[1], Sylvie Pierre[3], Benoit Sabot[3], Frédéric Chaput[1], Christophe Dujardin[2,4]

[1] Laboratoire de Chimie, ENS de Lyon, Université Claude Bernard Lyon 1, CNRS, UMR 5182, France
[2] Institut Lumière Matière, Université Claude Bernard Lyon 1, CNRS, UMR 5306, France
[3] Université Paris-Saclay, CEA, LIST, Laboratoire National Henri Becquerel, France
[4] Institut Universitaire de France (IUF)
*Presenting and corresponding author – E-mail: yannis.cheref@ens-lyon.fr

INTRODUCTION

The measurement of pure β emitting radioactive gases such as ^{3}H and ^{85}Kr is already of major importance for the nuclear safety authorities, and will meet an increasing demand with the expansion of nuclear-based energy production. Due to the short penetration length of β electrons in air, gaseous β emitters must be mixed with radiosensitive elements to enable detection. These are either gas-gas mixtures in an ionization chamber, or gas-liquid mixtures in liquid scintillation. However, none of these existing methods combine real-time analysis, sensitivity to multiple gases, and ease of deployment for on-site measurements. We demonstrate a new gas-solid mixture approach using inorganic aerogels as nanoporous scintillators.

EXPERIMENTAL STUDY

This presentation will focus on the preparation of scintillating aerogels. Scintillating nanoparticles were synthesized in the 10g-scale via a solvothermal route. After extensive washing, a controlled aggregation procedure allowed for their assembly into gels. These gels were then dried into transparent aerogels in supercritical CO_2. The aerogels were then exposed to known quantities of radioactive gases and their scintillation was measured. The procedure was initially developed to produce Ce^{4+}:YAG nanoparticles aerogels, and was subsequently applied to other scintillating nanomaterials.

RESULTS AND DISCUSSION

Transparent scintillating aerogels were obtained by the same method for Ce^{4+}:YAG (Fig. 1) and other nanomaterials. Statistical treatment of their measured scintillation allowed efficient, real-time measurement of ^{3}H and ^{85}Kr activity.

Fig. 1 - Aerogels before (left, Ce^{3+}:YAG, yellow sample) and after (right, Ce^{4+}:YAG, white sample) thermal treatment

CONCLUSION

We demonstrate a new gas-solid mixture approach using inorganic aerogels as nanoporous scintillators. This method combines the above criteria, allowing efficient real-time measurement of ^{3}H and ^{85}Kr activity.

ACKNOWLEDGMENTS

The authors acknowledge support from the European Community through grant n° 899293, HORIZON 2020 – SPARTE.

$Co_xFe_{3-x}O_4$ thin films for Photoelectrochemical degradation of rhodamine B : Experimental and response surface methodology approaches.

Yassine Elaadssi[1], Véronique Madigou[1], Madjid Arab[1].

[1] Université de Toulon, Aix-Marseille Université, CNRS, IM2NP, Toulon, France

INTRODUCTION

In recent years, Response Surface Methodology (RSM) has become widely used to optimize and evaluate the interactive effects of independent factors in many chemical processes. In this study, RSM was used to investigate the photoelectrocatalytic (PEC) activity of cobalt ferrite ($CoFe_2O_4$ and $Co_{1,5}Fe_{1,5}O_4$) thin films. These materials are known for their interesting catalytic activity [1].

EXPERIMENTAL/THEORETICAL STUDY

Cobalt ferrite thin films have been prepared by depositing $Co_xFe_{3-x}O_4$ powders (synthesized in our previous work) on indium tin oxide (ITO) substrates by the drop casting method. The crystallographic structure of thin films is the same as the powder, and the chemical composition was checked by energy dispersive spectroscopy (EDS). Mott-Schottky analysis was used also to determine the flat band potential. The study also included photocurrent measurements to assess the carrier density. The photoelectrocatalytic performance of the prepared $Co_xFe_{3-x}O_4$ thin films was evaluated for the removal of Rhodamine B from water under irradiation with a 390 nm light source using a photoreactor with three electrodes immersed in an electrolyte. Response surface methodology (RSM) was used to evaluate the effect of electrolyte concentration (Na_2SO_4), current density, dye concentration (RhB) and irradiation time, and to optimize the process.

RESULTS AND DISCUSSION

The band gap values of the samples estimated to be, approximately 2.32, 2.01 eV corresponding to $CoFe_2O_4$ and $Co_{1,5}Fe_{1,5}O_4$ respectively. Grain size distribution was broad, with a value between 6 and 12 nm. In addition, the flat band potential (V_{FB}) for the $CoFe_2O_4$ nanoparticles was obtained from the Mott-Schottky plots measured at 1000 Hz as shown in Figure 1.

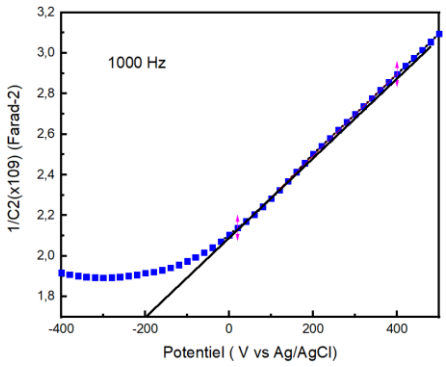

Fig. 1 Mott–Schottky plots of the $CoFe_2O_4$.

The positive slope of the plot indicates that the $CoFe_2O_4$ material is a n-type semiconductor, which agrees with the results of the literature [2]. The estimated V_{FB} value of the $CoFe_2O_4$ nanoparticles was 0.21 V vs. Ag/AgCl (Reference electrode). The $Co_xFe_{3-x}O_4$ thin films showed remarkable efficiency in the photoelectrocatalytic test and the RSM methodology established the most important parameters that affect the PEC activity and the optimum conditions to achieve the highest level of RhB degradation.

CONCLUSION

$Co_xFe_{3-x}O_4$ thin films were deposited on an ITO substrate by drop-coating cobalt ferrite powder for photoelectrocatalytic degradation of RhB. The photoelectrocatalytic tests showed interesting results and the RSM methodology was used to optimize the photoelectrocatalytic RhB removal and to achieve 100% RhB degradation.

REFERENCES

[1] André Luís Lopes-Moriyama, Véronique Madigou, Carlson Pereira de Souza, Christine Leroux, Controlled synthesis of CoFe2O4 nano-octahedra, Powder Technology, Volume 256, 2014, Pages 482-489.

[1] N. Labchir, A. Hannour, A. Ait Hssi, D. Vincent, K. Abouabassi, A. Ihlal, M. Sajieddine, Synthesis and characterization of CoFe2O4 thin films for solar absorber application, Materials Science in Semiconductor Processing, Volume 111, 2020, 104992.

Synthesis of cobalt ferrite nanoparticles for the photodegradation of Rhodamine B under simulated sunlight irradiation : Optimization by Response Surface Methodology.

Yassine Elaadssi[1], Véronique Madigou[1], Madjid Arab[1].

[1] Université de Toulon, Aix-Marseille Université, CNRS, IM2NP, Toulon, France

INTRODUCTION

The precursors and the methods of $Co_xFe_{3-x}O_4$ particles synthesis have strongly influenced several parameters like particle size, crystallinity, morphology, homogeneity, and distribution of ions in tetrahedral and octahedral sites[1]. In this study, the photocatalytic activity performance of cobalt ferrite was investigated for two chemical compositions: x=1 the most used and x=1.5 an original one. The effect of several experimental parameters on photocatalytic performance was evaluated by Response Surface Methodology (RSM).

EXPERIMENTAL/THEORETICAL STUDY

Cobalt ferrite nanoparticles have been synthesized by a hydrothermal method using nitrates as precursors and characterized using X-ray diffraction (XRD), transmission electron microscopy (TEM), Mott-Schottky analysis, UV-visible diffuse reflectance spectroscopy and BET technique. The photocatalytic performance of the synthesized $Co_xFe_{3-x}O_4$ nanoparticles was evaluated for the removal of Rhodamine B from water under visible light irradiation. The response surface methodology (RSM) based on the central composite design (CCD) model was used to evaluate the following set parameters: pH, dye concentration and catalyst weight and to optimize the RhB removal.

RESULTS AND DISCUSSION

The XRD and TEM analyses showed that the nanoparticles produced are single-phased with a nano-octahedral shape (Fig 1) and a size less than 10 nm. UV-Vis spectrophotometry revealed distinct optical band gap values for $CoFe_2O_4$ and $Co_{1,5}Fe_{1,5}O_4$ of 2.32 eV and 2.01 eV, respectively. In addition, the developed $Co_xFe_{3-x}O_4$ powders showed remarkable efficiency in the photodegradation of an aqueous Rhodamine B (RhB) solution (Fig 2).

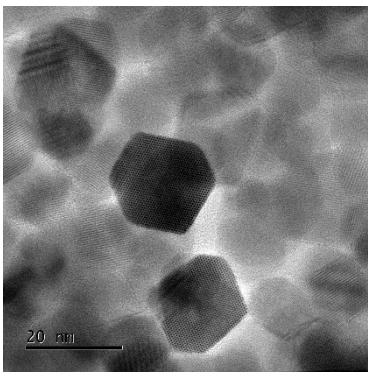

Fig 1: TEM image of $Co_{1.5}Fe_{1.5}O_4$ nano-octahedra.

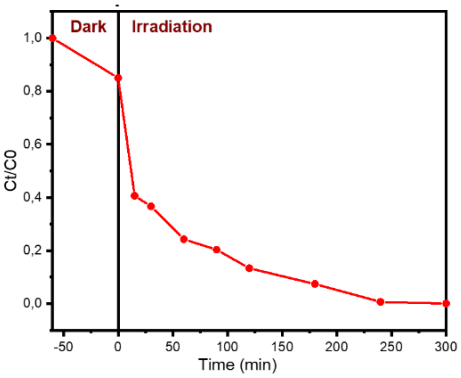

fig 2: Photodegradation of RhB solution in the optimum condition.

The results showed that the pH of the solution was the most effective parameter for the photocatalytic removal of RhB by $Co_xFe_{3-x}O_4$. The optimum condition to achieve the highest photocatalytic degradation with minimum catalyst weight (48mg) is obtained for a 6 ppm initial dye concentration, at pH 9. The predicted efficiency at the optimum condition is closed to 100% according to the experimental results.

CONCLUSION

The experimental photodegradation efficiency of $Co_xFe_{3-x}O_4$ has been investigated and the RSM methodology allowed to optimize the photocatalytic RhB removal (100%) for a set of three experimental parameters.

REFERENCES

[1] Fernandes de Medeiros, I.A., Madigou, V., Lopes-Moriyama, A.L. et al. Morphology and composition tailoring of Co x Fe3 − xO4 nanoparticles. J Nanopart Res 20, 3 (2018).

Polyimide Nonwoven Separators with Higher Electrochemical Performance for Lithium Ion Battery Applications

Youngkwon Kim* [1], Beum Jin Park [1] and Ji-Sang Yu [1]
[1]Advanced Batteries Research Center, Korea Electronics Technology Institute, Korea
(ykkim96@keti.re.kr)

INTRODUCTION

Polyolefin separators are widely used commercially due to their excellent mechanical properties. However, they are vulnerable to rate capability and to short circuits because of their poor thermal properties at high temperatures.[1] Polyimide-based separators can be a good alternative due to their inherent stability at elevated temperatures, making them suitable separators to prevent thermal failure.[1] As PI nonwoven separators have also high ionic conductivity and good electrolyte wettability, it is therefore expected to show excellent rate capability and cyclability.[1] Nevertheless, the pore sizes of nonwoven polyimide separators are often too large to provide appropriate electro-chemical properties. In this study, we controlled the pore sizes of polyimide (PI) nonwoven separators through simple coating.[2]

EXPERIMENTAL/THEORETICAL STUDY

The pore size controlled PI nonwoven separator was prepared by the dip coating method using the coating solution (polysiloxane and PvDF) at room temperature. The electrochemical performance of the coated separators were examined by 2 Ah pouch type full cell.

RESULTS AND DISCUSSION

This study demonstrates the ability to control the pore structure of PI nonwoven through polysiloxane coating. By employing hydrolysis and condensation reactions with three types of silane materials, we successfully coated polysiloxane onto the inner fibers. The resulting SI-PI separator has internal pores sized from 0.5 ~ 2 μm, a Gurley value of 0.6 $s \cdot 100\ cm^{-3}$, and 85 % porosity. It was intriguing to discover that the coated separator with controlled pores allowed for successful charging and discharging, unlike the PI nonwoven. LIBs assembled with the coated separator exhibited impressive rate capability, with discharge capacity of 2.77, 2.68, 2.61, 2.51 and 1.61 mAh at 0.2, 0.5, 1, 2, and 5 C discharge rates, respectively. Furthermore, the coated separator maintained 98.6 % of its capacity after 100 cycles.

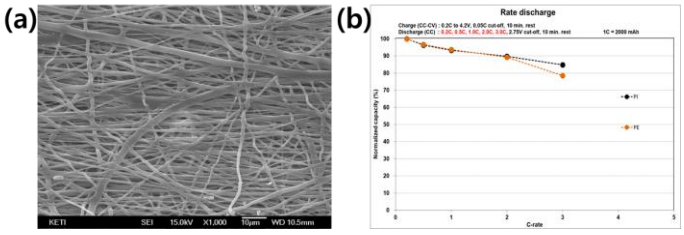

Fig. 1 (a) SEM image of polyimide nonwoven separator, (b) rate capability of 2Ah pouch type full cells with coated-PI and PE separators at a C-rate of 0.2, 0.5, 1.0, 2.0 and 3.0 C

CONCLUSION

The polysiloxane coating effectively controlled pore sizes, showing great potential as a lithium-ion battery (LIB) separator with outstanding thermal stability

REFERENCES

1. Z. Lu et. al, J. Energy Chem., 58, 170 (2021)
2. B. Park et. al, Next Energy, 3, 100090 (2024)

ACKNOWLEDGMENTS

This work was supported by the Industrial Technological Innovation Program (20010095) and the Korea Evaluation Institute of Industrial Technology (No. RS-2022-00155717 Development of High power Hybrid Lithium-ion Capacitors for Unmanned automatic logistics transport System) funded by the Ministry of Trade, Industry & Energy (MOTIE, Korea).

CFD simulation of the effect of in-cylinder water injection on the performance of a H2-diesel dual-fuel compression ignition engine

Qiang Zhang [1], Yusong Yu [2], Zhipeng Li [3], Yang Xu [3] and Xiangrong Li [1 *]
[1]School of Mechanical Engineering, Beijing Institute of Technology, Beijing 100081, China
[2]School of Mechanical, Electronic and Control engineering, Beijing Jiaotong University, Beijing, China
[3]China North Engine Research Institute, Tianjin, 300400, China

INTRODUCTION

Hydrogen-diesel dual-fuel compression ignition (CI) engines offer a cutting-edge solution, leveraging the clean-burning properties of hydrogen to enhance combustion efficiency and reduce emissions[1,2]. However, due to the high laminar combustion rate and wide flammability limits of hydrogen, blending hydrogen with diesel can easily lead to excessively high in-cylinder combustion pressure[3,4]. In this study, the H_2-diesel dual-fuel direct-injection (H2DDI) mode with in-cylinder water injection is implemented on a certain type diesel engine. By harnessing the latent heat of water evaporation and its impact on chemical reactions[5], we aim to achieve suppression of peak in-cylinder pressure and control over the rate of heat release during combustion.

EXPERIMENTAL/THEORETICAL STUDY

Using CFD simulation methods, the impact of hydrogen and water injection relative orientation, injection timing, water ratio on the ignition and in-cylinder combustion processes was studied. The RANS method is utilized for solving in-cylinder flow, employing the KH-RT atomization model to simulate the atomization of diesel and water. In-cylinder direct injection of hydrogen gas is achieved by setting pressure inlet boundaries. The turbulence model adopts the SST k-ω two-equation model.

RESULTS AND DISCUSSION

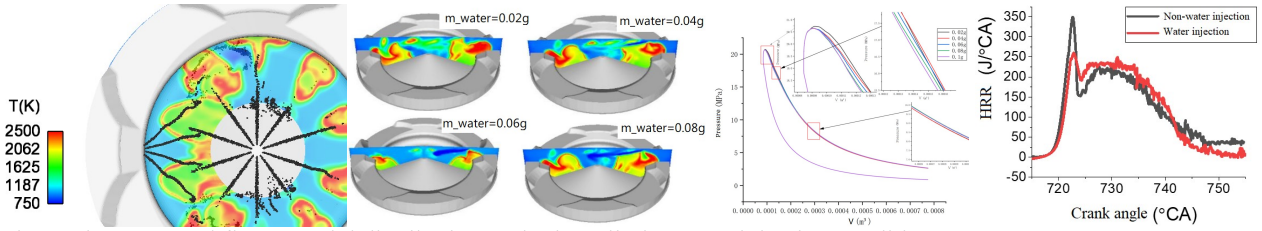

Fig. 1 The spray and flame spatial distribution under in-cylinder water injection conditions
Fig. 2 The flame distribution under different in-cylinder water injection mass (ranging from 0.02g to 0.08g) at ATDC 10°CA
Fig. 3 Pressure-volume (P-V) curves under different in-cylinder water injection mass
Fig. 4 The heat release rate curves under conditions of with and without in-cylinder water injection (water mass of 0.04g).

The spatial interaction between water spray and the jets of diesel and hydrogen has a significant impact on the heat release rate and the spatial distribution of in-cylinder flames. Due to water's high latent heat of evaporation, the evaporation of water spray can effectively reduce the temperature of in-cylinder flames, thereby effectively lowering the peak pressure of in-cylinder combustion. The water vapor generated by water evaporation provides additional volume expansion work, and along with water vapor participating in decomposition, it promotes the generation of free radicals such as OH and H, thereby promoting the improvement of thermal efficiency.

CONCLUSION

This study demonstrates that in-cylinder water injection is an effective approach to both effectively mitigate excessive peak pressure in hydrogen-diesel engine combustion and enhance thermal efficiency. There exists a critical water injection volume, beyond which engine thermal efficiency decreases rather than increases.

REFERENCES

1. T. Tsujimura, et. al, Int. J. Hydrog. Energy 42, 19, 14019-14029 (2017).
2. N. Gültekin, et. al, Int. J. Hydrog. Energy 49, 352-366 (2024).
3. P. Rorimpandey, et. al, Int. J. Hydrog. Energy 48, 2, 766-783 (2023).
4. X. Liu, et. al, Int. J. Hydrog. Energy 57, 904-917 (2024).
5. J. Mortimer, et. al, Fuel 335, 126652 (2023).

Radio Frequency Magnetron Sputtering deposition of MoS_2 electrocatalyst thin films for Anion Exchange Membrane Water Electrolysis

Giulia Di Gregorio[1,2], Matteo Testi[1], Nadhira Laidani[1], Gloria Gottardi[1], and Matteo Miola[2]

[1] Fondazione Bruno Kessler, Via Sommarive, 18, 38123 Povo (TN), Italy
[2]Enphos, Via Giuseppe Zorzi 7, 37138 Verona, Italy

INTRODUCTION

In light of the urgent global imperative to achieve carbon neutrality by 2050, hydrogen production via water electrolysis has become increasingly crucial. Research efforts aimed at enhancing performance and reducing costs of water electrolysis technologies have led to the development of a novel system: anion exchange membrane water electrolysis (AEMWE). AEMWE's distinct advantages lie in its reliance on alkaline feeds, making it compatible with cost-effective platinum-group-metal-free (PGM-free) electrocatalysts. Therefore, the fabrication of highly efficient PGM-free electrocatalysts is imperative for fostering the commercial growth of AEMWE. Conventionally, electrocatalysts are prepared in powder form, then mixed with binders/ionomers, and applied onto supports through spraying or painting, a multi-stage fabrication approach that hinders precise control over physico-chemical properties and often results in undesirable by-products. Magnetron sputtering (MS) is thus emerging as an environmentally friendly, industrially scalable, and highly reproducible one-step fabrication technique for catalyst deposition[1]. MS enables precise control over the deposited catalyst properties, allowing for tailoring the composition of the material, optimizing its microstructure, and controlling the loading and thickness on the substrate. Moreover, MS can avoid the need to mix ionomers with catalysts, facilitating the development of self-supported electrocatalysts[2].

EXPERIMENTAL/THEORETICAL STUDY

Herein, we present a versatile method for fabricating self-supported molybdenum disulfide (MoS2) electrocatalysts onto nickel fiber papers using Radio-Frequency (RF) MS at room temperature. A comprehensive ex-situ characterization of the physico-chemical properties was performed to evaluate the influence of sputtering parameters, using X-ray photoelectron spectroscopy (XPS), X-ray diffraction (XRD), and scanning electron microscopy with energy dispersive X-Ray spectroscopy (SEM-EDX). The hydrogen evolution reaction (HER) electrocatalytic performance of the as-sputtered thin films was assessed using a FlexCell® three electrode half-cell setup, with a Pt wire serving as the counter electrode and a HydroFlex® electrode as the reference electrode. A solution of 1 M KOH served as the electrolyte. For benchmarking, a commercial available PGM-free electrocatalyst deposited on the same nickel fiber paper substrate, manufactured by Dioxide Materials, was used.

RESULTS AND DISCUSSION

XRD spectra showed no peaks corresponding to the crystalline phases of MoS_2, indicating the amorphous structure of the samples. In contrast, XPS analysis demonstrated that slight variations in sputtering power influence the chemical bonding and oxidation states of the thin films. SEM-EDX revealed a rough surface morphology that closely followed the laminated nature of the substrate. Our electrochemical studies unveiled that the sputtering power also influences the HER performance of the MoS_2 electrocatalysts. Intriguingly, the MoS_2 sample deposited at the lowest sputtering power exhibited higher electrocatalytic activity for HER than the benchmark material (Fig.1).

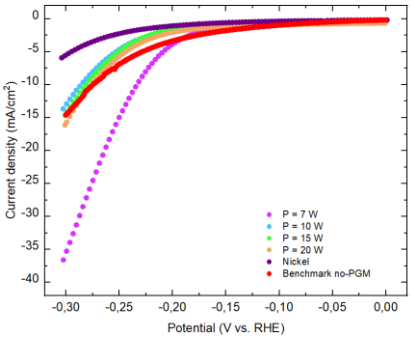

Fig.1 Polarization curves of MoS_2 samples compared to the substrate and benchmark

CONCLUSION

Our findings underscore the potential of RF-MS for depositing diverse catalyst motifs with precise control over both the physico-chemical and electrochemical properties.

REFERENCES

[1] J. Liang et al, Green Chemistry 23.8 (2021): 2834-2867.

[2] E. López-Fernández Ester et al, Molecules 26.21 (2021): 6326.

Preparation of Template-free ZSM-5 Zeolite Membranes by Secondary Hydrothermal Treatment on Supports Made from Rice Husk Ash and α-alumina

Amerícia Bento, Thaís Neves*, Rayssa Xavier, Dirléia Lima, Nilson Marcilio, and Isabel Tessaro
Department of Chemical Engineering, Universidade Federal do Rio Grande do Sul, Brazil
thais.tneves@gmail.com

INTRODUCTION

Zeolite membranes are of great interest because they have a narrow pore size distribution on a molecular scale, as well as chemical and thermal stability. These membranes can be used as membranes to separate species in gaseous or liquid solutions[1]. These membranes are usually supported on tubes or plates made of high-cost materials such as alumina, silica, aluminum, or stainless steel1. In the synthesis of zeolites, organic structure-directing agents are used, which then have to be removed to activate the membrane pores by calcination. This process can result in the formation of cracks in the membrane, reducing its separation efficiency. In addition, organic structure-directing agents are expensive, usually toxic, and generate polluting gases during calcination[2]. Therefore, this work aims to prepare ZSM-5 zeolite membranes on supports made from rice husk ash and α-alumina using the hydrothermal treatment technique. Also, the effect of the rice husk ash on membrane performance is evaluated.

EXPERIMENTAL/THEORETICAL STUDY

The zeolite membranes were prepared on ceramic supports prepared from pure alumina (M1) and supports containing a mixture of alumina and rice husk ash (M2). Colloidal silica LUDOX® SM (Sigma Aldrich), sodium aluminate (Sigma Aldrich), sodium hydroxide (Dinâmica), and deionized water were used to prepare the synthesis solution with a molar composition of SiO_2: 0.3 Na_2O: 0.01 Al_2O_3: 114 H_2O. The zeolite membranes were prepared by secondary hydrothermal techniques, which include a seeding stage for the support and a hydrothermal treatment stage. The experimental procedure also includes pre-synthesis cleaning of the support, preparation of the seed suspension, preparation of the synthesis solution, and post-synthesis treatment. The residual powder and membrane were characterized by X-ray diffraction (XRD) to identify the crystalline phase. The M1 and M2 membranes were photographed by scanning electron microscopy (SEM) to determine the morphology and thickness of the zeolitic layer. Gas permeation was performed in the membranes for the single gases helium, carbon dioxide, and nitrogen.

RESULTS AND DISCUSSION

It was found that just one synthesis cycle was enough to obtain a continuous and homogeneous zeolite membrane. For both membranes, the permeance is higher for helium gas and lower for carbon dioxide as shown in Figure 1.

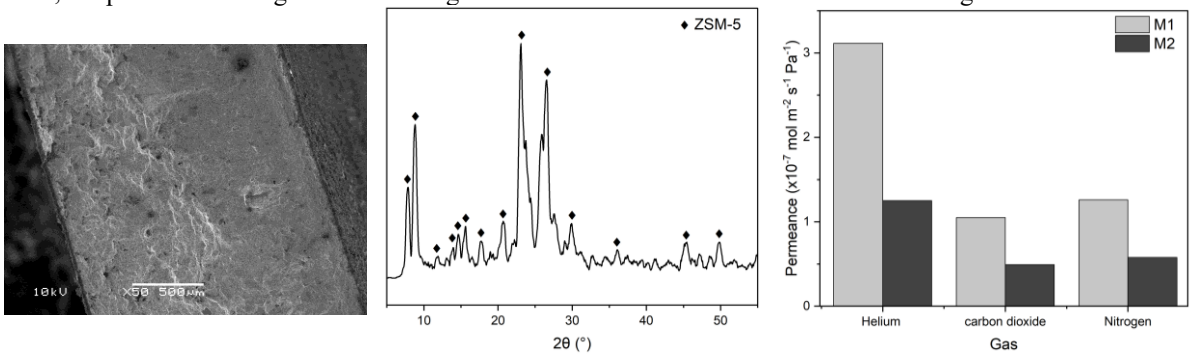

Fig. 1 Cross-sectional micrographs at 50x magnification of the M2, the diffractogram of the powder formed during the hydrothermal synthesis, and gas permeances.

CONCLUSION

The prepared membranes showed satisfactory results in terms of morphology, composition, and gas permeation.

REFERENCES

1. FONG, Y. Y. et al. Chemical Engineering Journal, v. 139, p. 172–193, Maio (2008).
2. ALGIERI, C.; DRIOLI, E. Separation and Purification Technology, v. 278, p. 119295, jan. (2022)

ACKNOWLEDGMENTS

The authors thank the financial support of CAPES, FAPERGS and Almatis for a donation of the raw ceramic powder.